NASA / TP-1998-208705

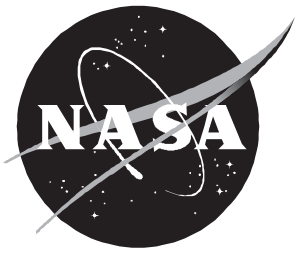

Overview of Laminar Flow Control

Ronald D. Joslin
Langley Research Center, Hampton, Virginia

October 1998

The NASA STI Program Office . . . in Profile

Since its founding, NASA has been dedicated to the advancement of aeronautics and space science. The NASA Scientific and Technical Information (STI) Program Office plays a key part in helping NASA maintain this important role.

The NASA STI Program Office is operated by Langley Research Center, the lead center for NASA's scientific and technical information. The NASA STI Program Office provides access to the NASA STI Database, the largest collection of aeronautical and space science STI in the world. The Program Office is also NASA's institutional mechanism for disseminating the results of its research and development activities. These results are published by NASA in the NASA STI Report Series, which includes the following report types:

- TECHNICAL PUBLICATION. Reports of completed research or a major significant phase of research that present the results of NASA programs and include extensive data or theoretical analysis. Includes compilations of significant scientific and technical data and information deemed to be of continuing reference value. NASA counter-part or peer-reviewed formal professional papers, but having less stringent limitations on manuscript length and extent of graphic presentations.

- TECHNICAL MEMORANDUM. Scientific and technical findings that are preliminary or of specialized interest, e.g., quick release reports, working papers, and bibliographies that contain minimal annotation. Does not contain extensive analysis.

- CONTRACTOR REPORT. Scientific and technical findings by NASA-sponsored contractors and grantees.

- CONFERENCE PUBLICATION. Collected papers from scientific and technical conferences, symposia, seminars, or other meetings sponsored or co-sponsored by NASA.

- SPECIAL PUBLICATION. Scientific, technical, or historical information from NASA programs, projects, and missions, often concerned with subjects having substantial public interest.

- TECHNICAL TRANSLATION. English-language translations of foreign scientific and technical material pertinent to NASA's mission.

Specialized services that help round out the STI Program Office's diverse offerings include creating custom thesauri, building customized databases, organizing and publishing research results . . . even providing videos.

For more information about the NASA STI Program Office, see the following:

- Access the NASA STI Program Home Page at ***http://www.sti.nasa.gov***

- Email your question via the Internet to help@sti.nasa.gov

- Fax your question to the NASA Access Help Desk at (301) 621-0134

- Phone the NASA Access Help Desk at (301) 621-0390

- Write to:
  NASA Access Help Desk
  NASA Center for AeroSpace Information
  7121 Standard Drive
  Hanover, MD 21076-1320

NASA / TP-1998-208705

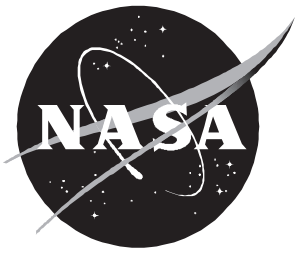

Overview of Laminar Flow Control

Ronald D. Joslin
Langley Research Center, Hampton, Virginia

National Aeronautics and
Space Administration

Langley Research Center
Hampton, Virginia 23681-2199

October 1998

Acknowledgments

The author's only intent in generating this overview was to summarize the available literature from a historical prospective while making no judgement on the value of any contribution. This publication is dedicated to the many scientists, engineers, and managers who have devoted a portion of their careers toward developing technologies which would someday lead to aircraft with laminar flow.

Special thanks to Anna Ruzecki and Dee Bullock for graphics services which led to the reproduced figures, Eloise Johnson for technical editing services, and Patricia Gottschall for typesetting services. Gratitude is expressed to the following companies and reviewers of this manuscript or a portion of this manuscript: Scott G. Anders, Dennis M. Bushnell, Michael C. Fischer, Jerry N. Hefner, Dal V. Maddalon, William L. Sellers III, Richard A. Thompson, and Michael J. Walsh, Langley Research Center; Paul Johnson and Jeff Crouch, The Boeing Company; E. Kevin Hertzler, Lockheed Martin Corporation; and Feng Jiang, McDonnell Douglas Corporation.

Available from the following:

NASA Center for AeroSpace Information (CASI)
7121 Standard Drive
Hanover, MD 21076-1320
(301) 621-0390

National Technical Information Service (NTIS)
5285 Port Royal Road
Springfield, VA 22161-2171
(703) 487-4650

Contents

Tables

Figures

Abbreviations and Symbols

ACEE	Aircraft Energy Efficiency
AEDC	Arnold Engineering and Development Center
a	double wave amplitude, ft
BF	block fuel
BLC	boundary-layer control
BMFT	German Ministry of Research and Technology
$C_{D,t}$	total drag coefficient, nondimensionalized by free-stream dynamic pressure and reference area
C_f	skin-friction coefficient
C_L	lift coefficient
C_p	pressure coefficient
C_q	suction coefficient
$C_{q,t}$	total suction coefficient, nondimensionalized by free-stream velocity and density and reference area
CERT	Centre d'Études et de Recherches de Toulouse
CF	crossflow
CFD	computational fluid dynamics
c	chord, ft
DLR	German Aerospace Research Establishment
DOC	direct operating cost
ELFIN	European Laminar Flow Investigation
F	fuselage
FB	fuel burn
g	acceleration, 32.2 ft/sec^2
g	gap width, ft
H	horizontal tail

HLFC	Hybrid Laminar Flow Control
HSCT	High-Speed Civil Transport
HSR	High-Speed Research
h	altitude
IBL	interacting boundary layer
k	roughness height
L/D	lift-to-drag ratio at cruise
L.E.	leading edge
LF	laminar flow
LFC	Laminar Flow Control
LTPT	Langley Low-Turbulence Pressure Tunnel
M	Mach number
N	$= \int_{s_0}^{s_1} -\alpha \, ds$
N	nacelle
N_t	number of Fourier series modes in time
N_z	number of Fourier series modes in spanwise direction
NLF	Natural Laminar Flow
OEW	operating empty weight
ONERA	Office National d'Etudes et de Recherches Aerospatiales
OPEC	Organization of Petroleum Exporting Countries
PSE	parabolized stability equations
R	range
RAE	Royal Aircraft Establishment
Re	Reynolds number
Re_c	chord Reynolds number
Re_T	transition Reynolds number

Re_θ	momentum-thickness Reynolds number
$Re_{\theta,N}$	momentum-thickness Reynolds number at neutral stability
$Re_{\theta,T}$	momentum-thickness Reynolds number at transition
SLDT	Langley Supersonic Low-Disturbance Tunnel
SLFC	Supersonic Laminar Flow Control
s	marching coordinate for N-factor determination
TOGW	takeoff gross weight
TPT	Langley 8-Foot Transonic Pressure Tunnel
TS	Tollmien-Schlichting
t	time
U	velocity
U_k	local velocity at top of roughness particle
U_l	local potential velocity
u, v, w, p	disturbance velocities and pressure
$\bar{u}, \bar{v}, \bar{w}, \bar{p}$	mean velocities
$\tilde{u}, \tilde{v}, \tilde{w}, \tilde{p}$	instantaneous velocities and pressure
V	airspeed
V	vertical tail
V_s	suction flow velocity
VSTFE	Variable Sweep Transition Flight Experiment
W	wing
x, y, z	Cartesian coordinate system
x/l	nondimensional length
α	disturbance streamwise wave number
β	disturbance spanwise wave number
γ	growth rate for N-factor determination

δ	boundary-layer thickness
θ	momentum thickness
Λ	wing sweep, deg
λ	surface wavelength, ft
ν	kinematic viscosity
ν_k	local kinematic viscosity at roughness
Φ	disturbance profile
ϕ	radial coordinate
ϕ_g	group velocity angle
ω	disturbance frequency
2D	two-dimensional
3D	three-dimensional

Subscripts:

k	roughness element
max	maximum
θ	momentum thickness
∞	free stream

A tilde (~) over a symbol indicates instantaneous; a bar (-), mean; a caret (^), complex eigen function.

Abstract

The history of Laminar Flow Control (LFC) from the 1930s through the 1990s is reviewed and the current status of the technology is assessed. Early studies related to the natural laminar boundary-layer flow physics, manufacturing tolerances for laminar flow, and insect-contamination avoidance are discussed. Although most of this publication is about slot-, porous-, and perforated-suction LFC concept studies in wind tunnel and flight experiments, some mention is made of thermal LFC. Theoretical and computational tools to describe the LFC aerodynamics are included for completeness.

1. Introduction

This overview reviews Laminar Flow Control (LFC) research that began in the 1930s and flourished through the early 1960s until it was de-emphasized because of a change in national priorities. During the 1970s when the oil embargo by OPEC led to a fuel shortage and high-cost fuel, LFC research became important again because of the aerodynamic performance benefits it could potentially produce for commercial aircraft. The next 20 years of research resulted in numerous significant achievements in LFC through wind tunnel and flight experiments in the United States and Europe.

The balance of this publication presents wind tunnel investigations, flight research activities, and LFC design tool methodology development in the United States and Europe that are devoted to advancing the state of the art and reducing the risk associated with the application of LFC technology to subsonic, transonic, and supersonic commercial and military transports. Because this publication is a review, it encompasses much of the nearly 60-year history of LFC research and LFC-related research to highlight the many basic flow physics experiments and theory development which have enabled successful hardware demonstrations.

Figure 1 and tables 1 through 3 summarize the LFC projects that are discussed in this overview and highlight the reference, LFC information, and accomplishment for each project. In section 2, definitions appropriate to LFC are presented and the numerous benefit studies are summarized. In section 3, the many fundamental studies which have led to the current understanding of the flow physics, the manufacturing tolerances necessary for laminar flow, and the design tools used to predict the extent of laminar flow (including transition prediction methods) are discussed. In section 4, issues relating to operating LFC aircraft are reviewed, including the potential impacts of insect and ice accumulation on laminar flow extent. From figure 1, two clear eras can be (subjectively) identified over the history of LFC. The first era is the early wind tunnel and flight experiments and design tool advancements in slot-, porous- and perforated-suction systems through the mid-1960s prior to the OPEC oil embargo, which are covered in section 5. Although many successful LFC demonstrations occurred in that era, the Vietnam Conflict caused a shift in U.S. national priorities and the demise of the major LFC projects.

Early in the 1970s, the OPEC oil embargo caused the United States to generate national programs which focused on improved aerodynamic efficiencies. This focus reenergized LFC under the NASA Aircraft Energy Efficiency (ACEE) Program. Many of the major natural laminar flow (NLF) and LFC projects under ACEE demonstrated the achievement of laminar flow in flight. Sparked by this U.S. success in the NLF and LFC programs, Bulgubure and Arnal (1992) noted that laminar flow projects began in France in 1984 to gather data that were currently not available in France. Aérospatiale, Dassault Aviation, and a number of research organizations (including ONERA) were involved in the French program. Then in 1989, the European Laminar Flow Investigation (ELFIN) Project was initiated, consisting of four primary elements concentrating on the development of laminar flow technology for application to commercial transport aircraft. These elements were

1. A transonic wind tunnel evaluation of the hybrid laminar flow control (HLFC) concept on a large-scale model

2. The development of a boundary-layer suction device and the development of new wind tunnel and flight test techniques for LFC

3. The development of improved computational methods for laminar-to-turbulent flow prediction capability

4. A partial-span flight demonstration of natural laminar flow (Birch 1992)

According to Mecham (1992), the project team consisted of 24 organizations, including Deutsche Airbus (project leader), Aérospatiale, Alenia, British Aerospace, CASA, Dassault Aviation, Dornier, Fokker, Saab, several smaller companies, six national aeronautical research institutes, and nine universities. Among these institutes and universities were ONERA, CIRA INTA, DLR, and the Universities of Manchester, Bristol, Galway, Lisbon, Lyngby, Darmstadt, Delft, Madrid, and Zaragoza. Section 6 summarizes the major U.S. and European LFC programs for the time frame beginning with the OPEC oil embargo.

This overview publication attests to the enormous amount of research pertaining to NLF and LFC in the literature. Additional discussions of LFC can be found in Harris and Hefner (1987), Wagner et al. (1988), Wagner et al. (1992), and Hefner (1992). A few bibliographies of LFC are available by Bushnell and Tuttle (1979), Tuttle and Maddalon (1982, 1993), and Kopkin and Rife (1977). Holmes and Obara (1992) and Holmes, Obara, and Yip (1984) review and focus on NLF flight research; Somers (1992) and Pfenninger and Vemuru (1992) discuss laminar flow airfoils; Wagner, Maddalon, and Fischer (1984); and Braslow and Fischer (1985) discuss the overall status of LFC. Finally, refer to *Research in Natural Laminar Flow and Laminar-Flow Control* (NASA CP-2387, 1987) and *First European Forum on Laminar Flow Technology* (DGLR-Bericht 92-06, 1992) for a selection of papers presented during those workshops. More recently, the second European forum on LFC occurred.

2. Background

In the following sections, the definition of NLF, LFC, and HLFC are outlined and the benefits of using LFC are discussed by summarizing numerous benefit studies.

2.1. Definition of LFC

LFC is an active boundary-layer flow control (usually suction) technique employed to maintain the laminar state at chord Reynolds numbers beyond that which is normally characterized as being transitional or turbulent in the absence of control. Understanding this definition is an important first step toward understanding the goals of the technology. Often, a reader mistakenly assumes that LFC implies the relaminarization of a turbulent flow state. These are two different flow physics phenomena; although the same control system may be employed for both problems, the energy requirements for relaminarization could typically be an order of magnitude greater than that required for LFC. Finally, LFC is a capability that is designed to benefit an aircraft during cruise by reducing the drag.

An alternate concept of drag reduction is referred to as “natural laminar flow (NLF).” NLF employs a favorable pressure gradient to delay the transition process. Inherent in practical NLF wings is low sweep and aircraft of small to moderate size. As the wing is swept, aerodynamic performance benefits are realized for high-speed aircraft; however, the now three-dimensional (3D) flow field becomes vulnerable to a boundary-layer instability termed “crossflow vortex instability” (discussed in section 3). This instability causes the NLF design to become ineffective and the boundary-layer state to become turbulent very near the wing leading edge. For nacelles, the application of the NLF design has been shown to produce unacceptable low-speed performance; however, some modern NLF nacelles have overcome earlier design deficiencies. An active system is usually required to prevent these boundary-layer instabilities from causing the laminar flow to become turbulent.

A significant advancement made in the development of LFC technology is the concept of Hybrid Laminar Flow Control (HLFC). Shown in figure 2, HLFC integrates the concepts of NLF with LFC to reduce suction requirements and reduce system complexity. LFC is complex, involving suction (and ducts, flutes, and pump source) over the whole-wing chord

(or engine nacelle or tail section). The key features of HLFC are

1. Suction is required only in the leading-edge region ahead of the front spar

2. NLF is maintained over the wing through proper tailoring of the geometry (pressure)

3. The HLFC wing design has good performance in the turbulent mode

These concepts integrated in figure 2 with the Krueger flap (for high lift and ice and insect-contamination prevention) show one potential practical application of HLFC on a wing.

2.2. Benefits of LFC

The benefits of LFC are configuration dependent; change with time because of changes in fuel cost, system cost, manufacturing technology efficiency improvements; and are closely linked to the amount of laminar flow and a host of other variables (including the weight of a passenger for the overall payload weight). Throughout the history of LFC, numerous benefit studies have been carried out on a host of configurations. The outcome of these studies is described in this section along with a discussion of the impact of fuel cost on LFC benefit.

Antonatos (1966) presented a review of the concepts and applications of LFC, beginning with the realization that skin friction drag could amount to approximately 75 percent of the total drag for an aircraft. Shown in figure 3, Thibert, Reneaux, and Schmitt (1990) attributed friction drag to approximately 45 percent of the total drag. Because laminar skin friction can be as much as 90 percent less than turbulent skin friction at the same Reynolds number, laminar flow would obviously be more desirable than turbulent flow for reducing the drag of aerodynamic vehicles (except in recovery regions where a severe pressure drag penalty can occur because of boundary-layer separation). A vehicle with laminar flow would have much less skin friction drag than a vehicle with turbulent flow. An example of the benefits of laminar flow are shown in figure 4 for a subsonic business jet (Holmes et al. 1985). Unfortunately, achieving laminar flow over the entire configuration is impractical because of the sensitivity of the laminar flow to external and vehicle disturbances (e.g., panel-panel joints, fasteners, access doors). However, drag reduction due to laminar flow over select portions of a vehicle is achievable. For an aircraft, the wings, engine nacelles, fuselage nose, and horizontal and vertical tail are candidates for achieving laminar flow. Although the summation of these individual drag reductions would indicate a benefit due to laminar flow (fig. 4), the maximum or optimal benefits of LFC are achieved by resizing the vehicle utilizing the benefits of laminar flow. Thus LFC could yield reductions in takeoff gross weight (TOGW), operating empty weight (OEW), and block fuel (BF) for a given mission, and significant improvements in cruise lift-to-drag ratio (L/D). Associated benefits may include reductions in both emissions (pollution) and noise and smaller engine requirements.

Lachmann (1961) discussed the design and operational economies of low-drag aircraft, including LFC. This presentation was one of the few that listed the equations and assumptions of the equations that led to projected performance. Lachmann noted that the benefits of laminar flow obtained by LFC increased with the size of the candidate aircraft, with benefits maximized for an all-wing aircraft. Also, if 39 percent of the aircraft fuselage could be laminarized for a typical trans-Atlantic airline, Lachmann (1961) predicted a 10-percent increase in L/D.

Chuprun and Cahill (1966) discussed the performance improvements of aircraft with LFC technology from the systems perspective and noted that the impact of any technology must involve the integrated result of aerodynamics, structures, propulsion, cost, risk, reliability, schedules (operations), and the sensitivity of the proposed concept to the design goals. This integrated result heavily determines the cost-effectiveness of the design concept and whether the technology will be implemented on the candidate aircraft. When compared with the turbulent baseline aircraft, the important improvement to the aircraft because of LFC would be an increase in L/D. The amount of improvement would depend on the amount of laminar flow achieved for a given surface geometry and flight condition and the structural weight penalties incurred by the addition of the pumping system. At a minimum, the benefits of the LFC technology must overcome the penalties incurred by such a system. The effect of the

LFC weight penalties on the range of an aircraft is a function of the ratio of fuel weight to gross weight. LFC weight penalties have less effect on range for aircraft with high ratios of fuel to gross weight. Finally, the performance benefits of LFC on a modified C-5A transport aircraft were compared with the C-5A baseline; this comparison yielded range increases for constant payload and payload increases with constant range for the LFC version of the aircraft (quantified in figs. 5 and 6). Clearly, the benefits of LFC became pronounced compared with the turbulent baseline for long-range medium payload aircraft, with 20 to 25 percent improvement in range on the LFC aircraft. Carefully noted by Chuprun and Cahill (1966), the 1966 development, production, and operation costs were projected to be 10 to 20 percent higher for the LFC aircraft compared with the turbulent baseline aircraft.

By noting that LFC benefits increase with increased aircraft range, Goethert (1966) demonstrated the performance benefit by example. A long-range aircraft designed to carry a payload of 150 000 lb some 5000 n.mi. could carry the same payload 6250 n.mi. by employing LFC technology, or the LFC aircraft would be able to carry a reduced payload of 100 000 lb some 8000 n.mi.

Later, Sturgeon et al. (1976) performed a systems study to determine the benefits of LFC on long-range subsonic transports. Based on a range of 5500 n.mi. and payloads of 200 (52 400 lb) and 400 (104 800 lb) passengers, the LFC transport would improve fuel efficiency by 39.4 percent over advanced technology turbulent aircraft; therefore fuel consumption would be reduced by 28.2 percent and operating costs by 8.4 percent.

Pearce (1982) presented the benefits of a LFC subsonic transport compared with an advanced comparable turbulent configuration. The benefits of using LFC were shown to be consistent with the results already cited; however, unlike many of the studies, Pearce showed the significance of both laminar flow extent (i.e., transition location on the wing) and fuel cost. For example, a rise in fuel cost from 45 cents to 1 dollar would cause direct operating cost (DOC) to be increased from 3 to 8 percent with LFC compared with the turbulent configuration.

Pfenninger (1987) explored an unconventional long-range LFC transport concept. Using large-span, large-aspect-ratio, strut-braced wings, a cruise L/D of 39.4 was estimated with laminar flow assumed on the wings, nacelles, tail, and struts. Such an aircraft would carry 50 000 kg of payload (or 250 passengers + cargo) and cruise at a Mach number of 0.83. Weak suction was positioned from 5 to 30 percent chord and it was predicted to achieve laminar flow on about 70 percent chord on the upper surface of the wing (HLFC).

As illustrated in figure 5, Kirchner (1987) showed that the benefits of LFC (HLFC and NLF) increased with the increased size and range of the candidate airplane. This figure indicates that the benefits of LFC on a long-range subsonic transport could lead to significant fuel savings.

Clark, Lange, and Wagner (1990) reported the benefits of LFC for advanced military transport aircraft. Based on a 132 500-lb payload transported 6500 n.mi. at a Mach number of 0.77, the LFC transport would lead to reductions in TOGW of 4 to 7 percent, fuel weight of 13.4 to 17 percent, and thrust of 10.6 to 13 percent and an increase in cruise L/D of 18.4 to 19.2 percent compared with the turbulent baseline configuration. The lower and higher values corresponded to low-wing and high-wing HLFC configurations, respectively.

Arcara, Bartlett, and McCullers (1991) performed a LFC benefit study for an advanced subsonic, twin-engine commercial transport with projected 1995 engine, structure, and aerodynamic technology improvements into a HLFC. With laminar flow assumed on 50 percent chord on the upper wing surfaces and horizontal and vertical tails and 40 percent on the engine nacelles, figure 6 shows reductions in TOGW of 9.9 percent, OEW of 5.7 percent, and BF of 18.2 percent. Additionally, an increase in cruise L/D of 14.7 percent was achieved compared with that of the turbulent baseline. The figure shows the very important location of the suction and resulting laminar flow extent. The analysis included conservative estimates of the HLFC system weight and engine bleed air (to drive the suction device) requirements. Satisfaction of all operational and Federal Aviation Regulations (FAR) requirements, such as fuel reserves and

balanced field length, was achieved. A brief section on the impact of fuel cost on the benefits was included in the analysis. Fuel at 65 cents per gallon had a reduction in DOC of 5.8 percent as a result of HLFC compared with fuel at 2 dollars per gallon having a reduction in DOC of 8.8 percent.

Robert (1992a) discussed the potential benefits of HLFC applied to the Airbus A320 and A340 class of subsonic transports. The study sought to determine

1. Differences for short- or long-haul aircraft

2. What size aircraft should be laminarized

3. Where laminarization is advantageous

4. What fuel reduction could be achieved

For the A320 with a range of 500 n.mi., cruise represented only 35 percent of the total FB, whereas for the A340 with a range of 3000 n.mi., cruise represented 80 percent of the total FB. Because LFC is a cruise technology, the A340 would benefit more from the application of LFC than the A320. If HLFC is used over the first 15 to 20 percent chord for the larger A340 class aircraft, a projected drag reduction of 14 percent could be obtained by using laminar flow concepts on the wing, horizontal tail, vertical tail, and nacelles. The A320 and A340 studies indicated that 60 percent of the performance gain came from the upper surface of the wing and 30 percent came from the lower surface of the wing. Robert noted that there was no point in laminarizing the lower surface because the costs of incorporating access doors and the Krueger flap within laminar flow tolerances offset the advantages of drag reduction on the lower surface. For the issue of DOC, if a 2.8-percent increase in the cost of maintenance is assumed, the DOC would be reduced by 0.8 percent for a 3000-n.mi. cruise and FB by 5 percent. The benefits increased with fuel cost and aircraft mission. Finally, Robert summarized that a long-range technical program could be established to enable Airbus Industrie to offer a future aircraft with laminar wings. This plan has been pursued in the 1990s with wind tunnel tests, flight tests, fundamental concept studies, and with advanced design tool development. (See section 6.)

Supersonic laminar flow control (SLFC) implies that the test vehicle flies at supersonic Mach numbers and that either LFC or HLFC is employed on the vehicle. Feasibility studies by Boeing Commercial Airplane Company (Parikh and Nagel 1990) and McDonnell Douglas Corporation (Powell, Agrawal, and Lacey 1989) were conducted to determine the benefits of SLFC applied to the HSCT configuration. The Boeing configuration was designed to cruise at a Mach number of 2.4 and carry 247 passengers (745 000 lb TOGW) 5000 and 6500 n.mi. The inboard wing was a modified airfoil from the NACA 65A-series and had a sweep of 75° (normal Mach number of 0.62 at cruise), whereas the outboard portion of the wing had a sharp supersonic leading edge with 47° of sweep (normal Mach number of 1.64 at cruise). The SLFC feasibility study estimated benefits to be reductions in TOGW of 8.5 percent, in OEW of 6.2 percent, and in FB of 12 percent. These numbers took into account the estimated 8500-lb suction-system weight penalty. The benefits were greater for an aircraft resized for a range of 6500 n.mi. and are shown in figure 7. With laminar flow covering 40 percent of the wing wetted area, reductions in TOGW, OEW, and FB of 12.6, 9.8, and 16.0 percent, respectively, were projected when compared with the turbulent version of the supersonic aircraft for a range of 6500 n.mi. Based on a TOGW of 750 000 lb for the turbulent baseline HSCT aircraft, the projected reduction in TOGW for the laminar aircraft is roughly equivalent to the payload fraction of the aircraft OEW.

The McDonnell Douglas configuration was designed to cruise at a Mach number of 2.2 and carry 308 passengers (750 000 lb TOGW) 5750 n.mi. The wing was a cranked arrow wing with most of the sweep at 71° and the outboard 30 percent span of the wing swept 61.5°. The SLFC feasibility study for application to the HSCT found reductions in TOGW of 8 percent and FB of 15 percent and an increase in cruise L/D of 15 percent. Whereas the Boeing concept employed a leading-edge suction strip and a second spanwise suction strip at about 40 percent chord, the McDonnell Douglas concept had large leading-edge suction and a continuous low level of suction back to the control surfaces.

Based on limited supersonic data, Kirchner (1987) showed in our figure 8 that an increase of 10 to

30 percent in L/D is expected by using SLFC on the supersonic high-speed civil transport. Pfenninger and Vemuru (1988) presented a strut-braced, highly swept wing SLFC long-range transport design which was capable of acquiring values of L/D of 19 to 27 at a Mach number of 2 and 16 to 22 at a Mach number of 2.5.

Aerodynamic performance benefits bought by skin friction drag reduction can translate into reduced operating costs of an aircraft. Figure 9 shows the jet fuel cost per gallon and jet fuel as a percentage of the cash operating cost for the industry over some 20 yr. From these data (Anon. 1985, 1995a), the critical times in the industry are evident when fuel costs grew in the late 1970s and early 1980s and briefly in the 1990s. The rapid increase in fuel cost in the 1970s inspired the drag reduction program in the United States, including NLF and LFC flight test programs. In the 1990s the cost of fuel has become a small fraction of the operating cost for the industry and, therefore, the demand for technologies such as LFC have diminished. However, similar to the OPEC oil embargo in the early 1970s that led to a diminished supply of fuel and subsequent rise in prices (large demand and low supply), technologists in the government laboratories and in industry must be poised to cope with future uncertainty in fuel cost (one of many external influences on the demand for innovation). Note, that the rise in fuel price in the early 1990s was spawned by the Iraq invasion of Kuwait. The yearly consumption of $10.5 billion in 1981 has only dropped to $7.7 billion in 1994, which reflects a reduction in fuel cost and an increase in fuel consumption.

In summary, LFC can lead to reduced skin friction drag and thereby reduced fuel consumption. This benefit can lead to either an extension in range for the same aircraft or to reduced aircraft weight for a fixed range. For the latter case, less engine power is required and reduced emissions, noise, and operating costs can be expected from the LFC aircraft. Noise and emission reductions have become ever more important and global pollution becomes an important variable in the design concepts of the future. Although fuel cost has decreased in recent years, the total volume of fuel consumption has increased and the potential fuel savings due to LFC remain a significant cost savings to the industry.

3. Laminar Flow Control Design Methodology

For a LFC design (a wing, for example), the analysis begins by defining an initial wing geometry. With wing geometry defined, the wing pressures and velocities can be obtained by using transonic wing theory and/or Computational Fluid Dynamics (CFD). The inverse approach of prescribing a target pressure distribution and solving for the wing geometry is then used. After obtaining the external flow field for the final geometry, boundary-layer and stability theory calculations are used for determining the suction flow rates and distribution for the desired transition locations. With the suction flow rate determined from boundary-layer stability considerations, the pressure drop through the skin must be set to obtain a reasonable subsurface compartmentation scheme and perforation spacing distribution for the desired suction distribution. The process is iterative until an acceptable design is obtained. Finally, the suction system ducting and compressor specifications are prescribed.

Other key issues, covered in this section, that must be understood for LFC design are

1. The physics associated with the laminar to turbulent boundary-layer transition process

2. Impact of surface tolerances—roughness, waviness, steps, and gaps—on laminar flow extent (required for manufacturing)

3. Slot, porous, and perforated suction and thermal LFC schemes

4. Issues relating to manufacturing LFC articles

5. The methodology and limitations of transition prediction (determining laminar flow extent for projecting benefits to aircraft)

3.1. Boundary-Layer Instability Issues

As stated in section 2, the reason laminar flow is usually more desirable than turbulent flow for external aerodynamic vehicles lies with the reduction of the viscous drag penalty. (See fig. 4.) Do we have a

sufficient understanding of the fundamental flow physics for the problem to design an optimal, reliable, cost-effective system to control the flow? The answer is encouraging!

The first major theoretical contributions to the study of boundary-layer transition were made by Helmholtz (1868), Kelvin (1880), Reynolds (1883), and Rayleigh (1879, 1880, 1887). Although these early investigations neglected the effects of viscosity, the second derivative of the mean velocity proved to be of key importance in explaining boundary-layer instabilities. These fundamental studies proved to be the basis for future breakthroughs in theoretical development, including inviscid jet-flow instabilities and shear-layer instabilities. Adding viscous effects, Orr (1907) and Sommerfeld (1908) developed an ordinary differential equation (Orr-Sommerfeld equation) that governs the linear instability of two-dimensional disturbances in incompressible boundary-layer flow on flat plates. Later, Squire (1933) accounted for three-dimensional waves by introducing a transformation from three to two dimensions. This analysis showed that two-dimensional waves were dominant in flat-plate boundary layers. Tollmien (1929) and Schlichting (1932) discovered convective traveling-wave instabilities (fig. 10) now termed Tollmien-Schlichting (TS) instabilities, and Liepmann (1943) and Schubauer and Skramstad (1947) experimentally confirmed the existence and amplification of these TS instabilities in the boundary layer. One can visualize this disturbance by remembering the image of water waves created by dropping a pebble into a still lake or puddle. In this image, the waves which are generated decay as they travel from the source. Such is the case in boundary-layer flow, except that the waves will grow in strength when certain critical flow parameters (say Reynolds number) are reached and lead to turbulent flow.

Taylor-Görtler vortex disturbances arise when the surface geometry becomes concave and are reminiscent of counterrotating vortices. A sketch of this vortex-disturbance structure is shown in figure 11. The design engineer would have to be sensitive to this disturbance only if there is concave curvature such as on the lower surface of some wings; otherwise, this disturbance is not too significant for LFC applications. See Smith (1955), Wortmann (1969), and Hall (1983) for more detailed discussions of Taylor-Görtler disturbances.

In addition to transition dominated by TS disturbance, a dynamic instability, termed the crossflow (CF) disturbance, is an important factor in the extent of laminar flow realized. The presence of TS and CF disturbances in the boundary-layer flow is dependent on the pressure gradient and on the wing sweep angle. As shown by Gray (1952), Anscombe and Illingworth (1956), and Boltz, Kenyon, and Allen (1960) for swept wings and by Gregory, Stuart, and Walker (1955) and Reilly and Pfenninger (1955) for rotating-disk flow, CF disturbances are characterized by corotating vortices (sketched in fig. 12). For example, Anscombe and Illingworth (1956) used a symmetric airfoil with a 4-ft chord in a wind tunnel experiment to study the flow on the wing swept from 0° to 50°. The results showed that at angles above 25° to 30°, a critical speed could be found which led to “striations” in the surface flow visualization with transition between 50 and 60 percent chord. As the speed of the free stream increased, the transition moved forward. This effect of sweep and Reynolds number on transition is shown in figure 13 (Anscombe and Illingworth 1956). The figure serves to provide a visual qualitative influence of wing sweep. They further noted that as the transition front moved forward, the laminar boundary layer became more sensitive to surface conditions and the number of turbulent wedges increased. This sensitivity was a unit Reynolds number influence; whereby the critical height of a roughness element affecting transition decreased with increase in unit Reynolds number (discussed in section 3.2).

At the same time, Gray (1952) investigated the effect of wing sweep in flight using the Armstrong Whitworth AW.52 aircraft. Visualization was achieved through sublimation, or liquid evaporation from china clay techniques. Most of the results are for sweep angles of 25° to 50°, chord locations from 3 to 17 ft, and speeds from 50 to 500 knots at an altitude of 40 000 ft. Additionally, a Meteor Fin with 25° sweep, a Sabre F.86 with 39° wing sweep, an Avro 707A Delta, and a Hawker P1052 were also tested. Gray (1952) concluded that the leading-edge radius was a direct measure of the limit of laminar flow for all modern flight speeds for sweep angles more than 20° or 25°. The amount of laminar flow decreases with increased leading-edge radius. Similar to the results presented by Anscombe and Illingworth (1956), the results of Gray (1952) showed that for a given sweep angle, laminar flow was lost as the speed is increased to a critical speed. Since those early experiments,

numerous flight experiments have shown that natural transition moves forward on the wing with increase in wing sweep. Flight and wind tunnel measurements of transition location with wing sweep are shown in figure 14 (Wagner et al. 1992).

Because a favorable pressure gradient leads to decreased TS-disturbance growth and increased CF-disturbance growth (Arnal 1992, for example), the NLF wing design engineer would seek to optimize the pressure distribution and sweep for prescribed Reynolds number and Mach number such that the pressure gradient causes the minimum growth of both the TS and the CF disturbances over the chord of the wing (or nacelle, etc.). For large sweep angles, LFC or HLFC suction is used in the leading-edge region to suppress the normally rapid growth of the CF disturbances, and then the pressure on the wing surface is tailored to minimize the growth of all disturbances.

In addition to TS and CF disturbances which lead to transition over the wing chord, attachment-line instabilities are possible and can be correlated for natural transition in the linear limit with the Reynolds number of the flow. If transition were to occur at some location on the attachment line, the outboard portion of the whole wing would have turbulent flow. Clearly, this can be understood by viewing the illustration in figure 15 (from Wentz, Ahmed, and Nyenhuis 1985) for the attachment-line region of a swept wing. Turbulence (or attachment-line contamination) from the fuselage boundary-layer flow can sweep out onto the attachment line and cause the entire wing to be engulfed in turbulent flow. However, a turbulence diverter such as Gaster's bump (Gaster 1965) can be effectively used to establish a laminar attachment line; this allows the potential for continued laminar flow on the attachment line. Some methods which can be used to prevent turbulent attachment-line contamination are illustrated in figure 16 (from Maddalon and Braslow 1990). For LFC or HLFC, strong suction can also be used at the fuselage–wing juncture to relaminarize the flow, and mild suction can be used thereafter on the leading edge to maintain laminar flow.

Transition along the attachment line can be prevented by designing the attachment-line Reynolds number not to exceed some critical value. This was drawn out in experiments by Gaster (1967), where small-amplitude disturbances were acoustically excited along the attachment line of a swept cylinder model. Gaster generated sine waves with various frequencies that were detected in the flow by a hot-film gauge on the attachment line. He noted that the recorded oscillations had preferred frequency bands that changed with tunnel speed and that this behavior was reminiscent of traveling-wave instabilities. From his measurements, he concluded that the small-amplitude disturbances in an attachment-line boundary layer were stable for momentum-thickness Reynolds numbers Re_θ below 170. Later, Cumpsty and Head (1969) experimentally studied large-amplitude disturbances and turbulent flow along the attachment line of a swept-wing model. Without artificially tripping the boundary-layer instabilities, they observed that laminar flow was stable to small-amplitude disturbances up to $\mathrm{Re}_\theta \approx 245$ (which corresponds to the top speed of the tunnel). At the same time, Pfenninger and Bacon (1969) used a wing sweep of 45° to study the attachment-line instabilities in a wind tunnel capable of reaching speeds sufficient to obtain unstable disturbances. With hot wires, they observed regular sinusoidal oscillations with frequencies comparable with the most unstable two-dimensional modes of theory; these modes caused transition to occur at about $\mathrm{Re}_\theta \approx 240$. A continued interest in the transition initiated near the attachment line of swept wings led Poll (1979, 1980) to perform additional experiments with the swept circular model of Cumpsty and Head (1969). Like Pfenninger and Bacon (1969), Poll observed disturbances that amplified along the attachment line. He noted that no unstable modes were observed below $\mathrm{Re}_\theta \approx 230$.

Accounting for all linear terms and using an eigenvalue-problem approach, Hall, Malik, and Poll (1984) studied the linear stability of the attachment-line boundary-layer flow called swept Hiemenz flow. This three-dimensional base flow was a similarity solution of the Navier-Stokes equations; hence, its use is advantageous in stability analyses. With a nonparallel theory, Hall, Malik, and Poll (1984) determined neutral curves with and without steady suction and blowing and demonstrated that the attachment-line boundary layer can theoretically be stabilized with small amounts of suction. The linear results were shown to be in good agreement with direct numerical simulations of Spalart (1989), Theofilis (1993), and Joslin (1995, 1996).

Based on these theoretical and experimental studies, the critical Reynolds number for the two-dimensional linear instability of subsonic flows is $Re_\theta \approx 245$. Additional understanding of the instability of the attachment-line flow to three-dimensional disturbances must be gained to formulate theories of design and implement devices to prevent instability growth.

In studying leading-edge contamination, Pfenninger (1965) discovered through flight experiments that laminar flow could be obtained for $Re_\theta < 100$ but leading-edge contamination occurred for $Re_\theta > 100$. Gregory and Love (1965) found that complete turbulence occurred for $Re_\theta > 95$ in their wind tunnel experiments on a swept airfoil. Flight experiments by Gaster (1967) showed that turbulent spots were first observed for $Re_\theta > 88$. Cumpsty and Head (1969) and later Poll (1985) used a swept model in a wind tunnel to show that turbulence was damped for $Re_\theta < 99$ and the leading edge was fully turbulent for $Re_\theta > 114$. Arnal, Juillen, and Casalis (1992) used a swept-wing model in a wind tunnel to show that leading-edge contamination was observed at $Re_\theta \approx 101 \pm 4$. Using the Jetstar LFC flight test aircraft, Maddalon et al. (1989) indicated that turbulent contamination caused transition on the attachment line of the test article for $Re_\theta > 94$. Hence, for $Re_\theta < 100$ disturbances are damped, and for $Re_\theta > 100$ the flow becomes turbulent. Between $Re_\theta \approx 100$ and the linear critical Re_θ care must be taken so that the flow is not tripped. Wind tunnel experiments by Carlson (1964) indicated that the Reynolds number based on boundary-layer momentum thickness at the front of the attachment line should be $Re_\theta \leq 150$ for very small disturbances and $Re_\theta \leq 100$ for large disturbances. As many flight experiments have shown, maintaining NLF on the attachment line is possible, and the momentum-thickness Reynolds number can be lowered by reducing the leading-edge radius or unit Reynolds number. Decreasing the leading-edge radius has the compounded benefit of decreasing the chordwise extent of the crossflow region and providing a more rapid acceleration of the flow over the wing.

Additionally, a turbulent wedge, originating at the fuselage–wing-leading-edge juncture, can sweep out over a portion of the wing root region and is a concern for NLF and LFC wing design. Clearly, one would attempt to optimize the fuselage–wing juncture point to cause this wedge to cling to the fuselage as much as possible; thereby, laminar flow would occur in a region close to the fuselage. The author knows of no study which has investigated the potential instability of the interface between a turbulent wedge and laminar flow over a wing; however, Hilton (1955) has used the concept of tailoring the streamlines to the fuselage to obtain a drag reduction.

In summary, for wing sweeps from 0° to 10°, TS disturbances amplify and cause natural transition. If the design pressure gradient is favorable (accelerating flow), longer runs of laminar flow can be realized because the TS-disturbance growth rate is suppressed, whereas the opposite is true with an adverse pressure gradient. Wing design should minimize the growth of these disturbances to enable long runs of laminar flow. Between wing sweep angles of 10° and 30°, both TS and CF disturbances are present, amplify, and cause transition; much of the flow physics associated with the nonlinear interaction of these modes is unknown. For wings swept greater than 30°, CF disturbances dominate, amplify, and cause transition—often very near the leading edge of the wing. Hence, LFC is required to achieve laminar flow on highly swept wings. Also, the leading-edge radius affects the stability limits of flow along the attachment line, with increased leading-edge radius being destabilizing to the flow.

3.2. Surface Tolerances for Laminar Flow

Roughness, waviness, steps, and gaps are issues related to manufacturing tolerances. Joints, rivets, screw heads, and panel joints contribute to the roughness-steps-gaps issue, and stiffness of the skin with imposed loads and overall manufactured skin smoothness are ingredients in the waviness issue. Since the early days of filling, sanding, and smoothing of test articles, the present day standard production-quality manufacturing techniques have enabled the waviness issue to be surmountable. A thorough review of the manufacturing tolerance issue is described by Carmichael (1979) and Holmes et al. (1985).

In the First Wright Brothers' Lecture (in honor of the famous aeronautical pioneers Wilbur and Orville Wright) held at Columbia University, New York, on December 17, 1937, B. Melvill Jones presented an overview of flight test experiments conducted

(mainly) at Cambridge University in England. Jones (1938) stated that the main conclusions from those flight experiments were

1. Drag predictions for moderately thick wing shapes can be made based on smooth flat-plate skin friction data if the transition points were known for the wing

2. Laminar flow could be maintained up to 30 percent chord (with drag reductions of 30 to 35 percent) for chord Reynolds numbers of 5×10^6 to 10×10^6

3. Small roughness and waviness moved transition points forward (increased drag)

The flight and wind tunnel tests have provided our current understanding of the mechanisms which cause transition to move forward because of surface imperfections. The impact of a surface imperfection (such as a rivet head) on the transition location can be viewed either by looking at the transition location as a function of imperfection size for a fixed unit Reynolds number or by keeping the size of the imperfection fixed and looking at transition location as a function of unit Reynolds number. The illustration in figure 17 (Holmes et al. 1985) depicts the latter case, where the amount of laminar flow is decreased as Reynolds number is increased. The problem is then to determine what roughness height and shape for a given Reynolds number will cause a reduction in the amount of laminar flow obtainable. In either case, the imperfection stimulates eigenmodes in the boundary layer; the linear stability of the flow dictates whether these modes will grow or decay as they evolve in the flow. However, as the height of the imperfection or unit Reynolds number increases, a point is reached when flow separation occurs because of the surface imperfection. At this point, inviscid instability arising from the inflectional velocity profile can grow and induce transition. Or if the imperfection is sufficiently large, linear instability amplification is “bypassed” and transition follows by way of a nonlinear process. Our current understanding of imperfections suggests that larger critical step heights can be realized with rounded steps because a reduced region of separation and reduced inflectional instability growth are encountered in the experiments.

In experiments to examine transition in flight, Stephens and Haslam (1938) used a Hart K1442 aircraft which had a 2D wing test section and a Snark L6103 aircraft which had a mildly swept-wing test section. Among the reported results, spanwise ridges of height 0.002 in. caused transition to move forward at chord Reynolds numbers of 5×10^6 and more; the database did not provide sufficient information for transition prediction (or correlation).

Surface roughness flight experiments described by Bicknell (1939) were conducted on a Northrop A-17A single-engine attack airplane. The focus of the study was to characterize the impact of conventional manufacturer-induced roughness and gaps (rivets, lap joints, access panels, and hinges) on drag. The results for a standard wing were compared with a smooth wing at a chord Reynolds number up to 15×10^6. The wing was made smooth by filling lap joints and cementing pieces of rubber sheeting to build up the areas of rivet protuberance. The results show that a 50-percent increase in the profile-drag coefficient was obtained with the rough wing compared with the smoother wing.

At the Royal Aircraft Establishment (RAE) in England, Young, Serby, and Morris (1939) reported on the impact of camouflage paint, snap rivets, flush rivets, lap joints, and leading-edge slats on wing drag of the prototype Battle. The Battle had wings with low sweep, with each wing containing three bomb doors on the underside of the wings (reason for joint study). The tests were conducted by fitting specially prepared skins over portions of the wings (approximately, NACA 2417 airfoils). The range of chord Reynolds number was 12×10^6 to 18×10^6 with approximate unit Reynolds numbers per foot of 1.2×10^6 to 1.8×10^6. Both the drag due to the variation of transition location (due to protuberance) and drag due to the protuberance itself were measured in the course of the flight test. For the Reynolds number per foot of 1.8×10^6, transition was forced upstream of the protuberance of interest. In brief, the conclusions of this flight test were

1. Camouflage paint did not influence the transition points; however, painting the wings of the Battle-type aircraft reduced its top speed by about 3 to 4 percent

2. Span rivets both increased drag and affected the transition point; for example, completely fastening the wings of the Battle-type aircraft with rivets 0.04 in. high and 0.25 in. wide caused a decrease in the top speed of the aircraft by about 2.5 percent

3. Flush rivet drag was negligible but the transition point was affected with this type of rivet; the implementation of flush rivets should be as far back from the leading edge of the wing as possible

4. Ten unchamfered rearward facing lap joints (1/16 in. high) decreased the top speed of the Battle-type aircraft by 2.5 percent; however, chamfered to a gradient of 1:5 led to only a 1.5-percent speed reduction

5. The addition of a leading-edge slat to half the wing of an aircraft with transition occurring near the leading edge led to a top speed reduction of 1 to 2 percent for a very well-fit slat and of about 2.5 percent for an average-fit slat; if transition was not at the leading-edge region, then the slat-incurred drag would be greater than if it were

6. Formulas for estimating the drag effects due to rivets and lap joints were shown to be in good agreement with experimental results; although the formulas for describing the drag due to rivets and lap joints are very important for turbulent configurations, the capability to predict the impact of the protuberance on the transition location is more significant for NLF and LFC applications

Wetmore, Zalovcik, and Platt (1941) performed a flight investigation to study the boundary-layer characteristics and profile drag of a 2D laminar flow airfoil at high Reynolds numbers. They used a Douglas B-18 aircraft modified with an NACA 35-215, 17-ft chord by 10-ft span test panel positioned on the wing 13 in. outboard of the propeller-pulled engine of the aircraft. The test covered Reynolds numbers from 20×10^6 to 30×10^6 and included variations in power and surface conditions. Engine power variations were made to determine the impact of the engines on profile drag. Although there was no fixed relationship between the lift coefficient and Reynolds number (i.e., quantitative evaluation was not possible), some qualitative comparisons can be made with reference to surface and engine conditions. A two-tube rack was used to measure the transition location. For the design lift coefficient ($C_L = 0.2$) and Reynolds number of 26.7×10^6, transition occurred at 42.4 percent chord (for engine-off conditions). The pressure minimum for this airfoil is at approximately 45 percent chord. For this best laminar flow case, the surface had a waviness amplitude of 0.001 in., which was obtained through polishing the surface. For the same flight conditions and a surface waviness amplitude of 0.005 in., transition occurred at 32.5 percent chord. This early work gave an indication of the influence of waviness on laminar flow extent; however, because no surface wavelengths were presented, the flight data cannot be used for waviness correlations. Finally, it was recognized that differences in flight test results and wind tunnel results were directly impacted by residual turbulence, even in the "quiet tunnels" of that time.

Fage (1943) performed the first systematic wind tunnel experiment to characterize the surface waviness impact on laminar flow (point of transition) for a flat-plate boundary-layer flow. The experiments were carried out using "corrugations"—smooth bulges and hollows and flat ridges—on one side of a smooth flat aluminum plate which had an elliptical leading edge. Although the tunnel could produce sufficiently clean flows up to a tunnel speed of 140 fps, the experiments were carried out so that the corrugations impact transition well below 140 fps and are not affected by free-stream turbulence in the wind tunnel. Positioned 20 in. downstream of the leading edge, a strip of spring steel was used to form bulges and hollows and a piano wire was used for ridges. Small surface tubes (mounted on the plate) were used to indicate when a corrugation caused transition to move forward as the tunnel speed was varied.

For this zero pressure gradient case, Fage (1943) found empirical expressions which gave an estimate for the minimum height of spanwise bulges, hollows, and ridges that affects the position of transition in the experiments. The experiments showed that the minimum height is not especially dependent on the form of the corrugation, and it appeared that the flow conditions that impact the transition location were related to the local separation of the laminar boundary layer.

However, as Fage noted, it was not expected that these simple relations take into consideration all flow conditions. In particular, only flow separation was considered and the stability of the flow downstream of the corrugation should be accounted for as well. Fage's work did not include the effects of compressibility or sweep.

At the same time, Braslow (1944) was studying the impact of roughness on transition in a less systematic manner than Fage (1943). The effect of various camouflage paints and the painting procedures on the drag characteristics on an NACA 65-420 airfoil section were examined. Using the Langley Low-Turbulence Pressure Tunnel (LTPT), Braslow (1944) showed that a carefully applied camouflage painted surface could retain the low-drag characteristics of the airfoil up to chord Reynolds numbers of 22×10^6. This maximum Reynolds number could not be overcome unless some light sanding was applied to the painted finish. This experiment demonstrated the impact roughness could have on drag (or transition) with unit Reynolds number variation.

Smith and Higton (1945) reported the results of King Cobra flight tests to determine the (surface) criteria for laminar flow and the practicality of meeting the necessary requirements. The impact of rain, dust, insects, and surface-finish polish on the flow was assessed. Dust and water accumulation did not increase the measured drag, whereas as the temperatures increased in April 1945, it became impossible to fly without insect contamination affecting drag measured in flight. Also, the results showed that reducing the waviness to ±0.001 in. led to runs of laminar flow to 60 to 65 percent chord. Gray and Fullam (1950) reported wind tunnel tests for the King Cobra wing model in the RAE No. 2 11.5- by 8-foot tunnel. Consistent with the flight experiments, low drag was realized for Reynolds numbers of 15×10^6; however, the existence of turbulence in the wind tunnel, which is not present in free flight, caused some degradation of the range of C_L and a ragged transition front.

Plascott (1946) and Plascott et al. (1946) conducted a flight test with a Hurricane II aircraft to measure improvements in laminar flow extent by reducing surface waviness. The manufactured wing was found to have waviness which prevented significant regions of laminar flow. The manufacturer reduced the waviness by the use of appropriate filler and careful rubbing down the surface. Surface waviness was measured to be less than 0.001 in. The results showed a 26-percent decrease in the drag coefficient compared with previous flight test results. Laminar flow was realized to between 50 and 60 percent chord of the test section (the pressure minimum was designed for about 50 percent chord). The conclusions from this flight test were in agreement with the previous King Cobra test; namely, reducing the surface waviness to 0.001 in. led to significant runs of laminar flow for flight Reynolds numbers in the range of 20×10^6.

The earlier wind tunnel and flight experiments served to illustrate the impact of surface smoothness (roughness and waviness) by demonstration. The following subsections present the current understanding of surface smoothness, building upon these earlier tests.

3.2.1. Waviness

Carmichael, Whites, and Pfenninger (1957), Carmichael (1959), and Carmichael and Pfenninger (1959) developed the basis for "allowable waviness criteria" for swept and unswept wing surfaces, influenced by compressibility, suction, single bulges, multiple waves, and wing sweep. The criteria are still valid today and were based on the available flight test observations. Flight test experiments were carried out by using the F-94A airplane with 69 suction slots as described by Groth et al. (1957). Sinusoidal waves were obtained over the width of the test section by applying paint with the wavelength specified by masking tape. Wave height and length were varied in a region of growth (28 percent chord) prior to the suction influencing the disturbance evolution. The results showed that the extent of laminar flow was more sensitive to the chordwise pressure distribution than variations in Reynolds number for the critical wave; an increase in a favorable chordwise pressure gradient was required to maintain laminar flow in the presence of a surface wave. The relationship found between the critical wave height and wavelength was h^2/λ = Constant. Sinusoidal waves at 15 percent chord were also studied. Only small increases in allowable waviness were realized in this strong favorable pressure gradient region, probably because the boundary layer was thinner compared with the 28-percent chord case.

The flight test results showed that waves above a surface caused sinusoidal pressure disturbances which affect the TS-disturbance growth. The relationship between the surface wavelength and critical TS wavelength could lead to a detrimental resonance condition or not impact transition if nonresonant. From the research results of Fage (1943) and Carmichael et al. (1959), the mechanisms for causing transition to move forward due to surface imperfections were realized. First, a local separation region due to the surface imperfection could cause Rayleigh's inflectional instability. Second, the local adverse pressure gradient could cause amplification of TS disturbances. The impact of compressibility is both favorable and unfavorable in a countercompeting manner. Although compressibility is stabilizing to TS disturbances, compressibility increases the amplitude of the pressure disturbance of the surface imperfection; however, which effect dominates is not clear.

Wing sweep was observed by Carmichael and Pfenninger (1959) to lead to a reduction in the allowable waviness, probably because of the impact of both TS disturbance growth and CF disturbance growth. Shown by Carmichael (1979), Braslow and Fischer (1985), and Braslow et al. (1990), the critical size for waviness parallel to the wing span and involving a single wave was

$$\frac{a}{\lambda} = \left(\frac{59\,000 c \cos^2 \Lambda}{\lambda \mathrm{Re}_c^{3/2}} \right)^{1/2} \tag{1}$$

For multiple waves parallel to the wing span, the critical waviness becomes one third of the single-wave criteria, and chordwise wave criteria are found by doubling the spanwise criteria (Braslow et al. 1990). An example of the waviness criteria for a LFC airplane with a given wing sweep, Mach number, and altitude is shown in figure 18 (from Braslow and Fischer 1985).

3.2.2. Two-Dimensional Surface Discontinuities

Criterion for two-dimensional surface discontinuities can be found in Braslow and Fischer (1985) and Braslow et al. (1990). The allowable step height h for forward-facing steps is

$$(\mathrm{Re/ft})\mathrm{h} = 1800 \tag{2}$$

The allowable height for aft-facing steps is one half the allowable for forward-facing steps. The allowable gaps for flow over the gap is

$$(\mathrm{Re/ft})\mathrm{g} = 15\,000 \tag{3}$$

and the allowable gap width for flow along the gap is one seventh the gap width for flow across the gap.

3.2.3. Three-Dimensional Surface Discontinuities

The flow tolerance to roughness was also investigated in the flight test. Single and multiple spherical-shaped glass beads and steel disks were used as roughness on the test section. At 22 percent chord, critical roughness heights of 0.0105, 0.007, and 0.0055 in. were obtained for a single sphere, a single disk (Height/Diameter = 0.167), and a multibead band of distributed roughness, respectively, for a Mach number of 0.68 and altitude of 26 000 ft. At 2.5 percent chord, where the boundary layer was much thinner, the critical heights decreased to 0.007 in. for a single sphere and to 0.004 in. for the single disk for the same Mach number and altitude. Carmichael, Whites, and Pfenninger (1957) explored the definition of the critical roughness condition

$$\mathrm{Re}_K = \frac{U_l k}{\nu} \tag{4a}$$

$$\mathrm{Re}_k = \frac{U_k k}{\nu_k} \tag{4b}$$

where k is the height of the roughness, U_k is the local velocity at the top of the roughness particle, ν_k is the local kinematic viscosity, and U_l is the local potential velocity. Equation (4a) should be used to determine critical roughness heights near the leading edge of the wing, and equation (4b) should be used in other than the leading-edge region. Essentially, the flight test results showed that these parameters were a linear function of the roughness height.

Braslow and Knox (1958) proposed a method for determining the critical height of three-dimensional roughness particles which would cause premature laminar-to-turbulent boundary-layer transition. An equation was derived which related the critical roughness height to local flow conditions (i.e., the local

temperature and velocity conditions in the boundary layer). The results were presented for zero-pressure gradient flow for Mach numbers from 0 to 5. A roughness Reynolds number Re_k of between 250 and 600 for Mach numbers up to 2 apparently caused premature transition. Then, based on the assumed Re_k which caused transition for known values of Mach number, unit Reynolds number, and roughness location, the critical roughness height could be determined.

Braslow and Maddalon (1993, 1994) discussed roughness-related results of the Jetstar LFC flight test. A ratio of roughness diameter to height between 0.5 and 5.0 is permissible in the high crossflow region of swept-wing flow.

An example of the critical roughness height with altitude for a fixed Mach number is shown in figure 19 (Braslow and Fischer 1985). As the altitude increases, the unit Reynolds number decreases and the allowable critical roughness heights can therefore increase.

The current understanding of the mechanisms which cause transition to move forward due to surface imperfections includes

1. A local separation region due to the surface imperfection could cause Rayleigh's inflectional instability, which could cause transition to move forward

2. The local adverse pressure gradient induced by the surface imperfection could cause the amplification of TS disturbances, which would cause premature transition

3. Depending on the relationship between surface wavelength and the disturbance (TS or CF), transition can move forward or be postponed in the CF-disturbance regions (due to wave superposition and relative wave phase)

4. The critical wave height decreases with increased number of waves

5. Forward-facing rounded steps near the leading edge had nearly a 50-percent increase in the critical step height compared with forward-facing square steps

These wind tunnel and flight experiments demonstrated the sensitivity of the flow to the surface definition. They also showed that with some careful surface preparation, laminar flow could be obtainable. The stringent surface smoothness and waviness criteria (tolerances) for laminar flow posed a major challenge for research in the 1950s and 1960s. A partial explanation for the descope of subsonic LFC in the 1950s was attributable to the severe surface manufacturing tolerances required to achieve laminar flow. However the manufacturing technologies of the 1990s have matured to the point that surface definition tolerances are more readily achievable.

3.3. Critical Suction Parameters for LFC

As part of the Saric (1985) review of LFC control with suction for AGARD, the issue of transition caused by local streamwise vorticity generated in the boundary-layer flow over a suction hole was briefly covered. Essentially, the threshold parameters are not known when these vortices appear nor what strength and impact they have on the flow instabilities. These parameters involve hole size, suction flow rate, hole spacing and geometry, and hole inclination.

The earliest fundamental understanding of the critical suction issue was reported by Goldsmith (1955, 1957), where experiments were conducted in the Northrop 2-in-diameter laminar flow tube to determine universal critical suction curves that would be used to design suction through isolated holes or a row of holes. Nondimensional parameters were determined from results over a large range of boundary-layer Reynolds numbers, tube velocities, and hole configurations. Tube velocities were determined from pressure-tap records, and the state of the boundary layer was determined to be either laminar or turbulent with a stethoscope. The critical suction was affected by the hole diameter, the hole spacing, and the boundary-layer thickness. The suction was adjusted from a flow condition which was turbulent until the flow became laminar. This suction level which led to laminar flow was called the critical maximum value. When a sufficiently low suction level is reached that any further decrease in the suction would lead to a turbulent flow, the minimum suction values were obtained. The critical maximum suction arose because with suction higher than this value, the three-dimensionality of the flow into the hole would cause

premature transition. Goldsmith (1955) noted that the critical suction quantities were dependent more on the gap between adjacent holes than on the diameter or centerline spacing. Also, the critical suction was reduced for holes aligned at an angle (swept) to the stream tube compared with holes perpendicular to the stream-tube axis. Significant to Goldsmith (1957) was the discussion of the impact of parameter variations on multiple rows of holes. Namely, the action of vortices from holes in different rows can lead to horseshoe vortices, which then lead to turbulence. This undesirable flow phenomenon can happen with lower suction compared with the isolated hole or row of holes. Goldsmith noted that the associated flow pattern with multiple rows of holes was complicated and may be sensitive to the suction distribution and pressure gradients.

Rogers (1957) reported results of experiments intended to extend the database of knowledge from low Reynolds number pressure drop through holes and slots to the intermediate regime. As the Reynolds number increased, presumably a vortex formed at the inlet edge of the hole or slot causing a flow-separation region. Reattachment could be rather abrupt downstream of the hole or slot. No theory was available to predict the behavior of the flow in this intermediate region. Pressure recovery coefficients versus slot width were presented. Because this report was essentially a contractor progress report, no conclusions were drawn; however, the author did make the interesting point that there was some uncharted regime between laminar suction attached flow at low Reynolds number and free-jet flow at high Reynolds number. For sharp-edge holes and slots, the experimental results agreed with theory for the pressure drop coefficient at low Reynolds number flow. As the Reynolds number increased, the experimental pressure drop coefficient broke away from the theory and at high Reynolds numbers approached the asymptotic nonviscous free-jet flow theory. However, for the holes and slots with rounded edges, no development of unstable vortices or separation was observed in the experiments. The results suggested that (if practical from manufacturing operations) rounded edges for suction LFC are preferred to conventional sharp edges.

Gregory (1961) reviewed the status of suction surfaces for LFC application, including the surfaces used among previous investigators, and summarized the results. Noting the decline in the feasibility of suction slots for swept-wing configurations, Gregory pointed out that as the wing was swept, the effective distance between slots increased. Hence, a loss of the slot effectiveness for control occurred especially near the leading edge. Hence, the advantages of a wholly perforated suction surface become pronounced with no "obvious" flow-directional dependence for such a LFC surface. Gregory listed the 1961 known materials for LFC to be sintered metals, fiberglass compacts, perforated sheets, wire cloth, electro-deposited mesh, slits, and organic fibers. The criticality of issues such as roughness and porosity varied depending on the material used.

Meitz and Fasel (1994) used an unsteady Navier-Stokes solver (direct numerical simulation, DNS) to study the flow field adjacent and downstream of suction holes. The Goldsmith (1957) parameter space was studied where low suction-induced vortices decayed with downstream distance and high suction-induced vortices coalesced with vortices from adjacent holes to cause premature transition to turbulence. In agreement with the Goldsmith experiments, the simulations of Meitz and Fasel showed that low suction through the holes generated a pair of vortices which decayed with downstream distance. As the suction increased to some critical value, the vortices became unstable. Larger suction led to vortex shedding at the suction hole location.

Supported by the European Communities Industrial and Materials Technology Program under the Laminar Flow Investigation (ELFIN) II Project, MacManus and Eaton (1996) performed three-dimensional Navier-Stokes simulations of the suction through holes to study the local flow physics involving single and multiple rows of holes. Variations in hole diameter, bore shape, inlet shape, and inclination of the hole to the surface on the resulting flow were evaluated with the simulations. See figure 20 for an illustration of the holes studied by MacManus and Eaton (1996). Although a detailed survey of the impact of the geometrical variations on the flow is very important for the design of LFC systems, only selected results were presented by MacManus and Eaton, most likely because of page limitations. From those select cases, the conclusions were (1) irregularities of the

hole shape had minimal effect on the induced flow, (2) it was undesirable to have holes inclined to the surface, (3) the flow field at the hole inlet was highly three-dimensional, (4) the sucked stream tube was approximately the shape of a circle segment, (5) the pressure drop and mass flow rate were insensitive to the hole inlet geometry, and (6) interhole flow field effects existed for staggered multiple rows of holes. (Incidentally, the adjacent rows of holes were staggered.) MacManus et al. (1996) performed complementing experiments to study the flow in the vicinity of a LFC suction hole. The LDV measurements confirmed that the flow field near the hole was highly three-dimensional.

Anselmet, Mérlgaud, and Fulachier (1992) used an IMST water tunnel in France and laser Doppler velocimeter and other flow visualization to determine the flow structure of suction through and near a single orifice to determine the optimal dimension of the hole and flow rate. The experiments showed that if suction was too large, premature transition would occur. The study focused only on single-hole flows and concluded by noting the importance of multiple-hole alignment studies toward the LFC problem.

To evaluate the potential use of perforated suction strips of LFC, Cornelius (1987) used a low-turbulence wind tunnel at Lockheed-Georgia Company and compared the strip results with slot suction. A flat plate was used with a slot thickness of 16 percent of the local displacement thickness and a perforated strip with a width of 15 percent of the displacement thickness as the test article. The slot thickness of 0.25 mm was cut with a saw, and the perforated strip had 45 rows of 0.25-mm-diameter electron-beam-drilled holes. The results showed a distinct difference between the slot and perforated strip with very large magnitude shear near the downstream end of the slot. With a portion of the perforated strip (80 percent of the width was covered with tape), suppression of the disturbance amplification was equivalent to using the suction slot. Compared with the results using the wider perforated strip, it is demonstrated that suction through the slots or narrow perforated strips have a greater beneficial effect on the boundary-layer stability. These results suggested that analysis which used continuous suction (wide strips) would be a conservative approximation to suction slots or thin perforated strips.

3.4. Manufacturing Issues

In the early years of airplanes, thin metal skins, multiple spanwise stringers, and countless fasteners (e.g., rivets) on the surface prevented achieving laminar flow. On research aircraft, fillers were used even into the 1980s to smooth problem areas of the surface. With the advent of bonded sandwich construction methods, the production surface became as good as the production mold definition. The surface structure became sufficiently stiff so that adequate waviness criteria could be maintained under loads (in subsonic and transonic aircraft) and the new production capability in the 1990s has solved (in principle) the task of manufacturing laminar flow quality surfaces.

3.4.1. Joints

Potential issues still remain associated with structural joints. The issue of critical waviness caused by these intersections must be part of the design process. The intersection of these major structures may have fasteners which protrude above the surface and cause flow interruption by way of steps and gaps. To avoid this problem, a recessed intersection region could be employed, which would remove the fastener issue and could require a flush-fill technique to cover the recessed connection area. Similar to the structural joints issue, access doors are a normal feature on aircraft and require special attention for laminar flow to be achievable. Flush mounting to within a few thousands of an inch is required; sealing the access panel is also required to prevent air bleed from the panel.

3.4.2. Holes

Comparable with early analysis on the Jetstar (Powell 1987), Boeing 757, and F-16XL (Norris 1994) LFC flight test articles, Parikh et al. (1990) studied the suction system requirements (based on computational analysis) for SLFC on a High-Speed Civil Transport (HSCT). In the analysis, the perforated skin had hole diameters on the order of 0.002 in. (0.05 mm), hole spacing of 0.01 in. (0.025 mm), and a skin thickness of 0.04 in. (0.1 mm). With this information, it is clear that millions to billions of holes are required for a large-scale wing. For example, the hole spacing suggests that 10 000 holes are contained in a square inch or 1.4 million holes are found in a square foot. For a large application such as the proposed HSCT,

420 million holes would be required on the wing if HLFC were applied to the leading-edge region (assuming a region of 100 ft of span by 3 ft of chord). If the entire wing was used for LFC, then approximately 12 billion holes would be required and obviously will become a significant manufacturing task. This large number of holes is an overly conservative estimate because the hole size and spacing are a function of the suction level and the placement (e.g., on the attachment line versus on the wing rooftop region).

In Germany, Schwab (1992) discussed the electron-beam drilling process for creating holes in a surface for suction LFC. Note that the Jetstar flight test (Powell 1987) made use of this hole-drilling technique. With this method, some 3000 holes could be generated per second with hole diameters as small as 0.04 mm in 0.5-mm-thick sheets of stainless steel to 0.06 mm in 1.0-mm-thick sheets. As the material thickness increased, the minimum hole diameter increased. To control the geometrical definition of the hole, a pulse procedure was required. Essentially, a high-power electron beam impinged on the surface to melt and vaporize the material at impact. Cross sections of the drilled holes indicated that the uppermost part of the drilled holes was 2 to 2.5 times larger in diameter than the exit diameter, with the exit of the hole being absolutely burr-fee and round. (See fig. 20(b) for an illustration.) This drilling technique suggested that holes drilled for LFC should be drilled from the interior to exterior so that the interior hole diameter is bigger than the exterior. Therefore, for example, if a piece of dust (or insect) enters a hole due to suction, the article will be able to freely exit the hole into the suction chamber and not get lodged in the hole. In addition to the electron-beam drilling process, laser drilling has been successfully used for LFC applications. Both the Boeing 757 HLFC (Collier 1993) and the F-16XL SLFC (Norris 1994) flight tests had skins which had their holes drilled with a laser. The laser would produce holes with characteristics similar to the electron beam.

Supported by the ELFIN Program, Poll, Danks, and Humphreys (1992) looked at the aerodynamic performance of laser-drilled suction holes relative to the pressure drop across a given surface for a given mass flow rate and hole diameter. They observed that laser drilling produced a random variety of hole shapes with no particular characteristic diameter (without a statistical determination of the hole diameter). The flow through the hole was characterized by incompressible laminar pipelike flow. The flow rates of interest led to the pressure drop being a quadratic function of the mass flow rate.

Buxbaum and Höhne (1996) outlined the testing of two perforated titanium sections to be used in a LFC wind tunnel experiment at Arizona State University. The first panel was a uniform aligned panel, and the second panel has a sine pattern to the hole alignment. Observation of the sections indicates that the laser-drilled holes range in spacing (0.35 to 0.95 mm) and shape. The holes were noted to be seldom circular as designed. LDV and hot wires were used to measure the flow resulting from suction through the holes. Although measurements of each individual hole were unobtainable, an innovative approach using a small funnel placed perpendicular to the surface was used to make measurements to about 1.5 mm. The drilling direction during the manufacturing process was presumed to have a large impact on the quality of the resulting holes. The measurements revealed that the deviation from the desired uniform velocity was 2 percent (0.05 m/sec) for the uniform panel and 14 percent (0.18 m/sec) for the sinusoidal panel.

3.5. Transition Prediction Design Tool Methodology

The improvements in aerodynamic efficiency directly scale with the amount of laminar flow achieved. Hence, the designer must be able to accurately predict the location of boundary-layer transition on complex, three-dimensional geometries as a function of suction distribution and suction level (or the accurate prediction of the suction distribution for a given target transition location). Pressure gradient, surface curvature and deformation, wall temperature, wall mass transfer, and unit Reynolds number are known to influence the stability of the boundary layer and transition location. For practical HLFC designs, it is imperative to be able to accurately predict the required amount, location, and distribution of wall suction (or thermal control or any other control technique) to attain a given (“designed for”) transition location.

This section describes the conventional and advanced transition prediction tools, some of which include prediction of perturbations to the laminar boundary layer, the spectrum and amplitudes of these perturbations, and the linear and nonlinear propagation of these perturbations, which ultimately leads to transition. For literature focusing on the theoretical and computational aspect of transition prediction and LFC, refer to Cousteix (1992) and Arnal (1984, 1994).

3.5.1. Granville Criterion

Granville (1953) reported on a procedure for calculating viscous drag on bodies of revolution and developed an empirical criterion for locating the transition location associated with low-turbulence flows. Low (or zero) turbulence characteristic of flight or low-turbulence wind tunnels and high turbulence characteristic of most wind tunnels are the two problems considered relative to a transition criterion. The low-turbulence case assumed that transition was TS disturbance dominated and began with infinitesimally small-amplitude disturbances. Walz (in Oudart 1949) suggested that rough empirical criteria for transition would indicate transition occurred at three times the neutral stability Reynolds number. With data from Dryden (1936), Hall and Hislop (1938), Schubauer (1939), and Schubauer and Skramstad (1948), Granville (1953) showed that a variety of flight and low-turbulence wind tunnel data collapsed into a criterion (curve) based on $\mathrm{Re}_{\theta,T} - \mathrm{Re}_{\theta,N}$, which is the difference between the momentum thickness Reynolds number at transition and at the neutral point, versus $\overline{\frac{\theta^2}{\nu}\frac{d\tilde{u}}{d\tilde{x}}}$, which is the average pressure gradient parameter. This correlation was demonstrated for two-dimensional flows and is shown in figure 21 with data from Braslow and Visconti (1948). Granville used a transformation to convert this information to a body-of-rotation problem. The data were also correlated with turbulence level in the free stream as shown in figure 22. Extrapolation of the criteria would work for a two-dimensional airfoil dominated by TS transition (Holmes et al. 1983), whereby the existing database included this form of transition. However, when the design configuration begins to significantly differ from the existing database, this transition prediction criteria would likely fail.

3.5.2. C1 and C2 Criteria

At ONERA, Arnal, Juillen, and Casalis (1991) performed *N*-factor correlations with wind tunnel experimental results of a LFC suction infinite swept wing. The motivation for the study was to gain fundamental understanding of the transition process with suction and to test the methodologies developed at ONERA-CERT for three-dimensional flows. The streamwise instability criteria were based on an extension of Granville (1953). Two crossflow transition criteria have been developed by Arnal, Habiballah, and Coustols (1984) at ONERA and are referred to as C1 and C2. The C1 criterion involves a correlation of transition onset integral values of the crossflow Reynolds number and the streamwise shape factor. The C2 criterion is a correlation of transition onset with a Reynolds number computed in the direction of the most unstable wave, the streamwise shape factor, and the free-stream turbulence level. The results demonstrate that the transition criteria cannot be applied in regions where the pressure gradient is mild because there is a large range of unstable directions. In that region, one cannot look only at pure streamwise or crossflow instabilities. The C1 criterion gives bad results with wall suction present; however, the C2 criterion correctly accounts for wall suction.

3.5.3. Linear Stability Theory

The equations governing the linear stability of disturbances in boundary layers were first described by Orr (1907), Sommerfeld (1908), and Squire (1933). These equations are ordinary differential equations and are referred to as the “Orr-Sommerfeld and Squire equations.” Although the growth or decay of small-amplitude disturbances in a viscous boundary layer could be predicted by the Orr-Sommerfeld and Squire equations (within the quasi-parallel approximation), the ability to predict transition came in the 1950s with the semi-empirical method by Smith (1953). This transition-prediction method—called e^N or *N*-factor method—correlates the predicted disturbance growth with measured transition locations. Although limited to empirical correlations of available experimental data, it is the main tool in use through the 1990s.

Linear stability theory represents the current state of the art for transition location prediction for three-dimensional subsonic, transonic, and supersonic

flows. To begin a transition prediction analysis, the steady, laminar mean flow must first be obtained (either by Navier-Stokes solutions or by boundary-layer equations). Then the three-dimensional boundary-layer stability equations (Orr-Sommerfeld and Squire ordinary differential equations) are solved for the amplification rate at each point along the surface, based on the assumption of small-amplitude disturbances.

Significant advances have been made in the understanding of the fundamentals of two- and three-dimensional, unsteady, viscous boundary-layer flow physics associated with transition (see reviews by Reshotko (1976); Herbert (1988); Bayly, Orszag, and Herbert (1988); Reed and Saric (1989); and Kachanov (1994)) and CFD mean-flow capabilities in complex geometries, turbulence modeling efforts, and in the direct numerical simulation of the unsteady flow physics (Kleiser and Zang 1991). However, a transition-prediction methodology devised in the 1950s is considered state of the art and is being used by industry for LFC-related design through the 1990s. This transition-prediction methodology termed the e^N method is semi-empirical and relies on experimental data to determine the *N*-factor value at transition.

To derive the stability equations, take the velocities $\tilde{u},\tilde{v},\tilde{w}$ and the pressure $\tilde{p}$ as solutions of the incompressible, unsteady Navier-Stokes equations. The instantaneous velocities and the pressure may be decomposed into base and disturbance components as

$$\left.\begin{aligned} \{\tilde{u},\tilde{v},\tilde{w}\}(x,y,z,t) &= \{\bar{u},\bar{v},\bar{w}\}(x,y,z) \\ &\quad + \{u,v,w\}(x,y,z,t) \\ \tilde{p}(x,y,z,t) &= \bar{p}(x,y,z) + p(x,y,z,t) \end{aligned}\right\} \quad (5)$$

where the base flow is given by the velocities $\bar{u},\bar{v},\bar{w}$ and the pressure $\bar{p}$, and the disturbance component is given by the velocities u,v,w and the pressure p. In the Cartesian coordinate system (x,y,z), x is aligned with the chordwise direction, y is normal to the wall, and z corresponds to the spanwise direction. To illustrate the stability tools, the Cartesian coordinate system and incompressible equations are used herein. In general, curvilinear or generalized coordinates are used to solve the govern system of compressible equations to predict the location of transition from laminar to turbulent flow.

The disturbance evolution and transition prediction tools require an accurate representation of the mean flow (velocity profiles). Either the velocity profiles can be extracted from Navier-Stokes solutions or are derived from solutions of a coupled Euler and boundary-layer equation solver. Harris, Iyer, and Radwan (1987) and Iyer (1990, 1993, 1995) presented approaches for the Euler and boundary-layer equation solver. Harris, Iyer, and Radwan (1987) demonstrate the accuracy of a fourth-order finite-difference method for a Cessna aircraft fuselage forebody flow, flat-plate boundary-layer flow, flow around a cylinder on a flat plate, a prolate spheroid, and flow on an NACA 0012 swept wing. In terms of computational efficiency, the Euler and boundary-layer approach for obtaining accurate mean flows will be the solution of choice for most of the preliminary design stages; however, Navier-Stokes solvers can be used for LFC design. A limiting factor for the Navier-Stokes mean flows is the demanding convergence required for the suitability of the results in the boundary-layer stability codes.

To obtain the stability equations, begin with the full incompressible Navier-Stokes equations that are

$$\frac{\partial\tilde{u}}{\partial x} + \frac{\partial\tilde{v}}{\partial y} + \frac{\partial\tilde{w}}{\partial z} = 0 \quad (6)$$

$$\frac{\partial\tilde{u}}{\partial t} + \tilde{u}\frac{\partial\tilde{u}}{\partial x} + \tilde{v}\frac{\partial\tilde{u}}{\partial y} + \tilde{w}\frac{\partial\tilde{u}}{\partial z} = -\frac{\partial\tilde{p}}{\partial x} + \frac{1}{\mathrm{Re}}\left(\frac{\partial^2\tilde{u}}{\partial x^2} + \frac{\partial^2\tilde{u}}{\partial y^2} + \frac{\partial^2\tilde{u}}{\partial z^2}\right) \quad (7)$$

$$\frac{\partial\tilde{v}}{\partial t} + \tilde{u}\frac{\partial\tilde{v}}{\partial x} + \tilde{v}\frac{\partial\tilde{v}}{\partial y} + \tilde{w}\frac{\partial\tilde{v}}{\partial z} = -\frac{\partial\tilde{p}}{\partial y} + \frac{1}{\mathrm{Re}}\left(\frac{\partial^2\tilde{v}}{\partial x^2} + \frac{\partial^2\tilde{v}}{\partial y^2} + \frac{\partial^2\tilde{v}}{\partial z^2}\right) \quad (8)$$

$$\frac{\partial\tilde{w}}{\partial t} + \tilde{u}\frac{\partial\tilde{w}}{\partial x} + \tilde{v}\frac{\partial\tilde{w}}{\partial y} + \tilde{w}\frac{\partial\tilde{w}}{\partial z} = -\frac{\partial\tilde{p}}{\partial z} + \frac{1}{\mathrm{Re}}\left(\frac{\partial^2\tilde{w}}{\partial x^2} + \frac{\partial^2\tilde{w}}{\partial y^2} + \frac{\partial^2\tilde{w}}{\partial z^2}\right) \quad (9)$$

A Reynolds number can be defined as $\mathrm{Re} = U\delta/\nu$, where U is the velocity, δ is the characteristic length, and ν is the kinematic viscosity.

For hydrodynamic linear stability theory, which makes use of the quasi-parallel flow assumption, $\bar{u}(y)$ and $\bar{w}(y)$ are functions of distance from the wall only and $v = 0$. Substituting equations (5) into the Navier-Stokes equations, the following linear system results:

$$\frac{\partial u}{\partial x} + \frac{\partial v}{\partial y} + \frac{\partial w}{\partial z} = 0 \tag{10}$$

$$\frac{\partial u}{\partial t} + \bar{u}\frac{\partial u}{\partial x} + v\frac{d\bar{u}}{dy} + \bar{w}\frac{\partial u}{\partial z} = -\frac{\partial p}{\partial x} + \frac{1}{\mathrm{Re}}\left(\frac{\partial^2 u}{\partial x^2} + \frac{\partial^2 u}{\partial y^2} + \frac{\partial^2 u}{\partial z^2}\right) \tag{11}$$

$$\frac{\partial v}{\partial t} + \bar{u}\frac{\partial v}{\partial x} + \bar{w}\frac{\partial v}{\partial z} = -\frac{\partial p}{\partial y} + \frac{1}{\mathrm{Re}}\left(\frac{\partial^2 v}{\partial x^2} + \frac{\partial^2 v}{\partial y^2} + \frac{\partial^2 v}{\partial z^2}\right) \tag{12}$$

$$\frac{\partial w}{\partial t} + \bar{u}\frac{\partial w}{\partial x} + v\frac{dw}{dy} + \bar{w}\frac{\partial w}{\partial z} = -\frac{\partial p}{\partial z} + \frac{1}{\mathrm{Re}}\left(\frac{\partial^2 w}{\partial x^2} + \frac{\partial^2 w}{\partial y^2} + \frac{\partial^2 w}{\partial z^2}\right) \tag{13}$$

According to the conventional normal mode assumption used to derive the Orr-Sommerfeld and Squire equation, the eigensolutions take the form

$$\{u,v,w,p\} = \{\hat{u},\hat{v},\hat{w},\hat{p}\}(y)\,\exp[i(\alpha x + \beta z - \omega t)] \tag{14}$$

where $i = \sqrt{-1}$, α and β are the nondimensional wave numbers (proportional to wavelengths) in the streamwise and spanwise directions, ω is the frequency, and $\{\hat{u},\hat{v},\hat{w},\hat{p}\}$ describe the velocity profile. Substituting equation (14) into the linear equations (eqs. (10) to (13)), the following Orr-Sommerfeld and Squire equations may be obtained:

$$\left(\frac{d^2}{dy^2} - \alpha^2 - \beta^2\right)^2 \hat{v} - i\mathrm{Re}\left[-\alpha\frac{d^2\bar{u}}{dy^2} - \beta\frac{d^2\bar{w}}{dy^2} + (\alpha\bar{u} + \beta\bar{w} - \omega)\left(\frac{d^2}{dy^2} - \alpha^2 - \beta^2\right)\right]\hat{v} = 0 \tag{15}$$

$$\frac{d^2\hat{\Omega}}{dy^2} - [\alpha^2 + \beta^2 - i\mathrm{Re}(\alpha\bar{u} + \beta\bar{w} - \omega)]\frac{d\hat{\Omega}}{dy} = i\mathrm{Re}\left(\alpha\frac{d\bar{u}}{dy} + \beta\frac{d\bar{w}}{dy}\right)\hat{v} \tag{16}$$

where $\hat{\Omega}$ is the wall normal vorticity and d^n/dy^n is the nth derivative in the wall normal direction. The standard wall boundary conditions are

$$\hat{v},\ \frac{d\hat{v}}{dy},\ \hat{\Omega} = 0 \qquad (y = 0) \tag{17}$$

and the free-stream boundary conditions are

$$\hat{v},\ \frac{d\hat{v}}{dy},\ \hat{\Omega} \to 0 \qquad (y \to \infty) \tag{18}$$

Either spatial or temporal stability analysis may be performed, whereby the temporal analysis is less expensive and the spatial analysis is more physical. In addition to the Reynolds number, Mach number, and other parameters that must be prescribed, a stability analysis requires that the mean flow and its first and second wall-normal derivatives be known very accurately. A small deviation in the mean flow could cause significant changes in the second derivative and contaminate the stability calculation. Once the mean flow is obtained, a stability problem has to determine six unknowns: $\{\alpha_r,\alpha_i,\beta_r,\beta_i,\omega_r,\omega_i\}$, which are the streamwise wave number, streamwise (spatial) growth rate, spanwise wave number and growth rate, wave frequency, and temporal growth rate. For the temporal formulation, α and β are real numbers and ω is a complex number that is determined through an eigenvalue solver. For the spatial approach, α and β are complex, and ω is the wave frequency.

Because the spatial formulation is more representative of the real boundary-layer instability physics and the temporal-to-spatial conversion is only valid on

the neutral curve, the remaining transition prediction methodologies are described via the spatial approach. However, the temporal approach was introduced first by Srokowski and Orszag (1977) in the SALLY code and later by Malik (1982) in the COSAL code. The COSAL code included the effect of compressibility in the equations. For the spatial approach in three-dimensional flows, the frequency ω_r is fixed, $\omega_i = 0$, and $\{\alpha_r,\alpha_i,\beta_r,\beta_i\}$ are parameters to be determined. Although an eigenvalue analysis will provide two of these values, the main issue with the application of the e^N methodology to three-dimensional flows is the specification (or determination) of the remaining two parameters. Figure 23 illustrates the instability concept within linear stability theory. A certain parameter range exists whereby a certain combination of wave numbers and frequencies characterize disturbances which decay at low Reynolds numbers, amplify over a range of Reynolds numbers, and then decay with the remaining Reynolds numbers. The Reynolds numbers nondimensionally represent the spatial chordwise location on a wing (for example). The boundary between regions of amplification (unstable) and decay (stable) is termed the neutral curve (location where disturbances neither amplify nor decay).

If a method is assumed available to determine the two remaining free parameters, the *N*-factor correlation with experiments could be carried out. By integrating from the neutral point with arbitrary disturbance amplitude A_0, the amplification of the disturbance is tracked until the maximum amplitude A_1 is reached at which a decay ensues. Being a linear method, the amplitudes A_0 and A_1 are never really used; rather, the *N*-factor relation of interest is defined as

$$N = \ln \frac{A_1}{A_0} = \int_{s_0}^{s_1} \gamma \, ds \tag{19}$$

where s_0 is the point at which the disturbance first begins to grow, s_1 is the point at which transition is correlated, and γ is the characteristic growth rate of the disturbance. Figure 24 illustrates the amplification and decay of four disturbances (wave-number–frequency combinations) leading to four *N*-values. The envelope of all individual *N*-values leads to the *N*-factor curve. By correlating this *N*-factor with many transition cases, the amplification factor for which transition is likely or expected for similar flow situations can be inferred. The resulting *N*-factor is correlated with the location of transition for a variety of experimental data (sketched in fig. 24). This information is then used in determining the laminar flow extent (crucial to LFC design). Hence, this methodology is critically dependent on the value of the experimental databases and the translation of the *N*-factor value to a new design.

The saddle point, fixed wave angle, and fixed spanwise wavelength methods are three approaches which have been devised to determine the two free parameters for three-dimensional flows.

Strictly valid only in parallel flows, the saddle point method suggests that the derivative of $\alpha x + \beta z$ with respect to β equals zero. As noted by Nayfeh (1980) and Cebeci and Stewartson (1980), carrying out this derivative implies that $d\alpha/d\beta$ must be real or

$$\frac{\partial \alpha_i}{\partial \beta_r} = 0 \tag{20}$$

The group velocity angle ϕ_g is given by $\partial\alpha_r/\partial\beta_r$ or

$$\phi_g = \tan^{-1}(\partial\alpha_r/\partial\beta_r) \tag{21}$$

The final condition to close the problem requires that the growth rate be maximized along the group velocity trajectory. Then the *N*-factor (or integrated growth) would be

$$N = \int_{s_0}^{s_1} \gamma \, ds \tag{22}$$

where

$$\gamma = \frac{-\left(\alpha_i - \beta_i \dfrac{\partial \alpha_r}{\partial \beta_r}\right)}{1 + \left(\dfrac{\partial \alpha_r}{\partial \beta_r}\right)^2}$$

s_0 is the location where the growth rate γ is zero, and s_1 is the distance along the tangent of the group velocity direction.

For the next method developed by Arnal, Casalis, and Juillen (1990), the fixed wave angle approach sets $\beta_i = 0$ and the *N*-factors are computed with a fixed wave orientation or

$$N = \int_{s_0}^{s_1} -\alpha \, ds \tag{23}$$

Many calculations have to be carried out over the range of wave angles to determine the highest value of *N*.

The last method, the fixed spanwise wavelength approach, proposed by Mack (1989) sets $\beta_i = 0$ and β_r is held fixed over the *N*-factor calculation, computed by equation (23). Many calculations have to be carried out over the range of β_r to determine the highest value of *N*. It is not clear what the significance of holding β_r to a constant has in three-dimensional flows.

A major obstacle in validating or calibrating current and future transition prediction tools results from insufficient information in wind tunnel and flight test databases. For example, Rozendaal (1986) correlated *N*-factor tools for TS and CF disturbances on a flight test database for the Cessna Citation III business jet. The database consisted of transition locations measured with hot-film devices for points that varied from 5 to 35 percent chord on both upper and lower wing surfaces for Mach numbers ranging from 0.3 to 0.8 and altitudes ranging from 10 000 to 43 000 ft. The results showed that CF and TS disturbances may interact and that CF disturbances probably dominated. CF *N*-factors were scattered around 5 and TS *N*-factors varied from 0 to 8. The stability analysis showed no relationship between Mach number and disturbance amplification at transition. Rozendaal (1986) noted that the quality of the results was suspect because no information on surface quality existed, an unresolved shift in the pressure data occurred, and an inadequate density of transition sensors on the upper wing surface was used. Furthermore, the impact of the engine placement relative to the wing could be added as a potential contributing factor. The Rozendaal analysis reinforced that the *N*-factor method is reliant on good experimental data.

In a discussion of the application of linear stability theory and e^N method in LFC, Malik (1987) describes the methodology for both incompressible and compressible flows and presents a variety of test cases. In situations where transition occurs near the leading edge of wings, the *N*-factors can be quite large compared with the range $N = 9$ to 11 applicable for transition in the latter portion of a wing. Malik makes an important contribution to this understanding by noting that the linear quasi-parallel stability theory normally does not account for surface curvature effects (terms). However, for transition near the leading edge of a wing, the stabilizing effects of curvature are significant and must be included to achieve *N*-factors of 9 to 11. The rest of this subsection documents samples of the extended use of the *N*-factor method for predicting laminar flow extent.

Schrauf, Bieler, and Thiede (1992) indicate that transition prediction is a key problem of laminar flow technology. They present a description of the *N*-factor code developed and used at Deutsche Airbus, documenting the influence of pressure gradient, compressibility, sweep angle, and curvature during calibrations with flight tests and wind tunnel experiments.

Among others, Vijgen et al. (1986) used *N*-factor linear stability theory to look at the influence of compressibility on disturbance amplification. They compared TS-disturbance growth for incompressible flow over a NLF fuselage with the compressible formulation. They noted that compressibility is a stabilizing influence on the disturbances (1st mode). For the NLF and LFC, an increase in Mach number (enhanced compressibility) is stabilizing to all instabilities for subsonic to low supersonic flow.

Nayfeh (1987) used the method of multiple scales to account for the growth of the boundary layer (nonparallel effects). The nonparallel results showed increased growth rates compared with the parallel-flow assumption. These results indicate that nonparallel flow effects are destabilizing to the instabilities. Singer, Choudhari, and Li (1995) attempted to quantify the effect of nonparallelism on the growth of stationary crossflow disturbances in three-dimensional boundary layers by using the multiple scales analysis. The results indicate that multiple scales can accurately represent the nonparallel effects when nonparallelism

is weak; however, as the nonparallel effects increase, multiple scales results diminish in accuracy.

Finally, Hefner and Bushnell (1980) looked at the status of linear stability theory and the *N*-factor methodology for predicting transition location. They note that the main features lacking in the methodology are the inability to account for the ingestion and characterization of the instabilities entering the boundary layer (the receptivity problem). In section 3.5.6, the issue of predicting boundary-layer receptivity is discussed, but first, advance transition prediction methodologies are presented in sections 3.5.4 and 3.5.5.

3.5.4. Parabolized Stability Equations Theory

Because the *N*-factor methodology based on linear stability theory has limitations, other methods must be considered that account for nonparallelism, curvature effects, and ultimately nonlinear interactions. The final method considered relative to the evolution of disturbances in boundary-layer flow is the PSE theory or method. Unlike the Orr-Sommerfeld equation *N*-factor method, which assumes a parallel mean flow, the PSE method enables disturbance-evolution computations in a growing boundary-layer mean flow. As first suggested by Herbert (1991) and Bertolotti (1991), PSE theory assumes that the dependence of the convective disturbances on downstream development events is negligible and that no rapid streamwise variations occur in the wavelength, growth rate, and mean velocity profile and disturbance profiles. At present, the disturbance $\Phi = (u,v,w,p)$ in the PSE formulation assumes periodicity in the spanwise direction (uniform spanwise mean flow) and time (temporally uniform) and takes the form

$$\Phi = \sum_{m=-N_z}^{N_z} \sum_{n=-N_z}^{N_t} \hat{\Phi}_{m,n}(x,y) \times \exp\left[i\left(\int_{x_o}^{x} \alpha_{m,n}\, dx + m\beta z - n\omega t \right) \right] \quad (24)$$

where N_z and N_t are the total numbers of modes kept in the truncated Fourier series. The convective direction, or streamwise direction, has decomposition into a fast-oscillatory wave part and a slow-varying shape function part. Because the disturbance profile $\hat{\Phi}$ is a function of x and y, partial differential equations describing the shape function result. These equations take the matrix form

$$[\mathbf{L}]\hat{\Phi} + [\mathbf{M}]\frac{\hat{\Phi}}{dx} + [\mathbf{N}]\frac{d\alpha}{dx} = f \quad (25)$$

Because the fast variations of the streamwise wave number, the second derivatives in the shape function are negligible. By the proper choice of $\alpha_{n,m}$, this system can be solved by marching in x. For small-amplitude disturbances, $f = 0$, whereas for finite-amplitude disturbances, f in physical space is simply the nonlinear terms of the Navier-Stokes equations or

$$F = (u \cdot \nabla)u \quad (26)$$

After the initial values of $\alpha_{n,m}$ are selected, a sequence of iterations is required during the streamwise marching procedure to satisfy the shape-function equations at each streamwise location.

Joslin, Streett, and Chang (1992, 1993) and Pruett and Chang (1995) have shown that the PSE solutions agree with direct numerical simulation results for the case of incompressible flat-plate boundary-layer transition and for compressible transition on a cone, respectively.

Haynes and Reed (1996) present the nonlinear evolution of stationary crossflow disturbances over a 45° swept wing computed with nonlinear PSE theory compared with the experiments of Reibert et al. (1996). The nonlinear computational results agree with the experiments in that the stationary disturbances reach a saturation state (confirmed with DNS by Joslin and Streett 1994 and Joslin 1995), whereas the linear *N*-factor type results suggest that the disturbances continue to grow. Hence, the linear predictions inadequately predict the behavior of the disturbances.

Finally, theoretical and computational tools are being developed to predict the rich variety of instabilities which could be growing along the attachment line of a swept wing. Lin and Malik (1994, 1995, 1996) describe a two-dimensional eigenvalue method which predicts symmetric and asymmetric disturbances about incompressible and compressible attachment-line flows which are growing along the attachment line. Such methodologies could provide important

parametric information for the design of NLF and LFC swept wings.

3.5.5. Transition Prediction Coupled to Turbulence Modeling

In this subsection, a relatively new concept is outlined which involves coupling transition prediction methodology with a two-equation turbulence model approach. Warren and Hassan (1997a, 1997b) pose the transition prediction problem within a nonlinear system of equations involving the kinetic energy and enstrophy. The exact governing equations provide a link between the laminar boundary-layer flow instabilities, the nonlinear transitional flow state, and the fully turbulent flow fluctuations. If the breakdown is initiated by a disturbance with a frequency reminiscent of the dominate growing instability, the simulations are initiated. The influence of free-stream turbulence and surface roughness on the transition location was accounted for by a relationship between turbulence level and roughness height with initial amplitude of the disturbance. The initial comparisons with flat-plate, swept flat-plate, and infinite swept-wing wind tunnel experiments suggest a good correlation between the computations and experiments for a variety of free-stream turbulence levels and surface conditions. Approaches relating flow instability and transition and turbulence modeling show promise for future computations of LFC-related aerodynamic configurations.

3.5.6. Receptivity—The Ingestion of Disturbances

Morkovin (1969) is usually given the credit for coining the process called receptivity. Receptivity is the process by which free-stream turbulence perturbs the boundary layer by free-stream disturbances originating at the edge of the boundary layer. Although believed by many to be a significant piece of the transition process, only brief mention is given to receptivity in this review. The rationale for this brief mention lies with the fact that receptivity has not been an active part in the history of LFC. However, receptivity will inevitably play an important role in the future of NLF and LFC technologies.

Let us quote Reshotko (1984) for a description of transition and the role of receptivity. “In an environment where initial disturbance levels are small, the transition Reynolds number of a boundary layer is very much dependent upon the nature and spectrum of the disturbance environment, the signatures in the boundary layer of these disturbances and their excitation of the normal modes (“receptivity”), and finally the linear and nonlinear amplification of the growing modes.”

This description gives a view of what future LFC design tools should involve to accurately capture the unsteady transition process. The receptivity tools will provide the disturbance spectrum and initial amplitudes to be used by the linear and/or nonlinear evolution module (e.g., linear stability theory, PSE theory) to predict the transition location or provide a means to correlate the transition location. Such capability already exists for the simplest of disturbance initiation processes as described by Bertolotti and Crouch (1992).

Leehey and Shapiro (1980), Kachanov and Tararykin (1990), Saric, Hoos, and Radeztsky (1991), and Wiegel and Wlezien (1993) have conducted receptivity experiments; Kerschen (1987), Tadjfar and Bodonyi (1992), Fedorov and Khokhlov (1993), Choudhari and Streett (1994), Choudhari (1994), and Crouch (1994) have conducted theoretical studies of receptivity to extend the knowledge base and capability for predicting the receptivity process. Acoustic noise, turbulence, and vorticity are free-stream influences and couple with single and distributed roughness, steps and gaps, surface waviness, and other things to produce disturbances in the viscous boundary-layer flow which are relevant to NLF and LFC applications. These ingestion mechanisms are referred to as “natural receptivity”; however, there are forced and natural categories of receptivity. Because the dominant instabilities in a boundary-layer flow are of a short scale, the receptivity initiation must input energy into the short-scale spectrum for the most efficient excitation of disturbances. As Kerschen (1989) pointed out, forced receptivity usually involves the intentional generation of instability waves by supplying energy to the flow at finite and selected wavelengths and frequencies that match the boundary-layer disturbance components. Examples of forced receptivity include unsteady wall suction and blowing or heating and cooling (used for active flow control).

Forced theoretical and computational receptivity is linked to the linear stability theory (section 3.5.3)

through forcing a boundary condition. The following equation is introduced as the boundary condition for the generation of a disturbance by suction and blowing through a single orifice in the wall (or boundary):

$$v = f(x) \exp(-i\omega t) \tag{27}$$

where ω is the frequency of the disturbance which one desires to initiate, $f(x)$ is the shape of the suction and blowing distribution (generally a sine or cosine bubble shape), and v is the resulting wall-normal velocity component at the wall. Similar techniques can be used for unsteady thermal forcing and to excite disturbances in a wind tunnel experiment.

Natural receptivity is more complicated in that free-stream acoustic, turbulence, and vorticity are of much longer wavelengths than the boundary-layer disturbance. Complicating the matter, the free-stream disturbance in nature has a well-defined propagation speed and energy concentrated at specific wavelengths. Hence, the free-stream disturbance has no energy in wavelengths that correspond to the boundary-layer disturbance. So a mechanism must effectively (and efficiently) be able to transfer energy from the long-wavelength range to the short wavelengths. Mechanisms to accomplish this transfer include the leading edge (of a plate and wing) and surface discontinuities (e.g., bugs, surface roughness, rivets).

To determine (or describe) this process of length scale conversion, Goldstein (1983, 1985) and Goldstein, Leib, and Cowley (1987) showed that the primary means of conversion was through nonparallel mean flow effects. Hence the two cases where nonparallel effects are strongest are (1) regions of rapid boundary-layer growth as at the leading edge where the boundary layer is thin and rapidly growing and (2) downstream at a surface discontinuity such as a bump on the wall.

To determine the receptivity of the boundary layer in the leading-edge region of a particular geometry to free-stream disturbances, solutions of the linearized unsteady boundary-layer equations are required. These solutions match downstream with the Orr-Sommerfeld equation, which governs the linear instability and serves to provide a means for determining the amplitude of the viscous boundary-layer disturbance.

Finally, the second class of natural receptivity involves the interaction of long-wavelength free-stream disturbances with local mechanisms (i.e., wall roughness, LFC suction, steps) to generate boundary-layer disturbances. In this case, adjustments made to the mean flow cannot be obtained with standard boundary-layer equations. In this situation, the triple-deck asymptotic approximation to the Navier-Stokes equations is used. The triple deck produces an interactive relationship between the pressure and the displacement thickness due to matching of the requirements between the three decks. The middle deck or main deck responds inviscidly to the short-scale wall discontinuities. The viscous layer (lower deck) between the main deck and the surface is required to ensure that a no-slip boundary condition is enforced at the wall. Finally, the rapid change in displacement thickness at the surface discontinuity induces a correction to the outer potential flow. This correction takes place in the upper deck. The mean flow gradients due to the discontinuity serve as forcing terms for the disturbance equations. Therefore, although much understanding about receptivity has been gained over the past few years, significant research must be conducted, especially in the three-dimensional effects and in supersonic flows, before the tools become widely used as design tools. Again, receptivity is included in this LFC review because it will inherently play a role in future transition prediction for NLF and LFC design tools.

3.5.7. Optimize Linear Design for LFC

Pertaining to the determination of what “optimal” suction distributions should be used on LFC systems, Nelson and Rioual (1994) posed a determination by means of minimizing the power requirements to achieve transition at a specified location, by applying suction through a sequence of controllable panels. Their paper had the problem formulated as a nonlinear constrained optimization problem and focused more on the stability of the algorithm than on the fluids mechanics of the LFC system. In a comparable study, Hackenberg, Tutty, and Nelson (1994) showed convergence optimization of 2 or 4 panels is less than 10 iterations for the problem of transition on a flat plate.

More recently, Balakumar and Hall (1996) employed optimal control theory and incompressible linear boundary-layer stability theory (*N*-factor of

9 assumed) to predict the suction distribution under the constraint of fixed mass flow (fixed energy requirement). The beginning of the suction region was imposed upstream of the neutral point and the end of the suction was prescribed downstream of the transition point. For simplicity, the mean flow was determined by solving incompressible boundary-layer equations. Although optimal suction is demonstrated for TS wave control in a flat-plate boundary-layer flow (Blasius), the resulting suction distributions for traveling and stationary crossflow disturbances in swept Hiemenz flow are quite relevant to HLFC implemented on a swept wing at low speed. Interestingly, the region of maximum suction occurred very near the location of the onset of disturbance amplification and progressively decreased through the region of disturbance growth. In addition, Balakumar and Hall concluded that over an order of magnitude more suction is required to control crossflow disturbances compared with that required to control TS disturbances.

Stock (1990) posed an interesting way of viewing boundary-layer instability with suction. The problem was transformed from the problem of a boundary-layer flow with a pressure gradient and suction to the problem of an equivalent pressure gradient without suction. The equivalence is imposed based on an identical form parameter, or shape factor H. Using integral and finite-difference methods, the stability results for the case with and without suction were shown to be in agreement.

3.5.8. Thermal LFC

As early as the 1950s, the thermal concept was recognized as a potential means for boundary-layer stabilization. Dunn and Lin (1953) realized and demonstrated that mild surface cooling was able to stabilize viscous boundary-layer instabilities which would otherwise amplify and lead to transition. In fact, the calculations showed that 2D disturbances could be completely stabilized at Mach number of 1.6 for the ratio of wall to free-stream temperature of 1.073, which implies a small amount of cooling.

A more recent study by Boeing (Parihk and Nagel 1990), showed that with stability theory cooling can be stabilizing to both TS and CF disturbances with application to supersonic LFC transports.

The application of thermal control for LFC aircraft is in an infancy stage compared with suction LFC. Issues relating to the thermal surface are unresolved as of this publication. One of these potential issues involves the possibility of surface waves being generated through the use of strips of thermal control. Whether such an application would generate waves intolerable to laminar flow has not been studied yet.

3.5.9. Advanced Prediction of Manufacturing Tolerances

Innovative tools have been developed to predict the impact of manufacturing tolerances on the extent of laminar flow; however, very little validation of these tools has been documented. As Masad (1996a, 1996b) shows, interacting boundary-layer (IBL) theory, which accounts for the viscous-inviscid interaction, can be coupled with either linear stability theory or PSE theory to parameterize the allowable dimensions of steps, gaps, rivets, and other things, which can be used and not impact the laminar flow.

Nayfeh, Ragab, and Al-Maaitah (1987, 1988) looked at the issue of manufacturing tolerances by performing a study of boundary-layer instability around humps and dips. Interacting boundary-layer theory was used to account for the viscous-inviscid interaction associated with potential separation bubbles, and the amplification of disturbances in the presence of humps with various height-to-width ratios and at various locations was studied. The results suggest that $N = 9$ correlates well with the transition location. In addition, the size of the separation bubble is influenced by the height-to-width ratio and Reynolds number, and the disturbance instability is affected by the height-to-width ratio and the location of the imperfection from the leading edge of the plate and branch I of the neutral curve.

4. Laminar Flow Control Aircraft Operations

The operational maintenance of laminar flow, including controlling the accumulation of ice and insects, is paramount to the incorporation of LFC on aircraft. Both ice and insects generate roughness-induced premature loss of laminar flow. Although anti-icing systems have been operational for many years on the leading edge of wings and on nacelles,

only limited research results for realistic insect-prevention systems are available. This section focuses primarily on the issue of insect accumulation and prevention; brief discussions on aircraft icing research, the impact of atmospheric particulates on laminar flow, and boundary-layer control for high lift will follow. Finally, a discussion of operational maintenance of laminar flow closes this section.

4.1. Insect Contamination

The population density of insects (or insects per volume) depends on temperature, moisture, humidity, local terrain, vegetation, climate, wind speed, altitude, and vehicle surface definition (e.g., wing shape). Insect contamination along with ice adherence are two of the most crucial operational issues which affect NLF and LFC systems. A summary of the studies addressing this issue follows.

On August 10, 1926, the first known attempt to use an airplane in collecting insects was made under the direction of E. P. Felt at Tallulah, Louisiana, in the United States (lower Mississippi valley) and at Tlahualilo, Durango, Mexico. Much of the test area is swamp country, encompassing hundreds of small lakes, bayous, rivers, and great forests. The project of collecting insect data was conducted from August 1926 to October 1931 and the results are reported by Glick (1939) in a Department of Agriculture Technical Bulletin. The investigation is of importance to LFC (and aircraft in general) and documented the numbers and kinds of insects, spiders, and mites with atmospheric conditions and altitude. DeHaviland H1 army biplanes were used for the study and covered some 150 000 miles. For the measure of insect density, traps of 1 ft^2 embedded with fine-mesh copper screens were placed between the biplane wings. A protective cover was used to control the duration and altitude of exposure to the screens. All measurements were made with 10-min exposures at known speeds.

Although the altitudes ranged from 20 to 16 000 ft, the systematic studies were conducted at 200, 1000, 2000, 3000, and 5000 ft for daytime collections and 1000, 2000, 3000, and 5000 ft for nighttime collections. Over all altitudes, Glick (1939) reported that the greatest number of insects was taken in May, with November and September following. The fewest insects were taken in January and December. For nighttime collections, the greatest numbers were taken in October followed by May. Results over the 5-yr period indicated that the largest density of insects was measured at low altitudes, with the number of insects decreasing rapidly with increased altitude. Glick (1939) also noted that temperature was one of the most important meteorological factors in the control and distribution of insects. He showed that the maximum densities were measured at temperatures of 75° to 80°F. Finally, Glick (1939) noted that the insects and mites captured at high altitude (and one spider at 15 000 ft) were very small and completely at the mercy of the air currents. The size, weight, and buoyancy of the insects contributed directly to the height to which the air currents carried it and hence to the presence of insects at high altitudes.

Hardy and Milne (1938) reported on the distribution of insects with altitudes from 150 to 2000 ft. The measurements were made with traps and nets carried into the sky by kites in England. Their study conducted from 1932 to 1935 resulted in 839 insects captured in 124.5 hr of flight. Of interest here is that the population density qualitatively agreed with Glick (1939) in that the largest density was at low altitude. Although all insects were affected somewhat differently by the weather conditions, high temperature and low humidity were determined to be more favorable to aerial drift than the reverse conditions. Freeman (1945), under the direction of Hardy, expanded on the early kite-flown study and found that the greatest numbers and varieties of insects occurred in May, June, and September. Although the information in these studies were significant for the NLF technology, the primary goals of the studies focused on characterizing the insect families and the motion of agricultural “pests” from one location to another.

Incidentally, in the flight testing of the Hurricane II reported by Plascott et al. (1946), no flies or insect debris was observed in this NLF flight test. However, the drag measurements from previous flight tests where flies and insects were picked up indicated an increase in the drag due to insect debris. Hence, the full advantages of laminar flow and the subsequent low drag would require some method to prevent the insects from adhering to the surface.

Atkins (1951) formally looked at the insect-contamination problem by generating correlations

using the Dakota, Wirraway, Mustang, and Vampire aircraft. The results gathered from 24 flights showed that contamination extended to about 14 percent chord on the upper surface and about 9 percent chord on the lower wing surface. A bug hit was only recorded if it had sufficient mass to trip the boundary layer. Furthermore, it was reported that insect contamination was evident in the winter, even though Melbourne, Australia, had a cool climate.

As numerous articles in the literature have previously stated, Coleman (1961) presented one of the first comprehensive discussions (reviews) of the issue of insect contamination. Coleman noted that correlating the numerous environmental conditions to predict the insect density was hindered by the fact that a variation in one parameter (e.g., humidity) was accompanied by simultaneous changes in other parameters (e.g., temperature, pressure). No consistent correlations have been identified for barometric pressure, humidity, light intensity, precipitation, or the electrical state of the atmosphere with insect population density. However, air temperature of 22° to 26°C and wind velocities of between 5 to 12 mph have been shown individually to be areas of maximum population densities. Also, the insect populations were maximized near ground level and rapidly decreased up to an altitude of 500 ft. The temperature and altitude correlations were consistent with the study by Glick (1939). Also, the region of influence for the aircraft was during takeoff and initial climb. Coleman proceeded to discuss the entomological impact of the insect on influencing laminar flow. The insect either remains intact or disintegrates when it impacts the surface. This account was determined by the critical impact velocity (or rupture velocity) of the insect; the rupture velocity was clearly dependent on the anatomical structure of the insect. Field and wind tunnel experiments revealed that rupture velocities between 22.5 and 44.9 mph were found for the variety of insects tested. Coleman also noted that smaller (1 to 3 mm) insects were more numerous than larger (>3 mm) insects.

Croom and Holmes (1985) reported on a flight experiment using a Cessna 206 to study the insect contamination problem. The airspeed, altitude, and angle of attack were recorded on magnetic tape. The surface winds, temperatures, and insect counts were manually recorded. The tests were conducted in a high insect population area to provide the potential for large density (insect/1×10^6 ft^3) accumulation. Flight durations lasted from 10 to 50 min and the airspeed ranged from 80 to 130 mph. The present flight test results shown in figure 25 were consistent with the earlier studies of Glick (1939), Hardy and Milne (1938), Freeman (1945), Coleman (1961) and Maresh and Bragg (1984). (Note, the population densities were normalized by the largest values.) Clearly, the largest number of strikes occurred near 77°F in 4 to 8 mph winds and rapidly dropped off in cooler and hotter temperatures. Furthermore, the insect density rapidly dropped off with increased altitude and the insect protection was not necessary at the higher altitudes above 500 ft.

Estimating the insect impact on the resulting "roughness size" was a difficult correlation to measure because the impact was a function of both incidence and speed of the insect-surface connection. Normally, the accumulation of insects was measured after the aircraft landed, without regard to the incidence and speed. However, some limited observations were made in the wind tunnel. To model the insect in reference to the wing (or most other parts) of the aircraft, the insect was assumed to be an inanimate object for the purpose of dynamic analysis. This assumption is made because the drag which an insect experiences due to the induced velocity in the vicinity of the wing significantly exceeds the propulsive force that the insect exerts. Based on the inanimate model of the insect, the theoretical streamwise extent of the roughness has shown some agreement with available data for 2D incompressible flow. The theoretical and experimental results agreed quite well for 2D airfoils and mildly swept wings. The conclusion of this comparison was that if the chordwise velocity component was much larger than the spanwise velocity component, the insect accumulation (and resulting roughness) was essentially a 2D process.

Low-speed wind tunnel results indicated that the resulting excrescence height for various geometry airfoils at small angle of attack was maximized near the leading edge of the wings and decreased in size to about 30 percent chord (upper and lower surface), where insect accumulation ceased except for high angle of attack.

Maresh and Bragg (1984) developed a method to predict the contamination of an airfoil by insects and the resultant performance penalty. The model

neglected any lift that may be produced by the body of the insect and assumed that three planes of symmetry existed about the insect and that the forces acting on the insect were known. The velocity flow field about the airfoil was required (neglecting the viscous effects in the boundary layer) and the insect drag and lift coefficients were required to compute insect trajectories. Additionally, the rupture velocity of an insect was a function of the shell hardness and amount of body fluid contained within it. The results showed that (1) angle of attack, Reynolds number, and accretion conditions influenced the insect contamination extent; (2) the effect of contamination for a given airfoil varied for different insect sizes and types; and (3) the airfoil geometry played a significant role in determining the insect accretion pattern.

Coleman (1961) closed the discussion of insect contamination by discussing techniques to either eliminate or prevent the roughness-induced effects of the insect to laminar flow. Preventive techniques discussed include (1) paper covers which cover the surface until sufficient altitude is reached and the cover is either released or extracted into the aircraft, (2) mechanical scrapers which scrape the surface, (3) deflectors which either catch the insects or cause their paths to be deflected away from the surface, (4) a highly viscous fluid layer in which the insects were trapped and carried away in flight by the high shear, (5) a cover which is dissolvable by fluid discharge, (6) a cover which is removed by a thermal process, (7) relaminarization downstream of the critical insect strike area, and (8) continuous liquid discharge.

4.1.1. Paper Cover

Covering the test section with paper was the simplest (or least mechanical) anti-insect device. This device was successfully used in the major laminar flight tests, including Gray and Davies (1952) with the King Cobra flight test; Head, Johnson, and Coxon (1955) with the Vampire porous-suction flight test; Groth et al. (1957) with the F-94 slot-suction flight test; and Runyan et al. (1987) with the Boeing 757 NLF flight test.

Gray and Davies (1952) reported on King Cobra flight tests at the Royal Aircraft Establishment in England. As the Spring days became warmer, the insect contamination problem increased (even if the flight tests were conducted early in the morning). This observation is consistent with the insect density increase with temperature discussed earlier. To avoid the insect problem, a sheet of paper covered 0 to 30 percent chord on the upper and lower surface of the test section. After the aircraft takeoff and climb to sufficient altitude, the pilot could jettison the paper by pulling a string attached to the paper and retrieving the paper inside the cockpit through a piece of pitot tubing.

To avoid insect contamination for the Vampire porous-suction flight tests reported by Head, Johnson, and Coxon (1955), the test-section sleeve was protected during takeoff and climb by a strip of tracing paper that covered from the leading edge to about 10 percent chord and was fixed to the surface with adhesive tape. Takeoff was delayed until 100 knots had been reached. This speed was maintained during takeoff and climb, and at “sufficient altitude,” the tracing paper was jettisoned by reducing the speed to 90 knots.

To avoid insect contamination for the F-94A flight tests of a slot-suction LFC experiment reported by Groth et al. (1957), the first 30 percent of the upper and lower surface of the test section on the wing was protected with a cover of blotting paper taped to the wing. This paper remained attached through takeoff and climb, then the plane was decelerated to remove the covering. Without this covering, turbulent wedges were generated from the insect remains. However, full laminar flow could be regained by climbing to higher altitudes (25 000 ft). This regaining of laminar flow is understood to be a unit Reynolds number effect. For constant Mach number, a climb in altitude decreases the unit Reynolds number and, as discussed in section 2, a lower unit Reynolds number flow is more tolerant to a roughness (insect impact) of given size.

For the Boeing 757 NLF flight tests (Runyan et al. 1987), the glove was protected from insect strikes during takeoff and climb by using a paper covering until the airplane reached 5000 ft at which time the paper was pulled into the cabin via a nylon cord. On flights not using the protective covering, loss of laminar flow was observed during the flight and evidence of insect accumulation near the attachment line was measured after landing.

4.1.2. Scrapers

Wires and felt pads have each been tested with some success in wind tunnel experiments, the latter working for painted surfaces. The problem of drag penalty due to the device was not evaluated; however, the device must either be contained in the skin of the aircraft during cruise flight or be jettisoned to avoid an unreasonable drag penalty (Coleman 1961).

4.1.3. Deflectors

Deflectors consist of a surface (or plate) that forms a nose flap which protects the leading edge of the wing from insects and absorbs the insect impacts. Tamigniaux, Stark, and Brune (1987) discussed a wind tunnel experiment to test the effectiveness of the Krueger high-lift device used as a shield against insects (although the insects used were larger relative to the model size than would be encountered in flight). Note, figure 2 shows a leading-edge Krueger device, which would be retracted after takeoff and climb, leaving a clean leading edge for cruise. The 2-ft model consisted of a slotted-leading-edge Krueger flap on a wing section. The insects were injected into the wind tunnel at a free-stream velocity of 4 ft/sec upstream of the wing leading edge. Without insects, the Krueger flap was varied for 37 different positions, optimizing for maximum high-lift characteristics. The optimal position was a 45° deflection and the optimal gap and trailing-edge gap were both 2 percent of the airfoil reference chord. The results showed that lighter insects impacted farther aft of the stagnation line than heavier insects; this indicates that heavier insects have straighter trajectories than lighter insects. A particle trajectory code was developed for two-dimensional multielement airfoils; the calculated results were in good agreement with the experiment. Insects impacting at an angle less than 7° left negligible body remnants on the wing upper surface to trip the laminar boundary layer. The Krueger concept has been demonstrated to be effective in flight on Jetstar LEFT aircraft (Powell 1987); however, incorporating an anti-icing system into the Krueger device remains an issue.

This concept has been developed into the modern day Krueger flap and demonstrated on the Jetstar flight test (Maddalon and Braslow 1990) described in section 6.3. Also, this concept was successful for the Boeing 757 HLFC flight experiment (Collier 1993) as described in section 6.6. The results indicated that it was possible to protect the upper surface but it was not possible to protect the lower surface. However, the plate device caused considerable drag and a pitching moment. The retracted reflector could introduce significant ridges. The Krueger flap serves to both protect the surface from insect strikes and improve lift.

4.1.4. Fluidic Cover

Coleman (1952) discussed wind tunnel tests that employed the application of glycerine, glycerine and gelatine, and soap and methanol to wing sections. These solutions would be wiped away as the aircraft reaches sufficient speed to cause the shear to remove the fluid (and insects). Although these solutions were shown to decrease the accumulation of insects on the test article, complete elimination of the insects was not possible. Continuous spraying of the solution was shown to be effective and required a penalty of 0.2 to 0.5 of the TOGW of the aircraft.

4.1.5. Thermal Cover

Under the concept of thermal covers, flammable covers which could be electrically ignited can be rendered out of possible solutions because of safety (and pollution) concerns. Heating (rather cooking) the insects until they are consumed has been suggested, but the high temperatures required would be undesirable to the wing structure. Imposing a layer of ice on the structure has been suggested and such a concept would be ideal in terms of preventing insect accumulation. This layer of ice would then be removed after takeoff and climb by the conventional de-icing systems. The application of the ice layer to the aircraft, potentially damaging effects of large ice pieces breaking away from the wing, the required thickness of ice required to prevent insect contamination, the minimum time to remove the ice layer, and the associated performance penalty during takeoff are issues that must be addressed. Coleman (1952) discussed some wind tunnel tests addressing some of these issues.

4.1.6. Relaminarization

Coleman (1961) noted that relaminarization through the use of suction slots was investigated by Cumming, Gregory, and Walker (1953). The results of their wind tunnel experiment indicated that the pump

drag increased because of the suction approximately balancing the profile drag due to the insect-roughened surface; hence, no apparent performance gain was realized with the suction slot.

4.1.7. Liquid Discharge

Peterson and Fisher (1978) reported on insect contamination by using a Jetstar aircraft. The goals of the experiment were investigating the extent of the insect problem at large airports, determine whether insect accumulation would erode in cruise flight, test the ability of the then new surface coatings to alleviate the insect accumulation problem, and test leading-edge sprays for anti-insect protection. In November 1977, the Jetstar was flown on 15 takeoff and climb missions to estimate the insect accumulation problem at Los Angeles, Sacramento, and San Francisco airports under normal airline-type operations. Insects were accumulated on 13 of the 15 flights and caused premature transition. The initial flights confirmed that insect accumulation and resulting premature transition required an anti-insect accumulation system. At the trailing edge of the flaps, boundary-layer probes recorded the state of the boundary layer. Next, five spanwise segments of the leading-edge flap were treated with (a) an aluminum alloy untreated surface, (b) a spray-on DuPont Teflon coating, (c) DuPont Teflon pressure-sensitive tape, (d) organosilicone hydrophobic coating, and (e) random rain repellent coating. Flights were then conducted from many airports in the United States ranging from California to Texas to Florida. Insects were encountered on all flights and the coatings were insufficient to remove the insect contamination interrupting laminar flow. The insect accumulation on super-slick Teflon surfaces and hydrophobic coatings was compared with standard reference aluminum. The flight test results showed that none of the surfaces tested showed any significant advantages in alleviating the insect contamination. Five types of flight tests were conducted with the spray insect-avoidance system: (1) no spray, (2) water-detergent spray after all low passes, (3) large-droplet water detergent spray after low passes, (4) continuous water spray during low passes, and (5) intermittent water-detergent spray during two passes. The first test was used as the calibration or reference flight. The flight test with continuous spray was most effective and no insect remains were observed in the spray area (consistent with the results of Coleman, 1952). Once insects have accumulated on dry surfaces, they could not be removed in flight with water and detergent spray.

In the Croom and Holmes (1985) flight experiment, three different fluids were considered for the purpose of both insect prevention and ice protection. The solutions were (1) monoethylene glycol (Aeroshell 07) and water solution, (2) propylene glycolmethyl ether, and (3) monoethylene glycol (MEG) and water. The fluid was discharged through either slots or perforated holes, where the holes had a diameter of 0.0025 in. and were spaced about 0.0205 in. apart. The TKS anti-icing system served as the method for the current test, partially because the system has already been certified for several aircraft. The left wing which had no insect protection was used as the baseline. The tests showed that the insect-protection system should be activated before insect impact. The ratio of water to MEG in the fluid system and the flow rate played significant roles in the effectiveness of the insect protection system. The MEG/water solution of 20/80 percent was very ineffective in reducing the number of insect strikes. Approximately 10-percent fewer strikes were realized by using this solution. However, with 80/20 percent solution, a 75-percent (or greater) reduction in the number of recorded insect strikes was realized. As the flow rate was increased, the total insect accumulation decreased. Croom and Holmes (1985) noted that only a 3-in. perforated region on the panel and a flow rate of 0.16 to 0.33 gal/min were required to achieve a 68- to 82-percent reduction in the insect accumulation.

Bulgubure and Arnal (1992) and Courty, Bulgubure, and Arnal (1993) reported the use of a TKS insect avoidance system for the HLFC flight tests using a Falcon 50 test aircraft. Monopropylene glycol (MPG) was the fluid chosen for use in this system. During low-altitude flight tests over insect-infested areas, the port (untreated) side of the aircraft had 600 insects/m^2 impact the leading edge in the region of interest, whereas on the starboard (treated) side with the MPG fluid, no insect contamination was noted. Hence, the TKS system was very effective for insect avoidance.

4.1.8. Flexible Surface or Cover

Compared with protective coverings or continuous spray techniques, Wortmann (1963) proposed using a

flexible surface to prevent insect contamination. The transfer of kinetic energy from the incoming insect to the surface would be absorbed by the surface and used to repel the insect. Experiments carried out by dropping a fluid drop onto a silicone rubber surface at 150 m/sec showed that most of the fluid was repelled due to the energy transfer relationship. Further experiments in wind tunnels and with automobiles and aircraft indicated that only small amounts of residue remain after impingement by using the silicone foam rubber (Silikonschaumgummi) consisting of a powdered foam layer and large air content. However, permanent surface damages caused by rain and hail were issues of concern for these coatings.

Finally, General Electric Aircraft Engines performed wind tunnel experiments (Fernandez et al. 1996) to determine if a test article covered with a coating designed to repel insects (similar to the concept by Wortmann 1963) would solve the insect-adhesion problem for NLF and LFC applications. Subsequent flight tests with a NASA Learjet were carried out under a cooperative agreement between NASA Lewis and Langley Research Centers and the General Electric Company. The results are not available for this publication.

From these studies, we find that predicting and preventing insect contamination can require very complicated (but necessary) systems to maintain laminar flow. Some of the results suggest

1. The rupture and attachment of insects on NLF/LFC surfaces can lead to premature transition (turbulent wedges)

2. Insect contamination is usually limited to the leading-edge region from 0 to 30 percent chord

3. The greatest density of insects falls below 500 ft

4. Insect accumulation rates are a strong function of temperature, with maximum accumulation near 77°F

5. Insect accumulation rates are a function of windspeed, with maximum accumulation near 4 to 8 mph

Of the anti-insect devices tested, paper coverings, continuous liquid discharge, and deflectors have been demonstrated in flight to prevent insect accumulation. Anti-icing systems such as TKS can be used to reduce the impact of insect accumulation. Solutions of MEG and water prevents insect accumulation (up to 82 percent) but is rather ineffective in removing insects from the surface after adhesion. Reduced insect accumulation occurs with increased solution fluid flow rates. The modern-day Krueger flap can be used for insect prevention and for increased lift during takeoff and landing.

4.2. Ice Accumulation and Atmospheric Particulates

The accumulation of ice on the leading edge of wings can significantly alter the geometry of the wing and cause drag penalty and performance degradation (and in the worst case, safety can be affected). In addition, degradation of laminar flow can occur due to particulates in the atmosphere, most evident during cloud encounters.

4.2.1. Ice Accumulation

The National Advisory Committee for Aeronautics (now the National Aeronautics and Space Administration) started studying the accumulation and prevention of ice on aircraft in 1928. An icing research tunnel was built at the Lewis Research Center in 1944 to perform ground-based testing. Additional effort was placed on accompanying simulation tools to predict the accumulation and prevention. Refer to Britton 1990, Perkins and Rieke l993, and Bergrun 1995 for discussion of the icing issues; to Reinmann 1981 for a bibliography of ice-related research; and to Ranaudo, Reehorst, and Potapczuk 1988 for a more recent review of the NASA Aircraft Icing Research Program. Although much research has been performed for standard configurations, little has been done for LFC-related aircraft.

As described by Etchberger et al. (1983) and Lange (1984, 1987), the Jetstar slotted wing had six slots in the leading-edge region to control the flow and to provide fluid for ice-accumulation (and insect-contamination) protection. A 60/40 mixture of propylene glycol methyl ether and water was expelled through the slots. After climb out to 4000 ft, the fluid

ejection system was purged from the slots, and suction was applied to obtain laminar flow.

Similar to the non-LFC aircraft, a LFC-type aircraft must account for potential ice accumulation and prevent such a detrimental and dangerous obstacle with anti-icing techniques—either by applying heat or by dispelling anti-freeze agents. The icing issue for NLF and LFC is more a system design problem than a technical obstacle to achieving laminar flow.

4.2.2. Atmospheric Particulates

Fowell and Antonatos (1965) noted the impact of atmospheric particles on achieving laminar flow during the flight test. Figure 26 shows a sketch estimating the LFC performance with ice particles in the air. The figure indicates that ice particles can influence laminar flow if the size and density of particles are sufficiently large. The flight results indicated that laminar flow was lost as the size and density of particles increased.

Hall (1964) set out to explain why the X-21 LFC flight experiment lost laminar flow when the aircraft flew through visible clouds. The explanation began by looking at the impact of the wake from a discrete particle on the otherwise laminar boundary layer; this suggests that local turbulent spots could be initiated in the boundary layer, depending on the particle Reynolds number and geometry. Next, the impact of surface roughness was reviewed, concluding that the roughness did not affect the boundary-layer stability below some critical roughness height or roughness Reynolds number of 600 for spheres (3D roughness) and 200 for cylindrical roughness (2D roughness). From the experiments, Hall concluded that the local boundary-layer Reynolds number, pressure gradient, and free-stream turbulence had no effect on the critical roughness Reynolds number; however, an increase in Mach number led to an increased critical Reynolds number. From this review, Hall concluded that transition induced by the wake of a particle was a local effect independent of the usual parameters (e.g., pressure gradient) influencing boundary-layer transition. To connect this impact of particles and roughness to the loss of laminar flow on the X-21 experiences, the particles in the clouds must be of sufficient size and density for sufficient duration to produce and sustain turbulence. Based on sparse data, the ice crystal size, density, and length of existence observed in the atmosphere correlated with observed loss of laminar flow on the X-21. Namely, ice crystals were generally larger than the critical diameters of 17 and 32 μm at respective altitudes of 25 000 ft and 40 000 ft. The duration of a particle passing through the boundary layer on the X-21 was an order of magnitude greater than the minimum time required to initiate turbulence, and the predicted flux of ice particles in Cirrus clouds with visibility of 5000 ft to 10 000 ft was high enough to cause the loss of laminar flow on the X-21 aircraft.

Davis et al. (1986, 1987, 1989) discussed the effect of the cloud encounters on the laminar flow extent in the Jetstar flight test program. A cloud-particle spectrometer (Knollenberg probe) and a particle detector (charging patch) were used to measure the free-stream particle environment. A degradation of the flow was observed during a cloud encounter coinciding with a charge-current increase on the instrumentation; however, full laminar flow was regained within a few seconds after the cloud encounter. Indicated by Fisher and Fischer (1987) and shown in figure 27, the Jetstar ice-encounter results agreed with the Hall criteria.

Finally, Anderson and Meyer (1990) showed flight data for the F-14 NLF flight experiment that indicated turbulent bursts were measured during cloud encounters. The charge patch indicated the presence of ice particles during the loss of laminar flow while in the clouds.

Meifarth and Heinrich (1992) discussed issues relating to maintaining NLF and LFC in flight. In agreement with the insect-contamination issue at low altitudes, figure 28 suggests that atmospheric pollution may be an issue at high altitudes, even up to 10 000 m. The uncertainty of the reliability of LFC systems operating in a polluted environment could be an additional risk to the implementation of the technology on a commercial transport; however, no degradation of the laminar flow extent was observed for the Jetstar LEFT test (see section 6.3) even though the Jetstar encountered pollution, dirt, and so forth at the various airports.

4.3. Boundary-Layer Control for Takeoff and Landing

Although boundary-layer control (BLC) is beyond the scope of this review, a comment will be made here

because BLC is related to LFC in that the suction system used for LFC could potentially be used for BLC.

An aircraft in high-lift mode droops the leading-edge flaps to enhance *L*/*D* (increased camber). This can lead to a region of flow separation over the flap and reattachment near the hinge line. One proposed BLC concept involves drooping the leading-edge flap more than conventional and use BLC suction to attach the otherwise separated flow. BLC would be applied just downstream of the hinge line.

Parikh et al. (1990) did a Euler computational analysis of the BLC suction concept with application to a supersonic transport. An assessment of the impact on aerodynamic performance with BLC was compared with the simple flap device without BLC. Boeing's 3D inviscid flow code—PANAIR—was used for a portion of the study. The Euler analysis was deemed sufficient for the study since previous studies have shown that the inviscid analysis was capable of capturing the vortex formation and nonlinear evolution on sharp leading-edge wings. The Euler analysis provided the pressure distributions, which were then used in a 3D boundary-layer analysis to determine the state of the viscous flow. The significance of Reynolds number scaling was an important factor drawn out in the analysis. At flight Reynolds numbers, the inboard portion of the wing indicated attached flow. However, at lower Reynolds numbers (but same unit Reynolds number), the flow separated on models which were less than 1/4-scale. The calculations were repeated to include unit Reynolds number variations. The conclusion was that flow separation was only impacted by chord Reynolds number effects. However, the unit Reynolds number calculations did not take into account the additional sensitivity of the flow to roughness (steps, gaps, joints). For the outboard portion of the wing, separation was encountered (when transition was assumed to occur at 5 percent chord). The effect of BLC and suction-region extent were then studied for the separated flow problem. The "optimized" results showed that for the four spanwise regions studied, a chordwise extent beginning at the suction peak location and covering 1 percent chord was sufficient for separation control. The results showed that $C_q = 0.003$ inboard and $C_q = 0.004$ outboard were sufficient to prevent flow separation. Lower C_q was required inboard because of the smaller suction peak. These suction levels indicate that BLC required an order of magnitude more suction than LFC. The resulting pressure drop was 10 psf for supersonic LFC and 20 to 40 psf for BLC. The BLC led to a drag improvement of about 10 percent over the optimized flap configuration. Parikh et al. (1990) noted that a more definitive assessment of performance benefits due to BLC should be made through wind tunnel tests.

4.4. Operational Maintenance of Laminar Flow

The maintenance and manufacturing of smooth surfaces is a significant issue in achieving laminar flow, potentially creating an additional burden on the day-to-day operations of NLF and LFC aircraft.

Gray and Davies (1952) reported on the experiences gained at the RAE in England dealing with surface deterioration issues. In the King Cobra flight tests, the test section of the wing was coated with two coats of primer and one coat of filler, followed by additional smoothing when deemed necessary. Over a 6-month period, the surface deteriorated only in the skin joints regions. The aircraft was exposed to weather for about 200 hr and 50 flights entailing about 40 hr. The rest of the time it was housed in a hangar. For different King Cobra aircraft, which was in the open for about 2 years, the skin surface was chalky (dirty) and rivet and joints areas were the only areas of the wing that had any surface damage (cracking). The surface degradation results at the rivet-gap-joint areas were consistent with those found by Plascott (1946) and Plascott et al. (1946) for the Hurricane II flight test program. Gray and Davies (1952) noted that once the ground crews became habitually aware of the sensitivity required for handling the wing surface for the Hurricane and King Cobra programs, protective coverings for the surface became unnecessary.

In the description of a porous-suction flight experiment on a Vampire aircraft, Head, Johnson, and Coxon (1955) noted an operational issue that must be addressed when using powered suction systems. If the suction pump were to fail, then outflow could cause premature separation at high lift coefficients. This potential problem could be alleviated with simple non-return valves to prevent outflow conditions.

Related to the issue of maintaining laminar flow in a variety of flight environments and maneuvers, Groth

et al. (1957) noted that 100 percent laminar flow was maintained in horizontal flight, during climb, turns, and descent for a range of Mach numbers. Both 12-slot and 69-slot tests realized a loss of laminar flow flying through clouds (consistent with the X-21 flight test observations); laminar flow was regained within 30 sec after emerging from the cloud. Also, laminar flow was maintained in moderately gusty weather. However, strong atmospheric turbulence levels can lead to a loss of laminar flow. This was demonstrated in 2-sec 0.5*g* and 30-sec 0.3*g* accelerations for chord Reynolds numbers of 22×10^6 and 27×10^6, respectively.

Later, Carmichael, Whites, and Pfenninger (1957) studied the impact of slot blockage on laminar flow extent for the 69 slot-suction test on the F-94A airplane. The tests were confined to the second slot of chamber 5 (or the 22nd slot of 69 at 63.42 percent chord). Paint plugs of slot chord length and with spans of 0.007, 0.0115, 0.015, 0.030, 0.20, 0.50, and 1.0 in. were individually tested. All slots maintained the normal suction distribution, whereas the suction in the slots in chamber 5 was varied. The results are summarized as (1) for the 0.007-in. plug, no turbulence was observed for the range of normal to maximum suction; (2) for the 0.0115-in. plug, turbulence was realized only after the suction was increased beyond 2.4 times the normal value; (3) for the 0.015- and 0.03-in. plugs, normal suction produced turbulence and reducing the level by 80 percent reestablished laminar flow; (4) for 0.2-, 0.5-, and 1.0-in. plugs, greater than normal suction values were limiting; and (5) the upper suction limit increased with increasing Reynolds number. Essentially, the slot blockage can cause a pair of adjacent vortices to combine and form a horseshoe vortex and lead to turbulence.

Because the X-21A wings were built from many panels spliced together on the wing, epoxy fills were required over the panel splices to meet the high unit Reynolds number step and waviness tolerances (Fowell and Antonatos, 1965). However, the epoxy encountered *cracking* and *chipping* under the wing loading and temperature changes of flight. The bonding process proved to be the cause of the fill unreliability and the process was successfully changed to achieve reliable tolerances. However, most of the ground maintenance time was charged to the repair and maintenance of these joint areas. Further laminar flow tests must carefully address this issue.

Meifarth and Heinrich (1992) had an in-depth discussion of issues relating to achieving and maintaining NLF and LFC from the operations perspective. A flow chart of multidisciplinary issues which must be addressed prior to the use and reliance of laminar flow on aircraft performance was presented. Issues which would cause an increase in DOC for aircraft and those which would cause a decrease in DOC are connected. Some issues include the need for additional spare parts and maintenance due to the suction system, uncertainties in the potential contamination due to pollution residue on the structural surface, and operational plan for suction-system failure. The latter concern affects a decrease in range and increase in fuel burn as a result of the unexpected turbulent drag.

5. Laminar Flow Control Prior to OPEC Oil Embargo

In this section, LFC projects are discussed for the time frame prior to the OPEC oil embargo. Each section has the configuration or model information, project goals, and summarized results.

5.1. B-18 Slot-Suction Glove Flight Test (1941)

Following the NLF flight test of Wetmore, Zalovcik, and Platt (1941), results of a 1941 LFC flight test experiment were reported in an NACA Wartime Report by Zalovcik, Wetmore, and Von Doenhoff (1944). A test panel with nine spanwise suction slots was mounted on the left wing (NACA 35-215 airfoil) of a B-18 airplane (provided by the Army Air Corps). The test panel shown in figure 29 had a chord of 204 in. and a spanwise extent of 120 in. at the leading edge and tapered to 60 in. at the trailing edge. The nine original suction slots were spaced 5 percent chord apart and were located from 20 to 60 percent chord. The eight additional slots were later added between each of the original slots. Suction was supplied by an 85-hp Ford engine. Below each slot, the external flow was drawn through 0.25-in-diameter holes drilled in the wood panel spaced 0.75 in. apart.

The airflow was manually regulated by butterfly valves located in the cabin. Static-pressure orifices

located in the ducts or tubes were used to measure the airflow through the slots. Numerous coats of paint, filling, and sanding were employed to smooth the surface and to achieve an acceptable surface-waviness limit. Five-tube rakes were used to measure boundary-layer profiles, and two-tube rakes were used to measure the transition location.

The flight tests were conducted for chord Reynolds numbers between 21.7×10^6 and 30.8×10^6 with airspeeds from 147 to 216 mph. Uniformly increasing, level, and uniformly decreasing suction in the chordwise direction were applied. Laminar flow back to 45 percent chord (pressure minimum point) was maintained over the range of Reynolds number and lift coefficient for suction mass flow C_q of 1.7×10^{-5} in slot 1 and decreasing to almost zero suction in slot 5. If suction was further decreased in slot 5, reverse flow in that slot led to abrupt transition. Increasing the level of suction had no additional favorable or adverse effect on the transition point. However, for uniform level or increasing suction distributions, a critical maximum level of suction ($C_q > 3.5 \times 10^{-5}$ in slot 1) led to turbulence regardless of the flight conditions. Finally, the results with 17 slots (2.5-percent-chord spacing of slots) were inconclusive because several small chordwise cracks appeared near the leading edge of the panel.

5.2. LFC Wind Tunnel Tests (1949–1963)

This section describes the early subsonic wind tunnel experiments which focused on the LFC technology.

5.2.1. Wind Tunnel Test With Porous Bronze Airfoil

Because Braslow, Visconti, and Burrows (1948) indicated that suction through a porous surface could lead to performance gain, Braslow et al. (1951) conducted a LFC experiment involving a porous-suction model in a low-turbulence wind tunnel. Using a model with a 3-ft chord and 3-ft span, experiments were carried out in the Langley Low-Turbulence Pressure Tunnel (LTPT). The upper and lower surfaces of the model were constructed from a single sheet of continuous bronze giving a single joint at the trailing edge. An estimate of the surface waviness indicated that ±0.003-in. variation occurred between the bronze surface and the inner aluminum shell. Figure 30 shows a sketch of the bronze porous sheet covering a core NACA 64A010 airfoil model perforated with 1-in-diameter holes over the center of the model and 1-in. slits at the leading and trailing edges of the model. Suction airflow measurements were made through an orifice plate in the suction duct, and suction was regulated by varying the blower speed and plate orifice diameter. Boundary-layer measurements were made on the upper surface to 83 percent chord. Laminar flow was observed to 83 percent chord for suction up to a Reynolds number of 8×10^6. An accompanying theoretical study suggested that, in the absence of roughness, full-chord laminar flow should be expected to higher Reynolds numbers if the experimental suction distribution could be made uniform.

In a follow-on test, Braslow et al. (1951) reported the wind tunnel results of an experiment using the same model but with less porosity. Full-chord laminar flow was observed up to a Reynolds number of 24×10^6. The measured drag for the laminar flow control airfoil was roughly one third of the model without suction; however, the results could not be repeated because the bronze skin buckled during testing.

5.2.2. University of Michigan Slot-Suction Wind Tunnel Tests

Pfenninger, Gross, and Bacon (1957) described the results of the LFC slot-suction experiments in the University of Michigan 5-Ft. by 7-Ft. Tunnel conducted in 1949 and 1950. Suction was applied through 86 fine slots from 25 to 95 percent chord on a 30° swept 12-percent-thick symmetric wing model. Total pressure, static pressure, boundary-layer crossflow, and the transition location were measured during the experiment. Measurements were made at various Reynolds numbers for model angles of attack of 0° and ±1°. The suction for each test case was selected based on theory. Full-chord laminar flow was observed at an angle of attack of 0° at a chord Reynolds number of 11.8×10^6. The measured minimum critical suction levels were slightly smaller than theoretical predictions; however, the measured drag closely matched the theoretical predictions. The suction level on the 30° wing was slightly larger than a 2D wing because crossflow disturbances had to be stabilized. At an angle of attack of −1°, turbulent bursts occurred for lower Reynolds numbers; this was correctly attributed to stronger crossflow.

5.2.3. Douglas Slot-Suction Wind Tunnel Test

Smith (1953) presented a review of LFC/BLC research at the Douglas Aircraft Company and noted that the program began early in 1948. The studies suggested that as the Reynolds number increased the slots must become thinner and thinner; this caused doubt about the structural feasibility of the concept. Smith conceived the idea of having several velocity discontinuities and regions of favorable velocity gradients for boundary-layer stabilization. However, such an airfoil must not separate if suction power was lost. The nature of the concept may cause shock formation at each jump; however, the suction would be sufficient to prevent separation.

To test the concept, a 2D airfoil ($G0010_7$) model was installed in a Douglas wind tunnel. The wind tunnel could reach a maximum Reynolds number of 4.25×10^6 and had a maximum fluctuating velocity of 0.1 percent of the free-stream value. The model had a 42-in. chord and had the first pressure jump at 20 percent chord. The first suction slot was put at 5 percent chord to control possible disturbances caused by simulated debris. The last 19 percent of the model was a flap covered with a sheet of porous bronze mesh for suction control. Laminar flow was easily achieved back to the flap (81 percent chord). When a flap alignment problem was corrected, laminar flow was observed back to 98 percent chord. These initial low Reynolds number wind tunnel results provided a proof of concept for the slot-suction concept with a pressure jump and verified the idea that at a pressure jump all fluid having a velocity pressure less than the prescribed pressure rise must be removed from the flow for boundary-layer stability.

The success of the wind tunnel experiment led to the development of a high Reynolds number airfoil. The new airfoil (DESA-2) had laminar flow designed to a chord Reynolds number of 50×10^6 using what is presently known as the *N*-factor correlation method (normally attributed to Smith 1956; Smith and Gamberoni 1956; and Van Ingen 1956). Note that the earlier document (Smith 1953) was classified until recently. By using the *N*-factor correlation, $N = 10$ at the trailing edge was selected as the design constraint. For $N = 6$, the critical Reynolds number was reduced to 35×10^6. Shown in figure 31, the DESA-2 model had a 6-ft chord, 9 slots on the upper surface, and 7 slots on the lower surface. Full-chord laminar flow was easily obtained up to a chord Reynolds number of 6.5×10^6 in the TDPT. Laminar flow was progressively lost with an additional increase in wind tunnel speed. Hot-wire surveys behind each slot revealed the presence of wild disturbances behind slot 6 (55 percent chord), which were most likely attributable to a 0.003-in. step. Great care was then taken to remove all discontinuities in the model. Additional tests showed that laminar flow was again lost, even though the flow was theoretically stable to TS disturbances. The results suggested that the flow was very sensitive to surface roughness. Because of the surface-roughness problems, the test data were insufficient to make any conclusions about the sawtooth pressure-jump distribution concept combined with slot suction for BLC/LFC.

5.3. Anson Mk.1 Porous-Suction Flight Test (1948–1950)

Based on porous-suction LFC wind tunnel experiments by Kay (1948), Head (1955) used an Anson Mk.1 aircraft to test the porous concept in flight tests. The goals of the study were to study laminar boundary-layer flow with uniform suction distributions for zero and adverse pressure gradients, to determine the minimum suction required for laminar flow, and to determine the effectiveness of suction in controlling transition induced by roughness and waviness.

The test section was a 2D symmetric airfoil covered with a porous nylon material (120-mesh phosphor bronze gauze) covering the suction box. In testing the concept, the results demonstrated that laminar flow was achieved at all rates of suction; turbulent flow was found on the same test section with no suction (generated by covering the suction area with an impermeable paper). For high rates of suction, loss of laminar flow occurred (in some cases), probably because of surface imperfections. Finally, Head showed that small amounts of distributed suction were ineffective in preventing transition induced by roughness; however, larger critical roughness existed with suction.

5.4. Vampire Porous-Suction Flight Test (1953–1954)

In England, LFC flight test experiments were carried out with the Vampire III single-seat fighter aircraft powered with a single Coblin II jet engine.

Head, Johnson, and Coxon (1955) reported details of the experiment, including rational for the suction system design and drag reductions obtained with suction as part of the test section. The flight tests demonstrated that full-chord laminar flow could be obtained in flight by using continuous distributed porous suction.

As sketched in figure 32, a suction sleeve (or glove) was mounted to the Vampire wing near the midspan region after the taper of the wing. The leading-edge sweep of the wing was 11.5°. The porous sleeve covered from 6 percent to 98 percent chord of the wing, with suction power drawn from a turbopump unit driven by air bled from the compressor of the aircraft engine. The sleeve was constructed such that a porous Monel Metal cloth surface was bonded to the skin which had premilled recesses to extract the air. The sleeve was compartmented to form 19 ducts, which led the air through two venturi tubes to the pump (mounted at the wing root).

No attempt was made to theoretically design an optimal glove geometry; instead the basic wing shape was used to simplify the sleeve construction. Calculations for an optimum suction distribution were made at a chord Reynolds number of 20×10^6. The resulting suction distribution which led to a neutral laminar boundary layer was used as a guide for designing the suction system. Surface waviness was limited by applying filling; the maximum waviness was measured at ±0.005 in., which was very good for production-type standards of that time.

Approximately 90 copper tubes were run in the sleeve to measure the external surface pressures, pressures in the ducts, and pressures downstream of the orifice plates. From the difference between the pressure in and out of the duct, a chordwise suction distribution could be obtained. The boundary-layer velocity profile at the trailing edge of the wing, the chordwise pressure distribution around the sleeve and leading edge, and the total suction flow from each collector were recorded during the flight. The pilot could vary the suction flow and pump operating conditions while in flight.

See section 4.1 for a discussion of the method used during the Vampire flight test to avoid insect contamination.

The initial flights with and without suction indicated that transition occurred very near the leading edge of the sleeve and that this was likely roughness-induced transition due to the surface quality of the Monel Metal cloth. Instead of trying to improve the Monel Metal cloth surface quality, a nylon parachute fabric was added to cover the cloth. After carefully applying this fabric, full-chord laminar flow could be achieved for chord Reynolds numbers of 16.4×10^6. For higher Reynolds numbers, roughness-induced transition occurred due to flaws in the nylon covering. However, for the lower Reynolds numbers, the results showed that a 70- to 80-percent overall reduction in profile drag (accounting for suction penalties) was realized with the porous-suction LFC system.

In the final series of flight tests, significant and careful effort was concentrated on reducing the roughness in the leading-edge region up to about 15 percent chord. By doing this, full-chord laminar flow was realized for a Mach number of 0.70 and chord Reynolds number of 26×10^6. Laminar flow at higher Reynolds numbers was not achieved (likely) because of surface waviness.

A comparison of the calculated and measured velocity profiles showed significant disagreement; this suggests that the suction flow through the surface was less than what the ventures recorded or that the theoretical description of the problem was not adequate. Unlike many of the LFC flight test experiments, the report by Head, Johnson, and Coxon (1955) pointed to deficiencies in the theoretical prediction capability of that era. Namely, the inability to determine slot-suction spacing and minimum suction requirements for laminar flow were noted along with the inability to determine suitable hole sizes and spacings for porous suction. As seen in section 6.1.3, some 40 years have passed since this flight experiment and these issues are only now being addressed by careful wind tunnel experiments.

5.5. F-94A Slot-Suction Glove Flight Test (1953–1956)

Supported by the U.S. Air Force and conducted at Northrop Aircraft, Inc., Pfenninger et al. (1955) and Carmichael, Whites, and Pfenninger (1957) describe the LFC slot-suction experiment using a glove on the F-94A airplane. The flight test was conducted to

extend the use of suction LFC in flight at high Reynolds numbers. Because turbulence levels and roughness effects due to high unit Reynolds numbers impact the laminar flow extent in the wind tunnels, it was determined that flight experiments were necessary for concept validation. To make a comparison with the wind tunnel results of Pfenninger (1951), the suction wing for the flight test was designed with a similar suction arrangement. As shown in the sketch of figure 33, the glove was mounted on the left wing of the F-94A, where suction was implemented on the upper surface only. Twelve suction slots were located between 41.5 and 95 percent chord. Remote control was used to adjust needle valves to change the chordwise suction distribution; the suction compressor was externally mounted in a pod on the fuselage behind the wing.

Low surface waviness was achieved by sanding and polishing the test article. No roughness-induced transition was realized up to chord Reynolds numbers of 28×10^6 (unit Reynolds number per foot of 3.73×10^6). Static pressure and temperature measurements of the suction chamber, static pressure on the upper surface of the glove, and boundary-layer measurements at the trailing edge of the upper surface were made in the course of the flight test.

Full-chord laminar flow was observed on 21 of 23 consecutive flights. Two flights were not successful because of leading-edge contamination by bugs and sand particulate. For chord Reynolds numbers ranging from 12×10^6 to 30×10^6 and Mach numbers 0.6 to 0.65, the glove had 100 percent laminar flow. The drag decreased with increased Reynolds number until a minimum was reached at the chord Reynolds number of 22×10^6. As the Reynolds number was increased, the drag unexplainably increased with Reynolds number. (No mention was made of C_q levels.)

In follow-on studies, Groth et al. (1957) and Pfenninger and Groth (1961) reported the results for an LFC slot-suction experiment using the F-94A airplane and a glove with 69 suction slots. The justification for the additional slots was that such a multiple slot configuration would be applicable to an actual airplane wing (i.e., the distance between slots should be minimized to avoid premature transition to turbulence in a high chord Reynolds number flow).

The design of the 69-slot glove was based on the pressure and suction distribution measured on the 12-slot glove. However, a variation in the hole sizes for each slot accounted for the different pressure losses of the sucked air resulting from a variation in the chord pressure along a chamber. The slot widths were selected to balance a local deceleration of the flow due to wide slots (potentially causing premature transition) and high flow velocities in narrow slots (causing unnecessary pressure losses). Furthermore, the issue of surface waviness was controlled by polishing the surface until the waviness was reduced to 1/3000 in/in (height-to-length ratio) or less.

The flight measurements with the 69-slot experiment were made in the same manner as the 12-slot study. Laminar flow was achieved and maintained in flight for chord Reynolds numbers ranging from 12.25×10^6 to 36.34×10^6, resulting in drag reductions for all cases. No attempt was made to minimize the drag by varying the suction distribution. Unlike the drag rise with maximum chord Reynolds number for the 12-slot configuration, no drag rise was realized in the 69-slot test. Groth et al. (1957) postulated that the increase in drag for the wider spaced slots could be caused by the amplification of three-dimensional disturbances (crossflow and/or Görtler) or two-dimensional disturbances that may have locally been amplified between the slots. If the drag increase was due to crossflow disturbances, then stronger suction would be required at higher Reynolds numbers; this would result in increased suction drag and wing profile drag. In addition, the flight tests showed that lower Mach numbers (reduced flight speeds) caused an increase in lift coefficient, a forward shift of the pressure minimum, and, therefore, a loss of 100 percent laminar flow. For flights conducted at high subsonic Mach numbers (≈0.70), regions of local supersonic flow on the glove limited the desired 100 percent laminar flow. For local Mach numbers greater than 1.10, it was not possible to maintain laminar flow back to the trailing edge of the test section.

See section 4.1 for a discussion of insect contamination avoidance during the slot-suction LFC F-94A flight test.

Pfenninger and Groth (1961) additionally discussed an 81 slot-suction experiment which used the 69-slot approach with 12 additional slots (and

4 chambers) in the region of 8 to 41 percent chord. For higher Reynolds numbers, the 81-slot configuration had a drag increase compared with the 69-slot configuration; however, at lower Reynolds numbers and higher lift coefficients the drag was less than the previous 69-slot test.

5.6. Later Subsonic Slot-Suction Wind Tunnel Tests (1958)

Carmichael and Pfenninger (1959) reported the results of slot-suction LFC wind tunnel experiments on a 30° swept-wing model. The tests were carried out in the University of Michigan 5-Ft by 7-Ft and the NORAIR 7-Ft by 10-Ft Low-Turbulence Tunnels with the goal of determining whether surface waviness was more critical on swept suction wings compared with unswept suction wings. Previous results by Pfenninger, Gross, and Bacon (1957) and by Bacon, Tucker, and Pfenninger (1959) obtained full-chord laminar flow to the trailing edge of a swept wing with 93 suction slots for LFC. The model had a 7-ft chord and the tunnels operated at unit Reynolds number per foot of 1.7×10^6 or a chord Reynolds number of approximately 12×10^6. The surface waviness of the model was 1/3000 in/in, and suction slots were located from 0.5 to 97 percent chord. Fairings were applied at the tunnel walls to remove three-dimensional effects, and an angle of attack of 0° was imposed on the test article. The F-94A flight test parameters were used to guide the wind tunnel experiment. Sine-curve waves were constructed of Reynolds Wrap aluminum foil and layered using silicone adhesive. The experiments were conducted with the slots covered by the waves (foil). The results showed that waves of different length become critical when h^2/λ is a constant (consistent with the work of Fage (1943) and the F-94A flight test results). From the database, the critical waviness for swept laminar suction wings was defined as outlined in section 3.2. However, from the limited results it appears that multiple waves have smaller allowable wave ratios than single-wave allowables. Finally, by sealing some of the slots, the slot spacing was increased from 0.55 percent (0.4 in.) to 2.2 percent (1.6 in.) chord to determine a measure of sensitivity for more practical applications. No significant difference in the results was observed in the experiments with fewer slots.

Gross (1964) reported the results of experiments that were conducted in the NORAIR 7- by 10-Foot Wind Tunnel using a 17-ft chord, two-dimensional, 4-percent-thick slot-suction laminar flow airfoil. One hundred suction slots were located from 1 to 97.2 percent chord. The spanwise extent of the slots reduced from 77.4 in. at the first slot to 15.2 in. at the last slot. Full-chord laminar flow was achieved up to a chord Reynolds number of 26×10^6. It was suspected that the wind tunnel flow quality contaminated the laminar flow for larger Reynolds numbers.

Bacon, Pfenninger, and Moore (1964) reported the experimental results of (1) a 4-percent-thick straight laminar suction wing and (2) a 30° swept, 12-percent-thick, 7-ft chord laminar suction wing in the NORAIR 7- by 10-Foot Wind Tunnel to investigate the influence of sound and vibration on the laminar flow extent achieved with LFC suction through slots. Naphthalene sublimation pictures showed that the introduction of sound for the swept wing resulted in transition in the flat pressure region of the wing and the appearance of crossflow vortex signatures prior to transition. The straight wing results indicated that the frequency dependence of transition and sound correlated with the theory for Tollmien-Schlichting waves. For vibration, additional suction was required to maintain laminar flow.

Gross and Bossel (1964) discussed the experiments and theoretical analysis of a LFC slot-suction body of revolution. The experiments were conducted in the NORAIR 7- by 10-Foot Wind Tunnel, and the 30° swept-wing model had 120 suction slots. The suction slots were connected to 13 suction chambers. The 0.003-in. slots were spaced 2 in. apart from 4.84 to 75 percent of the model length and were spaced 0.5 in. from 75 to 100.4 percent of the model. (Note, 100.4 percent of the model indicates that the last slot was partially positioned on the sting.) Laminar flow to a length Reynolds number of 20.1×10^6 was realized with the LFC. The theoretical analysis was comparable with the experiments; however, some disagreement was found because the experiments could not attain the pure axisymmetric-symmetric flow assumed in the theory.

Gross, Bacon, and Tucker (1964) reported the results of a LFC slot-suction experiment conducted in

the Ames 12-Foot Pressure Tunnel. The model had 93 slots of 0.004 to 0.005 in. wide extending to 97 percent chord of the model. The results showed laminar flow extent to a chord Reynolds number of 29×10^6.

5.7. Supersonic Slot-Suction Wind Tunnel Tests (1957–1965)

Virtually all the wind tunnel and flight test experiments relating to LFC were conducted in the subsonic flow environment. However, there are a few unclassified supersonic LFC-related wind tunnel experiments.

Groth (1961) reported the results of supersonic LFC slot-suction wind tunnel experiments conducted during 1957 and 1958. Groth, Pate, and Nenni (1965) reported the results contracted to Northrop Aircraft from the U.S. Air Force through 1965. The first study was conducted in a supersonic wind tunnel at the U.S. Navy Ordinance Aeronautical Laboratory in Texas. The model was a biconvex, 5-percent-thick, 20-in-chord two-dimensional airfoil. Tests were run for Mach numbers of 2.23 and 2.77. Between 23.5 and 90 percent chord, 19 slots were cut in the model with suction extracted into four chambers. The spanwise extent of the slots decreased from 6.28 in. for the first slot to 2.56 in. for the last slot, corresponding to the 8° taper consistent with observed turbulent wedge spreading angle. Pressure orifices, thermocouples, and boundary-layer rakes were used for the measurements. Boundary-layer measurements were made for several suction distributions. For the preliminary tests with no suction, transition occurred at 40 and 30 percent chord for Mach numbers of 2.23 and 2.77; this resulted in transition Reynolds numbers of 5.1×10^6 and 3.9×10^6, respectively. With the suction model, shock waves were observed originating from each slot. The strength of the waves increased with increased suction. Laminar flow was observed at an angle of attack of 0° for the suction distributions used.

Groth (1961) noted that additional tests at Mach numbers of 2.5, 3.0, and 3.5 were conducted in 1958 in tunnel E1 at Arnold Engineering Development Center (AEDC) in Tennessee. A 20-caliber ogive cylinder, 3.25 in. in diameter (maximum) and 14.443 in. long, was used for the model; 16 suction slots were located between 5 and 22 in. of the cylinder with 4 slots connected to one chamber. (Note, the ogive cylinder model was connected to a cylinder to form a total model length of 40 in.) For a Mach number of 2.5, the drag without suction was 1.35 times the friction drag of a laminar flat plate and the flow was laminar to a Reynolds number of 6×10^6. To recover the same drag by using suction to achieve laminar flow, the Reynolds number was 9×10^6. Drag increased as the Reynolds number was increased. For a Mach number of 3.0, the test article with no suction had laminar flow for a Reynolds number of 4.5×10^6. With suction, the same drag could be achieved with a Reynolds number of 6×10^6.

A single-slot, 9.25-caliber ogive cylinder was tested at a Mach number of 2.9 in the 8-Inch by 13-Inch Supersonic Blow-Down Tunnel at the University of Michigan to study the flow physics near a slot. Boundary-layer profiles were measured ahead and aft of the slot with a total-pressure survey. A discussion was given by Groth of the local Mach number and pressure variations near the slot and its impact. Shock waves emulating from the suction slot increased the suction drag by approximately 10 to 15 percent. Groth (1961) suggested that the installation of many fine slots would reduce this shock-induced drag.

Groth (1964a), Jones and Pate (1961), and Groth, Pate, and Nenni (1965) reported on experiments conducted in 1961 in the 1-m × 1-m (40-in. × 40-in.) supersonic tunnel at Arnold Engineering and Development Center. A flat-plate model with a 41-in. chord, 40-in. span, and 76 spanwise suction slots was used in a Mach number 2 to 3.5 supersonic flow to study the feasibility of LFC for supersonic flows. The slot width ranged from 0.004 in. in the front to 0.005 in. in the rear of the model. Below the slots, 0.2-in-deep holes with diameters of 0.042 to 0.062 in. were drilled 0.25 in. apart. The instrumentation could measure surface pressures on the model, suction chamber and metering box pressures, and temperatures. A rake was positioned at the rear of the model to determine the state of the boundary layer. For Mach numbers of 2.5, 3.0, and 3.5, full-chord laminar flow was observed to Reynolds numbers of 21.8×10^6, 25.7×10^6, and 21.4×10^6, respectively (up to the tunnel limit). The resulting reduction in skin friction drag of 28 and 43 percent of the turbulent plate values was achieved with suction mass flow coefficients of 2×10^{-4} and 3×10^{-4}. These laminar flows were obtained by TS-disturbance stabilization where compressibility

helps considerably; crossflow disturbances were absent from this two-dimensional flow. The measured boundary-layer thickness and wake drag coefficients were 40 to 80 percent larger than the theoretical data for the same suction coefficients. This difference may be attributable to spanwise contamination in the experiments or the presence and influence of a detached shock wave from the blunt leading-edge plate, which is not accounted for in the theory.

Shock-wave boundary-layer interaction studies were conducted by Greber (1959) at Massachusetts Institute of Technology and in 1962 by Groth (1964a) at AEDC to determine if slot-suction could be used to achieve laminar flow behind a shock wave. Using strong suction in the shock-interaction zone, both studies observed laminar boundary layers downstream of the shock impingement area; this means that with suction, a stronger shock was required to separate the flow. Again, crossflow disturbances were not present in these LFC shock–boundary-layer interaction studies.

Additional tests were reported by Groth (1964b) at Mach numbers of 2.5, 3.0, and 3.5, which were conducted in 1961 in tunnel E1 at Arnold Engineering Development Center. A 20-caliber ogive cylinder, 3.25 in. in diameter (maximum) and 14.443 in. long, was used for the model, which had the same dimensions as the 1958 model. An improved suction system was used and 29 closely spaced suction slots were located between 4.5 in. and 18 in. at spacings of 0.5 in.; this led to a more continuous distribution of suction compared with the 1958 LFC model. A total-pressure head rake was mounted aft of the last slot to measure the state of the boundary layer. Full laminar flow was observed for chord Reynolds numbers of 15.3×10^6 for Mach number 2.5, 11.5×10^6 for Mach number 3.0, and 6.3×10^6 for Mach number 3.5. The experimental boundary-layer thickness measurements were shown to be 22 percent thicker than theoretical estimates; however, the theory did not account for potential shock waves emanating from the slots. Additionally, the effect of surface roughness on the laminar flow extent was measured at Mach number 3.0 and unit Reynolds number per foot of 10×10^6. A 0.093-in-diameter disk with height of 0.0035 in. was placed at 2.0 in. on the model. With no suction, transition moved upstream from 14 to 12 in. with the roughness present for a Reynolds number of 6.3×10^6; however, with suction, laminar flow was maintained. At higher Reynolds numbers suction could not maintain laminar flow. The critical roughness heights of 0.001 to 0.002 in. were determined for this high unit Reynolds number.

Pate (1965) and Groth, Pate, and Nenni (1965) reported on wind tunnel results of a LFC 9.2-in. cylindrical body of revolution. Suction was applied through 150 slots on the model. Laminar flow was observed at Mach number 2.5 to a length Reynolds number of 42×10^6 and at Mach number 3.0 to a Reynolds number of 51.5×10^6. The total drag at Mach number 3.0 was only 23 percent of the turbulent friction drag on a flat plate.

To verify the benefits of suction LFC for swept supersonic wings, Groth (1964c) and Pate and Deitering (1963) reported the results of experiments with a 3-percent-thick, 36° biconvex suction-slot wing tested in 1962 in the 1-m × 1-m tunnel at AEDC for Mach numbers 2.5, 3.0, and 3.5. The purpose of the test was to demonstrate supersonic slot-suction LFC in the presence of crossflow disturbances. The wing had a 39-in. flow-direction chord (31.5-in. perpendicular chord) and 66 slots. Two models were tested. The first model, which had insufficient suction distribution at high Mach numbers, had the first slot at 1.6 in. aft of the leading edge. No laminar flow was observed with the first model for Mach number 3.5. The second model (or modified model) had the first slot at 0.76 in. down from the leading edge. Full laminar flow was observed for length Reynolds numbers of 17×10^6 for Mach number 2.5, 25×10^6 for Mach number 3.0, and 20×10^6 for Mach number 3.5. However, the drag coefficient was somewhat higher and was presumed to be influenced by three-dimensionality in the tunnel.

Goldsmith (1964) reported results conducted in 1963 in the same AEDC tunnel but with a 72° swept-wing model and at flow conditions of Mach numbers of 2.0 and 2.25, giving a subsonic leading edge to a supercritical leading edge. Contoured wind tunnel wall liners were installed to simulate an infinite (two-dimensional flow) swept wing. The model had a 10-in. chord perpendicular to the leading edge and a 33-in. chord in the streamwise direction. Sweeping the wing beyond the Mach angle zeros the lift wave drag; however, this benefit may be offset by increases in induced drag. To prevent this increase in induced drag, the aspect ratio of the highly swept wing must lead to an

increased wetted area. Increases in wetted area would suggest the benefits of LFC (skin-friction reductions) would be profitable. Slot suction was used with slots being as narrow as 0.003 to 0.0035 in. and spaced 0.08 in. (0.27 in. in the streamline direction) apart. Three rows of 13 pressure taps were used in addition to the measurements made by Groth (1964a) for the LFC suction system. The total drag measurements for the flow at a Reynolds number of 9×10^6 were low and indicated that the flow was laminar; the drag rose quickly for an increase in Reynolds number. Turbulent contamination along the attachment line was suggested as the culprit for the sudden drag increase. The results at Mach number 2.25 were sparse and inconclusive.

Further study of highly swept wings by Goldsmith (1964) focused on the influence of the spanwise velocity component on slot losses. Previous incompressible calculations have assumed that the slots were two-dimensional channels with no density changes in the slot; however, for supersonic flows, the calculated losses should account for density variations. In addition, an account of the spanwise velocity component should be considered for swept slots. The procedure for calculating the losses through a swept slot was rather lengthy compared with that for unswept slots; however, the new procedure indicated a 22-percent increase in losses for an example problem of a 72° swept slot. This value indicated the potential significance of including the spanwise component. The new procedure used for an unswept case gave the same results as the prior two-dimensional approach.

Finally, Pate (1964) and Groth, Pate, and Nenni (1965) reported the results of slot-suction LFC swept-wing models tested in the 1-m × 1-m supersonic tunnel at AEDC. As sketched in figure 34, 36° and 50° swept-wing models with 68 and 67 slots, respectively, were used for the tests. For Mach numbers of 2.5, 3.0, and 3.5, laminar flow was achieved on both models, with full-chord laminar flow being observed on the 36° model. These results shown in figure 35 demonstrate that drag reductions can be achieved by using LFC in supersonic flow. More specifically, the slot-suction LFC flat-plate and swept-wing results are compared with one-third turbulent skin friction on a flat plate. Then the total drag using LFC was a fraction of the turbulent flow skin friction. Groth, Pate, and Nenni (1965) noted that suction requirements increased with increased Mach number and with increased crossflow. Unlike the flat-plate model, the swept-wing models were sensitive to the local suction distribution. Two additional slots were added to the 36° model in the leading-edge region to provide adequate suction with increased Mach and Reynolds numbers.

5.8. X-21A (WB-66) Slot-Suction Flight Test (1960–1965)

The July 1966 issue of AIAA *Astronautics and Aeronautics* was devoted to discussions on the prospects of Laminar Flow Control and the X-21 LFC flight test. This section summarizes the content of those articles (which primarily focused on work by Northrop and the Air Force Systems Command), the June 1967 report of the Northrop Corporation (Kosin 1967), papers by Whites, Sudderth, and Wheldon (1966) and Pfenninger and Reed (1966), and AGARD reports by Pfenninger (1965) and Fowell and Antonatos (1965), which summarized the X-21A slot-suction flight experiment and the state of the art in LFC aircraft of that era. Northrop modified two WB-66 aircraft to incorporate LFC technology on the wings to demonstrate the feasibility and practicality of the design, manufacturing, operation, and maintenance of LFC aircraft systems. Modifications of the WB-66 aircraft included the removal of the original wings and their replacement with LFC slot-suction wings, the removal of the engines and replacement with aft-mounted engines, and the installation of LFC suction compressors in pods mounted under the wings. Figure 36 shows a modified X-21A aircraft.

Nenni and Gluyas (1966) discussed the aerodynamic analysis involved with slot-suction LFC design. In the 1960s, the analysis consisted of defining a wing pressure and velocity distribution, followed by calculations of the viscous boundary-layer flow over the wing, then the suction required to stabilize the boundary layer was determined, and finally the slot spacing and size and the suction system were prescribed. The process was iterative until the desired design was obtained. By establishing the wing geometry, the wing pressures and velocities can be obtained with transonic wing theory. Notably, the pressure isobars should be straight and constant along the wing span both to allow the suction slot to see a constant pressure and to minimize the boundary-layer crossflow over a large

portion of the wing. The inverse problem of prescribing the pressure and solving for the wing geometry could not be tackled at that time. Local deviations from the desired pressure did not hinder the attainment of laminar flow (for full-chord LFC applications). After obtaining the external flow field, boundary-layer calculations provided velocity profiles and integral thicknesses for comparison with established criteria for the boundary-layer instability to determine transition locations. If the ideal straight isobar wing was approached, the three-dimensional boundary-layer system could be simplified with a conical flow assumption. This assumption was used over most of the X-21A wing, with full three-dimensional calculations being made at the wingtip and wing root.

The X-21 had a wing sweep of 30° and a flight envelope with Mach numbers from 0.3 to 0.8 at altitudes from 5000 to 44 000 ft. Approximately 160 hr of high-speed and 1300 hr of low-speed wind tunnel tests were carried out with a model X-21A wing to validate the wing-design concept. Good correlation was later found in comparing the wind tunnel and flight experiment results for the effects of aeroelasticity and flight pressure distributions on the wing. To prevent attachment-line contamination resulting from the wing–fuselage juncture, the X-21A used a fence, vertical slots, and a gutter.

For the suction system boundary-layer calculations, a continuous-area suction assumption was used to approximate the actually discrete distributed suction which occurred in steps. Boundary-layer stability analysis provided the necessary information for determining the adequate suction flow rates. A typical value of the slot Reynolds number was 100, and typical suction quantity coefficients range from $v/U_\infty = 5 \times 10^{-4}$ in relatively flat pressure regions to $v/U_\infty = 10 \times 10^{-4}$ near the leading edge of the wing. In the leading-edge region, the chordwise slots were 0.0035 in. wide and spaced 0.75 in. apart and were used to control the flow on the attachment line. Strong suction was required near or on the attachment line so that the momentum-thickness Reynolds number did not exceed 100. In the spanwise direction, the slots were varied in width so that the velocity would gradually be reduced to zero as the end of the slot was reached to minimize the potential for vortex formation there. Typical values of the slot spacing/width include 1.1/0.003–0.004, 2.0/0.006–0.007, and 1.2/0.005 in/in for regions on the wing of 1 to 5, 5 to 40, and 40 to 100 percent chord, respectively. The flow passed from the slot in the skin through the holes in the structure below the skin, to the duct via the plenum chambers beneath the slots, and through the plenum ducts and flowmeter nozzles through the inner skin. These slot plenum and holes were designed to provide a uniform suction distribution along the suction slot to minimize the potential for disturbances. For the X-21A suction system, 96 suction control valves were employed to independently control the suction in each slot. The airflow rates for the system were operational from 85 to 130 percent of the designed nominal flow rate to provide variations to validate the unproven method for estimating the airflow. For example, the flight condition at an altitude of 43 000 ft and a Mach number of 0.75 had airflow ranging from 1.94 to 7.18 lb/sec. For the theoretical description of the suction system involving a continuous distribution, the flight-observed and theoretically predicted suction over the wing chord agreed reasonably well except for the lower surface outboard region. Whites, Sudderth, and Wheldon (1966) showed that for a Mach number of 0.74 and altitude of 41 400 ft, the flight measured and predicted suction distribution agreed in shape but differed in level by 50 percent, with theory underpredicting the requirements.

To measure the local state of the boundary layer, total-pressure rakes were mounted at the trailing edge of the wing. Single probes were positioned at a height slightly above the laminar boundary-layer thickness. When the state of the boundary layer was laminar, the probe recorded a full free-stream total pressure; otherwise, a smaller pressure was recorded due to the probe being immersed in a turbulent boundary layer. The relationship between the pressure loss and the transition location was made both analytically and in flight. Probes were used to measure velocity fluctuations within the boundary layer. Microphones mounted with diaphragms flush to the surface were used to measure both velocity fluctuations and to determine sound levels above the wing.

Concerning the issue of allowable or tolerable waviness and roughness, the report (Kosin 1967) documents the flight condition of a Mach number of 0.8 and an altitude of 45 000 ft, the permissible step heights were 0.02 in. for forward-facing steps, 0.009 in. for rearward-facing steps, and 0.25-in. widths for spanwise running gaps. The permissible

amplitude to wavelength was much less than 0.004 (waviness criteria). The flight tests showed that the wing can tolerate a 0.125-in. gap with a depth of 0.18 in. on the lower left outboard wing at 60 percent chord, 0.04-in. gaps at 44 percent, and 32 percent chord without the loss of laminar flow. The addition of gaps of 0.05 in. at 15 percent chord and 0.08 in. at 8 percent chord required a lowering of the suction in the forward ducts to maintain laminar flow. The results of waviness studies showed that waves as far apart as the front and rear spars can be treated by single wave criteria rather than multiple wave criteria.

The impact of acoustic disturbances on transition was also tested in the X-21A program. The sound was introduced ahead of the 15-percent-chord position (front spar). There was a lack of evidence that internal noise caused any deterioration of the laminar flow. This impact may be caused by insufficient intensity of the sound at the critical frequencies even with sound 10 to 15 percent above normal levels in the duct or it may be caused by the sound not being introduced at the most critical chordwise position. Slot Reynolds numbers from 120 to 140 were shown to create a disturbance at the slot-wing intersection that dominated any potential disturbance from the internal duct sound pressures. Finally, tests showed that structural vibrations within frequencies 400 to 1800 Hz at magnitudes above the normal vibration environment did not affect the laminar flow extent.

Companion wind tunnel tests were performed to verify that a sudden loss of laminar flow would not cause control problems on a LFC aircraft. The results showed that the lateral-directional and long-period longitudinal dynamic motions may require more stringent artificial damping than the minimum acceptable requirements on the turbulent aircraft. However, both motions are of sufficient duration that the pilot corrective action can be applied and the aircraft dynamics does not present a danger to flight safety.

An interesting conclusion from Kosin (1967) suggested that future studies should seek to reduce the boundary-layer disturbances which are generated in the wing-nose region of the aircraft.

For the flight tests beginning in 1963, the results showed progressively increasing regions of laminar flow, culminating at the end of the year with nearly 60-percent-chord laminar flow at a mean aerodynamic chord Reynolds number of 20×10^6. During 1964, the laminar flow region was extended to 70 percent chord at that Reynolds number and from 30- to 55-percent-chord laminar flow at a Reynolds number of 30×10^6. During 1965, laminar flow was realized up to 96, 81, and 59 percent chord for Reynolds numbers of 20×10^6, 30×10^6, and 40×10^6, respectively. The X-21A program completed more than 200 LFC flights. Figure 37 shows sample results obtained during the flight test for a Mach number of 0.7, altitude of 40 000 ft, and a chord Reynolds number of 20×10^6; 74 percent of the upper surface and 61 percent of the lower surface had laminar flow.

See section 4.2 for a discussion of the impact of cloud particulate on laminar flow during the X-21A flight test.

Using criteria from previous experiments, the analysis required that the momentum-thickness Reynolds number on the attachment line be less than 100. The second derivative of the velocity at the wall led to momentum-thickness Reynolds number correlations for both tangential and crossflow instabilities. Although suction was applied in discrete steps (slots), the calculated suction requirements assumed continuous suction on the surface. The suction system should be designed to keep slot Reynolds numbers below approximately 100 to prevent the generation of disturbances by the slot flow. With the suction flow rate determined from boundary-layer stability considerations, the pressure drop through the skin must be set to obtain the desired flow rate.

6. Laminar Flow Control After OPEC Oil Embargo

Because of the impact of the OPEC oil embargo on fuel prices in the United States in the 1970s, the Laminar Flow Control project (under the NASA ACEE Program) was formed to help improve aircraft cruise efficiency. The major NLF and LFC projects in the United States included various general aviation flight tests, F-111 TACT, F-14 VSTFE, Boeing 757 NLF glove flight experiments, a LFC wind tunnel experiment, advanced airfoil development for NLF, and the Jetstar LFC flight experiment. See appendix A for a discussion of many of the subsonic NLF results. This section contains LFC projects in the United States and Europe after the OPEC oil embargo.

6.1. Boeing Research Wind Tunnel LFC Test (1977–1978)

Kirchner (1987) discussed a slot-suction LFC swept-wing experiment that was conducted in the Boeing Research Wind Tunnel. The principal goals of the test were to demonstrate the functionality of the suction system, to establish the required suction distribution, and to explore the sensitivity of the flow to suction level. A 30° swept-wing model with a 20-ft chord was designed with slot suction over the first 30 percent chord for the upper surface and the first 15 percent chord for the lower surface for the design condition of Mach number 0.8. Confidence in the design and analysis tools and the experimental diagnostic tools were the only results reported as products of that LFC wind tunnel experiment.

6.2. Langley 8-Foot Transonic Pressure Tunnel LFC Wind Tunnel Test (1981–1988)

In 1975, Werner Pfenninger devised a wind tunnel experiment to determine the impact of a large supersonic zone on a supercritical wing (concept by Whitcomb and Clark 1965) and application of suction (slotted and perforated) LFC to control the boundary-layer stability characteristics (Bobbitt et al. 1992).

The tunnel of choice during 1976 was the Ames 12 Foot Pressure Tunnel because of its good flow quality, demonstrated by the previous achievement of full-chord laminar flow on a swept wing. (See Gross, Bacon, and Tucker, 1964.) However, funding commitments to make flow-quality improvements to the Langley 8-Foot Transonic Pressure Tunnel (TPT) changed the preferred tunnel to the 8-ft TPT in 1978. In the 1980 time frame, the scope of the experiment was modified from slot suction only to include a perforated-suction panel, and in 1985, the plan was modified to include the LFC capability with suction on the first 20 percent chord of the model. The first test with a slot-suction model began in 1981 and ended in 1985; perforated-suction testing began in 1985 and ended in 1987; the HLFC test began in the winter of 1987 and ended in 1988.

Harvey and Pride (1981) discussed the design of the LFC suction system and required modification to the tunnel. To minimize the impact of wind tunnel free-stream turbulence vorticity, noise, and thermal spottiness on transition, antiturbulence screens, honeycombs, and a sonic choke were employed in the 8-ft TPT. The level of u/U_∞ dropped to between 0.03 and 0.06 percent. To simulate an infinite wing flow, upper and lower tunnel wall effects were removed by installing foam wall liners. Figure 38 shows a sketch of the swept-wing model and wall liners installed in the 8-ft TPT wind tunnel with the anticipated turbulent regions.

Bobbitt et al. (1992) expanded on the discussion to include the design of the tunnel liner, swept LFC wing model, and the type and location of the instrumentation. For a 7.07-ft-chord model, the airfoil design had a 12-percent-thick 23° swept-wing model, Mach number 0.82, $C_L \approx 0.47$, and a chord Reynolds number of 20.2×10^6. In the design of the LFC model, CF disturbances were kept small to prevent CF-TS disturbance interactions because the linear design theory could not account for nonlinear interactions. To optimize the design, many iteration cycles were required consisting of computing the mean-flow fluid dynamics and the boundary-layer stability properties for specified suction levels. The SALLY (Srokowski and Orszag 1977) and MARIA (Dagenhart 1981) boundary-layer stability codes were used for the analysis. For all calculations, distributed suction over 1.5 to 25 percent chord was enforced with $C_q = -0.00015$. For the design, an adverse pressure gradient existed to about 25 percent chord followed by a favorable gradient. The model had suction capability to 96 percent chord on the upper surface and to 85 percent chord on the lower surface, with different pressure gradients providing the potential for studying both TS and CF disturbances. Partial-chord suction coupled with the favorable pressure gradient prevented the CF disturbances from growing beyond $N = 4$. The TS disturbances grew to $N = 10.36$ at 70 percent chord. A chief concern of the design process was the supersonic bubble height limitation (distance between model and tunnel wall) and the desire for stable upper surface flow.

Brooks and Harris (1987) noted that, for the slot-suction LFC test, full-chord laminar flow was obtained on the upper and lower surface for a Mach number of 0.82 and a chord Reynolds number of 12×10^6 (unit Reynolds number per foot of approximately 1.7×10^6). The sonic bubble associated with the flow on the upper surface of the model was slightly larger than designed, partially because of the inability

to adequately account for boundary-layer displacement effects in the design analysis. The flow remained shock free below a Reynolds number of 10×10^6. The required suction levels were higher in the experiment than predicted with the theory. A partial explanation for these higher suction requirements could be attributed to wind tunnel free-stream disturbance levels (not accounted for in the design), surface pressure irregularities, and upper surface high velocities.

The transition front for a Reynolds number of 10×10^6 has moved from the trailing edge upstream at a nonuniform rate (i.e., the simulated infinite wing had some wind tunnel wall influences) as the Reynolds number was increased. For Reynolds numbers between 11×10^6 and 13×10^6, transition on the upper surface moved upstream to about 80 percent chord and to about 65 percent chord as the chord Reynolds number approached 20×10^6. On the lower surface, transition moved to about 75 and 30 percent chord for Reynolds numbers of 13×10^6 and 15×10^6. A total drag reduction of about 60 percent was realized with the swept slot-suction supercritical wing compared with the unswept supercritical turbulent wing (Bobbitt et al. 1992).

The influence of Mach number on the transition location is shown in figure 39. Increasing the Mach number had a stabilizing influence on the boundary-layer instabilities and the transition location moved downstream, except at Mach number 0.811 where the transition location moved upstream. Bobbitt et al. (1996) noted that a significant change in the pressure took place near Mach number 0.8, which caused dramatic alterations. These alterations may be due to the supersonic bubble contacting the wind tunnel wall.

Using the slot-suction model, a simulation of HLFC was attempted simply by progressively turning off suction over the rear portion of the model until suction was only applied near the leading-edge region. For a chord Reynolds number of 10×10^6, full-chord laminar flow moved to 53-percent-chord laminar flow using suction only in the first 25 percent chord. At a chord Reynolds number of 15×10^6, the influence of chordwise suction extent on the amount of laminar flow is shown in figure 40. The results indicated that after about 15 percent chord, the extent of laminar flow significantly increased with additional suction from 15 to 20 percent chord.

The compressible boundary-layer stability code COSAL (Malik 1982) and the incompressible SALLY code (Srokowski and Orszag 1977) were used to analyze TS disturbances and MARIA (Dagenhart 1981) was used to analyze CF disturbances to correlate computed *N*-factors with the observed transition locations on the slot-suction wing model. For a Mach number of 0.6 and a chord Reynolds number of 10×10^6, incompressible TS-disturbance analysis showed that growth of the disturbances occurred over the first 15 percent chord and suggested that $N = 10$ would correlate with the observed transition location. Over the Mach number (less than 0.7) and Reynolds number range, *N*-factors correlated with the experiments ranged from 8.5 to 10.5 for TS disturbances. Incompressible CF-disturbance analysis showed that over the same range the amplification of the disturbance did not exceed $N = 2.5$; this indicated that the transition process on the wing was primarily TS-disturbance dominated. At a Mach number of 0.82 and a Reynolds number of 20×10^6, TS disturbances achieved $N = 10$ to 13 at the measured transition location of 20 to 28 percent chord. For this simulated HLFC test case, suction was applied only in the first 8 percent chord. For CF disturbances, $N = 4.5$ was reached in the first 5 percent chord followed by decay; hence, because the CF modes were decaying at the measured transition location, it was concluded that transition was caused by TS disturbances. For a Mach number 0.82 and a chord Reynolds number of 10×10^6, figure 41 shows correlations of incompressible TS-disturbance amplification with measured transition locations that were varied with suction variations. If transition occurred close to the leading edge, $N = 10.5$ correlated with the measurements, and if transition was observed at greater than 40 percent chord, $N = 7$ correlated with the measurements. (Section 3.5.3 indicated that higher *N*-factors are realized for transition in the leading-edge region of a wing if the surface curvature is not included in the *N*-factor calculation.) For a chord Reynolds number of 20×10^6, shock interference prevented any meaningful correlation. For the compressible analysis of TS disturbances, *N*-factors ranged from 5 to 7.5 for a Mach number of 0.82, a chord Reynolds number of 20×10^6, and suction applied only up to 10 percent chord. In conclusion, Berry et al. (1987) found transition to be TS-disturbance dominated with incompressible analyses correlating *N*-factors of 9 to 11 and compressible analyses correlating *N*-factors of 5 to 6. They also noted that the *N*-factor tool should be

used conservatively with LFC in the transonic flow regime.

Bobbitt et al. (1996) noted that the main results from the slot-suction LFC and HLFC wind tunnel experiments were

1. Full-chord laminar flow was achieved for the slot-suction model up to a chord Reynolds number of 10×10^6

2. Up to 60 percent total drag reductions were achieved for slot-suction test compared with unswept turbulent baseline

3. Suction mass flow required to maintain laminar flow to 60 percent chord on the upper surface was twice as high as predicted for free-air conditions

4. Suction over less than 20 percent chord caused transition to move rapidly forward

5. The drag coefficient increased as Mach number increased until Mach number 0.82 to 0.825 was reached, when an abrupt increase in laminar flow was observed (probably due to choking of the tunnel and decreased noise)

6. More research is needed to provide tools which better describe the effects of wind tunnel environment on boundary-layer receptivity and transition for more accurate prediction of suction level requirements for LFC and HLFC

6.3. Jetstar Leading-Edge Flight Test (1983–1986)

The Leading-Edge Flight Test (LEFT) on the NASA Jetstar (Lockheed C-140) aircraft was an element of laminar flow technology within the ACEE program. The Jetstar flight experiment had objectives which included addressing LFC leading-edge system integration questions and determining the practicality of the LFC system in operational environments via simulated airline operations. Douglas Aircraft Company and Lockheed-Georgia Company designed and constructed leading-edge test sections for the Jetstar right and left wings, respectively. An illustration of the aircraft with suction gloves is shown in figure 42. Details of the flight experiment are reported by Fischer, Wright, and Wagner (1983), Davis et al. (1989), and Maddalon and Braslow (1990).

As described by Etchberger (1983) and Lange (1984, 1987), the Lockheed LFC concept consisted of a fiberglass-epoxy substructure enclosing ducts which provided air passage for 27 suction slots. Shown in figure 43, the titanium skin had each slot cut to a width of 0.004 in. The holes under the slots were 0.03 in. in diameter and centered 0.2 in. apart. Suction was provided by a centrifugal air turbine compressor mounted inside the aircraft. The suction slots covered the upper surface back to the front spar (12 percent chord). In the leading-edge region, six slots served both to control the flow and to provide fluid for insect-contamination and ice-accumulation protection. A 60/40 mixture of propylene glycol methyl ether and water was expelled through the slots. After climb out to 4000 ft, the fluid ejection system was purged from the slots. The suction system and glove geometry were designed by using computer simulations and wind tunnel experiments. The construction of the test article required numerous manufacturing trial and error steps.

The Douglas concept, reported by McNay and Allen (1981), Pearce (1982), Pearce, McNay, and Thelander (1984), and Powell (1987) and shown in figure 44, involved an electron-beam-perforated titanium sheet bonded to a fiberglass corrugated substructure. Fifteen flutes were used to extract air through 0.0025-in. holes spaced 0.03 in. apart. Suction was applied from just below the attachment line back to the front spar. A Krueger shield was used at the leading edge to deflect or block insects. TKS anti-ice system was used on the Krueger shield, and a spray nozzle system was appended to the back of the Krueger shield as a backup system for anti-insect and anti-ice protection of the leading edge pending a Krueger system failure. The Krueger shield was retracted after reaching an altitude of 6000 ft, with the goal of leaving an insect-free leading edge for cruise flight.

Both LFC test articles were 61.25 in. long (20 percent of the spanwise extent of the wings) and extended from the leading edge to the front spar. At the end of the test article at the front spar, both designs had a fairing which was used to continue the contours of the test articles back to 65 percent chord. The contours were designed to simulate a supercritical pressure

distribution for the design conditions of Mach number 0.75 at an altitude of 38 000 ft. Off-design conditions ranged from Mach numbers of 0.7 to 0.8 and altitudes of 29 000 to 40 000 ft. The gloves had a leading-edge sweep of 30° and the local peak Mach number of 1.1.

Surface pitot tubes aligned along the front spar were used to determine the state of the boundary layer. Pitot probes were positioned at 13 percent chord at the laminar boundary-layer height to measure the state of the boundary layer. The differential between the pitot probe pressure and free-stream reference probe pressure gave the state of the boundary layer. For laminar flow, the differential would be zero, but for transitional and turbulent flow, a differential would exist because the pitot probe would be submerged in a turbulent boundary layer. Atmospheric cloud conditions were measured by a laser particle spectrometer to provide a qualitative picture of potential ice-particle contamination and interference. (Refer to fig. 45.)

At a Mach number of 0.78 and altitude of 32 000 ft, the test article only had 7 to 8 percent laminar flow. Disturbances along the attachment line caused transition to occur as the momentum-thickness Reynolds number increased above 110. Introducing a Gaster-type bump (fig. 16) on the inboard attachment line eliminated the turbulent contamination problem. Figure 45 shows a typical flight profile result. According to Fisher and Fischer (1987), laminar flow was realized back to the front spar by using the LFC system.

For the Douglas article, laminar flow was observed back to 83 percent of the article length for design conditions and back to 97 percent for the off-design condition of a Mach number of 0.705 and an altitude of 38 000 ft. Powell (1987) and Morris (1987) discussed the LFC technological accomplishments resulting from the Jetstar program for the Douglas Aircraft Company. In brief, electron-beam-perforated suction surface fabrication, simplified LFC suction panel construction, and a retractable Krueger shield for anti-insect contamination were devised and/or demonstrated on the Jetstar. Also, because the Krueger shield effectively prevented insect contamination on the test section, liquid discharge from the spray nozzle was not necessary.

A similar wood leading-edge bump was placed on the Lockheed test article to prevent attachment-line contamination. For a Mach number of 0.725 and an altitude of 32 000 ft, 97 percent laminar flow was observed on the Lockheed glove. At the design Mach number of 0.75, only 74 percent laminar flow was realized.

See section 4.2 for a discussion of the influence of ice-particulate on laminar flow for the Jetstar flight test. Note, that the aircraft encounter with clouds shown in figure 45 lasted on the order of minutes and that laminar flow was regained within a few seconds after exiting the cloud.

In addition to demonstrating that the LFC systems could be packaged in the leading-edge region, laminar flow could be obtained through the suction LFC systems, the simulated airline service demonstrated the robustness of the LFC systems under normal operating conditions of typical commercial aircraft (Maddalon and Braslow 1990). As Warwick (1985) noted, the X-21 program had difficulty keeping the LFC system free from insects and dirt or dust accumulation. The Jetstar overcame this difficulty by using a Krueger flap on the right wing and by applying a thin layer of fluid on the left wing during takeoff. As a demonstration of the concept, the Jetstar aircraft operated out of Atlanta, Georgia; Pittsburgh, Pennsylvania; and Cleveland, Ohio, and into many other airports in the United States in 1985 and 1986 (Maddalon and Braslow 1990). In this service, the aircraft was kept outside and exposed to the weather (e.g., rain, pollution). Results of the simulated airline service showed that no operational problems were evident with the LFC systems, no special maintenance was required, and LFC performance was proven through the realization of laminar flow on the test article.

6.4. Cessna Citation III Nacelle LFC Flight Test (1986)

Peterman (1987) presented a Cessna Aircraft Company perspective on NLF and LFC at a 1987 NASA symposium. Although the company focus had primarily been on NLF, mention was made of a LFC flight test that Cessna and Rohr Industries conducted in August and September 1986. The nacelle length was extended by 10 in. and the first 40 percent of the

nacelle on a Citation III was reskinned with a woven-wire porous surface called DYNAROHR. The surface pressures and boundary-layer transition locations were measured. Peterman did not discuss the LFC flight test results in his presentation.

6.5. Dassault Falcon 50 HLFC Flight Tests (1987–1990)

Bulgubure and Arnal (1992) and Courty, Bulgubure, and Arnal (1993) noted that the purpose of the flight tests on the Falcon 50 aircraft (fig. 46) was to acquire data to validate and improve design tools and to show the feasibility of the laminar flow concept in flight conditions covering a range of Mach number, Reynolds number, and sweep angle to a future laminar business aircraft. The project took place in two flight test phases plus a wind tunnel validation phase.

The first phase (1985–1987) aimed to demonstrate that a wing could fly with NLF (optimized airfoil for extended regions of laminar flow) and to determine the limits of this concept. The results of the program showed that transition criteria had been correlated and provided the knowledge required to proceed with the second phase—a HLFC demonstration. The second phase (1987–1990) of the flight test aimed to show the feasibility of HLFC in a highly three-dimensional region near the fuselage. The purpose of the follow-on flight experiments was to show that laminar flow could be realized for a 35° swept wing with flight Reynolds numbers ranging from 12×10^6 to 20×10^6.

The HLFC system was designed to provide leading-edge boundary-layer suction aft to 10 percent chord on the upper surface, anti-icing and insect contamination avoidance, and fuselage turbulence contamination avoidance along the attachment line. The design objective was 30-percent-chord laminar flow. Shown in figure 46, the perforated stainless steel suction article was placed over the existing inboard wing structure in close proximity to the fuselage of the Falcon 50 aircraft. The glove was faired into the existing wing with an epoxy resin fairing. Boundary-layer suction was distributed chordwise through six spanwise flutes. In addition, a TKS anti-icing system was integrated into the design and performed the additional task of insect contamination

Calculations showed that at unit Reynolds numbers above 4×10^6 (flight envelope), contamination from the fuselage would spill onto the attachment line and destroy the potential for laminar flow. Three-dimensional calculations were conducted to theoretically optimize a bump (Gaster 1965) to avoid the turbulent contamination problem. This bump was designed and constructed for the attachment-line region near the fuselage-wing juncture and tested in a wind tunnel. Results from the wind tunnel study of a simplified model showed that the bump enabled larger Reynolds numbers prior to turbulence onset. A bump was manufactured for the Falcon 50 aircraft.

As shown in figure 46, the installed instrumentation package included (1) 3 rows of static-pressure taps embedded in the suction article between the flutes to measure the pressure distribution C_p, (2) 3 rows of 12 hot films each for transition detection flush mounted in resin downstream of the suction article, (3) a series of 14 hot-film sensor arrays on the upper surface and 14 hot films oriented spanwise on the attachment line for attachment-line boundary-layer state detection (used only during the leading-edge transition–contamination measurements and removed for flight tests with suction), (4) a pod installed for either an infrared camera to record the transition location or a video camera for recording leading-edge anti-icing effectiveness, (5) 2 sensors for free-stream turbulence measurements, and (6) 6 velocimeters coupled with static pressure taps to measure the suction flow rate in each channel.

The first HLFC flight test phase was conducted initially without the Gaster bump; the primary objective of the flight investigation was the assessment of the TKS anti-icing and insect-avoidance system. (See section 4.1 for a discussion of the effect of the use of a TKS anti-insect system for the flight test.) In addition, the location of the attachment line was measured for proper placement to the Gaster bump. The second phase of flight tests was with the bump on the aircraft to determine the effectiveness of the Gaster bump for turbulence contamination avoidance along the attachment line, the effect of sweep angle on the chordwise extent of laminar flow, and the effect of suction flow rates and distribution on the chordwise extent of laminar flow. The flight tests were conducted such that the chord Reynolds number variation in the region of the test article was between 12×10^6 and 20×10^6. The leading-edge sweep angle of the test article was nominally 35°; however, additional testing was conducted

at sideslip of 5° which yielded a leading-edge sweep angle of 30°.

With boundary-layer suction and without the bump, the whole test article was turbulent. For various combinations of Reynolds number and sweep angle, the best case revealed only a very small area of intermittent boundary-layer flow outboard on the test article. With the Gaster bump installed on the leading edge at 150 mm from the fuselage and with the same suction rates as in the case of no bump, the boundary layer was observed to be mostly intermittent. With the Gaster bump installed at 300 mm from the wing root, figure 47 shows that most of the test article became fully laminar. As expected, when the boundary-layer suction turned off, the flow over the test article became completely turbulent.

The results of this two-phase flight test program demonstrated that laminar flow was a viable concept for at least the business-type aircraft. Hence, the ELFIN program was established to advance NLF and LFC technologies for subsonic flight. Figure 48 gives a schematic of the range of interest for the projects supported by the program.

6.6. Boeing 757 HLFC Flight Test (1990–1991)

In the 1980's, it was recognized that conventional aircraft production wing surfaces could be built to meet LFC design constraints. The NASA Jetstar flight test addressed LFC suction leading-edge systems and demonstrated extensive laminar flow in airline-type operations. A large, commercial transport demonstration was the natural next logical stage of development. In 1987, NASA, the U.S. Air Force Wright Laboratory, and Boeing Commercial Airplane Group initiated a cooperative flight test program on a Boeing 757 transport aircraft.

The Boeing 757 high Reynolds number HLFC flight experiment was designed (1) to develop a database on the effectiveness of the HLFC concept applied to a large, subsonic commercial transport, (2) to evaluate real-world performance and reliability at flight Reynolds numbers (including off-design conditions), and (3) to develop and validate integrated and practical high-lift, anti-ice, and HLFC systems. (See Collier 1993.)

A 22-ft span segment of the leading-edge box outboard of the engine nacelle pylon and on the left wing was replaced with a HLFC leading-edge box as shown in figure 49. This new leading-edge section consisted of a perforated titanium outer skin, suction flutes under the skin, and collection ducts to allow suction control of the boundary-layer CF- and TS-disturbance growth from the leading edge to the front spar. The leading edge included a Krueger shield integrated for high lift and insect protection and hot air deicing systems. The wing-box portion of the test area consisted of the original Boeing 757 surface and contour and only required minor clean-up (e.g., shaved-off exposed rivet heads) to meet surface waviness and smoothness requirements. The design point for the flight tests was Mach number 0.8 at C_L = 0.50. Flight tests of many off-design conditions were performed to investigate extent of laminar flow as a function of Mach number, unit Reynolds number, and lift coefficient. Flight testing began in February 1990 and ended in August 1991.

As shown in figure 49, flush-mounted pressure taps were positioned in the perforated leading edge and strip-a-tube belts were used to measure the external pressure distribution over the wing box. Hot-film sensors were used to determine the transition location on the wing box and along the attachment line. Limited infrared camera imaging was obtained and indicated that this technique was useful for boundary-layer transition detection. Finally, wake-survey probes were used to infer local drag-reduction estimates. The state of the laminar boundary layer, the internal and external pressure distributions, and the suction system were monitored in real time onboard the aircraft during the flight test.

The flight test demonstrated that the HLFC concept was extremely effective in delaying boundary-layer transition as far back as the rear spar around the design point. A sample test condition (fig. 50) shows that most of the hot films indicated laminar flow beyond 65 percent chord (Maddalon 1991, 1992; Shifrin 1991; Collier 1993). In fact, the suction rates required to achieve laminar flow to 65 percent chord were about one third of those predicted during the initial design (Maddalon, 1991). The wake-rake measurements indicated a local drag reduction on the order of 29 percent with the HLFC system operational,

which resulted in a projected 6-percent drag reduction for the aircraft (Maddalon 1991). However, because only about one third of the design suction was required to achieve laminar flow, significant uncertainty in the design tools was a by-product of the flight test. This uncertainty led to the HLFC wind tunnel experiment discussed in section 6.13.

6.7. HLFC ONERA-CERT T2 Wind Tunnel Test (1991)

In 1989, the European Laminar Flow Investigation (ELFIN) project was initiated and consisted of four primary elements that concentrated on the development of laminar flow technology for application to commercial transport aircraft. Three of these elements are related to LFC. These elements were a transonic wind tunnel evaluation of the HLFC concept on a large-scale model, the development of a boundary-layer suction device, the development of new wind tunnel and flight test techniques for LFC, and the development of improved computational methods for laminar-to-turbulent flow prediction capability (Birch 1992).

Reneaux and Blanchard (1992) discussed the design and testing of a HLFC airfoil model in the ONERA-CERT T2 cryogenic wind tunnel. The transition criterion of Arnal, Habiballah, and Coustols (1984) was used for the wing design. First, the Airbus transport turbulent wing was modified to achieve the best compromise between transonic performance and the HLFC wing. For the wing swept to 27.5°, suction was applied from the leading edge to 20 percent chord and a favorable pressure gradient was maintained to 60 percent chord on the upper surface and 55 percent chord on the lower surface. For a Mach number of 0.82, $C_L = 0.44$, and a maximum chord Reynolds number of 42×10^6, the computed transition location ranged from 25 percent chord at the wing root to 55 percent chord at the wingtip for a mean suction velocity of 0.1 m/sec. With upper and lower surface suction, the computed viscous drag of the HLFC wing was 45 percent less than the turbulent wing and the total drag was 10 percent less than the turbulent wing. Applying suction to the upper surface alone led to a viscous drag reduction of 29 percent and a total drag reduction of 6.3 percent.

Reneaux and Blanchard (1992) suggested that the maximum allowable roughness in the leading-edge region would be 0.2 mm and because of this criterion, research should focus on advancing manufacturing technology and insect-impact prevention. Additionally, because conventional slats cannot be used in laminar flow wings, leading-edge Krueger flaps or using suction to permit higher angles of attack should be explored for enhancing lift. Finally, the design of the perforated-suction system must focus attention on the hole diameter and spacing, hole pattern and alignment, and the thickness of the surface sheet. The suction must be such that premature transition is not induced, and the pressure drop is such that no outflow is observed. The hole spacing and size have to be small compared with the boundary-layer thickness; a hole diameter of 0.06 mm and spacing of 0.6 mm are typical examples of sizes studied.

To establish criteria for the design of the perforated surface, three tests were carried out in the T2 tunnel. The experiments studied the critical suction velocities for isolated holes, the influence of hole alignment, and validation of the transition prediction method. For the experiments, four holes were placed at 20 percent chord and five holes were placed at 40 percent chord of an airfoil model with hole diameters which ranged from 0.1 mm to 0.8 mm. Infrared thermography and liquid crystals were used to detect the transition location. Critical velocities were obtained and correlated to a proposed curve-fit criterion.

Square and triangle hole pattern and alignment were investigated. The critical suction velocities were larger for the triangles; the explanation for the larger velocities was attributed to the larger distance between the holes in the triangle alignment.

Next, hole alignment was investigated by varying the hole alignment to free-stream flow from spanwise to streamwise alignment. With a test section from 17 to 34 percent chord, the results indicate that the critical suction velocities decreased with decreased hole spacing. The hole spacing seems to have no effect on transition when the distance between holes is 10 diameters. The results also suggested that for hole alignment greater than 30°, the holes behave as though they were in isolation.

6.8. HLFC Nacelle Demonstration Flight Test (1992)

The encouraging results achieved on the Boeing 757 HLFC flight experiment and the potential for drag reduction on nacelles led General Electric Aircraft Engines (GEAE) to initiate a project with Rohr Industries, Inc., Allied Signal Aerospace, and NASA to explore the use of LFC on nacelles. The project was directed toward the flight demonstration of the HLFC concept applied to the external surface of large, turbofan engine nacelles. Bhutiani et al. (1993) stated that the main objective of the project was to demonstrate the feasibility of laminar flow nacelles for wide-body aircraft powered by modern high-bypass engines and to investigate the influence of aerodynamic characteristics and surface effects on the extent of laminar flow.

A production GEAE CF6-50C2 engine nacelle installed on the starboard wing of an Airbus A300/B2 commercial transport testbed aircraft was modified to incorporate two HLFC panels—one inboard and one outboard—as shown in figure 51. The panels were fabricated of a perforated composite material with suction from the highlight aft to the outer barrel-fan cowl juncture. Suction was applied to the surface utilizing circumferential flutes and was collected and ducted to a turbocompressor unit driven by engine bleed. For convenience, the turbocompressor unit was located in the storage bay of the aircraft. The flow through each flute was individually metered. The laminar flow contour extended aft over the fan cowl door and was accomplished through the use of a nonperforated composite structure blended back into the original nacelle contour ahead of the thrust reverser. No provisions were made for ice-accumulation or insect-contamination avoidance systems.

Static-pressure taps were mounted on the external surface and in the flutes. A boundary-layer rake was used to measure the state of the boundary layer. Hot-film gauges were used for boundary-layer transition detection. Surface embedded microphones were used to measure noise. A charge patch was used to measure the atmospheric particle concentration. An infrared camera was used for detecting the boundary-layer transition location. Real-time monitoring and analysis of the state of the boundary layer and suction system were accomplished onboard the aircraft.

The flight-test phase of the project extended over a period of 16 flights totaling 50 flight hr. As shown in figure 51, the HLFC concept was effective over the range of cruise altitude and Mach number and resulted in laminar flow to as much as 43 percent of the nacelle length (the design objective) independent of altitude (Bhutiani et al. 1993, Collier 1993, Fernandez et al. 1996). At this transition location, the static-pressure sensors indicated the onset of the pressure recovery region, which caused the laminar boundary layer to become turbulent. Without suction, significant laminar flow was achieved on the LFC panel; the extent of "natural" laminar flow increased with increasing altitude (perhaps due to passive suction).

6.9. NLF and LFC Nacelle Wind Tunnel Tests (1991–1993)

The earlier studies conducted in the United States suggested that significant performance benefits could be realized through the use of NLF and/or LFC on engine nacelles. Before 1991, no flight tests were conducted by the Rolls-Royce Company to study LFC; however, wind tunnel tests were conducted with a two-dimensional model of a LFC nacelle. The wind tunnel test demonstrated a region of substantial laminar flow with sufficient suction. Due to unacceptable levels of turbulence and noise in the tunnel, the extension of this effort was moved to a low-turbulence 9-ft by 7-ft tunnel at the University of Manchester. Mullender, Bergin, and Poll (1991) discussed the plan to perform a series of wind tunnel experiments and theoretical studies with NLF and LFC nacelles. The theoretical studies were aimed at validating the LFC design tools (including transition prediction) for use in optimization of nacelle designs.

Optimal nacelle designs pointed toward minimizing the length of the cowl to maximize internal performance and drag reduction benefits. For best high-speed performance, conventional nacelles have a peak pressure near the lip of the nacelle to distribute the largest pressure at the most forward face of the nacelle; the flow was then decelerated over most of the nacelle. This pressure distribution produced turbulent flow over most of the nacelle and a subsequent large skin friction. Because the circumferential curvature of the nacelle was smaller than the boundary-layer thickness on the nacelle, a two-dimensional model was used to mimic the nacelle flow. Hot-film,

total-pressure, and static-pressure measurements of the boundary layer were made during the wind tunnel experiment. Using LFC suction, laminar flow was observed on the nacelle model. By reducing the level of suction, TS disturbances were measurable, and with no suction the flow was turbulent. Variations in tunnel speed indicated that the suction was relatively constant near the nose over the speed range; however, in the mid nacelle region where the pressure gradient was nearly flat, notable differences in suction were observed for variation in tunnel speed. The linear calculations suggested that an inviscid instability (Rayleigh mode) developed and had greatest amplification at 1700 Hz for a tunnel speed of 36 m/sec and increased to 3500 Hz for 60 m/sec. In two-dimensional viscous boundary-layer stability, the frequency of the dominant mode would decrease with increased distance downstream. Theoretical *N*-factor correlations achieved 6.6 at a tunnel speed of 36 m/sec to 9.1 at 60 m/sec; this indicated that the TS disturbances never evolved sufficient to cause transition. Rather a separation bubble developed causing transition.

6.10. VFW 614 HLFC Transonic Wind Tunnel Test (1992)

In 1986, the German laminar flow technology program, supported by the German Ministry of Research and Technology (BMFT), began wind tunnel and flight experiments for NLF and LFC (Redeker et al. 1990). Körner (1990) noted that part of the program involved determining (or discriminating) between when NLF is preferred and when HLFC or LFC is a more appropriate choice for a particular aircraft. Two of the major milestones of this program involved NLF wind tunnel tests and flight research on a VFW 614 and Fokker 100 research aircraft to gain a database of TS-disturbance- and CF-disturbance-dominated transition for code calibration.

The successful VFW 614 and Fokker 100 NLF flight tests led to a transonic wind tunnel evaluation of the HLFC concept, evaluation of wind tunnel test techniques, and development of viable boundary-layer suction devices. In March and April of 1992, a 1:2 scale model of one of a VFW 614 wing was built with leading-edge suction and tested in the ONERA S1MA transonic tunnel—the first LFC test in the facility (Schmitt, Reneaux, and Pries 1993). The model had a span of 4.7 m and a mean chord of 1.58 m. The perforated leading edge was built into the midspan region of the wing and had a span of about 0.95 m. Suction was implemented to about 15 percent chord on both the upper and lower surfaces. The titanium outer skin was 0.9 mm thick and had holes which were 40 μm in diameter and spaced 0.5 mm apart. As shown in figure 52, the leading edge consisted of 38 suction flutes connected to 17 collection ducts. The suction flow rate through each collection duct was individually controlled and measured. The chordwise transition location was measured with infrared thermography as a function of suction flow velocity for a given transonic test condition. Figure 52 shows the measured transition location as a function of suction velocity. As suction was increased the transition front moved aft. Laminar flow was achieved to 50 percent chord on the upper surface and to 30 percent chord on the lower surface. Data gathered from the test were used for suction system design criteria and calibration of the laminar flow prediction methodology.

6.11. European NLF and HLFC Nacelle Demonstrator Flight Tests (1992–1993)

In 1992 and 1993, a cooperative program was conducted by DLR, Rolls Royce, and MTU with the goal of investigating in flight the prospects of achieving extensive laminar flow on aircraft engine nacelles (Barry et al. 1994). The test vehicle chosen for the project was the VFW 614 ATTAS aircraft which has twin Rolls-Snecma M45H turbofans. The placement of the nacelle on the aircraft is shown in figure 53. The program had the usual goals of demonstrating drag reduction with NLF and HLFC on a nacelle, verifying the design methodology, verifying manufacturing techniques, and validating the anti-insect transpiration system.

For the NLF portion of the test program, two new composite nacelles were constructed by Hurel-Dubois for the program. One nacelle consisted of baseline lines and the second nacelle consisted of a new set of aerodynamic lines, conducive to laminar flow. A third nacelle was designed for validation of the HLFC concept, which included a liquid transpiration insect contamination avoidance system. (See Humphreys 1992.)

Instrumentation to measure the pressure, temperature, and transition location is illustrated on the test section in figure 53. The flight test portion of the program consisted of about 93 hr which clearly demonstrated that laminar boundary-layer flow was achievable over 60 percent of the nacelle length in the installed environment over a large range of flight conditions for both laminar flow concepts tested. For the NLF concept, figure 54 shows the design and measured pressures at two radial locations. Very good agreement between the computed and observed pressures is realized at $\phi = 30°$; however, significant disagreement was found at $\phi = 140°$ near the pylon. This disagreement can be attributed to the computations not including the pylon in the design. Noise and vibration had little or no effect on the ability to achieve laminar flow for this design. The liquid transpiration-styled insect contamination avoidance system was operated successfully during the course of the flight testing.

6.12. A320 Laminar Fin Wind Tunnel and Flight Test Program (1993–1998)

Figure 55 shows an illustration of a 1987 plan by Airbus Industries in close collaboration with ONERA and DLR to enable LFC capability for subsonic transport aircraft. The program consisted of theoretical analysis, a large wind tunnel evaluation, and a flight test program of the vertical fin of the A320 aircraft (ultimately geared toward the application of laminar flow to wing and tail surfaces of a future advanced aircraft). The vertical fin of the A320 aircraft was chosen as the candidate to test the feasibility of HLFC because of the availability of an aircraft for flight testing, simple installation, no de-icing system, attainment of flight Reynolds number in an existing wind tunnel (ONERA S1MA at Modane), and minimized cost (Robert 1992a; Redeker, Quast, and Thibert 1992; Thibert, Reneaux, and Schmitt 1990).

Shown in figure 56, boundary-layer stability results indicated that laminar flow is expected to approximately 40 percent chord for the baseline A320 fin and to about 50 percent chord for the HLFC A320 fin (using a reasonable amount of suction). A benefit study with the projected amount of laminar flow indicates that an aircraft drag reduction of 1.0 to 1.5 percent is possible by laminarizing the vertical fin.

The second phase of the program involved the testing of the A320 vertical fin with leading-edge suction in the ONERA S1MA facility. The 1/2-scale model in the tunnel is shown in figure 57. The objectives of the wind tunnel experiment were to simulate flight Reynolds numbers on the model, calibrate the transition prediction tools, and establish LFC suction design criteria. Finally, Anon. (1995b) reported that the A320 HLFC fin flight test program was scheduled to be completed by 1996. (Prior to the publication of the present report, no flight test data were available.) The development of the A3XX program at Airbus has allowed for the success of the A320 LFC fin program by requiring the power plants of the A3XX to be positioned closer to the wing and for suction LFC nacelles (Birch 1996).

6.13. Langley 8-Foot Transonic Pressure Tunnel HLFC Wind Tunnel Test (1993–1995)

Although the Boeing 757 HLFC flight test experiment demonstrated significant runs of laminar flow using leading-edge suction, sufficient uncertainty in the design tools made the technology an unacceptable risk for the commercial market. To provide a better understanding of the complex physics of flow over a swept-wing geometry, to provide a calibration database for the LFC design tools, and to better understand the issues of suction-system design, a joint NASA/Boeing HLFC wind tunnel experiment was conducted in the Langley 8-Foot Transonic Pressure Tunnel (Phillips 1996).

A swept-wing model with a 7-ft span and 10-ft chord was installed in the tunnel in January 1995 and tests were conducted throughout the year. Tunnel liners were installed to simulate an infinite swept wing. Over 3000 infrared images and 6000 velocity profiles (hot-wire data) were obtained during the test, and the data were made available to the team of researchers in real time via encrypted World Wide Web communications (Phillips 1996).

As stated by Johnson (1996), an assessment of the LFC design criteria was made to help guide future designs. The influence of hole size and spacing and suction level and distribution on the transition location was recorded and correlated with the design tools. Laminar flow was easily obtained back to the pressure

minimum with sufficient suction levels. Detailed surface roughness and suction level measurements are underway to characterize the leading-edge panels.

Detailed results are not available in the literature for inclusion in this publication.

6.14. High-Speed Civil Transport (1986)

In 1986, NASA and the U.S. airframe and engine manufacturers determined that the long-range travel market was conducive to a supersonic airliner (high-speed civil transport, HSCT); however, significant technological advances were required. The advances would require an aircraft to fly slightly faster than the speed of the Concord but with nearly twice the range and three times the number of passengers at an affordable ticket price while not damaging the environment.

As shown by Kirchner (1987), laminar flow could lead to significant benefits for a supersonic transport. When considering the application of NLF and LFC technologies to the supersonic flow regime, the high cost and limited availability of flight test aircraft inhibits the advancement of these technologies. Military jet fighter aircraft, the Concord, and the Tupelov Tu-144 currently fly at supersonic Mach numbers and are potentially viable candidates to serve the LFC research community; however, the design and manufacturing of most of these aircraft were devoid of the future potential use for LFC missions and potentially have unacceptable surface waviness, roughness, and aircraft-specific obstacles. Wagner et al. (1990) presented the status of supersonic LFC through the 1980s.

In spite of these limitations, technology can be advanced by making use of these aircraft when they are made available. Toward the goal of advancing NLF supersonic technology, flight experiments were commenced in the United States toward gaining a better understanding of the viscous flow physics. A summary of the NLF results for supersonic aircraft are presented in appendix B.

Two fundamental approaches were posed for the supersonic laminar flow wing. The first approach was a low-sweep wing which involved the design of a NLF leading-edge region and low-suction (or thermal) LFC on a section on the wing to extend the laminar flow to higher chord Reynolds numbers. As discussed by Gottschalk (1996), such a concept proposed by Northrop Grumman Corporation would have a sharp supersonic leading edge and result in a thin attachment-line boundary layer and a very small momentum-thickness Reynolds number. Such a flow should be stable and have a laminar attachment line. Crossflow disturbances could be avoided with the low wing sweep and, with appropriate wing shaping, a partially NLF wing could be achieved. LFC would be required on the rooftop of the wing to extend the region of laminar flow to higher Reynolds numbers. Concerning the use of thermal LFC, Dunn and Lin (1953) have shown in the early 1950s that cooling can be used to suppress disturbances. As shown by Boeing (Parikh and Nagel 1990), cooling has a large impact on TS disturbances and only a subtle influence on CF disturbances; hence, cooling would not be useful in the leading-edge region of swept wings for CF stabilization.

In contrast to the low-sweep supersonic laminar flow concept proposed by Northrop Grumman, the highly swept wing would have a subsonic leading edge, a blunt nose, and higher momentum-thickness Reynolds number. As Wagner et al. (1990) noted, the turbulent baseline HSCT configurations by The Boeing Company and McDonnell Douglas Corporation were making use of the second approach. With this high-sweep wing, the issue of turbulent attachment-line contamination must be addressed and suction LFC would be required to control the CF-dominated transition process in the leading-edge region of the wing. For long chords typical of the HSCT configurations, an additional strip of suction (or thermal) LFC would be required on the wing to delay the TS-dominated transition process.

Williams (1995) noted that a proposed HSCT carrying 305 passengers and flying 5000 n.mi. with 1990 technology would weigh almost 1.25 million lb at takeoff and would not meet the current noise requirements. A technology development program would need to reduce the weight by almost 50 percent to make the HSCT feasible. Toward overcoming the technical obstacles, NASA commenced Phase I of a High-Speed Research (HSR) Program in partnership with U.S. industry. Phase I focused on developing reliable methods to predict engine-emission effects on the ozone, noise reduction technologies, and the potential

advantages of supersonic laminar flow control (SLFC).

Feasibility studies by Boeing Aircraft Company (Parikh and Nagel 1990) and McDonnell Douglas Aircraft Company (Powell, Agrawal, and Lacey 1989) were funded to determine the benefits of supersonic laminar flow control applied to the HSCT configuration. Reductions in gross takeoff weight, mission fuel burn, structural temperatures, emissions, and sonic boom were predicted by incorporating SLFC technology on a HSCT configuration (see section 2).

Because of the favorable results achieved with Phase I of the program, HSR Phase II was initiated to perform additional research toward advancing the state of technology to make the HSCT economically viable. As part of Phase II, the low-disturbance wind tunnels at Langley and Ames Research Centers and the F-16XL aircraft at Dryden Flight Research Center were used to advance the state of the art in supersonic laminar flow control. An overview of the understanding of SLFC up to 1987 was provided by Bushnell and Malik (1987).

6.15. Supersonic LFC Quiet-Tunnel Tests (1987–1996)

Conventional supersonic and hypersonic wind tunnels are dominated by acoustic disturbances radiated from the turbulent boundary layers on the tunnel walls. The emanation of these disturbances follow Mach lines. To study laminar flows (i.e., transition, boundary-layer instability, and LFC), the test section in the tunnel must be clean (defined as free-stream pressure fluctuations below 0.1 percent). This section focuses on the research primarily supported by the HSR project and conducted in the Langley Supersonic Low-Disturbance Tunnel (SLDT) and the Ames Laminar-Flow Supersonic Wind Tunnel (LFSWT). For more details about quiet tunnels, refer to the review of quiet tunnel technology by Wilkinson et al. (1992).

Beckwith, Chen, and Malik (1987, 1988) presented a method to maintain a test section free from acoustic disturbances which culminated in the Mach number 3.5 Supersonic Low-Disturbance Tunnel (SLDT) at Langley Research Center. The tunnel is a blowdown facility supplied with dry high-pressure air which exhausts into large vacuum spheres to provide run times on the order of 30 min. The nozzle throat is highly polished to maximize the extent of laminar flow on the nozzle walls. Upstream of the sonic throat, suction was used to remove the turbulent boundary layer that exists on the wall. The fresh laminar boundary layer evolved through the contoured nozzle until the boundary layer undergoes transition to turbulence. The location of this transition point governs the length of the low-disturbance test-section rhombus and is directly influenced by the unit Reynolds number of the flow. As the unit Reynolds number increases, the size of the quiet test-section rhombus decreases; however, the Reynolds number based on the length of the quiet test core increases. The tunnel was capable of operating in conventional noisy mode or in quiet (low-disturbance) mode.

In the SLDT, measured transition Reynolds numbers were shown to be comparable with transition observed in flight. Creel, Malik, and Beckwith (1987) and Creel, Beckwith, and Chen (1987) used the quiet tunnel to study boundary-layer instabilities on a leading edge of a swept cylinder. The results suggested that transition was affected by wind tunnel noise only when large roughness was present on the model, the local roughness Reynolds number correlated with the transition location for a wide range of Mach numbers, and linear stability theory showed good agreement for the experimental crossflow vortex wavelength of the dominant mode. Morrisette and Creel (1987) studied the effect of surface roughness and waviness on transition in the SLDT. Controlled roughness and waviness were imposed in the supersonic flow and compared with subsonic correlations. Eight 15-in. long and 5° half-angle wavy cones were tested, where the wavelength of the cones correspond to the most amplified TS disturbance for the smooth cone. A fixed surface pitot tube was used to measure transition as a function of total tunnel pressure. Results with wall waviness indicated that the tunnel running with a noisy environment led to lower transition Reynolds numbers compared with the results in the quiet environment. Also, the results suggested that the transition location was a function of aspect ratio (wave height over wavelength). The quiet tunnel results for roughness matched with the correlation by Van Driest and McCauley (1960) for three-dimensional roughness on cones. Morrisette and Creel (1987) concluded that

waviness had less effect on transition than a single trip of comparable height, and the effect of noise on critical and effective roughness Reynolds numbers appeared small.

In support of the F-16XL SLFC flight experiment, models were developed for the Langley quiet tunnel to calibrate the design tools for NLF and LFC and to study attachment-line transition. Iyer and Spall (1991) and Iyer, Spall, and Dagenhart (1992) performed linear stability theory calculations using CFL3D for the mean flow and COSAL for boundary-layer stability for the F-16XL leading-edge section model. The 15-in. model had a leading-edge sweep of 77.1° with a normal Mach number of 0.78. Traveling CF disturbances were found to have the largest amplification; however, distributed suction was shown to stabilize the flow so that $N = 10$ was not exceeded over the entire model. In addition, cooling was shown to be stabilizing for the flow. Cattafesta et al. (1994, 1995) and Cattafesta and Moore (1995, 1996) discussed temperature sensitive paint (TSP) transition measurement and the transition locations for the solid model. Shown in figure 58, the calculated *N*-factors correlated well for $N = 14$ over a range of free-stream unit Reynolds numbers and angle of attacks for the solid model. The results suggested that traveling crossflow disturbances probably dominated the transition process. A SLFC porous-suction model was developed and tested but the results are not available for this publication.

At the Ames Research Center, a Mach 1.6 quiet tunnel was constructed to minimize the free-stream disturbances. This was accomplished by using a low-disturbance settling chamber to produce steady supersonic diffuser flow and low structural vibration and included smooth (polished) walls to produce laminar boundary layers on the nozzle and test section. Wolf, Laub, and King (1994) presented results for flow quality and tunnel transition aspects of this continuous operation facility. Supporting the F-16XL SLFC flight experiment, a section of the passive glove was used to study the leading edge of the wing. A comparison of the surface pressure distributions measured in the tunnel compared well with CFD predictions at an angle of attack of 0°; however, the agreement was rather poor for flight test measurements. More recent attachment-line transition experiments on a swept cylinder were reported by Coleman et al. (1996) and Coleman, Poll, and Lin (1997) in the Ames tunnel. Schlieren photography was used to assess the state of the boundary layer on the cylinder for variations in free-stream conditions. Observations indicate that the boundary layer remained laminar up to and including the largest attachment-line Reynolds number of 760. Using trip wires to control the state of the boundary layer, the results suggested that the free-stream disturbance environment impacted the transition location; this confirmed that designs based on conventional noisy tunnels were too conservative.

6.16. F-16XL Supersonic LFC Flight Tests (1989–1996)

Supersonic LFC flight tests were conducted by a NASA and U.S. industry team to demonstrate the feasibility of laminar flow in supersonic flight. Two F-16XL aircraft (XL has delta wings) are on loan to NASA from the U.S. Air Force to serve as testbeds. The F-16XL wings have inboard sweep of 70° and outboard sweep of 50°, similar to the proposed HSCT wing configuration. NASA and Rockwell International Corporation carried out the flight tests with the F-16XL Ship 1; NASA, Rockwell, Boeing, and McDonnell Douglas carried out the flight tests for F-16XL Ship 2.

In 1990, flight testing began using a suction glove on the F-16XL Ship 1 (shown in fig. 59(a)). A Rockwell-designed perforated-suction glove was fabricated and installed on an existing wing of Ship 1 as sketched in figure 59(b). Because of the geometrical constraints of implementing a glove on Ship 1 (glove height of less than 2 in. above the existing wing surface and 10 in. in front of the leading edge), active suction was limited to the first 25 percent chord and attachment-line instabilities were the primary focus of the LFC experiment. Woan, Gingrich, and George (1991), Anderson and Bohn-Meyer (1992), and Norris (1994) noted that the perforated-suction glove on Ship 1 was designed for a Mach number of 1.6, altitude of 44 000 ft, angle of attack of 2°, momentum-thickness Reynolds number on the attachment line of less than 114, and a unit Reynolds number per foot of 2.53×10^6. No laminar flow was achieved at the design point; however, laminar flow was observed at off-design conditions. Figure 60 shows the amount of laminar flow with and without suction for a given flight test condition; hot-film data indicated laminar

flow to the outboard portion of the glove (Anderson and Bohn-Meyer 1992).

Woan, Gingrich, and George (1991) reported on the design, analysis, and validation of a coupled Navier-Stokes and compressible linear stability theory approach for supersonic LFC design. Validation was obtained by using the methodology to design the suction LFC glove for the F-16XL Ship 1 and then by making a comparison with flight-measured results. A technology goal of the methodology was to obtain a design which minimizes suction requirements and simultaneously defines a pressure which is conducive to stabilizing the boundary layer. Overall, the CFD results were in reasonably good agreement with the Ship 1 database. Mean-flow results from the Navier-Stokes codes were used with the COSAL boundary-layer stability code for correlations with the available transition Ship 1 data. Stability calculations (for an *N*-factor of 10) indicated that transition would occur at 1.5 in. from the leading edge without suction; shown in figure 60, laminar flow was restricted to very near the leading edge in the flight test with no suction. The computations showed three distinct shocks which must be tracked for laminar flow management. These shocks emanated from the nose, the canopy, and the engine inlet (underneath the aircraft).

Flores et al. (1991) used thin-layer Reynolds averaged Navier-Stokes equations to study the sensitivity of the attachment line and crossflow velocity profiles to changes in angle of attack for Ship 1. The results showed that as angle of attack increased (1) the boundary-layer thickness and streamwise velocity profiles had no significant changes, (2) the attachment line moved from the upper surface to the lower surface, and (3) the crossflow velocity component at a fixed location on the upper surface of the wing decreased. This information is important for determining the optimal amount of suction required for a given position on the wing to obtain laminar flow.

In the 1991–1992 time-frame, flight measurements were obtained for the flow on the F-16XL Ship 2 leading-edge passive glove. The passive glove had a 4.5-m span and 10-percent-chord section made of foam and fiberglass and was designed by McDonnell Douglas Corporation and built by NASA Dryden Flight Research Center. The goal of the first flight tests was to obtain surface pressure data to calibrate the Euler design codes, particularly in the leading-edge attachment-line region. Preventing the fuselage turbulent boundary layer from contaminating the attachment-line region of the wing was a second major technical issue which was addressed in the first phase of flight tests. The third technical area of interest involved characterizing the acoustic disturbance field and disturbances which could come from the fuselage turbulent boundary layer. The pressure and laminar flow extent data provided valuable attachment-line region information for the design of the Ship 2 suction glove.

The perforated-suction glove for Ship 2 was designed in a collaborative effort between Boeing, McDonnell Douglas, Rockwell, and NASA. A photograph of Ship 2 and a sketch of the LFC test article are shown in figure 61. Because of the asymmetry of Ship 2 with the suction glove, stability and control of the Ship 2 configuration was tested for safety assurance in a wind tunnel. For the flight article, the perforated-suction SLFC glove was constructed of inner and outer titanium skin and aluminum stringers. Suction was obtained by using a modified Boeing 707 turbocompressor. Norris (1994) noted that suction was applied through some 10 million holes and 20 individual suction regions on the glove surface. Wagner et al. (1990) and Fischer and Vemuru (1991) noted that the F-16XL Ship 2 SLFC flight experiment had objectives of achieving laminar flow over 50 to 60 percent chord on a highly swept wing, of delivering validated CFD codes and design methodology, and of establishing initial suction system design criteria for LFC at supersonic speeds. The suction glove was installed on Ship 2 and the first flight was conducted October 13, 1995. The first supersonic flight took place on November 22, 1995. The first suction-on supersonic flight test was accomplished January 24, 1996.

Similar to Ship 1, Ship 2 had aircraft-specific shock and expansion waves which influenced the flow on the wings. Although canopy and engine inlet shocks spreading out over the wings and expansion waves from beneath the wing caused a highly three-dimensional flow field and difficulties in obtaining laminar flow on the attachment-line region at the same test conditions, significant progress toward

accomplishing the goals was achieved. In spite of these test aircraft-dependent obstacles, Smith (1996) noted that the supersonic laminar flow control flight experiment achieved about 70 to 80 percent of the initial goals.

7. Concluding Remarks

This publication has reviewed some of the early foundational studies and more recent U.S. and European projects which had goals of solving technical obstacles associated with the application of laminar flow control to advanced transport aircraft. The technology has the potential to offer breakthrough improvements in aircraft efficiency by leading to significant reductions in aircraft fuel consumption, extending range or increased payload, reductions in emissions and noise, and increasing cruise lift and drag, and reducing maximum gross takeoff weight. Much progress has been accomplished toward the goal of commercial incorporation of laminar flow control (LFC) (and natural laminar flow (NLF)) on wings, tails, and engine nacelles. However, because the application of the technology leads to additional systems and some uncertainty in the maintenance requirements and long-term structural integrity due to the system, questions still remain which must be resolved relative to long-term operational and reliability characteristics of current hybrid laminar flow control (HLFC) concepts before the aircraft industry can guarantee the sustained performance of the LFC vehicle to their airline customers.

The 1980s and 1990s brought the successful demonstration of a LFC aircraft (Jetstar and Falcon 50 LFC flight tests) in airline operations and with insect-prevention systems, the achievement of laminar flow at high Reynolds numbers (Boeing 757 HLFC flight test), the achievement of laminar flow on a HLFC engine nacelle (A300/GE and VFW 614 nacelle flight tests), and various LFC wind tunnel tests (Langley 8-Foot Transonic Pressure Tunnel and ONERA S1MA LFC tests). However, from the airframe company perspective, some technology issues exist which require attention prior to the acceptance of LFC. These issues include the resolution of potential performance penalties versus projected HLFC benefits (leading-edge Krueger versus conventional leading-edge slat system); the development of HLFC compatible ice-protection systems; the development of viable high Reynolds number, wind tunnel test techniques for HLFC configuration development; the demonstration of acceptable reliability, maintainability, and operational characteristics for a HLFC configuration; and the ability to predict and guarantee benefits to the airline customers. In 1991, a Senior Vice President of an airframe systems manufacturer stated that before laminar flow control could be used on commercial aircraft, the long-term technical and economic viability of the technology must be demonstrated. Although many of these issues have been addressed subsequent to this statement, the future of subsonic and transonic LFC technology must reside in a large-scale demonstrator to study the long-term reliability of the performance and flight-safety operations, in refined design tool development, and in the longer term understanding of the effects of wind tunnel flow quality on the laminar flow (LF) extent. An alternative future resides in the demonstration of innovative LFC control systems. Perhaps, advances in micro-machine, synthetic-jet, smart-material technologies will lead to orders of magnitude improvements in efficiency, reliability, and cost-effectiveness of these future LFC systems, and LFC will be an integral part of this revolutionary new aircraft.

In the supersonic vehicle class, the 1990s brought the first flight demonstration of LF achieved by supersonic laminar flow control (SLFC) through the success of a NASA-industry team. In 1990, a General Manager of a major airline company stated in a talk on the high-speed market in the next three decades that, although the subsonic fleet will play the role of serving the low-yield mass traffic markets, the supersonic transport will be a big part of the intercontinental fleet of the future. Looking at historical data, the long-range aircraft entering the market and replacing an existing aircraft has never been smaller than the aircraft being replaced. Based on these data, the smallest intercontinental supersonic transport (SST) will have a capacity of no less than 300 seats (at moderately higher—20 percent—cost than the subsonic cost). The benefits of LFC increase with the size of the aircraft. If this subsonic trend of larger aircraft entering the market continues, the LFC technology could be an even more significant competitive advantage to a next generation airplane. Environmental issues, materials, systems, engines, and supersonic laminar flow control are some of the research which ought to be pursued for the development of a supersonic transport.

The reduced priority of LFC resides not with any unfeasibility of the technology but rather with the promise of benefits being intimately tied to the aircraft fuel prices. As the cost of fuel decreases in real dollar value, the benefits and hence future prospects of LFC decrease to obscurity; conversely, as fuel price increases, the benefits of LFC increase. Even if alternate fuels are introduced into the equation, the benefits of reduced noise and emissions (and heat stress on supersonic aircraft) remain attractive achievements with LFC.

NASA Langley Research Center
Hampton, VA 23681-2199
June 18, 1998

Appendix A

Subsonic Natural Laminar Flow Research

In this appendix, a bibliography of NLF research results is briefly given. Additional reviews of laminar flow flight testing are given by Wagner et al. (1988, 1989) and Hefner (1992). Holmes and Obara (1992) and Holmes, Obara, and Yip (1984) review and focus on NLF flight research, Somers (1992) and Pfenninger and Vemuru (1992) discuss laminar flow airfoils.

A.1. Cessna T210R (Late 1980s)

Research was performed to design NLF airfoils and implement these airfoils in full-scale wind tunnel and flight tests. For example, a Cessna T210R research aircraft was used in the late 1980s to validate the use of NLF for aerodynamic performance gains. This research airplane had a NLF wing and horizontal stabilizer and a smoothed vertical stabilizer. The airfoil was designed to achieve 70 percent NLF on both upper and lower surfaces; this resulted in low drag at a cruise Reynolds number of 10×10^6. Murri and Jordon (1987) and Befus et al. (1987) performed full-scale wind tunnel and flight tests of this aircraft. Under a joint research program, NASA, Cessna, and the Federal Aviation Administration (FAA) addressed the flight testing of a NLF aircraft to simulate FAR Part 3 certification. Related to certification, Manuel and Doty (1990) describe the impact of the loss of laminar flow on the Cessna T210R and make quantitative comparisons of the ability of the aircraft to meet certification under these conditions. Three test conditions were explored:

1. Natural transition on all surfaces

2. Fixed transition at 5 percent chord on the upper and lower surfaces of the wing, horizontal stabilizer, and both sides of the vertical stabilizer

3. Fixed transition at 5 percent chord on the upper and lower surfaces of the left wing and the remaining surfaces with natural transition

The conclusions were (1) the loss of NLF did not cause the aircraft to exhibit unacceptable stability and control behavior relative to FAR Part 23 and (2) climb performance decreased 10 percent, which was consistent with the increased drag associated with a tripped boundary-layer flow.

A.2. Bellanca Skyrocket II

Holmes et al. (1983) reported on a flight investigation of NLF on a high-performance, single-propeller, composite aircraft. The primary goals of the flight test were (1) to address the achievability of NLF on a modern composite production-quality surface and (2) to address some of the NLF-related maintainability issues (e.g., insect contamination). The flight envelope enables unit Reynolds numbers up to 1.9×10^6 and chord Reynolds numbers of 12×10^6. Without modification of contours or waviness, the flight test results indicated that laminar flow on the wings and empennage was responsible for the previously measured lower-than-expected zero-lift drag coefficient. No premature transition was observed due to waviness, contour discrepancies, or surface dents. Significant regions of laminar flow were realized in the slipstream region. Insect-debris contamination in flight indicated that 25 percent of the insects caused transition. The fact that transition was realized downstream of the minimum pressure suggests that acoustic, surface, or turbulence disturbances are not responsible for transition; rather, the amplification of TS disturbances or laminar separation in an adverse pressure gradient dominates the transition process. NLF was achieved on approximately 40 percent of the wing and 50 to 70 percent of the propeller. In a comparison of the waviness of the Bellanca Skyrocket II production quality with the filled and sanded wing test section of the King Cobra (see Smith and Higton 1945), it is clear that the production quality of more modern surfaces has less variation, sufficient for NLF and LFC technologies. *N*-factor calculations showed that a 3000-Hz TS wave correlated with the transition location for $N = 17$.

A.3. Gulfstream GA-7 Cougar

Howard, Miley, and Holmes (1985) studied the effects of the propeller slipstream on the laminar wing boundary layer. Hot-film measurements in flight and a wind tunnel show that the state of the boundary layer at any given point on the wing alternates between laminar and turbulent flow because of the periodic

external flow disturbances generated in the viscous wake of the propeller blade. Analytic studies reveal that the cyclic laminar and turbulent drag of the wing is lower than a fully turbulent wing. Hence, the NLF design yields drag-penalty reductions in the slipstream region of the wing and in regions not affected by the slipstream.

A.4. Cessna Citation III

Wentz, Ahmed, and Nyenhuis (1984, 1985) discussed the results of a Langley Research Center, Wichita State University, Cessna Aircraft Co., and Boeing Commercial Airplane Company joint research program on NLF. The study used a business jet aircraft with the following objectives:

1. To determine the transition location at various Mach numbers and Reynolds numbers

2. To determine the effects of wing sweep on transition

3. To determine impact of engine acoustics on transition

4. To check the validity of boundary-layer stability tools

Sublimating chemicals and hot-film anemometry are used to detect transition. The test section on the wing was covered with fiberglass and filled and smoothed to minimize roughness-related effects caused by joints, rivets, and screw heads. Plaster splashes of the upper and lower wing surfaces were made to measure waviness. The measured waviness was well below the maximum allowable for a single wave. (See Kosin 1967.) Transition was realized to about 15 percent chord for 20° wing sweep and to about 5 percent chord for 30° wing sweep. The amplification of TS disturbances is proposed to be the cause for transition because transition was realized in the region of adverse pressure gradient. The impact of engine noise on transition was inconclusive. The flight test results were not compared with theory.

A.5. F-111

A F-111 Transonic Aircraft Technology (TACT) airplane was tested with partial span NLF gloves attached to both wings. The primary goal of the study was to demonstrate laminar flow at higher Reynolds numbers for swept wings. The glove geometry consisted of a supercritical NLF airfoil designed by Boeing and NASA to investigate NLF at transonic speeds. For the design lift coefficient of 0.5 at a Mach number of 0.77 and a Reynolds number of 25×10^6, the airfoil had a favorable pressure gradient to about 70 percent chord on the upper surface (crossflow disturbances were not considered in the design). The glove was installed on the wing to achieve the desired pressure distribution at 10° wing sweep. The flight results showed that laminar flow was obtained to 56 percent chord on the upper surface at 9° sweep, to 21 percent chord at 25° sweep, with chord Reynolds numbers from 23×10^6 to 28×10^6, respectively. The maximum run of laminar flow on the lower surface was 51 percent wing chord at 16° wing sweep to 6 percent chord at 25° sweep (sideslip). The overall results from the F-111 TACT NLF flight experiment showed laminar flow but not as much as expected. Besides not accounting for potential crossflow-induced transition, the F-111 had a limited spanwise extent of test section and had a crude method for determining the transition location.

A.6. NASA NLF(1)-0414F Airfoil Experiment

In addition to flight tests, NLF wing design studies were conducted in the 1980s. For example, McGee et al. (1984) reported the results of testing a NLF wing (NASA NLF(1)-0414F airfoil) in the Langley Low-Turbulence Pressure Tunnel (LTPT). The airfoil was designed (Viken 1983) to achieve 70-percent-chord laminar flow on both upper and lower surfaces at the design Reynolds number of 10×10^6 and Mach number of less than 0.40. In the wind tunnel experiment, laminar flow was observed to 70 percent chord on both surfaces at design conditions.

A.7. F-14

Following the achievement of laminar flow on the F-111, the F-14 Variable Sweep Transition Flight Experiment (VSTFE) was initiated by NASA and Boeing Commercial Airplane Company (Anderson, Meyer, and Chiles 1988). Unlike the F-111 glove (which was not designed to minimize CF disturbance growth), the F-14 gloves were designed to optimize between TS- and CF-disturbance growth. The F-14

test used nearly all the span of the variable-sweep portion and hot films to detect transition onset in the boundary layer. Testing of the smooth clean-up glove ended in 1986 and testing with the Mach number 0.7 NLF glove ended in 1987. Test variations included wing sweep, Reynolds number, Mach number, and pressure gradients. Discussed by Meyer, Trujillo, and Bartlett (1987), the results from the F-14 VSTFE showed maximum transition Reynolds numbers of 17.6×10^6 for 15° wing sweep, 13.5×10^6 for 20° sweep, 12×10^6 for 25° sweep, and 5×10^6 for 3° sweep. Overall, the *N*-factor correlations gave a much broader distribution of *N*(CF) versus *N*(TS) for the F-14 flight test compared with the F-111. Hence, either the *N*(CF)-*N*(TS) graph does not collapse the transition points and correlations to a usable design tool or a more careful review and discrimination of the usable flight test points must be made to reduce the uncertainty and scatter in the results.

A.8. NLF Nacelle Flight Experiment

About the same time, a NLF nacelle flight experiment was conducted through a teaming effort led by General Electric Aircraft Engines. The experiment was pursued because the friction drag associated with modern turbofan nacelles may be as large as 4 to 5 percent of the total aircraft drag for a typical commercial transport and because potential specific fuel consumption (SFC) reductions on the order of 1 to 1.5 percent may be achieved for laminar boundary-layer flows on advanced nacelles. The first phase of the flight experiment involved flying a NLF fairing on the nacelle of a Citation aircraft to develop test techniques and to establish the feasibility of the concept. Hastings et al. (1986) reported the results of the first phase which achieved laminar flow to 37 percent of the fairing length. The analysis showed that the Granville (1953) criterion predicted the observed transition location for two of the four locations and that the pressure on the fairing induced a neutrally stable flow; this indicated that the flow was sensitive to external effects. The second phase of the flight test experiment involved flying a full-scale flow-through NLF nacelle (of various geometries) under the wing of a Grumman OV-1 Mohawk aircraft (Hastings 1987; Faust and Mungur 1987). Three nacelle shapes were selected and designed to have pressure distributions which led to flow fields which were susceptible to boundary-layer instabilities. The variation was to determine the potential influence of sound on the potentially unstable flows. Essentially, a less stable flow would be expected simply by thickening the nacelle lip. Obara and Dodbele (1987) reported the aerodynamic performance results realized during the flight experiment and Schoenster and Jones (1987) reported the effect of the acoustic sources. For a flight test at altitude of 1300 ft, Mach number of 0.25, and unit Reynolds number per foot of 1.8×10^6, subliming chemicals indicated laminar flow to 50 percent of the nacelle length, with transition occurring at the forebody-aftbody joint. At the same flight conditions, the noise sources had no noticeable impact on the transition locations. Away from the pylon, the measured pressure distributions were shown to be in good agreement with the design pressure back to the pressure peak.

A.9. Boeing 757 NFL Flight Test

The question of whether laminar flow could be maintained on a commercial transport with high-bypass-ratio wing-mounted turbofan engines led to another NASA-funded flight experiment. The Boeing Company used its Boeing 757 flight research aircraft with a part of one wing modified to reduce sweep and obtain more NLF and to obtain extensive noise field measurements on a commercial transport (Runyan et al. 1987). Primary goals of the experiment included the determination of the influence of noise on the laminar boundary-layer flow. A 21° swept-wing glove was mounted outboard of the engine on the right wing. The noise level was measured with microphones, surface pressures were measured with strip-a-tube belts, and transition locations with hot films as a function of engine power and flight condition. A large database was obtained during the course of the flight test experiment. The results suggest that the noise levels on the lower surface have engine power dependence; however, the upper surface did not show engine power dependence but did show Mach number dependence. At the design point, laminar flow was observed to 28 percent chord on the upper surface of the glove and to 18 percent chord on the lower surface. At the outboard portion of the glove, transition occurred at about 5 percent chord where the pressure peaked (not predicted by the transonic design code). The lower surface was more sensitive to engine power and 2 to 3 percent less laminar flow was observed at the higher power settings compared with lower power settings.

Concerning the calibration data for transition predictions codes, TS- and CF-disturbance *N*-factors showed fairly good agreement with the Boeing 757 and F-111 flight database.

A.10. VFW 614

In 1986, the German laminar flow technology program, supported by the German Ministry of Research and Technology (BMFT), began wind tunnel and flight experiments NLF and LFC (Redeker et al. 1990). Korner (1990) noted that part of the program involved determining (or discriminating) between when NLF is preferred and when HLFC or LFC is a more appropriate choice for a particular aircraft. Additionally, two of the major milestones of this program involved NLF wind tunnel tests and flight research on the 40-seat VFW 614 research aircraft (owned by DLR) during 1987 through 1990. The goal of the VFW 614 ATTAS NLF flight experiment was to gain a database of TS-disturbance- and CF-disturbance-dominated transition for code calibration. During the flight test, a database was obtained for variations in Mach numbers from 0.35 to 0.7, Reynolds numbers from 12×10^6 to 30×10^6, and sweep angles from 18° to 24° (obtained with sideslip). For a Mach number of 0.35, the transition front ranged from 8 to 50 percent chord dependent on flap and yaw settings (Horstmann et al. 1990). For TS-disturbance-dominated transition, the transition front was at nearly the same chordwise location across the span, whereas for CF-disturbance-dominated transition, a distinct sawtooth pattern arose (reminiscent of CF transition). As yaw was increased, the laminar attachment line became intermittently turbulent which was consistent with the threshold momentum Reynolds number of 100 on the attachment line. Following the VFW 614 NLF flight test, a Fokker 100 transport aircraft was fitted with a partial-span NLF glove to measure the drag reduction associated with a NLF wing design, validate laminar flow CFD methodology, and to establish the upper limits of NLF (transition Reynolds number for a given leading-edge sweep angle). The flight test consisted of three flights for a total of 12 hr. The observed results validated the design predictions of 15-percent drag reduction; this confirmed high-speed wind tunnel investigations conducted at the Dutch National Aerospace Laboratory (Mecham 1992).

Appendix B

Supersonic Natural Laminar Flow Research

In this section, a brief summary of supersonic NLF research is given.

B.1. F-104 Starfighter Flight Test

Some of the first transition-related supersonic flight tests were carried out at the NASA High-Speed Flight Station in California. In 1959, McTigue, Overton, and Petty (1959) reported on transition detection techniques tested in supersonic flight by using an F-104 Starfighter. A wing glove made of fiberglass cloth and epoxy resin was positioned on the wing of the fighter-type aircraft. Resistance thermometers and subliming chemicals were used to detect the transition location. Cameras were used to record the sublimation process in flight. Approximately 40 instrumented flights were flown up to a Mach number of 2.0 and an altitude of 55 000 ft. Photographs were presented in the report giving a measure of transition location (laminar flow extent) with various flight conditions. No detailed analysis of the transition location and mean-flow attributes was performed.

B.2. F-106 and F-15

An F-106 at Langley Research Center and an F-15 at Dryden Flight Research Center had a 6-month window of availability in 1985 which could be used to study supersonic boundary-layer transition (Collier and Johnson 1987). The F-15 twin-engine fighter was selected as a flight test vehicle because earlier flight tests have shown that pressures on the 45° swept wing would support small amounts of NLF. A surface clean-up glove was installed on the right wing of the F-15 to eliminate surface imperfections in the original wing. The glove was 4 ft wide, extended past 30 percent chord, and a notch-bump (fig. 15) was added to the inboard side of the leading edge of the test section to eliminate the potential for attachment-line contamination problems. The flight tests were flown at Mach numbers ranging from 0.7 to 1.8, altitudes of 20 000 to 55 000 ft, unit Reynolds numbers per foot of 1.2×10^6 to 4×10^6, and angles of attack of $-1°$ to 10°. Compressible stability calculations (using COSAL) for stationary crossflow disturbances at zero frequency were correlated with the flight-observed transition location. Ignoring surface curvature, *N*-factors of 10.5 and 11 matched the transition point for the Mach numbers of 0.98 and 1.16, where the transition points were measured at 20 and 15 percent chord, respectively. For transition occurring closer to the leading edge, *N*-factors of 5.5 and 6 were found for Mach numbers of 0.9 and 1.76. Surface clean-up gloves were mounted on both the right wing (leading-edge sweep of 60°) and the vertical tail (sweep of 55°) of the F-106. Gaster-type bumps were installed on the inboard portion of the gloves to prevent attachment-line contamination. Flight tests were conducted at Mach numbers ranging from 0.8 to 1.8, altitudes ranging from 30 000 to 50 000 ft, unit Reynolds numbers per foot of 1.6×10^6 to 5.2×10^6, and angles of attack of 3° to 14°. Turbulent flow was observed at the first hot-film gauge (0.5 percent chord) for all but four of the flight test points. All the transition points were observed within 5 percent chord of the leading edge. Either the attachment-line contamination prevention was not working properly or strong crossflow disturbances were generated by the large leading-edge sweep. Collier and Johnson (1987) showed theoretically that *N*-factor values could be significantly decreased by adding small quantities of suction in the first 12 percent chord of the vertical tail for a simulated F-106 test point. With this small amount of suction, disturbances were stable to 20 percent chord; this suggests that HLFC would lead to significant runs with laminar flow.

References

Anon. 1985: *85–86 Aerospace Facts & Figures*. Aerospace Industries Assoc. of America, Inc., pp. 94–95.

Anon. 1995a: *Aerospace Facts & Figures 1995-96*. Aerospace Industries Assoc. of America, Inc., pp. 92–93.

Anon. 1995b: Laminar-Flow Testing Begins on Airbus A320. *Flight Int*., Apr. 12–18, p.10.

Anderson, Bianca Trujillo; Meyer, Robert R., Jr.; and Chiles, Harry R. 1988: *Techniques Used in the F-14 Variable-Sweep Transition Flight Experiment*. NASA TM-100444.

Anderson, Bianca Trujillo; and Meyer, Robert R., Jr. 1990: *Effects of Wing Sweep on Boundary-Layer Transition for a Smooth F-14A Wing at Mach Numbers From 0.700 to 0.825*. NASA TM-101712.

Anderson, Bianca T.; and Bohn-Meyer, Marta 1992: Overview of Supersonic Laminar Flow Control Research on the F-16XL Ships 1 and 2. SAE Paper 921994.

Anscombe, A.; and Illingworth, L. N. 1956: *Wind-Tunnel Observations of Boundary-Layer Transition on a Wing at Various Angles of Sweepback*. R&M 2968, British A.R.C.

Anselmet, F.; Mérigaud, E.; and Fulachier, L. 1992: Effect of Hole Suction on Boundary Layer Transition. *First European Forum on Laminar Flow Technology*, DGLR-Bericht 92-06, pp. 67–72.

Antonatos, P. P. 1966: Laminar Flow Control—Concepts and Applications. *Astronaut. & Aeronaut*., vol. 4, no. 7, pp. 32–36.

Arcara, P. C., Jr.; Bartlett, D. W.; and McCullers, L. A. 1991: *Analysis for the Application of Hybrid Laminar Flow Control to a Long-Range Subsonic Transport Aircraft*. SAE Paper 912113.

Arnal, D. 1984: Description and Prediction of Transition in Two-Dimensional, Incompressible Flow. *Special Course on Stability and Transition of Laminar Flow*, AGARD Rep. 709.

Arnal, D.; Habiballah, M.; and Coustols, E. 1984: Laminar Instability Theory and Transition Criteria in Two- and Three-Dimensional Flow. *La Recherche Aerospatiale*, no. 2, pp. 45–63.

Arnal, D.; Casalis, G.; and Juillen, J. C. 1990: Experimental and Theoretical Analysis of Natural Transition on 'Infinite' Swept Wing. *Laminar-Turbulent Transition*, Springer-Verlag, pp. 311–325.

Arnal, D.; Juillen, J. C.; and Casalis, G. 1991: The Effects of Wall Suction on Laminar-Turbulent Transition in Three-Dimensional Flow. *Boundary Layer Stability and Transition to Turbulence*, FED-VOL. 114, ASME, pp. 155–162.

Arnal, D.; Juillen, J.-C.; and Casalis, G. 1992: Fundamental Studies Related to Laminar-Turbulent Transition Problems on Swept Wings. *First European Forum on Laminar Flow Technology*, DGLR-Bericht 92-06, pp. 35–44.

Arnal, D. 1992: Boundary Layer Transition: Prediction, Application to Drag Reduction. *Special Course on Skin Friction Drag Reduction*, AGARD Rep. 786. (Available from DTIC as AD A253 005.)

Arnal, Daniel 1994: Boundary Layer Transition: Predictions Based on Linear Theory. *Special Course on Progress in Transition Modelling*, AGARD Rep. 793.

Atkins, P. B. 1951: *Wing Leading Edge Contamination by Insects*. Flight Note 17, Aeronaut. Res. Lab. (Melbourne).

Bacon, J.; Tucker, V.; and Pfenninger, W. 1959: Michigan 5- by 7-Foot Tunnel Experiments on a 30° Swept 12% Thick Symmetric Laminar Suction Wing With Suction Extended Forward to 1% Chord. Rep. NOR-59-328 (BLC-119), Northrop Aircraft, Inc.

Bacon, J. W., Jr.; Pfenninger, W.; and Moore, C. R. 1964: Investigations of a 30° Swept and a 17-Foot Chord Straight Suction Wing in the Presence of Internal Sound, External Sound, and Mechanical Vibrations. *Summary of Laminar Boundary Layer Control Research*, Volume I, ASD-TDR-63-554, U.S. Air Force, pp. 120–154. (Available from DTIC as AD 605 185.)

Balakumar, P.; and Hall, P. 1996: Optimum Suction Distribution for Transition Control. AIAA-96-1950.

Barry, Brian; Parke, Simon J.; Bown, Nicholas W.; Riedel, Hansgeorg; and Sitzmann, Martin 1994: The Flight Testing of Natural and Hybrid Laminar Flow Nacelles. 94-GT-408, ASME.

Bayly, Bruce J.; Orszag, Steven A.; and Herbert, Thorwald 1988: Instability Mechanisms in Shear-Flow Transition. *Annual Review of Fluid Mechanics*, Volume 20, Ann. Rev., Inc., pp. 359–391.

Beckwith, Ivan E.; Chen, Fang-Jeng; and Malik, Mujeeb R. 1987: Design and Fabrication Requirements for Low Noise Supersonic/Hypersonic Wind Tunnels. *Research in Natural Laminar Flow and Laminar-Flow Control*, Jerry N. Hefner and Frances E. Sabo, compilers, NASA CP-2487, Part 3, pp. 947–964.

Beckwith, I. E.; Chen, F.-J.; and Malik, M. R. 1988: Design and Fabrication Requirements for Low-Noise Supersonic/Hypersonic Wind Tunnels. AIAA-88-0143.

Befus, Jack; Nelson, E. Randel; Ellis, David R.; and Latas, Joe 1987: Flight Test Investigations of a Wing Designed for Natural Laminar Flow. SAE Paper 871044.

Bergrun, Norman 1995: A Warming Trend for Icing Research. *Aerosp. America*, vol. 33, no. 8, pp. 22–27.

Berry, Scott; Dagenhart, J. R.; Brooks, C. W.; and Harris, C. D. 1987: Boundary-Layer Stability Analysis of LaRC 8-Foot LFC Experimental Data. *Research in Natural Laminar Flow and Laminar-Flow Control*. Jerry N. Hefner and Frances E. Sabo, compilers, NASA CP-2487, Part 2, pp. 471–489.

Bertolotti, Fabio Paolo 1991: Linear and Nonlinear Stability of Boundary Layers With Streamwise Varying Properties. Ph.D. Thesis, Ohio State Univ.

Bertolotti, Fabio P.; and Crouch, Jeffrey D. 1992: *Simulation of Boundary-Layer Transition: Receptivity to Spike Stage*. NASA CR-191413.

Bhutiani, P. K.; Keck, D. F.; Lahti, D. J.; Stringas, M. J. 1993: Investigating the Merits of a Hybrid Laminar Flow Nacelle. *The Leading Edge*, General Electric Co., Spring, pp. 32–35.

Bicknell, Joseph 1939: *Determination of the Profile Drag of an Airplane Wing in Flight at High Reynolds Numbers*. NACA Rep. 667.

Birch**,** S**.** 1992: Laminar Flow. *Aerosp. Eng*., vol. 12, no. 3, pp. 45–47.

Birch**,** S. 1996: Aerospatiale Looks to the Future. *Aerosp. Eng*., vol. 16, no. 6, pp. 28–30.

Bobbitt, Percy J.; Harvey, William D.; Harris, Charles D.; and Brooks, Cuyler W., Jr. 1992: *The Langley 8-Ft Transonic Pressure Tunnel Laminar-Flow-Control Experiment. Natural Laminar Flow and Laminar Flow Control*, R. W. Barnwell and M. Y. Hussaini, eds., Springer-Verlag, pp. 247–411.

Bobbitt, Percy J.; Ferris, James C.; Harvey, William D.; and Goradia, Suresh H. 1996: *Hybrid Laminar Flow Control Experiment Conducted in NASA Langley 8-Foot Transonic Pressure Tunnel*. NASA TP-3549.

Boltz, F. W.; Kenyon, G. C.; and Allen, C. Q. 1960: *Effects of Sweep Angle on the Boundary-Layer Stability Characteristics of an Untapered Wing at Low Speeds*. NASA TN D-338.

Braslow, Albert L. 1944: *Investigation of Effects of Various Camouflage Paints and Painting Procedures on the Drag Characteristics of an NACA $65_{(421)}$-420, a = 1.0 Airfoil Section*. NACA WR L-141. (Formerly NACA CB L4G17.)

Braslow, Albert L.; and Visconti, Fioravante 1948: *Investigation of Boundary-Layer Reynolds Number for Transition on an NACA $65_{(215)}$-114 Airfoil in the Langley Two-Dimensional Low-Turbulence Pressure Tunnel*. NACA TN 1704.

Braslow, Albert L.; Visconti, Fioravante; and Burrows, Dale L. 1948: *Preliminary Wind-Tunnel Investigation of the Effect of Area Suction on the Laminar Boundary Layer Over an NACA 64A010 Airfoil*. NACA RM L7L15.

Braslow, Albert L.; Burrows, Dale L.; Tetervin, Neal; and Visconti, Fioravante 1951: *Experimental and Theoretical Studies of Area Suction for the Control of the Laminar Boundary Layer on an NACA 64A010 Airfoil*. NACA Rep. 1025. (Supersedes NACA TN 1905 by Burrows, Braslow, and Tetervin and NACA TN 2112 by Braslow and Visconti.)

Braslow, Albert L.; and Knox, Eugene C. 1958: *Simplified Method for Determination of Critical Height of Distributed Roughness Particles for Boundary-Layer Transition at Mach Numbers From 0 to 5*. NACA TN 4363.

Braslow, Albert L.; and Fischer, Michael C. 1985: Design Considerations for Application of Laminar Flow Control Systems to Transport Aircraft. *Aircraft Drag Prediction and Reduction*, AGARD Rep. 723, pp. 4-1–4-27.

Braslow, A.L.; Maddalon, D. V.; Bartlett, D. W.; Wagner, R. D.; and Collier, F. S., Jr. 1990: Applied Aspects of Laminar-Flow Technology. *Viscous Drag Reduction in Boundary Layers*, Dennis M. Bushnell and Jerry Hefner, eds., AIAA, pp. 47–78.

Braslow, Albert L.; and Maddalon, Dal V. 1993: *Flight Tests of Three-Dimensional Surface Roughness in the High-Crossflow Region of a Swept Wing With Laminar-Flow Control*. NASA TM-109035.

Braslow, Albert L.; and Maddalon, Dal V. 1994: *Flight Tests of Surface Roughness Representative of Construction Rivets on a Swept Wing With Laminar-Flow Control*. NASA TM-109103.

Britton, Randall K. 1990: *Elevator Deflections on the Icing Process*. AIAA Student J., vol. 27, pp. 8–18.

Brooks, Cuyler W., Jr.; and Harris, Charles D. 1987: Results of LFC Experiment on Slotted Swept Supercritical Airfoil in Langley's 8-Foot Transonic Pressure Tunnel. *Research in Natural Laminar Flow and Laminar-Flow Control*, Jerry N. Hefner and Frances E. Sabo, compilers, NASA CP-2487, Part 2, pp. 453–469.

Bulgubure, C.; and Arnal, D. 1992: DASSAULT Falcon 50 Laminar Flow Flight Demonstrator. *First European Forum on Laminar Flow Technology*, DGLR-Bericht 92-06, pp.11–18.

Bushnell, D. M.; and Tuttle, M. H. 1979: *Survey and Bibliography on Attainment of Laminar Flow Control in Air Using Pressure Gradient and Suction—Volume 1*. NASA RP-1035.

Bushnell, D. M.; and Malik, M. R. 1987: Supersonic Laminar Flow Control. *Research in Natural Laminar Flow and Laminar-Flow Control*, Jerry N. Hefner and Frances E. Sabo, compilers, NASA CP-2487, Part 3, pp. 923–946.

Buxbaum, Jörg; and Höhne, Gordon 1996: Flow Measurements of Porous Titanium Suction Panels Designed for Laminar Flow Control. MS Thesis, Arizona State Univ.

Carlson, J. C. 1964: *Low Drag Boundary Layer Suction Experiments Using a 33° Swept 15 Percent Thick Laminar Suction Wing With Suction Slots Normal to the Leading Edge Aerodynamic Model and Test Report*. NOR-64-281, Northrop Corp. (Available From DTIC as AD 482 068.)

Carmichael, B. H.; Whites, Roy C.; and Pfenninger, W. 1957: *Low Drag Boundary Layer Suction Experiments in Flight on the Wing Glove of an F-94A Airplane*. Rep. No. NAI-57-1163 (BLC-101), Northrop Aircraft Inc.

Carmichael, B. H. 1959: *Surface Waviness Criteria for Swept and Unswept Laminar Suction Wings*. Rep. No. NOR-59-438 (BLC-123) (Contract AF33 (616)-3168), Northrop Aircraft, Inc.

Carmichael, B. H.; and Pfenninger, W. 1959: *Surface Imperfection Experiments on a Swept Laminar Suction Wing*. Rep. No. NOR-59-454 (BLC-124), Northrop Aircraft Inc.

Carmichael, B. H. 1979: *Summary of Past Experience in Natural Laminar Flow and Experimental Program for Resilient Leading Edge*. NASA CR-152276.

Cattafesta, L. N., III; Iyer, V.; Masad, J. A.; King, R. A.; and Dagenhart, J. R. 1994: Three-Dimensional Boundary-Layer Transition on a Swept Wing at Mach 3.5. AIAA-94-2375.

Cattafesta, L. N., III; Iyer, V.; Masad, J. A.; King, R. A.; and Dagenhart, J. R. 1995: Three-Dimensional Boundary-Layer Transition on a Swept Wing at Mach 3.5. *AIAA J.*, vol. 33, no. 11, pp. 2032–2037.

Cattafesta, L. N., III; and Moore, J. G. 1995: Uncertainty Estimates for Luminescent Temperature-Sensitive Paint Intensity Measurements. AIAA-95-2193.

Cattafesta, Louis N., III; and Moore, Jay G. 1996: Review and Application of Non-Topographic Photogrammetry to Quantitative Flow Visualization. AIAA-96-2180.

Cebeci, Tuncer; and Stewartson, Keith 1980: On Stability and Transition in Three-Dimensional Flows. *AIAA J.*, vol. 18, no. 4, pp. 398–405.

Choudhari, Meelan 1994: Roughness-Induced Generation of Crossflow Vortices in Three-Dimensional Boundary Layers. *Theoret. Comput. Fluid Dyn.*, vol. 6, pp. 1–30.

Choudhari, Meelan; and Streett, Craig 1994: Theoretical Prediction of Boundary-Layer Receptivity. AIAA-94-2223.

Chuprun, John; and Cahill, Jones F. 1966: LFC on Large Logistics Aircraft. *Astronaut. & Aeronaut.*, vol. 4, no. 7, pp. 58–62.

Clark, Rodney L.; Lange, Roy H.; and Wagner, Richard D. 1990: Application of Advanced Technologies to Future Military Transports. *Progress in Military Airlift*, AGARD-CP-495.

Coleman, W. S. 1952: *Wind Tunnel Experiments on the Prevention of Insect Contamination by Means of Soluble Films and Liquids Over the Surface*. BLCC Note 39.

Coleman, W. S. 1961: Roughness Due to Insects. *Boundary Layer and Flow Control*, Volume 2, G. V. Lachmann, ed., Pergamon Press, pp. 682–747.

Coleman, Colin P.; Poll, D. I. A.; Laub, James A.; and Wolf, Stephen W. D. 1996: Leading Edge Transition on a 76 Degree Swept Cylinder at Mach 1.6. AIAA-96-2082.

Coleman, Colin P.; Poll, D. I. A.; and Lin, Ray-Sing 1997: Experimental and Computational Investigation of Leading Edge Transition at Mach 1.6. AIAA-97-1776.

Collier, F. S., Jr.; and Johnson, J. B. 1987: Supersonic Boundary-Layer Transition on the LaRC F-106 and DFRF F-15 Aircraft—Part I: Transition Measurements and Stability Analysis. *Research in Natural Laminar Flow and Laminar-Flow Control*, Jerry N. Hefner and Frances E. Sabo, compilers, NASA CP-2487, Part 3, pp. 997–1014.

Collier, F. S., Jr. 1993: An Overview of Recent Subsonic Laminar Flow Control Flight Experiments. AIAA-93-2987.

Cornelius, Kenneth C. 1987: An Experimental Evaluation of Slots Versus Porous Strips for Laminar-Flow Applications. *Research in Natural Laminar Flow and Laminar-Flow Control*, Jerry N. Hefner and Frances E. Sabo, compilers, NASA CP-2487, Part 2, pp. 435–451.

Courty, J. C.; Bulgubure, C.; and Arnal, D 1993: Estudes d'ecoulements Laminaires Chez Dassault Aviation: Calculs et Essais en Vol (Studies on Laminar Flow Conducted at Dassault Aviation; Calculations and Test

Flights). *Recent Advances in Long Range and Long Endurance Operation of Aircraft,* AGARD CP-547.

Cousteix, Jean 1992: Basic Concepts on Boundary Layers. *Special Course on Skin Friction Drag Reduction.* AGARD Rep. 786. (Available from DTIC as AD A253 005.)

Creel, T. R., Jr.; Malik, M. R.; and Beckwith, I. E. 1987: Experimental and Theoretical Investigation of Boundary-Layer Instability Mechanisms on a Swept Leading Edge at Mach 3.5. *Research in Natural Laminar Flow and Laminar-Flow Contro*l, Jerry N. Hefner and Frances E. Sabo, compilers, NASA CP-2487, Part 3, pp. 981–995.

Creel, T. R., Jr.; Beckwith, I. E.; and Chen, F. J. 1987: Transition on Swept Leading Edges at Mach 3.5. *J. Aircr*., vol. 25, no. 10, pp. 710–717.

Croom, C. C.; and Holmes, B. J. 1985: Flight Evaluation of an Insect Contamination Protection System for Laminar Flow Wings. SAE Paper 850860.

Crouch, J. D. 1994: Theoretical Studies on the Receptivity of Boundary Layers. AIAA-94-2224.

Cumming, R. W.; Gregory, N.; and Walker, W. S. 1953: *An Investigation of the Use of an Auxiliary Slot To Re-Establish Laminar Flow on Low-Drag Aerofoils*. R. & M. No. 2742, British A.R.C.

Cumpsty, N. A.; and Head, M. R.1969: The Calculation of the Three-Dimensional Turbulent Boundary Layer—Part III. Comparison of Attachment-Line Calculations With Experiment. *Aeronaut. Q*., vol. XX, pp. 99–113.

Dagenhart, J. Ray 1981: *Amplified Crossflow Disturbances in the Laminar Boundary Layer on Swept Wings With Suction*. NASA TP-1902.

Davis, Richard E.; Fischer, Michael C.; Fisher, David F.; and Young, Ronald 1986: Cloud Particle Effects on Laminar Flow in the NASA LEFT Program: Preliminary Results. AIAA-86-9811.

Davis, Richard E.; Maddalon, Dal V.; and Wagner, Richard D. 1987: Performance of Laminar-Flow Leading-Edge Test Articles in Cloud Encounters. *Research in Natural Laminar Flow and Laminar-Flow Control*, Jerry N. Hefner and Frances E. Sabo, compilers, NASA CP-2487, Part 1, pp. 163–193.

Davis, Richard E.; Maddalon, Dal V.; Wagner, Richard D.; Fisher, David F.; and Young, Ronald 1989: *Evaluation of Cloud Detection Instruments and Performance of Laminar-Flow Leading-Edge Test Articles During NASA Leading-Edge Flight-Test Program.* NASA TP-2888.

Di Giorgio, L. 1990: The High Speed Market in the Next Three Decades. *Proceedings of the European Symposium on Future Supersonic Hypersonic Transportation Systems,* pp. 117–130.

Dryden, Hugh L. 1936: *Air Flow in the Boundary Layer Near a Plate*. NACA Rep. 562.

Dunn, D. W.; and Lin, C. C. 1953: On the Role of Three-Dimensional Disturbances in the Stability of Supersonic Boundary Layers. *J. Aeronat. Sci*., vol. 20, pp. 577–578.

Edwards, Brian 1977: Laminar Flow Control—Concepts, Experiences, Speculations. *Special Course on Concepts for Drag Reduction*. AGARD Rep. 654, pp. 4-1–4-41.

Etchberger, F. R.; et al. 1983: *LFC Leading Edge Glove Flight—Aircraft Modification Design, Test Article Development, and Systems Integration*. NASA CR-172136.

Fage, A. 1943: *The Smallest Size of a Spanwise Surface Corrugation Which Affects Boundary-Layer Transition on an Aerofoil*. R. & M. No. 2120, British A.R.C.

Faust, G. K.; and Mungur, P. 1987: Status Report on a Natural Laminar-Flow Nacelle Flight Experiment—Nacelle Design. *Research in Natural Laminar Flow and Laminar-Flow Control*, Jerry N. Hefner and Frances E. Sabo, compilers, NASA CP-2487, Part 3, pp. 891–907.

Fedorov, A. V.; and Khokhlov, A. P. 1993: Excitation and Evolution of Unstable Disturbances in Supersonic Boundary Layer. *Transitional and Turbulent Compressible Flows*, FED-Vol. 151, ASME.

Fernandez, Rene; Rylicki, Daniel S.; Maddalon, Dal V.; Dietrich, Donald; and McVey, Leslie 1996: Flight Tests of Anti-Insect Coatings on a Simulated Hybrid Laminar Flow Nacelle Surface. Paper presented at World Aviation Congress and Exposition 1996 (Los Angeles, California).

Fischer, M. C.; Wright, A. S., Jr.; and Wagner, R. D. 1983: *A Flight Test of Laminar Flow Control Leading-Edge Systems*. NASA TM-85712.

Fischer, Michael; and Vemuru, Chandra S. 1991: Application of Laminar Flow Control to the High Speed Civil Transport—The NASA Supersonic Laminar Flow Control Program. SAE Paper 912115.

Fisher, David F.; and Fischer, Michael C. 1987: Development Flight Tests of JetStar LFC Leading-Edge Flight Test Experiment. *Research in Natural Laminar Flow and Laminar-Flow Control*, Jerry N. Hefner and Frances E. Sabo, compilers, NASA CP-2487, Part 1, pp. 117–140.

Flores, Jolen; Tu, Eugene L.; Anderson, Bianca; and Landers, Stephen 1991: A Parametric Study of the

Leading Edge Attachment Line for the F-16XL. AIAA-91-1621.

Fowell, L. R.; and Antonatos, P. P. 1965: Some Results From the X-21A Program—Part 2: Laminar Flow Flight Test Results on the X-21A. *Recent Developments in Boundary Layer Research*—Part IV, AGARDograph 97.

Freeman, J. A. 1945: Studies in the Distribution of Insects by Aerial Currents—The Insect Population of the Air From Ground Level to 300 Feet. *J. Anim. Ecol.*, vol. 14, pp. 128–154.

Gaster, M. 1965: A Simple Device for Preventing Turbulent Contamination on Swept Leading Edges. *J. R. Aeronaut. Soc.*, vol. 69, no. 659, pp. 788–789.

Gaster, M. 1967: On the Flow Along Swept Leading Edges. *Aeronaut. Q.*, vol. XVIII, pt. 2, pp. 165–184.

Glick, P. A. 1939: *The Distribution of Insects, Spiders, and Mites in the Air*. Tech. Bull. No. 673, U.S. Dep. Agriculture.

Goethert, Bernhard 1966: Toward Long-Range Aircraft With Laminar Flow Control. *Astronaut. & Aeronaut.*, vol. 4, no. 7, pp. 56–57.

Goldsmith, John 1955: *Critical Suction Quantities and Pumping Losses Associated With Laminar Boundary Layer Suction Through Rows of Closely-Spaced Holes.* Rep. NAI-55-287 (BLC-72), Northrop Aircraft, Inc. (Available from DTIC as AD 74 865(b).)

Goldsmith, John 1957: *Critical Laminar Suction Parameters for Suction Into an Isolated Hole or a Single Row of Holes.* Rep. No. NAI-57-529 (BLC-95), Northrop Aircraft, Inc.

Goldsmith, John 1964: Investigation of Laminar Flow Control Airfoils Swept Behind the Mach Angle. *Summary of Laminar Boundary Layer Control Research*, Volume I, ASD-TDR-63-554, U.S. Air Force, pp. 487–547. (Available from DTIC as AD 605 185.)

Goldstein, M. E. 1983: The Evolution of Tollmien-Schlichting Waves Near a Leading Edge. *J. Fluid Mech.*, vol. 127, pp. 59–81.

Goldstein, M. E. 1985: Scattering of Acoustic Waves Into Tollmien-Schlichting Waves by Small Streamwise Variations in Surface Geometry. *J. Fluid Mech.*, vol. 154, pp. 509–529.

Goldstein, M. E.; Leib, S. J.; and Cowley, S. J. 1987: Generation of Tollmien-Schlichting Waves on Interactive Marginally Separated Flows. *J. Fluid Mech.*, vol. 181, pp. 485–517.

Gottschalk, Mark A. 1996: Going With the Flow. *Design News*, Sept. 9, pp. 23–24.

Granville, Paul S. 1953: *The Calculation of the Viscous Drag of Bodies of Revolution*. Rep. 849, David W. Taylor Model Basin.

Gray, W. E.; and Davies, H. 1952: *Note on the Maintenance of Laminar-Flow Wings*. R. & M. No. 2485, British A.R.C.

Gray, W. E. 1952: *The Effect of Wing Sweep on Laminar Flow*. Tech. Memo. No. Aero 255, British R.A.E.

Gray, W. E.; and Fullam, P. W. J. 1950: *Comparison of Flight and Tunnel Measurements of Transition on a Highly Finished Wing (King Cobra)*. Rep. No. Aero 2383, British R.A.E.

Greber, Isaac 1959: *Interaction of Oblique Shock Waves With Laminar Boundary Layers*. Tech. Rep. 59-2, MIT.

Gregory, N.; Stuart, J. T.; and Walker, W. S. 1955: On the Stability of Three-Dimensional Boundary Layers With Application to the Flow Due to a Rotating Disk. *Philos. Trans. R. Soc. London*, ser. A, vol. 248, no. 943, pp. 155–199.

Gregory, N. 1961: Research on Suction Surfaces for Laminar Flow. *Boundary Layer and Flow Control*, Volume 2, G. V. Lachmann, ed., Pergamon Press, pp. 924–960.

Gregory, N.; and Love, E. M. 1965: *Laminar Flow on a Swept Leading Edge: Final Progress Report*. NPL AERO. Memo. No. 26, British A.R.C.

Gross, L. W.; Bacon, J. W., Jr.; and Tucker, V. L. 1964: Experimental Investigation and Theoretical Analysis of Laminar Boundary Layer Suction on a 30° Swept, 12-Percent-Thick Wing in the NASA Ames 12-Foot Pressure Wind Tunnel. *Summary of Laminar Boundary Layer Control Research, Volume I*, ASD-TDR-63-554, U.S. Air Force, pp. 96–110. (Available from DTIC as AD 605 185.)

Gross, L. W. 1964: Experimental Investigation of a 4-Percent-Thick Straight Laminar Suction Wing of 17-Foot Chord in the NORAIR 7- by 10-Foot Wind Tunnel. *Summary of Laminar Boundary Layer Control Research*, Volume I, ASD-TDR-63-554, U.S. Air Force, pp. 111–119. (Available from DTIC as AD 605 185.)

Gross, L. W. 1964: Laminarization of a Sears-Haack Body of Revolution by Means of Boundary Layer Suction. *Summary of Laminar Boundary Layer Control Research*, Volume I, ASD-TDR-63-554, U.S. Air Force, pp. 155–165. (Available from DTIC as AD 605 185.)

Groth, E. E.; Carmichael, B. H.; Whites, Roy C.; and Pfenninger, W. 1957: *Low Drag Boundary Layer Suction Experiments in Flight on the Wing Glove of a F94-A Airplane—Phase II: Suction Through 69 Slots*. NAI-57-318 (BLC-94) (Contract AF-33(616-3108)), Northrop Aircraft, Inc.

Groth, E. E. 1961: Boundary Layer Suction Experiments at Supersonic Speeds. *Boundary Layer and Flow Control*. Volume 2, G. V. Lachmann, ed., Pergamon Press, pp. 1049–1076.

Groth, E. E. 1964a: Investigation of a Laminar Flat Plate With Suction Through Many Fine Slots With and Without Weak Incident Shock Waves. *Summary of Laminar Boundary Layer Control Research*. Volume I, ASD-TDR-63-554, U.S. Air Force, pp. 428–441. (Available from DTIC as AD 605 185.)

Groth, E. E. 1964b: Low Drag Boundary Layer Suction Experiments at Supersonic Speeds on an Ogive Cylinder With 29 Closely Spaced Slots. *Summary of Laminar Boundary Layer Control Research*. Volume I, ASD-TDR-63-554, U.S. Air Force, pp. 449–463. (Available from DTIC as AD 605 185.)

Groth, E. E. 1964c: Investigations of Swept Wings With Supersonic Leading Edges. *Summary of Laminar Boundary Layer Control Research*. Volume I, ASD-TDR-63-554, U.S. Air Force, pp. 464–479. (Available from DTIC as AD 605 185.)

Groth, E. E.; Pate, S. R.; and Nenni, J. P. 1965: Laminar Flow Control at Supersonic Speeds. *Recent Developments in Boundary Layer Research*—Part IV, AGARDograph 97.

Hackenberg P.; Tutty, O. R.: and Nelson, P. A. 1994: Numerical Studies of the Automatic Control of Boundary-Layer Transition via Multiple Suction Panels. AIAA-94-2214.

Hall, A. A.; and Hislop, G. S. 1938: *Experiments on the Transition of the Laminar Boundary Layer on a Flat Plate*. R. & M. No. 1843, British A.R.C.

Hall, G. R. 1964: *On the Mechanics of Transition Produced by Particles Passing Through an Initially Laminar Boundary Layer and the Estimated Effect on the LFC Performance of the X-21 Aircraft*. Northrop Corp.

Hall, P. 1983: The Linear Development of Görtler Vortices in Growing Boundary Layers. *J. Fluid Mech.*, vol. 130, pp. 41–58.

Hall, P.; Malik, M. R.; and Poll, D. I. A. 1984: On the Stability of an Infinite Swept Attachment Line Boundary Layer. *Proc. R. Soc. London*, ser. *A*, vol. 395, pp. 220–245.

Hardy, A. C.; and Milne, P. S. 1938: Studies in the Distribution of Insects by Aerial Currents—Experiments in Aerial Tow-Netting From Kites. *J. Anim. Ecol*., vol. 7, no. 2, pp. 199–229.

Harris, Julius E.; Iyer, Venkit; and Radwan, Samit 1987: Numerical Solutions of the Compressible 3-D Boundary-Layer Equations for Aerospace Configurations With Emphasis on LFC. *Research in Natural Laminar Flow and Laminar-Flow Contro*l, Jerry N. Hefner and Frances E. Sabo, compilers, NASA CP-2487, Part 2, pp. 517–545.

Harris, Roy V., Jr.; and Hefner, Jerry N. 1987: NASA Laminar-Flow Program—Past, Present, Future. *Research in Natural Laminar Flow and Laminar-Flow Control*, Jerry N. Hefner and Frances E. Sabo, compilers, NASA CP-2487, Part 1, pp. 1–23.

Harvey, W. D.; and Pride, J. D. 1981: NASA Langley Laminar Flow Control Airfoil Experiment. *Laminar Flow Control—1991 Research and Technology Studies*, Dal V. Maddalon, ed., NASA CP-2218, pp. 1–42.

Hastings, E. C.; Schoenster, J. A.; Obara, C. J.; and Dodbele, S. S. 1986: Flight Research on Natural Laminar Flow Nacelles: A Progress Report. AIAA-86-1629.

Hastings, Earl C., Jr. 1987: Status Report on a Natural Laminar Flow Flight Experiment— Summary. *Research in Natural Laminar Flow and Laminar-Flow Control*, Jerry N. Hefner and Frances E. Sabo, compilers, NASA CP-2487, Part 3, pp. 887–890.

Haynes, T. S.; and Reed, H. L. 1996: Computations in Nonlinear Saturation of Stationary Crossflow Vortices in a Swept-Wing Boundary Layer. AIAA-96-0182.

Head, M. R. 1955: *The Boundary Layer With Distributed Suction*. R. & M. No. 2783, British A.R.C. (Available from DTIC as AD B029 704.)

Head, M. R.; Johnson, D.; and Coxon, M. 1955: *Flight Experiments on Boundary-Layer Control for Low Drag*. R. & M. No. 3025, British A.R.C.

Hefner, Jerry N.; and Bushnell, Dennis M. 1980: *Status of Linear Boundary-Layer Stability Theory and the* e^n *Method, With Emphasis on Swept-Wing Applications*. NASA TP-1645.

Hefner, Jerry N. 1992: Laminar Flow Control: Introduction and Overview. *Natural Laminar Flow and Laminar Flow Control*, R. W. Barnwell and M. Y. Hussaini, eds., Springer-Verlag, pp. 1–22.

Helmholtz, H. 1868: Über discontinuirliche Flüssigkeits-Bewegungen. *Akad. Wiss*., Monatsber 215.

Herbert, Thorwald 1988: Secondary Instability of Boundary Layers. *Annual Review of Fluid Mechanics*, Volume 20, Ann. Rev., Inc., pp. 487–526.

Herbert, Th. 1991: Boundary-Layer Transition—Analysis and Prediction Revisited. AIAA-91-0737.

Hilton, W. F. 1955: Tests of a Fairing To Reduce the Drag of a Supersonic Swept-Wing Root. *J. Aeronaut. Sci.*, vol. 22, no. 3, pp. 173–178, 188.

Holmes, Bruce J.; Obara, Clifford J.; Gregorek, Gerald M.; Hoffman, Michael J.; and Freuler, Rick J. 1983: Flight Investigation of Natural Laminar Flow on the Bellanca Skyrocket II. SAE Paper 830717.

Holmes, Bruce J., Obara, Clifford J.; and Yip, Long P. 1984: *Natural Laminar Flow Experiments on Modern Airplane Surfaces*. NASA TP-2256.

Holmes, Bruce J.; Obara, Clifford J.; Martin, Glenn L.; and Domack, Christopher S. 1985: Manufacturing Tolerances for Natural Laminar Flow Airframe Surfaces. SAE Paper 850863.

Holmes, Bruce J.; and Obara, Clifford J. 1992: Flight Research on Natural Laminar Flow Applications. *Natural Laminar Flow and Laminar Flow Control*, R. W. Barnwell and M. Y. Hussaini, eds., Springer-Verlag, pp. 73–142.

Horstmann, K. H.; Redeker, G.; Quast, A.; Dressler, U.; and Bieler, H. 1990: Flight Tests With a Natural Laminar Flow Glove on a Transport Aircraft. AIAA-90-3044.

Howard, R. M.; Miley, S. J.; and Holmes, B. J. 1985: An Investigation of the Effects of the Propeller Slipstream on the Laminar Wing Boundary Layer. SAE Paper 850859.

Humphreys, B. E. 1992: Surface Contamination Avoidance for Laminar Flow Surfaces. *First European Forum on Laminar Flow Technology*, DGLR-Bericht 92-06, pp. 262–269.

Iyer, Venkit 1990: *Computation of Three-Dimensional Compressible Boundary Layers to Fourth-Order Accuracy on Wings and Fuselages*. NASA CR-4269.

Iyer, Venkit; and Spall, Robert 1991: Application of Linear Stability Theory in Laminar Flow Design. SAE Paper 912116.

Iyer, V.; Spall, R.; and Dagenhart, J. 1992: Computational Study of Transition Front on a Swept Wing Leading-Edge Model. AIAA-92-2630.

Iyer, Venkit 1993: *Three-Dimensional Boundary-Layer Program (BL3D) for Swept Subsonic or Supersonic Wings With Application to Laminar Flow Control*. NASA CR-4531.

Iyer, Venkit 1995: *Computer Program BL2D for Solving Two-Dimensional and Axisymmetric Boundary Layers*. NASA CR-4668.

Johnson, Paul L. 1996: Effects of Suction on Crossflow Disturbance Growth—NASA/BCAG Crossflow Experiment Results. Paper presented at World Aviation Congress and Exposition 1996 (Los Angeles, California).

Jones, B. Melvill 1938: Flight Experiments on the Boundary Layer. *J. Aeronaut. Sci.*, vol. 5, no. 3, pp. 81–101.

Jones, J. H.; and Pate, S. R. 1961: *Investigation of Boundary-Layer Suction on a Flat Plate at Mach Number 3*. AEDC-TN-61-128, U.S. Air Force.

Joslin, Ronald D.; Streett, Craig L.; and Chang, Chau-Lyan 1992: *Validation of Three-Dimensional Incompressible Spatial Direct Numerical Simulation Code—A Comparison With Linear Stability and Parabolic Stability Equation Theories for Boundary-Layer Transition on a Flat Plate*. NASA TP-3205.

Joslin, R. D.; Street, C. L.; and Chang, C.-L. 1993: Spatial Direct Numerical Simulation of Boundary-Layer Transition Mechanisms: Validation of PSE Theory. *Theoret. Comput. Fluid Dyn.*, vol. 4, pp. 271–288.

Joslin, R. D.; and Streett, C. L. 1994. The Role of Stationary Crossflow Vortices in Boundary-Layer Transition on Swept Wings. *Phys. Fluids*, vol. 6, no. 10, pp. 3442–3453.

Joslin, Ronald D. 1995: Direct Simulation of Evolution and Control of Three-Dimensional Instabilities in Attachment-Line Boundary Layers. *J. Fluid Mech.*, vol. 291, pp. 369–392.

Joslin, Ronald D. 1996: Simulation of Nonlinear Instabilities in an Attachment-Line Boundary Layer. *Fluid Dyn. Res.*, vol. 18, pp. 81–97.

Kachanov, Y. S.; and Tararykin, O. I. 1990: The Experimental Investigation of Stability and Receptivity of a Swept-Wing Flow. *Laminar-Turbulent Transition*, D. Arnal and R. Michel, eds., Springer-Verlag, pp. 499–509.

Kachanov, Yury S. 1994: Physical Mechanisms of Laminar-Boundary-Layer Transition. *Annual Review of Fluid Mechanics*, Volume 26, Ann. Rev., Inc., pp. 411–482.

Kay, J. M. 1953: *Boundary-Layer Flow Along a Flat Plate With Uniform Suction.* R. & M. 2628, British A.R.C.

Kelvin, Lord 1880: On Disturbance in Lord Rayleigh's Solution for Waves in a Plane Vortex Stratum. *Mathematical and Physical Papers*, Volume 4, pp. 186–187.

Kerschen, E. J. 1987: Boundary-Layer Receptivity and Laminar-Flow Airfoil Design. *Research in Natural Laminar Flow and Laminar-Flow Control*, Jerry N. Hefner and Frances E. Sabo, compilers, NASA CP-2487, Part 1, pp. 273–287.

Kerschen, E. 1989: Boundary Layer Receptivity. AIAA-89-1109.

Kirchner, M. E. 1987: Laminar Flow: Challenge and Potential. *Research in Natural Laminar Flow and Laminar-Flow Control*, Jerry N. Hefner and Frances E. Sabo, compilers, NASA CP-2487, Part 1, pp. 25–44.

Kleiser, Leonhard; and Zang, Thomas A. 1991: Numerical Simulation of Transition in Wall-Bounded Shear Flows. *Annual Review of Fluid Mechanics*, Volume 23, Ann. Rev., Inc., pp. 495–537.

Kopkin, T. J.; and Rife, C. D. 1977: *Laminar Flow Control Bibliography*. Rep. No. LG 77ER0018, Lockheed-Georgia Co. (Available from DTIC as AD B026 321L.)

Kosin, R. E. 1967: *LFC Aircraft Design Data Laminar Flow Control Demonstration Program*. NOR-67-136, Northrop Aircraft, Inc.

Körner, H. 1990: Natural Laminar Flow Research for Subsonic Transport Aircraft in the FRG. *Z. Flugwiss. Weltraumforsch.*, vol. 14, pp. 223–232.

Lachmann, G. V. 1961: Aspects of Design, Engineering and Operational Economy of Low Drag Aircraft. *Boundary Layer and Flow Control*, Volume 2, G. V. Lachmann, ed., Pergamon Press, pp. 1123–1166.

Lange, Roy H. 1984: Design Integration of Laminar Flow Control for Transport Aircraft. *J. Aircr.*, vol. 21, pp. 612–617.

Lange, Roy H. 1987: Lockheed Laminar-Flow Control Systems Development and Applications. *Research in Natural Laminar Flow and Laminar-Flow Control*. Jerry N. Hefner and Frances E. Sabo, compilers, NASA CP-2487, Part 1, pp. 53–77.

Ledy, J. P.; Charpin, F.; and Garcon, F. 1993: ELFIN (European Laminar Flow Investigation) Test in S1MA Wind Tunnel. *1992 Scientific and Technical Activities*, ONERA, pp. 60–61.

Leehey, P.; and Shapiro, P. J. 1980: Leading Edge Effect in Laminar Boundary Layer Excitation by Sound. *Laminar-Turbulent Transition*, R. Eppler and H. Fasel, eds., Springer-Verlag, pp. 321–331.

Liepmann, Hans W. 1943: *Investigations on Laminar Boundary-Layer Stability and Transition on Curved Boundaries*. NACA WR W-107. (Formerly NACA ACR 3H30.)

Lin, R.-S.; Edwards, J. R.; Wang, W.-P.; and Malik, M. R. 1996: Instabilities of a Mach 2.4 Slow-Expansion Square Nozzle Flow. AIAA-96-0784.

Lin, R.-S.; and Malik, M. R. 1994: The Stability of Incompressible Attachment-Line Boundary Layers—A 2D-Eigenvalue Approach. AIAA-94-2372.

Lin, R.-S.; and Malik, M. R. 1995: Stability and Transition in Compressible Attachment-Line Boundary-Layer Flow. SAE Paper 952041.

Lin, Ray-Sing; and Malik, Mujeeb R. 1996: On the Stability of Attachment-Line Boundary Layers. Part 1—The Incompressible Swept Hiemenz Flow. *J. Fluid Mech.*, vol. 311, pp. 239–255.

Lynch, Frank K.; and Klinge, Mark D. 1991: Some Practical Aspects of Viscous Drag Reduction Concepts. SAE Paper 912129.

Mack, L. M. 1989: Stability of Three-Dimensional Boundary Layers on Swept Wings at Transonic Speeds. *Symposium Transsonicum III*, J. Zierep and H. Oertel, eds., Springer-Verlag, pp. 209–224.

MacManus, D.; and Eaton, J. 1996: Micro-Scale Three-Dimensional Navier-Stokes Investigation Laminar Flow Control Suction Hole Configurations. AIAA-96-0544.

MacManus, David G.; Eaton, John A.; Barrett, Rod V.; Rickards, Jeremy; and Swales, Chris 1996: Mapping the Flow Field Induced by a HLFC Perforation Using a High Resolution LDV. AIAA-96-0097.

Maddalon, D. V.; Collier, F. S., Jr.; Montoya, L. C.; and Land, C. K. 1989: Transition Flight Experiments on a Swept Wing With Suction. AIAA-89-1893.

Maddalon, Dal V.; and Braslow, Albert L. 1990: *Simulated-Airline-Service Flight Tests of Laminar-Flow Control With Perforated-Surface Suction System*. NASA TP-2966.

Maddalon, Dal V. 1990: Boeing 757 Hybrid Laminar-Flow Control Flight Tests. *Langley Aerospace Test Highlights*, NASA TM-104090, p. 159.

Maddalon, Dal V. 1991: Hybrid Laminar-Flow Control Flight Research. *Research and Technology*, NASA TM-4331, p. 47.

Malik, Mujeeb R. 1982: *COSAL—A Black-Box Compressible Stability Analysis Code for Transition Prediction in Three-Dimensional Boundary Layers*. NASA CR-165925.

Malik, Mujeeb R. 1987: Stability Theory Applications to Laminar-Flow Control. *Research in Natural Laminar Flow and Laminar-Flow Control*, Jerry N. Hefner and

Frances E. Sabo, compilers, NASA CP-2487, Part 1, pp. 219–244.

Manuel, Gregory S.; and Doty, Wayne A. 1990: A Flight Test Investigation of Certification Requirements for Laminar-Flow General Aviation Airplanes. AIAA-90-1310.

Maresh, J. L.; and Bragg, M. B. 1984: The Role of Airfoil Geometry in Minimizing the Effect of Insect Contamination of Laminar Flow Sections. AIAA-84-2170.

Masad, J. 1996a: The Critical Allowable Height of a Backward-Facing Step. AIAA-96-0780.

Masad, Jamal A. 1996b: *Effect of Surface Waviness on Transition in Three-Dimensional Boundary-Layer Flow*. NASA CR-201641.

McGhee, Robert J.; Viken, Jeffrey K.; Pfenninger, Werner; Beasley, William D.; and Harvey, William D. 1984: *Experimental Results for a Flapped Natural-Laminar-Flow Airfoil With High Lift/Drag Ratio.* NASA TM-85788.

McNay, Dave; and Allen, John 1981: *Laminar Flow Control Leading Edge Glove Flight Test Article Development*. ACEE-21-PM-1632 (Contract NAS1-16220), McDonnell Douglas Corp.

McTigue, John G.; Overton, John D.; and Petty, Gilbert, Jr. 1959: *Two Techniques for Detecting Boundary-Layer Transition in Flight at Supersonic Speeds and at Altitudes Above 20,000 Feet*. NASA TN D-18.

Mecham, Michael 1992: Europeans Test New Laminar Flow Design, Target Lower Transport Operating Costs. *Aviat. Week & Space Tech.*, Feb. 3, p. 51.

Meifarth, K. U.; and Heinrich, S. 1992: The Environment for Aircraft With Laminar Flow Technology Within Airline Service. *First European Forum on Laminar Flow Technology*, DGLR-Bericht 92-06, pp. 251–255.

Meitz, Hubert L.; and Fasel, Hermann F. 1994: Navier-Stokes Simulations of the Effects of Suction Holes on a Flat Plate Boundary Layer. *Application of Direct and Large Eddy Simulation to Transition and Turbulence*, AGARD-CP-551.

Meyer, Robert R.; Trujillo, Bianca M.; and Bartlett, Dennis W. 1987: F-14 VSTFE and Results of the Cleanup Flight Test Program. *Research in Natural Laminar Flow and Laminar-Flow Control*, Jerry N. Hefner and Frances E. Sabo, compilers, NASA CP-2487, Part 3, pp. 819–844.

Morkovin, Mark V. 1969: On the Many Faces of Transition. *Viscous Drag Reduction*, C. Sinclair Wells, ed., Plenum Press, pp. 1–31.

Morris, John 1987: LFC—A Maturing Concept. *Research in Natural Laminar Flow and Laminar-Flow Control*, Jerry N. Hefner and Frances E. Sabo, compilers, NASA CP-2487, Part 1, pp. 45–51.

Morrisette, E. L.; and Creel, T. R., Jr. 1987: The Effects of Wall Surface Defects on Boundary-Layer Transition in Quiet and Noisy Supersonic Flow. *Research in Natural Laminar Flow and Laminar-Flow Control*, Jerry N. Hefner and Frances E. Sabo, compilers, NASA CP-2487, Part 3, pp. 965–980.

Mullender, A. J.; Bergin, A. L.; and Poll, D. I. A. 1991: Application of Laminar Flow to Aero Engine Nacelles. *Boundary Layer Transition & Control.* Rep. No. PNR-90916, ETN-92-92205, British R.A.E.

Murri, Daniel G.; and Jordon, Frank L., Jr. 1987: *Wind-Tunnel Investigation of a Full-Scale General Aviation Airplane Equipped With an Advanced Natural Laminar Flow Wing.* NASA TP-2772.

Nayfeh, A. 1980: Stability of Three-Dimensional Boundary Layers. *AIAA J.*, vol. 18, pp. 406–416.

Nayfeh, Ali H. 1987: Nonparallel Stability of Boundary Layers. *Research in Natural Laminar Flow and Laminar-Flow Control*, Jerry N. Hefner and Frances E. Sabo, compilers, NASA CP-2487, Part 1, pp. 245–259.

Nayfeh, Ali H.; Ragab, Saad A.; and Al-Maaitah, Ayman 1987: Effect of Roughness on the Stability of Boundary Layers. *Research in Natural Laminar Flow and Laminar-Flow Control*, Jerry N. Hefner and Frances E. Sabo, compilers, NASA CP-2487, Part 1, pp. 301–315.

Nayfeh, Ali H.; Ragab, Saad A.; and Al-Maaitah, Ayman A. 1988: Effect of Bulges on the Stability of Boundary Layers. *Phys. Fluids*, vol. 31, no. 4, pp. 796–806.

Nelson, P. A.; and Rioual, J.-L. 1994: *An Algorithm for the Automatic Control of Boundary Layer Flow*. ISVR Tech. Rep. No. 233, Univ. of Southhampton.

Nenni, Joseph P.; and Gluyas, George L. 1996: Aerodynamic Design and Analysis of an LFC Surface. *Astronaut. & Aeronaut.*, vol. 4, no. 7, pp. 52–57.

Norris, Guy 1994: Smooth and Supersonic. *Flight Int.*, vol. 145, no. 4421, pp. 32–33.

Obara, Clifford J.; and Dodbele, S. S. 1987: Status Report on a Natural Laminar-Flow Nacelle Flight Experiment—Nacelle Aerodynamic Performance. *Research in Natural Laminar Flow and Laminar-Flow Control*, Jerry N. Hefner and Frances E. Sabo, compilers, NASA CP-2487, Part 3, pp. 908–913.

Orr, William M'Fadden 1907: *The Stability or Instability of the Steady Motions of a Liquid. Part II: A Viscous*

Liquid. Proc. R. Irish Acad., vol. XXVII, section A, no. 3, pp. 69–138.

Oudart, Adalbert 1949: Le Calcul de la Couche Limite Laminaire ou Turbulente en Fluide Compressible: Les Methodes Semi-Empiriques Modernes et Les Travaux du Dr. Ing. Alfred Walz (The Calculation of the Laminar or Turbulent Boundary in a Compressible Fluid: The Modern Semi-Empirical Methods and Work of Dr. Alfred Walz). Publ. Sci. & Tech. No. 223, Ministére de l'Air (Paris).

Parikh, P. G.; Chen, A. W.; Yu, N. J.; Wyatt, G. H.; and Timar, T. 1990: Application of Boundary Layer Control to HSCT Low Speed Configuration. AIAA- 90-3199.

Parikh, P. G.; and Nagel, A. L. 1990: *Application of Laminar Flow Control to Supersonic Transport Configurations*. NASA CR-181917.

Pate, S. R. 1964: *Investigation of Drag Reduction by Boundary-Layer Suction on a 50-Deg Swept Tapered Wing at M_∞ = 2.5 to 4*. AEDC-TDR-64-221, U.S. Air Force. (Available from DTIC as AD 450 195.)

Pate, S. R. 1965: *Investigation of Drag Reduction by Boundary-Layer Suction on a Body of Revolution at Mach Numbers 2.5, 3, and 3.5*. AEDC-TR-65-36, U.S. Air Force. (Available from DTIC as AD 456 988.)

Pate, S. R.; and Deitering, J. S. 1963: *Investigation of Drag Reduction by Boundary-Layer Suction on a 36-Deg Swept Wing at M_∞ = 2.5 to 4*. AEDC-TDR-63-23, U.S. Air Force.

Pearce, W. E. 1981: Progress at Douglas on Laminar Flow Control Applied to Commercial Transport Aircraft. *Laminar Flow Control*. ACEE-23-PM-1630 (Contract NAS1-16234), McDonnell Douglas Corp.

Pearce, W. E. 1982: Progress at Douglas on Laminar Flow Control Applied to Commercial Transport Aircraft. *ICAS Proceedings, 1982*: *13th Congress of the International Council of the Aeronautical Sciences, AIAA Aircraft Systems and Technology Conference*, B. Laschka and R. Staufenbiel, eds.

Pearce, W. E.; McNay, D. E.; and Thelander, J. A. 1984: *Laminar Flow Control Leading Edge Glove Flight Test Article Development*. NASA CR-172137.

Perkins, Porter J.; and Rieke, William J.: Aircraft Icing Problems—After 50 years. AIAA-93-0392.

Peterman, B. E. 1987: Laminar Flow—The Cessna Perspective. *Research in Natural Laminar Flow and Laminar-Flow Control*, Jerry N. Hefner and Frances E. Sabo, compilers, NASA CP-2487, Part 1, pp. 79–88.

Peterson, John B., Jr.; and Fisher, David F. 1978: Flight Investigation of Insect Contamination and Its Alleviation. *CTOL Transport Technology—1978*, NASA CP-2036, Part I, pp. 357–373.

Pfenninger, W.; Groth, E. E.; Carmichael, B. H.; and Whites, R. C. 1955: *Low Drag Boundary Layer Suction Experiments in Flight on the Wing Glove of a F94-A Airplane. Phase I—Suction Through Twelve Slots*. Rep. No. NAI-55-458 (BLC-77), Northrop Aircraft, Inc. (Available from DTIC as AD 79 342(b).)

Pfenninger, Werner 1952: *Experiments With a 15% Thick Slotted Laminar Suction Wing Model in the Low Turbulence Tunnel (TDT) at the NACA, Langley Field, Virginia*. TR-5982, Northrop Aircraft, Inc.

Pfenninger, W.; Gross, Lloyd; and Bacon, John W., Jr. (appendix I by G. S. Raetz) 1957: *Experiments on a 30° Swept 12%-Thick Symmetrical Laminar Suction Wing in the 5-Ft by 7-Ft Michigan Tunnel*. Rep. No. NAI-57-317 (BLC-93), Northrop Aircraft, Inc.

Pfenninger, W.; and Groth, E. 1961: Low Drag Boundary Layer Suction Experiments in Flight on a Wing Glove of an F-94A Airplane With Suction Through a Large Number of Fine Slots. *Boundary Layer and Flow Control*, Volume 2, G. V. Lachmann, ed., Pergamon Press, pp. 981–999.

Pfenninger, W. 1965: Some Results From the X-21A Program—Part 1: Flow Phenomena at the Leading Edge of Swept Wings. *Recent Developments in Boundary Layer Research*—Part IV, AGARDograph 97.

Pfenninger, Werner; and Reed, Verlin D. 1966: Laminar-Flow Research and Experiments. *Astronaut. & Aeronaut.*, vol. 4, no. 7, pp. 44–50.

Pfenninger, W.; and Bacon, J. W., Jr. 1969: Amplified Laminar Boundary Layer Oscillations and Transition at the Front Attachment Line of a 45° Swept Flat-Nosed Wing With and Without Boundary Layer Suction. *Viscous Drag Reduction*, C. Sinclair Wells, ed., Plenum Press, pp. 85–105.

Pfenninger, W. 1987: Long-Range LFC Transport. *Research in Natural Laminar Flow and Laminar-Flow Control*, Jerry N. Hefner and Frances E. Sabo, compilers, NASA CP-2487, Part 1, pp. 89–115.

Pfenninger, Werner; and Vemuru, Chandra S. 1988: Design Aspects of Long Range Supersonic LFC Airplanes With Highly Swept Wings. SAE Paper 881397.

Pfenninger, Werner; and Vemuru, Chandra S. 1992: Design Philosophy of Long Range LFC Transports With Advanced Supercritical LFC Airfoils. *Natural Laminar Flow and Laminar Flow Control*, R. W. Barnwell and M. Y. Hussaini, eds., Springer-Verlag, pp. 177–222.

Phillips, Edward H. 1996: NASA Sends Test Data Via Web. *Aviat. Week & Space Technol*., Apr. 15, p. 37.

Plascott, R. H.; Higton, D. J.; Smith, F.; and Bramwell, A. R. 1946: *Flight Tests on Hurricane II, Z.3687 Fitted With Special Wings of "Low-Drag" Design*. R. & M. No. 2546, British A.R.C.

Poll, D. I. A. 1979: Transition in the Infinite Swept Attachment Line Boundary Layer. *Aeron. Quart.*, vol. XXX, pp. 607–628.

Poll, D. I. A. 1980: Three-Dimensional Boundary Layer Transition via the Mechanisms of Attachment Line Contamination and Cross Flow Instability. *Laminar Turbulent Transition*, R. Eppler and H. Fasel, eds., Springer-Verlag, pp. 253–262.

Poll, D. I. A. 1985: Some Observations of the Transition Process on the Windward Face of a Long Yawed Cylinder. *J. Fluid Mech.*, vol. 150, pp. 329–356.

Poll, D. I. A.; Danks, M.; and Humphreys, B. E. 1992: The Aerodynamic Performance of Laser Drilled Sheets. *First European Forum on Laminar Flow Technology*, DGLR-Bericht 92-06, pp. 274–277.

Powell, Arthur G. 1987: The Right Wing of the L.E.F.T. Airplane. *Research in Natural Laminar Flow and Laminar-Flow Control*, Jerry N. Hefner and Frances E. Sabo, compilers, NASA CP-2487, Part 1, pp. 141–161.

Powell, A. G.; Agrawal, S.; and Lacey, T. R. 1989: *Feasibility and Benefits of Laminar Flow Control on Supersonic Cruise Airplanes*. NASA CR-181817.

Pruett, C. David; and Chang, Chau-Lyan 1995: Spatial Direct Numerical Simulation of High-Speed Boundary-Layer Flows—Part II: Transition on a Cone in Mach 8 Flow. *Theoret. Comput. Fluid Dyn*., vol. 7, pp. 397–424.

Ranaudo, Richard J.; Reehorst, Andrew L.; and Potapczuk, Mark G. 1988: An Overview of the Current NASA Program on Aircraft Icing Research. SAE Paper 881386.

Rayleigh, Lord 1879: On the Instability of Jets. *Scientific Papers*, Volume I, Cambridge Univ. Press, pp. 361–371.

Rayleigh, Lord 1880: On the Stability or Instability of Certain Fluid Motions. *Proc. London Math. Soc.*, vol. 11, pp. 57–70.

Rayleigh, Lord 1887: On the Stability or Instability of Certain Fluid Motions II. *Proc. London Math. Soc.*, vol. 19, pp. 67–74.

Redeker, G.; Horstmann, K. H.; Köster, H; Thiede, P.; and Szodruch, J. 1990: Design of a Natural Laminar Flow Glove for a Transport Aircraft. AIAA-90-3043.

Redeker, G.; Quast, A.; and Thibert, J. J. 1992: Das A320 Laminar-Seitenleit Werks-Program. *Proceedings of JAHRBUSH 1992*, Volume III, DGLR, pp. 1259–1270.

Reed, Helen L.; and Saric, William S. 1989: Stability of Three-Dimensional Boundary Layers. *Annual Review of Fluid Mechanics*, Volume 21, Ann. Rev., Inc., pp. 235–284.

Reibert, M. S.; Saric, W. S.; Carrillo, R. B., Jr.; and Chapman, K. L. 1996: Experiments in Nonlinear Saturation of Stationary Crossflow Vortices in a Swept-Wing Boundary Layer. AIAA-96-0184.

Reilly, Richard J.; and Pfenninger, W. 1955: *Laminar Flow Observations on a Rotating Disc*. Rep. No. NAI-55-288 (BLC-73), Northrop Aircraft, Inc.

Reinmann, J. J. 1981: *Selected Bibliography of NACA-NASA Aircraft Icing Publications*. NASA TM-81651.

Reneaux, J.; and Blanchard, A. 1992: The Design and Testing of an Airfoil With Hybrid Laminar Flow Control. *First European Forum on Laminar Flow Technology*, DGLR-Bericht 92-06, pp. 164–174.

Reshotko, Eli 1976: Boundary-Layer Stability and Transition. *Annual Review of Fluid Mechanics*, Volume 8, Ann. Rev., Inc., pp. 311–349.

Reshotko, E. 1984: Environment and Receptivity. *Special Course on Stability and Transition of Laminar Flow*, AGARD Rep. 709, pp. 4-1–4-11.

Reynolds, Osborne 1883: An Experimental Investigation of the Circumstances Which Determine Whether the Motion of Water Shall Be Direct or Sinuous, and of the Law of Resistance in Parallel Channels. *Philosoph. Trans. R. Soc. London*, ser. A, vol. 174, pp. 935–982.

Robert, J.-P. 1992a: Hybrid Laminar Flow Control—A Challenge for a Manufacturer. *First European Forum on Laminar Flow Technology*, DGLR-Bericht 92-06, pp. 294–308.

Robert, J.-P. 1992b: Drag Reduction: An Industrial Challenge. *Special Course on Skin Friction Drag Reduction.* AGARD Rep. 786. (Available from DTIC as AD A253 005.)

Rogers, Kenneth H. 1955: *Investigation of the Pressure Distribution Along a Constant Area Suction Duct With 90 Degree Drilled-Hole Inlet*. Rep. No. NAI-55-286 (BLC-71), Northrop Aircraft, Inc.

Rogers, K. H. 1957: *Experimental and Theoretical Investigations of the Pressure-Drop Through Holes and Slots in Incompressible Viscous Flow*. Rep. No. NAI-58-19 (BLC-104), Northrop Aircraft, Inc. (Available from DTIC as AD 152 319.)

Rozendaal, R. A. 1986: *Natural Laminar Flow Flight Experiments on a Swept Wing Business Jet—Boundary Layer Stability Analyses*. NASA CR-3975.

Runyan, L. James; and George-Falvy, Dezso 1979: Amplification Factors at Transition on an Unswept Wing in Free Flight and on a Swept Wing in Wind Tunnel. AIAA-79-0267.

Runyan, L. J.; Bielak, G. W.; Behbehani, R.; Chen, A. W.; and Rozendaal, R. A. 1987: 757 NLF Glove Flight Test Results. *Research in Natural Laminar Flow and Laminar-Flow Control*, Jerry N. Hefner and Frances E. Sabo, compilers, NASA CP-2487, Part 3, pp. 795–818.

Saric, William S. 1985: Laminar Flow Control With Suction*:* Theory and Experiment*. Aircraft Drag Prediction and Reduction*, AGARD Rep. 723.

Saric, William S.; Hoos, Jon A.; and Radeztsky, Ronald H. 1991: Boundary-Layer Receptivity of Sound With Roughness. *Boundary Layer Stability and Transition to Turbulence*, FED-Vol. 114, ASME, pp. 17–22.

Schlichting, H. 1932: Concerning the Origin of Turbulence in a Rotating Cylinder. *Math. Phys. Klasse*, no. 2, pp. 160–198.

Schmitt, V.; Reneaux, J.; and Priest, J. 1993: Maintaining Laminarity by Boundary Layer Control. *1992 Scientific and Technical Activities*, ONERA, pp. 13–14.

Schoenster, James A.; and Jones, Michael G. 1987: Status Report on a Natural Laminar-Flow Nacelle Flight Experiment: Effects of Acoustic Sources. *Research in Natural Laminar Flow and Laminar-Flow Control*, Jerry N. Hefner and Frances E. Sabo, compilers, NASA CP-2487, Part 3, pp. 914–923.

Schrauf, G.; Bieler, H.; and Thiede, P. 1992: Transition Prediction—The Deutsche Airbus View. *First European Forum on Laminar Flow Technology*, DGLR-Bericht 92-06, pp. 73–82.

Schubauer, G. B. 1939: *Air Flow in the Boundary Layer of an Elliptic Cylinder*. NACA Rep. 652.

Schubauer, G. B.; and Skramstad, H. K. 1947: Laminar Boundary-Layer Oscillations and Stability of Laminar Flow. *J. Aeronaut. Sci.*, vol. 14, no. 2, pp. 69–78.

Schubauer, G. B.; and Skramstad, H. K. 1948: *Laminar-Boundary-Layer Oscillations and Transition on a Flat Plate.* NACA Rep. 909.

Schwab, U. 1992: Electron Beam Drilled Holes for Laminar Flow Control. *First European Forum on Laminar Flow Technology*, DGLR-Bericht 92-06, pp. 270–273.

Shifrin, Carole A. 1991: Hybrid Laminar Flow Tests Cut Drag, Fuel Burn on 757. *Aviat. Week & Space Technol.*, Dec. 2, pp. 36–37.

Singer, Bart A.; Choudhari, Meelan; and Li, Fei 1995: *Weakly Nonparallel and Curvature Effects on Stationary Crossflow Instability: Comparison of Results From Multiple-Scales Analysis and Parabolized Stability Equations.* NASA CR-198200.

Smith, A. M. O. 1953: *Review of Research on Laminar Boundary Layer Control at the Douglas Aircraft Co., El Segundo Division*. Rep. No. ES-19475, Douglas Aircraft Co.

Smith, A. M. O. 1955: On the Growth of Taylor-Görtler Vortices Along Highly Concave Walls. *Q. Appl. Math.*, vol. XIII, no. 3, pp. 233–262.

Smith, A. M. O. 1956: Transition, Pressure Gradient, and Stability Theory. *Proceedings of the International Congress of Applied Mechanics*, Volume 9, pp. 234–244.

Smith, A. M. O.; and Gamberoni, Nathalie 1956: Transition, Pressure Gradient, and Stability Theory. Rep. No. ES 26388, Douglas Aircraft Co., Inc.

Smith, Bruce A. 1995: F-16XL Flights Could Aid in HSCT Design. *Aviat. Week & Space Technol.*, Oct. 23, pp. 42–44.

Smith, Bruce A. 1996: Laminar Flow Data Evaluated. *Aviat. Week & Space Technol.*, Oct. 7, p. 30.

Smith, F.; and Higton, D. J. 1945: *Flight Tests on "King Cobra" FZ.440 To Investigate the Practical Requirements for the Achievement of Low Profile Drag Coefficients on a "Low Drag" Aerofoil*. R. & M. No. 2375, British A.R.C.

Somers, Dan M. 1992: Subsonic Natural-Laminar-Flow Airfoils. *Natural Laminar Flow and Laminar Flow Control*, R. W. Barnwell and M. Y. Hussaini, eds., Springer-Verlag, pp. 143–176.

Sommerfeld, A. 1908: Ein Beitrag zur Hydrodynamischen Erklaerung der Turbulenten Fluessigkeitsbewegungen. *Atti Int. Congress of Math.*, vol. 3, pp. 116–124.

Spalart, P. R. 1989: Direct Numerical Study of Leading-Edge Contamination. *Fluid Dynamics of 3-D Turbulent Shear Flows and Transition*, AGARD-CP-438, pp. 5.1–5.13.

Squire, H. B. 1933: On the Stability for Three-Dimensional Disturbances of Viscous Fluid Flow Between Parallel Walls. *Proc. R. Soc. London*, ser. A, vol. CXLII, pp. 621–628.

Srokowski, Andrew J.; and Orszag, Steven A. 1977: Mass Flow Requirements for LFC Wing Design. AIAA-77-1222.

Stephens, A. V.; and Haslam, J. A. G. 1938: *Flight Experiments on Boundary Layer Transition in Relation to Profile Drag.* R. & M. No. 1800, British A.R.C.

Stock, H. W. 1990: The Stability and Amplification Rates of Two-Dimensional, Incompressible Laminar Boundary Layers With Suction. *Z. Flugwiss. Weltraumforsch*, vol. 14, pp. 263–272.

Sturgeon, R. F.; Bennett, J. A.; Etchberger, F. R.; Ferrill, R. S.; and Meade, L. E. 1976: *Study of the Application of Advanced Technologies to Laminar-Flow Control Systems for Subsonic Transports. Volume II: Analyses.* NASA CR-144949.

Tadjfar, M.; and Bodonyi, R. J. 1992: Receptivity of a Laminar Boundary Layer to the Interaction of a Three-Dimensional Roughness Element With Time-Harmonic Free-Stream Disturbances. *J. Fluid Mech.*, vol. 242, pp. 701–720.

Tamigniaux, T. L. B.; Stark, S. E.; and Brune, G. W. 1987: An Experimental Investigation of the Insect Shielding Effectiveness of a Krueger Flap/Wing Airfoil Configuration. AIAA-87-2615.

Theofilis, Vassilios 1993a: Numerical Experiments on the Stability of Leading Edge Boundary Layer Flow: A Two-Dimensional Linear Study. *Int. J. Numer. Methods Fluids*, vol. 16, pp. 153–170.

Thibert, J. J.; Reneaux, J.; and Schmitt, Reneaus V. 1990: ONERA Activities on Drag Reduction. *Proceedings of the 17th Congress of the International Council of the Aeronautical Sciences*, pp. 1053–1059. (Available as ICAS-90-3.6.1.)

Tollmien, W. 1929: Über die Entstehung der Turbulenz. *Math.-Phys. Kl.*, pp. 21–44. (Translation available as NACA TM 609.)

Tuttle, Marie H.; and Maddalon, Dal V. 1982: *Laminar Flow Control (1976–1982)—A Selected, Annotated Bibliography*. NASA TM-84496.

Tuttle, Marie H.; and Maddalon, Dal V. 1993: *Laminar Flow Control—1976–1991: A Comprehensive, Annotated Bibliography*. NASA TM-107749.

Van Driest, E. R.; and McCauley, W. D. 1960: The Effect of Controlled Three-Dimensional Roughness on Boundary-Layer Transition at Supersonic Speeds. *J. Aerosp. Sci.*, vol. 27, no. 4, pp. 261–271, 303.

Van Ingen, J. L. 1956: *A Suggested Semi-Empirical Method for the Calculation of the Boundary Layer Transition Region.* Rep. V.T.H.-74, Tech. Hogeschool Vliegtuigbouwkunde.

Viken, Jeffrey K. 1983: Aerodynamic Design Considerations and Theoretical Results for a High Reynolds Number Natural Laminar Flow Airfoil. M.S. Thesis, George Washington Univ.

Vijgen, P. M. H. W.; Dodbele, S. S.; Holmes, B. J.; and Van Dam, C. P. 1986: Effects of Compressibility on Design of Subsonic Natural Laminar Flow Fuselages. AIAA-86-1825.

Von Doenhoff, Albert E. 1940: *Investigation of the Boundary Layer About a Symmetrical Airfoil in a Wind Tunnel of Low Turbulence.* NACA WR L-507.

Wagner, Richard D.; Maddalon, Dal V.; and Fischer, Michael C. 1984: Technology Developments for Laminar Boundary Layer Control on Subsonic Transport Aircraft. NASA paper presented at the 54th Meeting of the Fluid Dynamics Panel Symposium on Improvement of Aerodynamic Performance Through Boundary Layer Control and High Lift Systems (Brussels, Belgium).

Wagner, R. D.; Maddalon, D. V.; Bartlett, D. W.; and Collier, F. S., Jr. 1988: *Fifty Years of Laminar Flow Flight Testing*. SAE Paper 881393.

Wagner, Richard D.; Maddalon, Dal V.; Bartlett, D. W.; Collier, F. S., Jr.; and Braslow, A. L. 1989: Laminar-Flow Flight Experiments. *Transonic Symposium: Theory, Application and Experiment—Volume 2*, Jerome T. Foughner, compiler, NASA CP-3020, pp. 59–104.

Wagner, R. D.; Fischer, M. C.; Collier, F. S., Jr.; and Pfenninger, W. 1990: Supersonic Laminar Flow Control on Commercial Transports. *17th Congress of the International Council of the Aeronautical Sciences, ICAS Proceedings*.

Wagner, R. D.; Maddalon, D. V.; Bartlett, D. W.; Collier, F. S., Jr.; and Braslow, A. L. 1992: Laminar Flow Flight Experiments—A Review. *Natural Laminar Flow and Laminar Flow Control*, R. W. Barnwell and M. Y. Hussaini, eds., Springer-Verlag, pp. 23–72.

Warren, E. S.; and Hassan, H. A. 1997a: An Alternative to the e^n Method for Determining Onset of Transition. AIAA-97-0825.

Warren, E. S.; and Hassan, H. A. 1997b: A Transition Closure Model for Predicting Transition Onset. Session Code: 10A1, Presented at 1997 AIAA/SAE World Aviation Congress.

Warwick, Graham 1985: JetStar Smoothes the Way. *Flight Int.*, vol. 128, pp. 32–34.

Wentz, W. H., Jr.; Ahmed, A.; and Nyenhuis, R. 1984: Natural Laminar Flow Flight Experiments on a Swept-Wing Business Jet. AIAA-84-2189.

Wentz, W. H., Jr.; Ahmed, A.; and Nyenhuis, R. 1985: Further Results of Natural Laminar Flow Flight Test Experiments. *General Aviation Aircraft Aerodynamics,* SAE SP-621, pp. 37–50.

Wetmore, J. W.; Zalovcik, J. A.; and Platt, Robert C. 1941: *A Flight Investigation of the Boundary-Layer Characteristics and Profile Drag of the NACA 35-215 Laminar-Flow Airfoil at High Reynolds Numbers*. NACA WR L-532. (Formerly NACA MR May 5, 1941.)

Whitcomb, Richard T.; and Clark, Larry R. 1965: *An Airfoil Shape for Efficient Flight at Supercritical Mach Numbers*. NASA TM X-1109.

Whites, R. C.; Sudderth, R. W.; and Wheldon, W. G. 1966: Laminar Flow Control on the X-21. *Astronaut. & Aeronaut.*, vol. 4, no. 7, pp. 38–43.

Wiegel, M.; and Wlezien, R. W. 1993: Acoustic Receptivity of Laminar Boundary Layers Over Wavy Walls. AIAA-93-3280.

Wilkinson, S. P.; Anders, S. G.; Chen, F.-J.; and Beckwith, I. E. 1992: Supersonic and Hypersonic Quiet Tunnel Technology at NASA Langley. AIAA-92-3908.

Williams, Louis J. 1995: HSCT Research Gathers Speed. *Aerosp. America,* pp. 32–37.

Woan, C. J.; Gingrich, P. B.; and George, M. W. 1991: CFD Validation of a Supersonic Laminar Flow Control Concept. AIAA-91-0188.

Wolf, Stephen W. D.; Laub, James A.; and King, Lyndell S. 1994: Flow Characteristics of the NASA-Ames Laminar Flow Supersonic Wind Tunnel for Mach 1.6 Operation. AIAA-94-2502.

Wortmann, F. X. 1963: A Method for Avoiding Insect Roughness on Aircraft. *Luftahrettechnik Raumfahritechnik*, vol. 9, no. 9, pp. 272–274. (Translation available as NASA TT F-15454.)

Wortmann, F. X. 1969: Visualization of Transition. *J. Fluid Mech*., vol. 38, pt. 3, pp. 473–480.

Young, A. D.; Serby, J. E.; and Morris, D. E. 1939: *Flight Tests on the Effect of Surface Finish on Wing Drag*. R. & M. No. 2258, British A.R.C.

Zalovcik, John A.; Wetmore, J. W.; and Von Doenhoff, Albert E. 1944: *Flight Investigation of Boundary-Layer Control by Suction Slots on an NACA 35-215 Low-Drag Airfoil at High Reynolds Numbers*. NACA WR L-521. (Formerly NACA ACR 4B29.)

Zalovcik, John A.; and Skoog, Richard B. 1945: *Flight Investigation of Boundary-Layer Transition and Profile Drag of an Experimental Low-Drag Wing Installed on a Fighter-Type Airplane.* NACA WR L-94. (Formerly NACA ACR L5C08a.)

Table 1. Subsonic and Transonic LFC Wind Tunnel and Flight Experiments and Major Accomplishments

[Blank spaces indicate information not available]

Year	Reference	LFC type	Extent of LFC, percent x/c	Flight or tunnel	Laminar, percent x/c	Re	Notes
1941	Zalovcik, Wetmore, and Von Doenhoff 1944	9 slots	20 to 60	Flight B-18 2d glove	45	21.7×10^6 to 30.8×10^6	Pressure minimum at 45 percent x/c
1948	Braslow, Visconti, and Burrows 1948 Burrows et al. 1951	Porous		2D model	83	8×10^6	Measurements to 83 percent only
1948–1949	Smith 1953	16 slots	Spaced for acceleration	2D airfoil	100	6.5×10^6	First use of N-factor method
1949–1950	Pfenninger, Gross, and Bacon 1957	86 slots	25 to 95	30° swept-wing model	100	11.8×10^6	Measured drag close to theory
1950	Head 1955	Porous nylon		Anson Mk.1 2D wing			
1953–1954	Head, Johnson, and Coxon 1955	Porous	6 to 98	Vampire III 11.5° sweep	100	29×10^6	70 to 80 percent profile drag reduction
1955	Pfenninger et al. 1955	12 slots	41 to 95	F-94	100	12×10^6 to 30×10^6	$M = 0.6$ to 0.65
1955–1956	Groth et al. 1957 Carmichael, Whites and Pfenninger 1957	69 slots			100	36×10^6	Drag reduction Studied surface waves
1956	Pfenninger and Groth 1961	81 slots					Local $M = 1.1$
1957	Carmichael and Pfenninger 1959	93 slots	0.5 to 97	30° swept wing	100	12×10^6	Studied surface waves
1963	Gross 1964	100 slots	1 to 97.2	2D airfoil	100	26×10^6	
1963	Bacon, Pfenninger, and Moore 1964	100 slots 93 slots	1 to 97.2 1 to 97	2D model 30° swept model			Studied sound influence
1963	Gross and Bossel 1964	120 slots	4.8 to 100	Body of revolution	100	20.1×10^6	
1963	Gross, Bacon, and Tucker 1964	93 slots	1 to 97	30° swept model	100	29×10^6	
1963–1965	Pfenninger 1965 Fowell and Antonatos 1965	Slot		X-21 30° sweep	96 81 59	20×10^6 30×10^6 40×10^6	200 LFC flights

Table 2. Subsonic LFC Wind Tunnel and Flight Experiments and Major Accomplishments Prior to OPEC Oil Embargo (1970)

[Blank spaces indicate information not available]

Year	Reference	LFC type	Extent of LFC, percent x/c	Flight or tunnel	Laminar, percent x/c	Re	Mach number	Notes
1957–1958	Groth 1961	19 slots	23.5 to 90	5-percent-thick biconvex airfoil	93	12.5×10^6	2.23 to 2.77	Measurements at 93 percent chord
1958	Groth 1961	16 slots		Ogive Cylinder	 100 100	9×10^6 7.0×10^6 3.0×10^6	2.5 to 3.0 3.0 3.5	
1957	Groth 1964a Groth, Pate, and Nenni 1965	76 slots	5 to 97	Flat plate		21.8×10^6 25.7×10^6 21.4×10^6	2.5 3.0 3.5	Drag = 26–43 percent of turbulent skin friction
1958	Groth 1964b	29 slots	11 to 46	Ogive Cylinder	100 100 100	15.3×10^6 11.5×10^6 6.3×10^6	2.5 3.0 3.5	Critical roughness studied
1962	Groth 1964c Pate and Deitering 1963 Groth, Pate, and Nenni 1965	66 slots	Began at 2	36° biconvex swept wing		17×10^6 25×10^6 20×10^6	2.5 3.0 3.5	
1963	Goldsmith 1964	Slots		72.5° wing		9×10^6	1.99 to 2.25	
1962	Pate 1965 Groth, Pate, and Nenni 1965	150 slots	Began at 2	9.2-in. body of revolution		42×10^6 51.5×10^6	2.5 3.0	Drag = 23 percent of turbulent flat plate
1964	Pate 1964 Groth, Pate, and Nenni 1965	68 slots		50° swept wing	100 100 100		2.5 3.0 3.5	Drag = $\frac{1}{3} C_f$ of turbulent flat plate

Table 3. LFC Wind Tunnel and Flight Experiments and Major Accomplishments After OPEC Oil Embargo

[Blank spaces indicate information not available]

(a) Subsonic

Year	Reference	LFC type	Extent of LFC, percent x/c	Flight or tunnel	Laminar, percent x/c	Re	Notes
1977–1978	Kirchner 1987	Slot	0 to 30	30° swept model			
1981–1985 1985–1987	Bobbitt et al. 1992 Bobbitt et al. 1996	Slot Perforated	0 to 96 0 to 96	23° swept model	100 65	10×10^6 20×10^6	Tunnel interference
1986	Powell 1987 Lange 1987	Perforated 27 slots	0 to 12 0 to 12	Jetstar	97 100		Anti-insect system OK
1986	Peterman 1987	Porous		Citation III nacelle			
1987	Bulgubure and Arnal 1992	Perforated	0 to 10	Falcon 50	12 to 20		Anti-insects
1990–1991	Maddalon 1991, 1992	Perforated	0 to 22	Boeing 757	65		29 percent C_D reduction
1991–1992	Bhutiani et al. 1993	Perforated	–43	Nacelle	43		All altitudes
1992	Schmitt, Reneaux, and Priest 1993	Perforated	0 to 15	ATTAS wing model	50		
1996	Phillips 1996	Perforated		35° wing			

(b) Supersonic

Year	Reference	LFC type	Extent of LFC, percent x/c	Flight or tunnel	Laminar, percent x/c	Re	Mach number	Notes
1991	Anderson and Bohn-Meyer 1992	Perforated		F-16XL Ship 1			1.6	
1995	Unpublished	Perforated		Swept model			3.5	
1995–1996	Smith 1995, 1996	Perforated		F-16XL Ship 2			1.9 to 2.0	

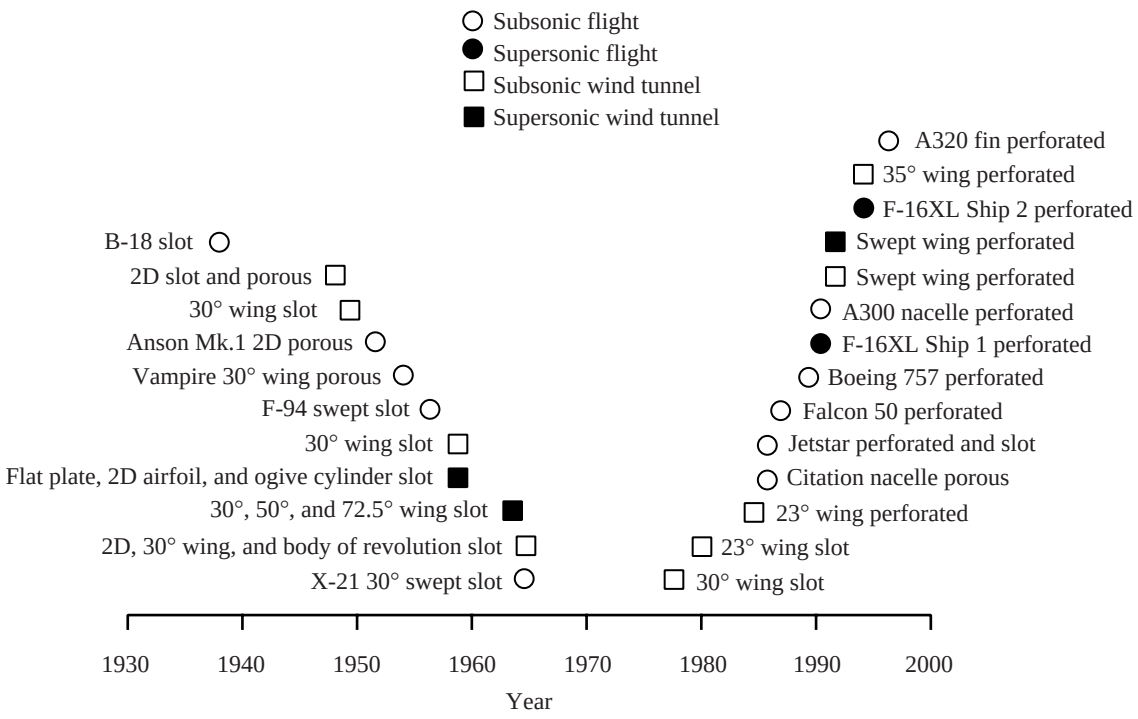

Figure 1. Overview of Laminar Flow Control Projects.

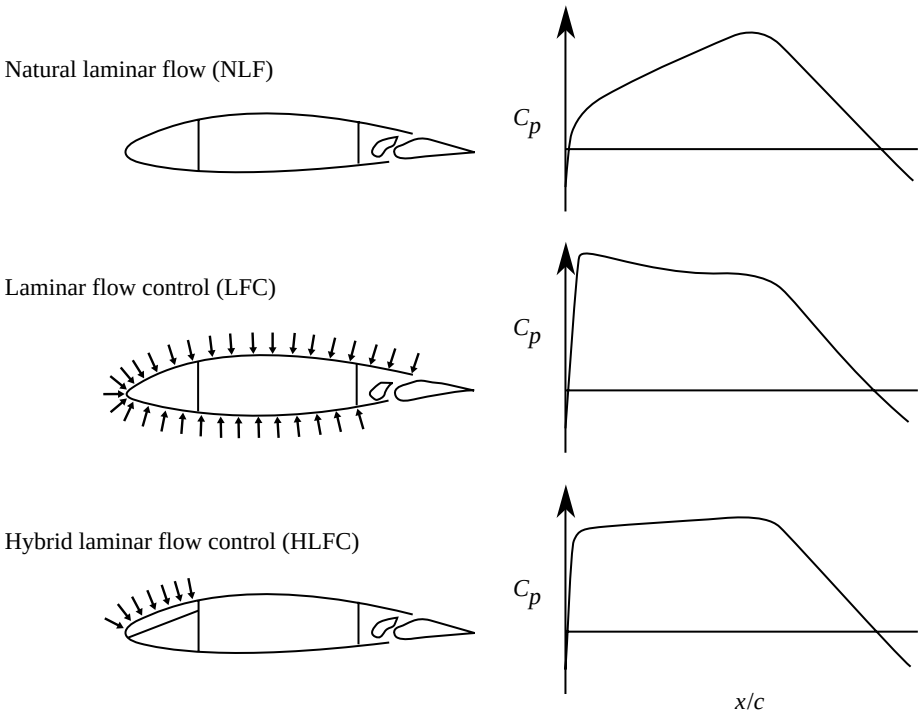

(a) NLF, LFC, and HLFC concepts for wing.

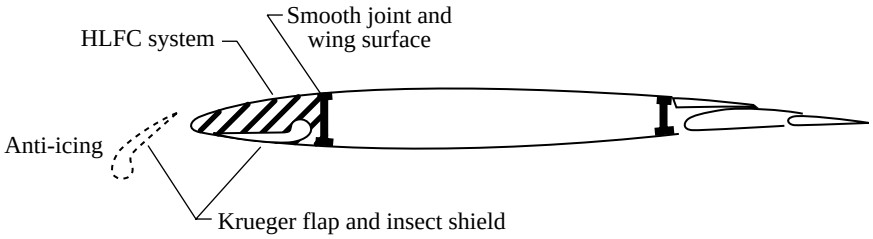

(b) Practical application of HLFC wing.

Figure 2. Concepts and practical application. (From Collier 1993.)

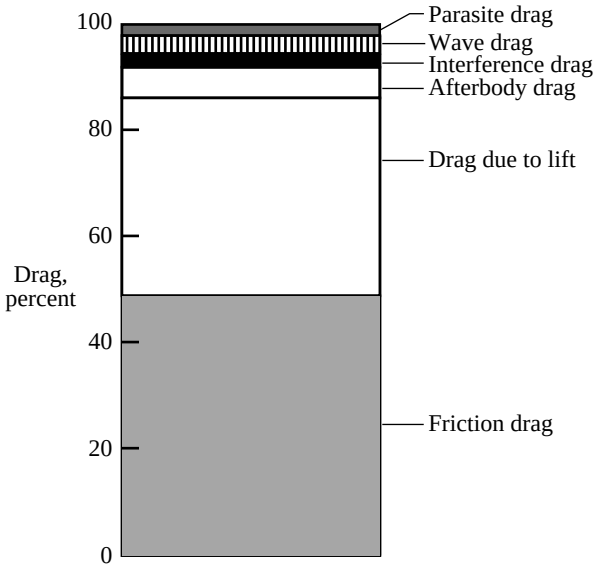

Figure 3. Aircraft drag breakdown. (From Thibert, Reneaux, and Schmitt 1990.)

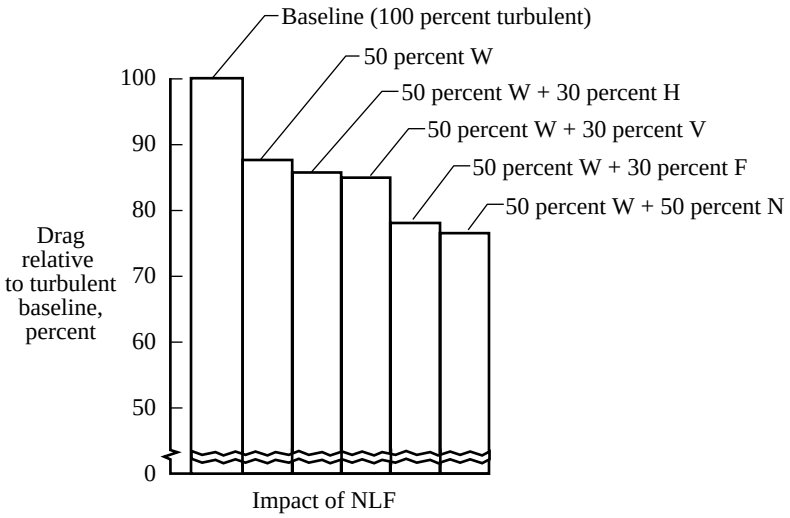

Figure 4. Predicted drag benefits of laminar flow on subsonic business jet. (From Holmes et al. 1985.)

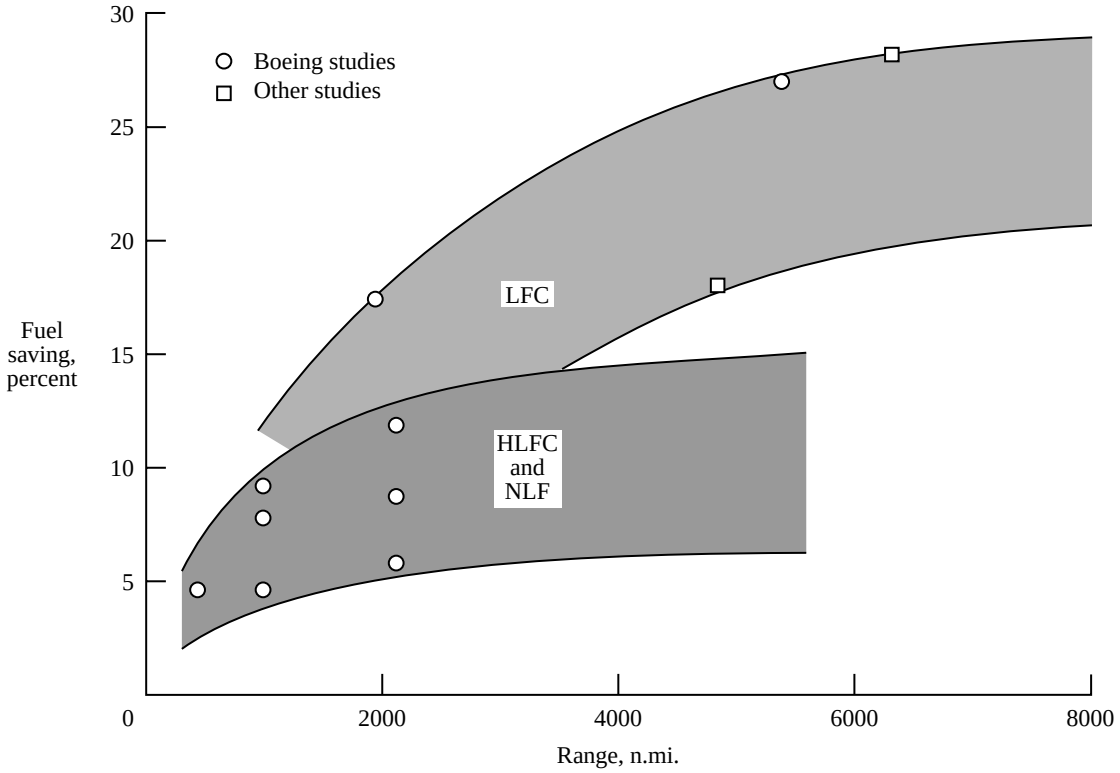

Figure 5. Benefits of LFC with range for subsonic aircraft. (From Kirchner l987.)

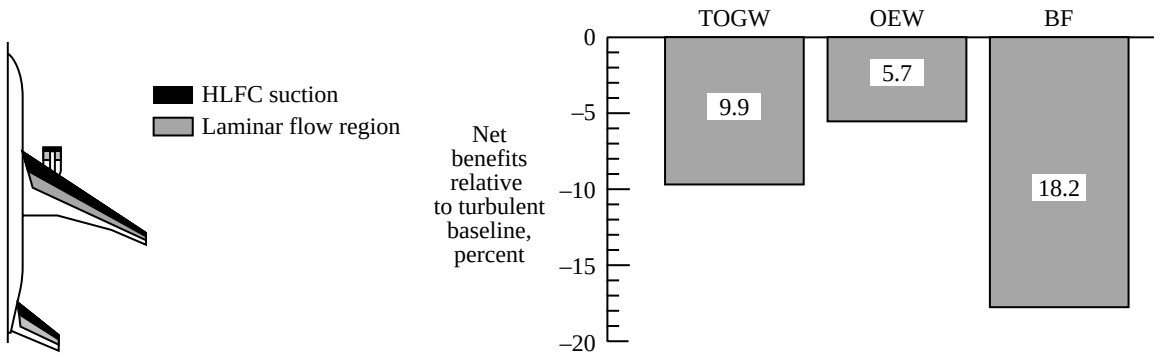

Figure 6. Potential benefits of HLFC on advanced subsonic transport. M = 0.85; R = 6500 n.mi.; 300 passengers. (From Arcara, Bartlett, and McCullers 1991.)

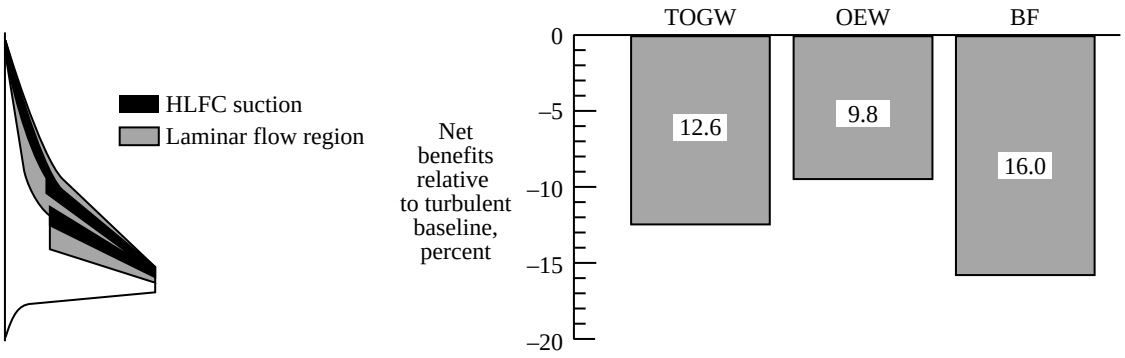

Figure 7. Potential benefits of HLFC on advanced supersonic transport. M = 2.4; R = 6500 n.mi.; 247 passengers. (From Parikh and Nagel 1990.)

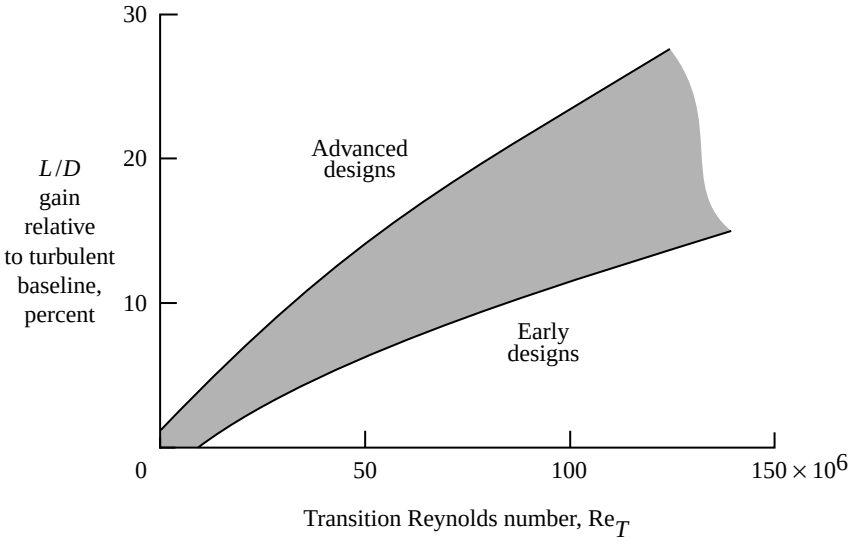

Figure 8. Benefits of SLFC on supersonic aircraft. M = 2.5. (From Kirchner 1987.)

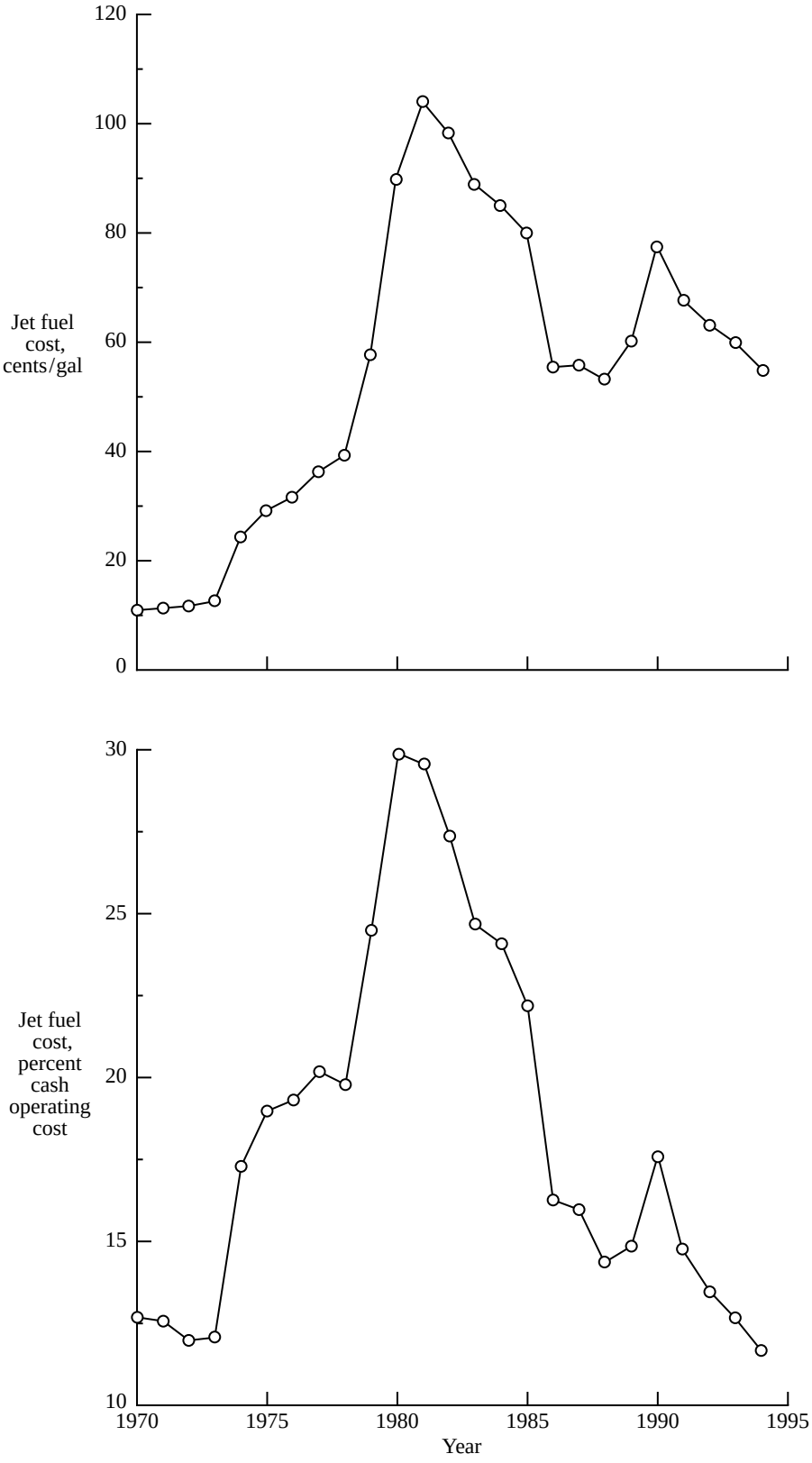

Figure 9. Cost of jet fuel to airline industry. (Data from Anon. 1985, 1995a.)

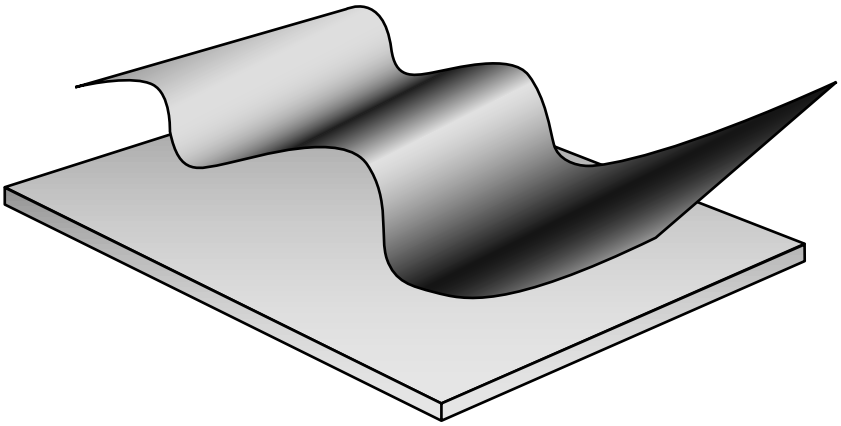

Figure 10. Sketch of Tollmien-Schlichting traveling wave.

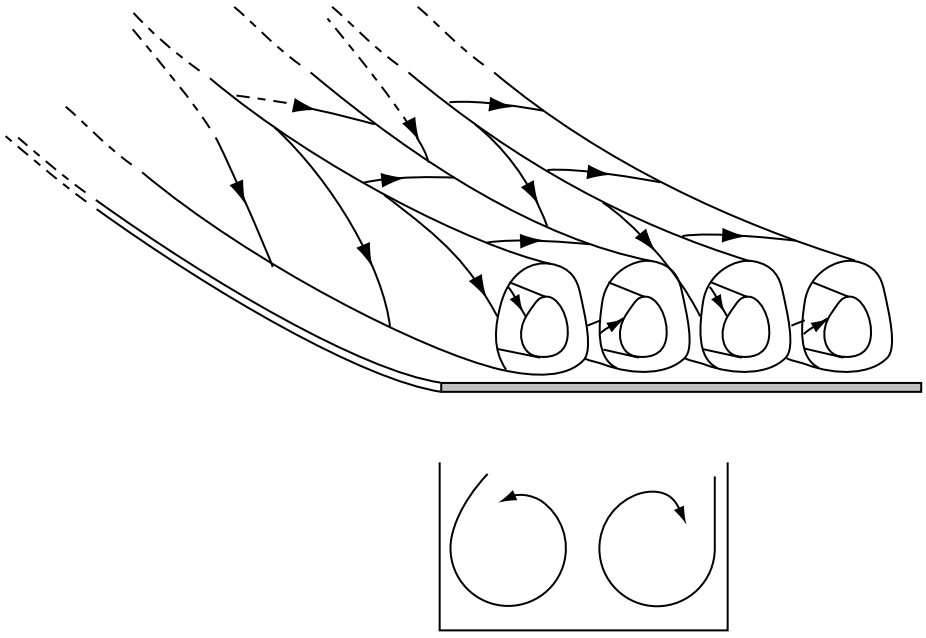

Figure 11. Sketch of Taylor-Görtler vortices over concave surface.

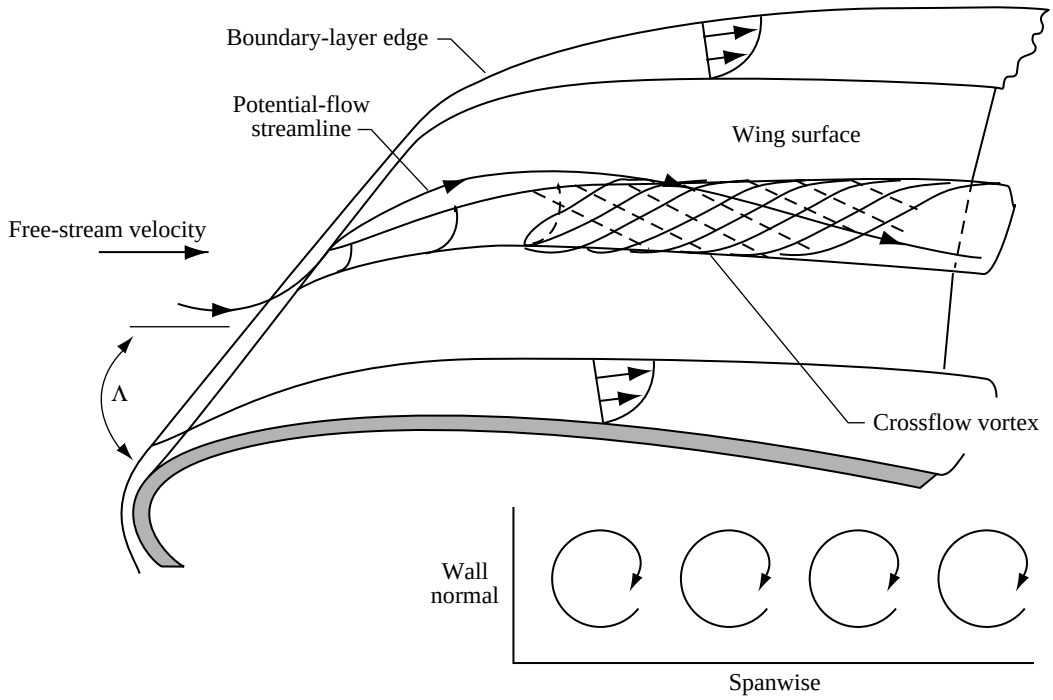

Figure 12. Sketch of crossflow vortices over swept wing.

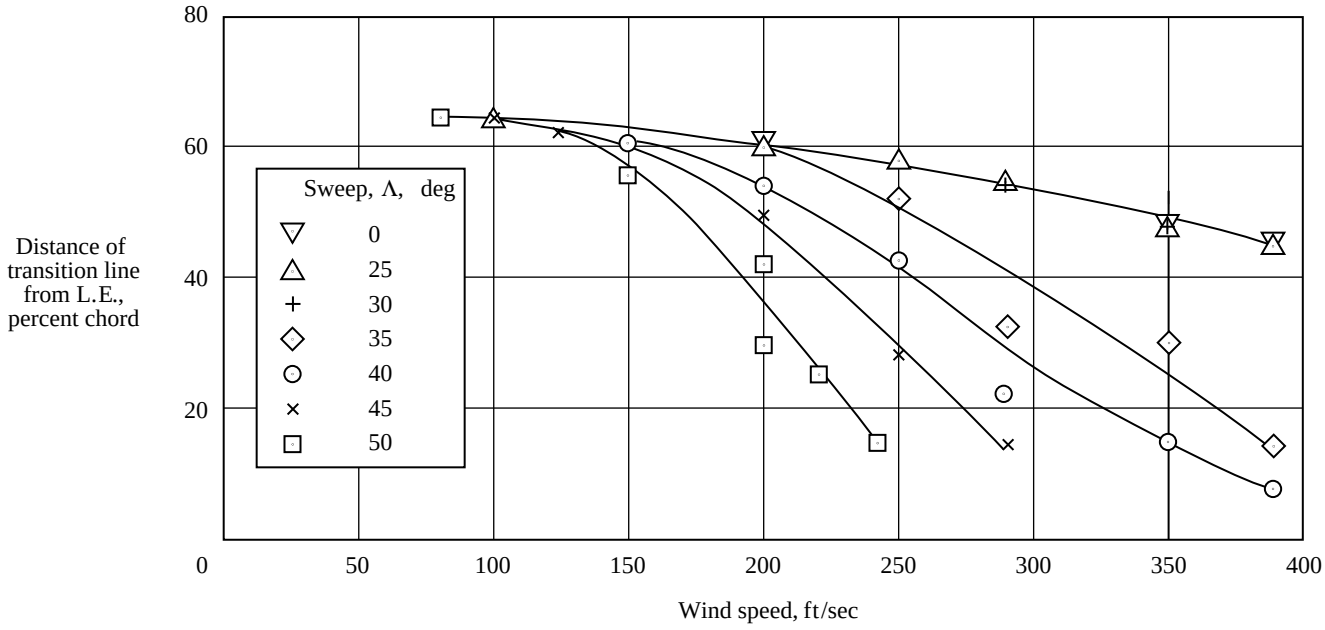

Figure 13. Effect of wind speed and wing sweepback on transition. (From Anscombe and Illingworth 1956.)

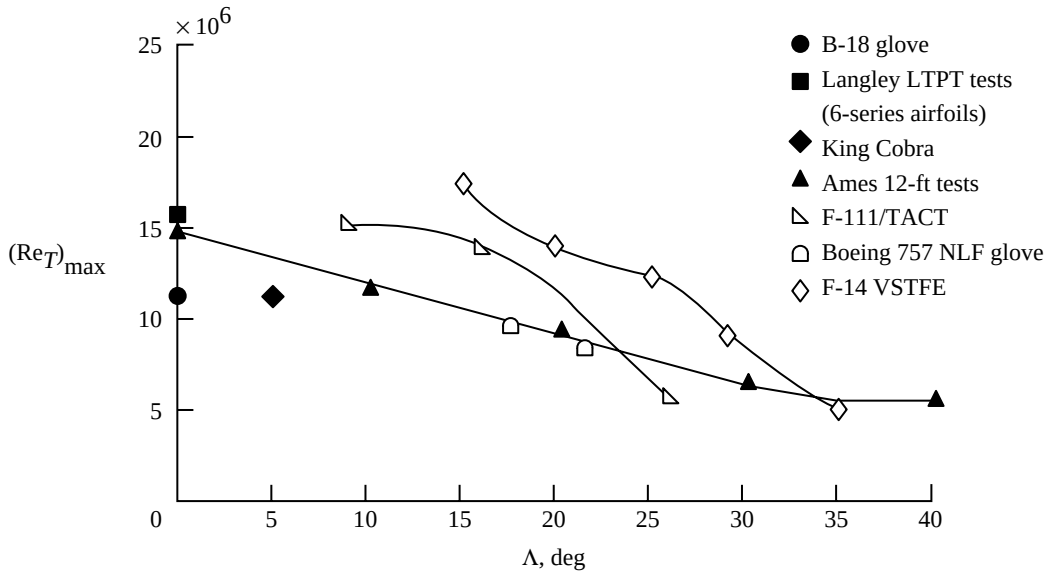

Figure 14. Maximum transition Reynolds number with wing sweep. (From Wagner et al. 1992.)

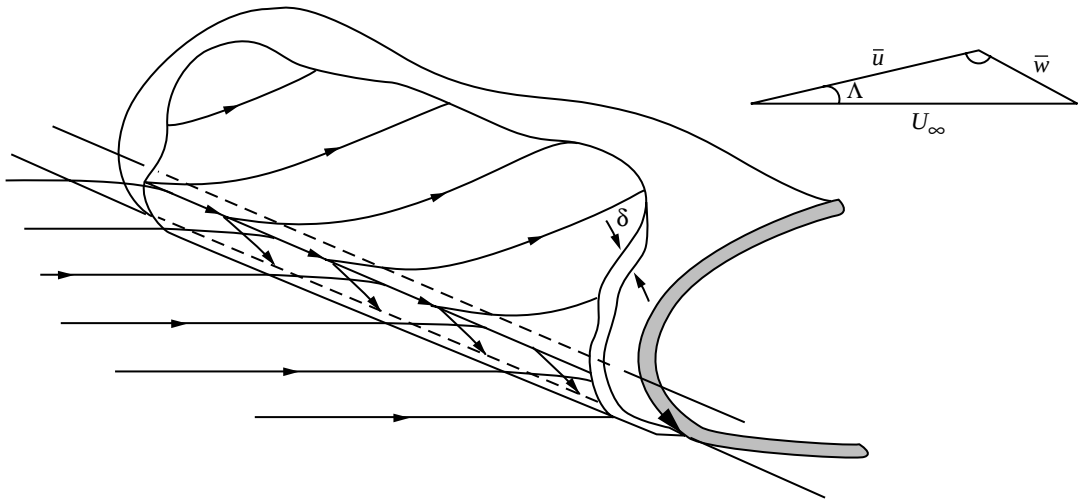

Figure 15. Sketch of attachment-line flow. (From Wentz, Ahmed, and Nyenhuis 1985.)

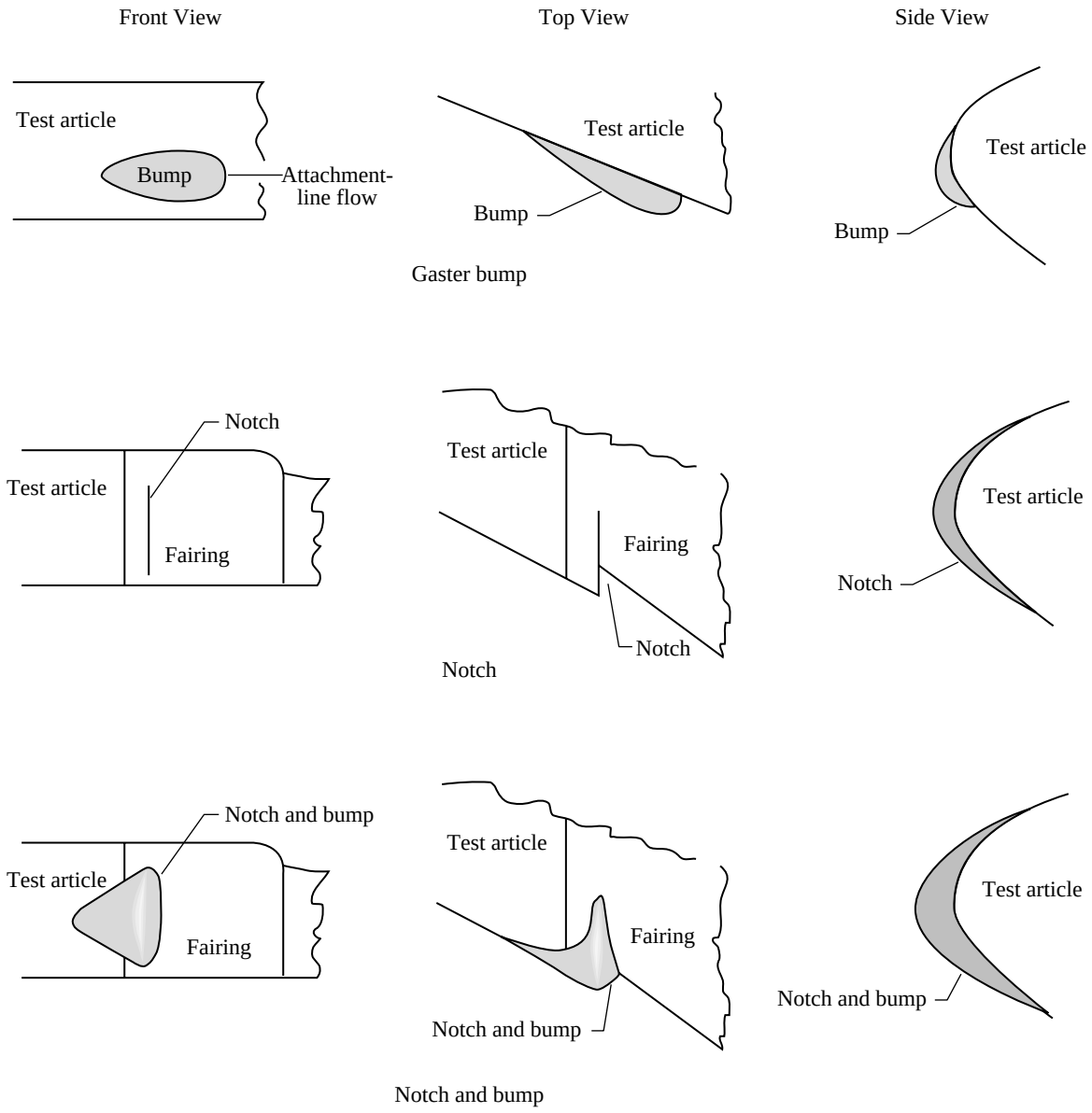

Figure 16. Devices used to prevent attachment-line contamination. (From Maddalon and Braslow 1990.)

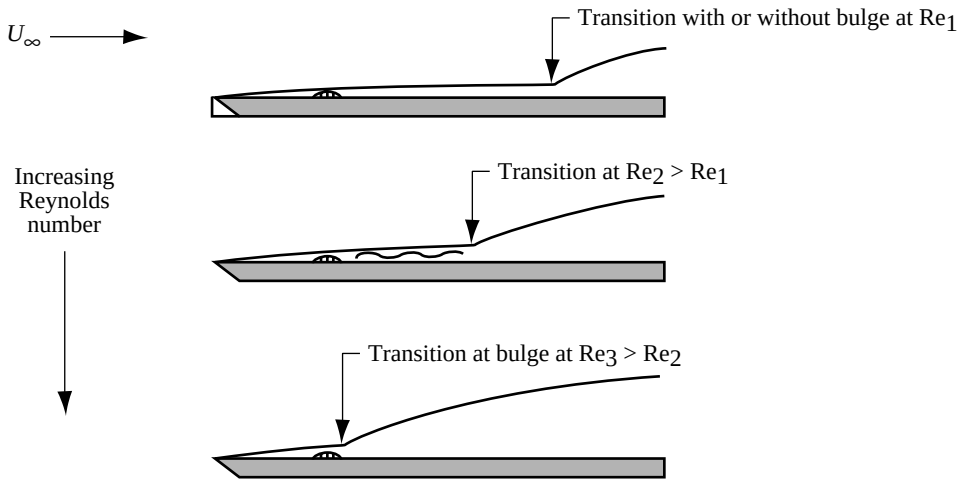

Figure 17. Effects of two-dimensional surface imperfection on laminar flow extend. (From Holmes et al. 1985.)

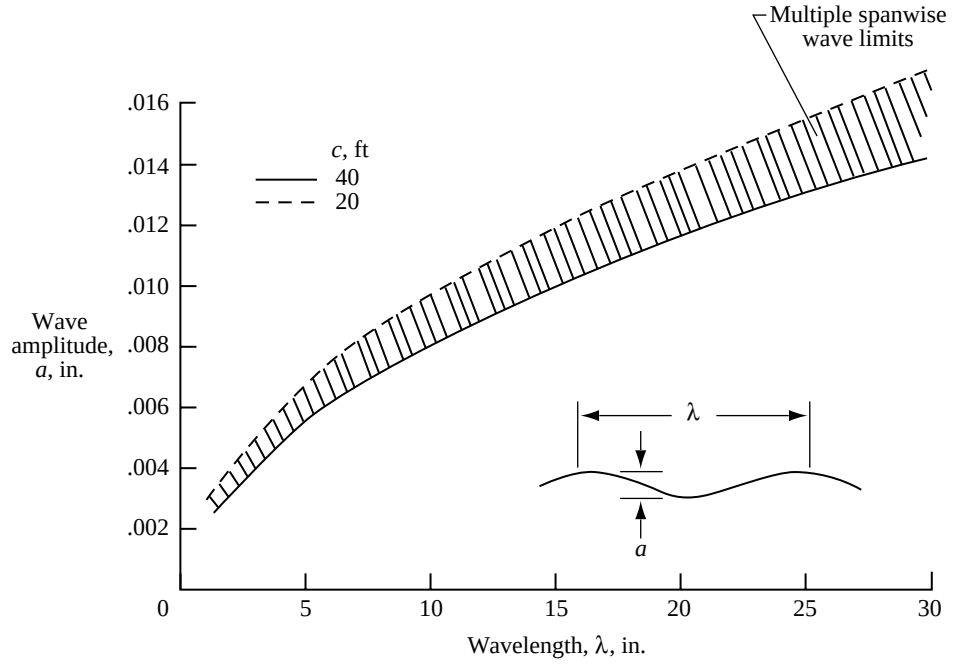

Figure 18. Typical permissible surface waviness. $M = 0.8$; $h = 38\,000$ ft; $\Lambda = 25°$. (From Braslow and Fischer 1985.)

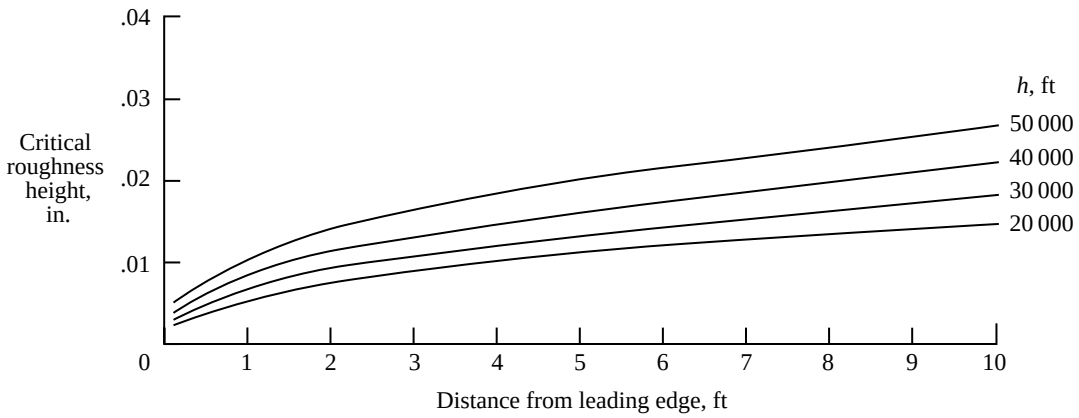

Figure 19. Typical permissible three-dimensional type of surface protuberances. $M = 0.8$. (From Braslow and Fischer 1985.)

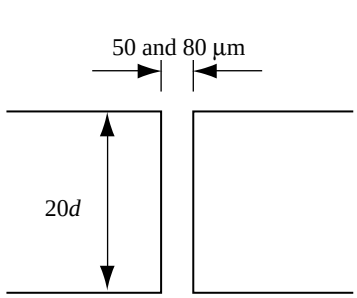

(a) Idealized cylindrical hole.

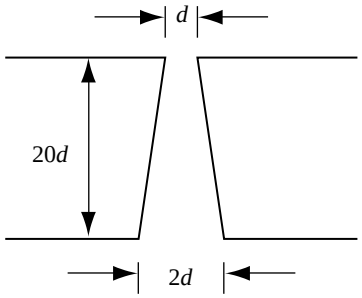

(b) Conical hole.

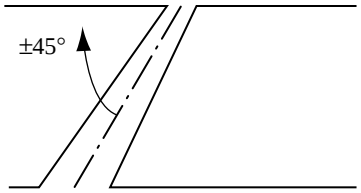

(c) Inclined conical hole.

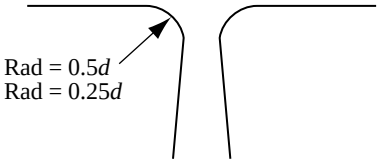

(d) Radiused inlet.

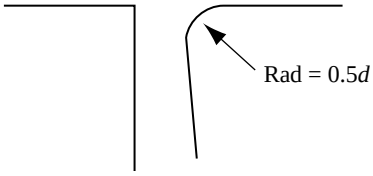

(e) Asymmetrically radiused inlet.

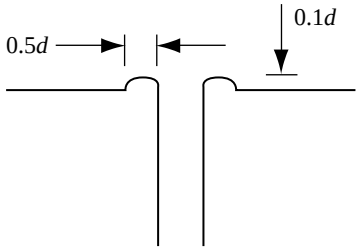

(f) Raised rounded inlets.

Figure 20. Hole geometries and inlet region shapes. Not drawn to scale. (From MacManus and Eaton 1996.)

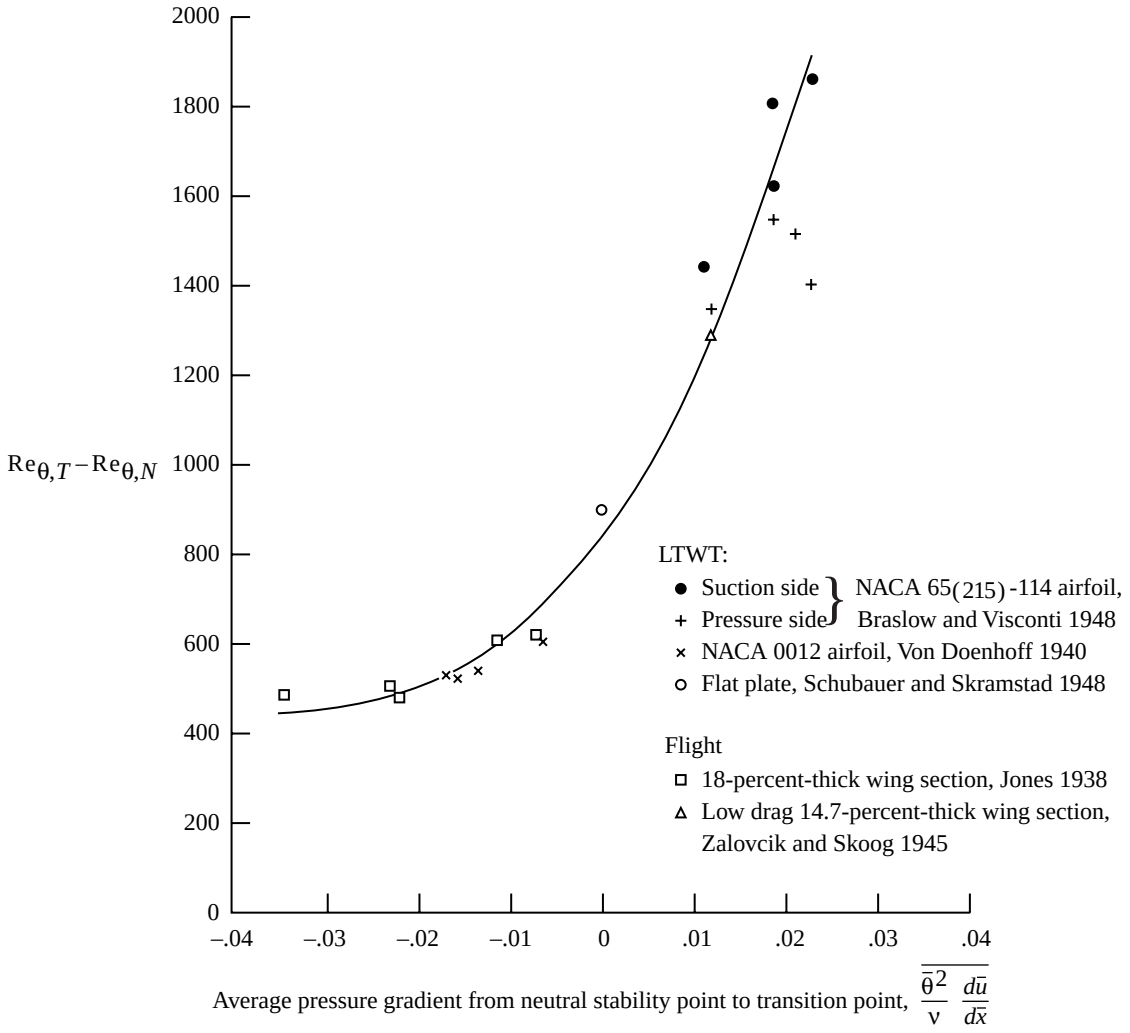

Figure 21. Transition location as function of average pressure gradient. (From Granville 1953.)

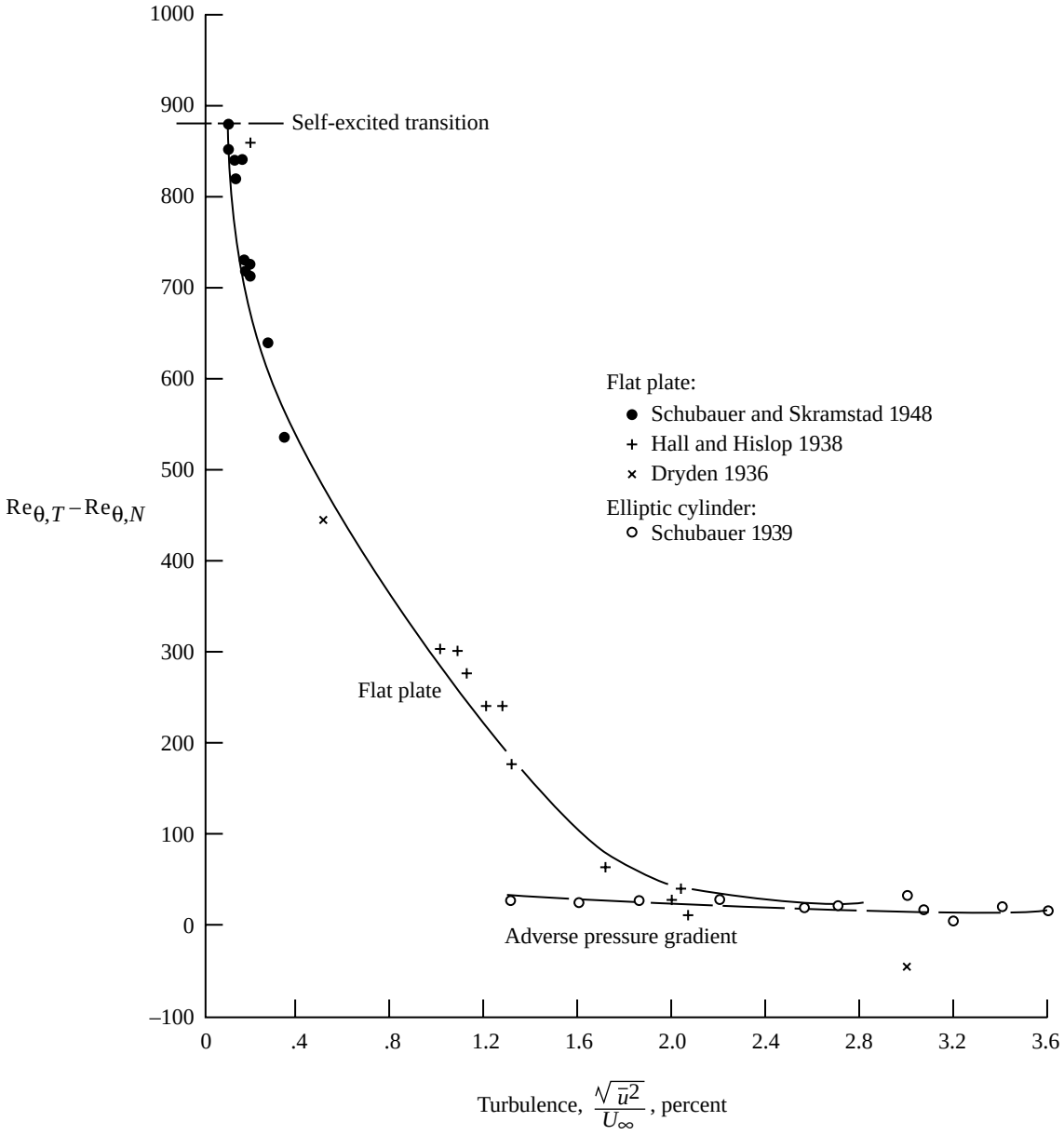

Figure 22. Transition location as function of turbulence level. (From Granville 1953.)

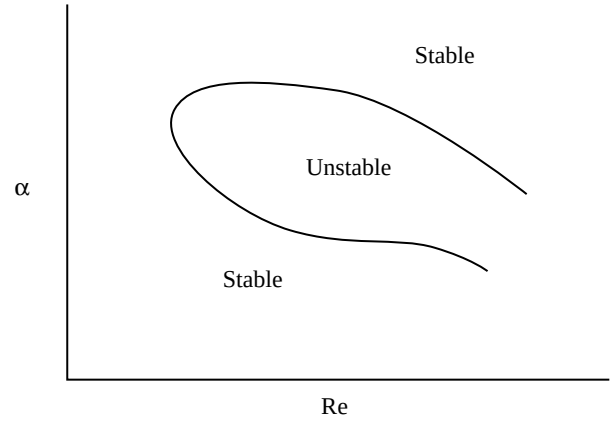

Figure 23. Illustration of neutral curve for linear stability theory.

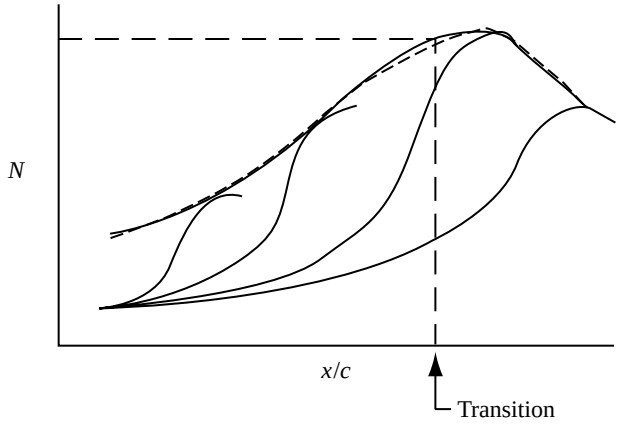

Figure 24. Amplification of four waves of different frequency to illustrate determination of *N*-factor curve.

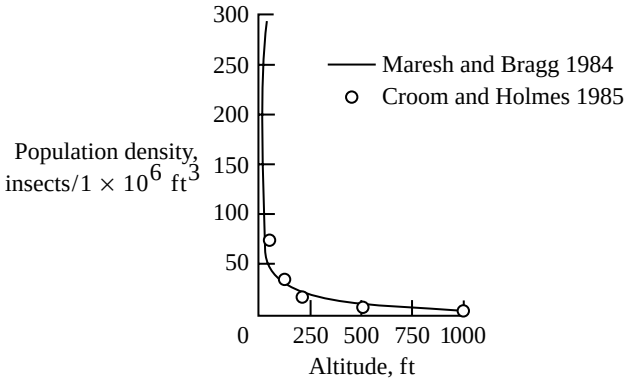

(a) Vertical distribution of population density.

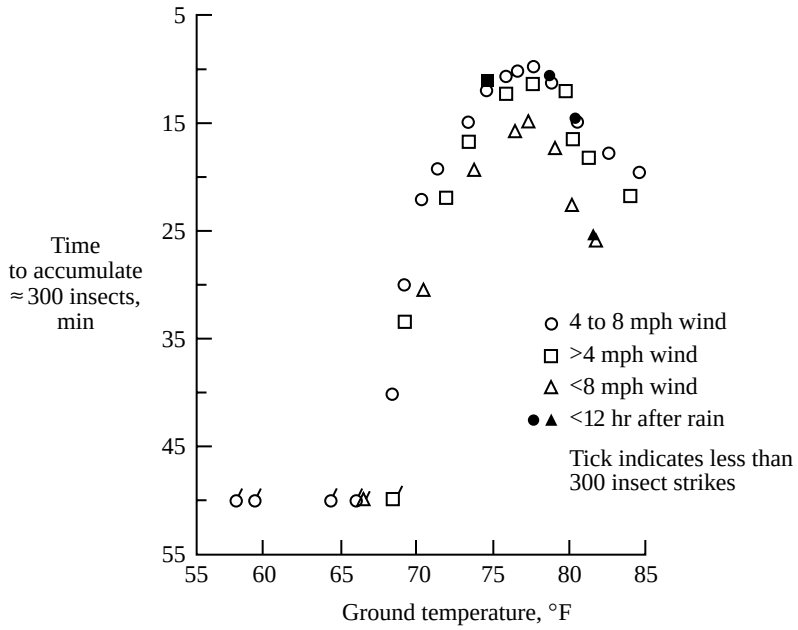

(b) Effect of meteorological conditions on rate of insect accumulation; V = 130 mph; h = 50 ft.

Figure 25. Cessna 206 anti-insect flight test results. (From Croom and Holmes 1985.)

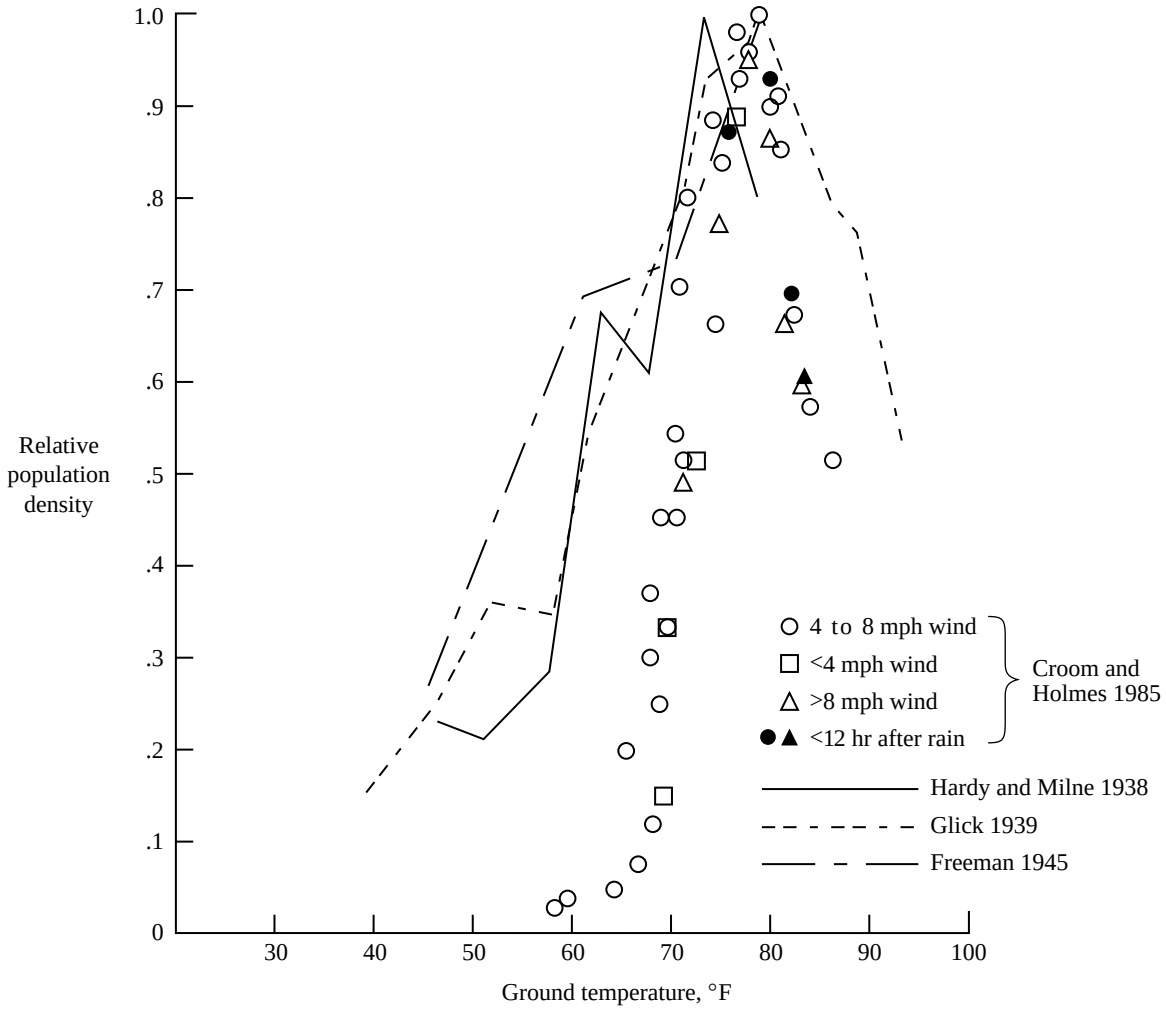

(c) Effect of temperature on normalized insect population density; V = 130 mph; h = 50 ft.

Figure 25. Continued.

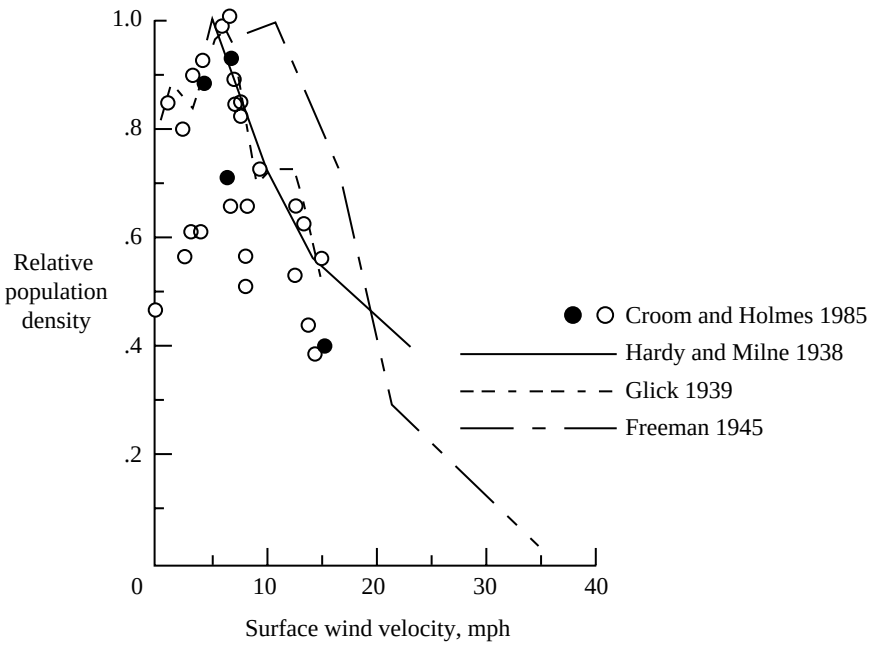

(d) Effect of wind velocity on normalized insect population density; V = 130 mph; h = 50 ft.

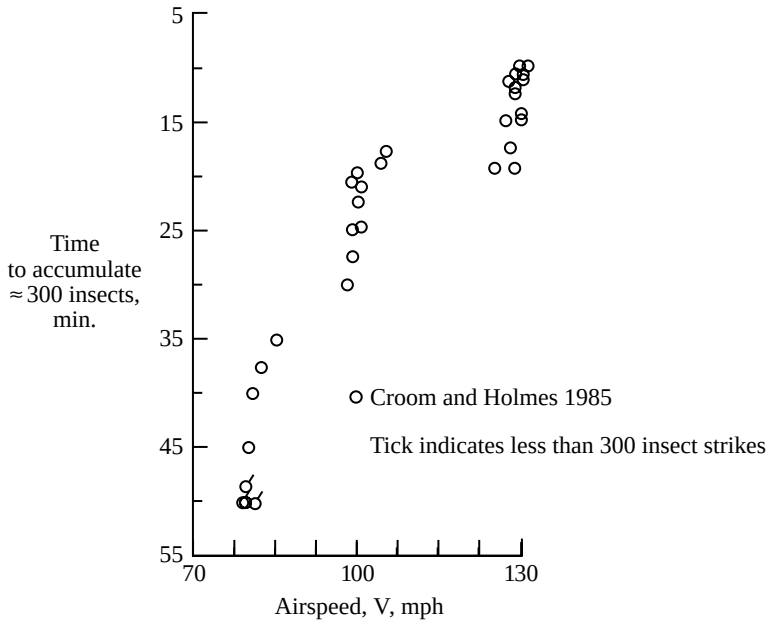

(e) Effect of airspeed in rate of insect accumulation; h = 50 ft; surface windspeed, 4 to 8 mph; surface temperature, 70°F.

Figure 25. Concluded.

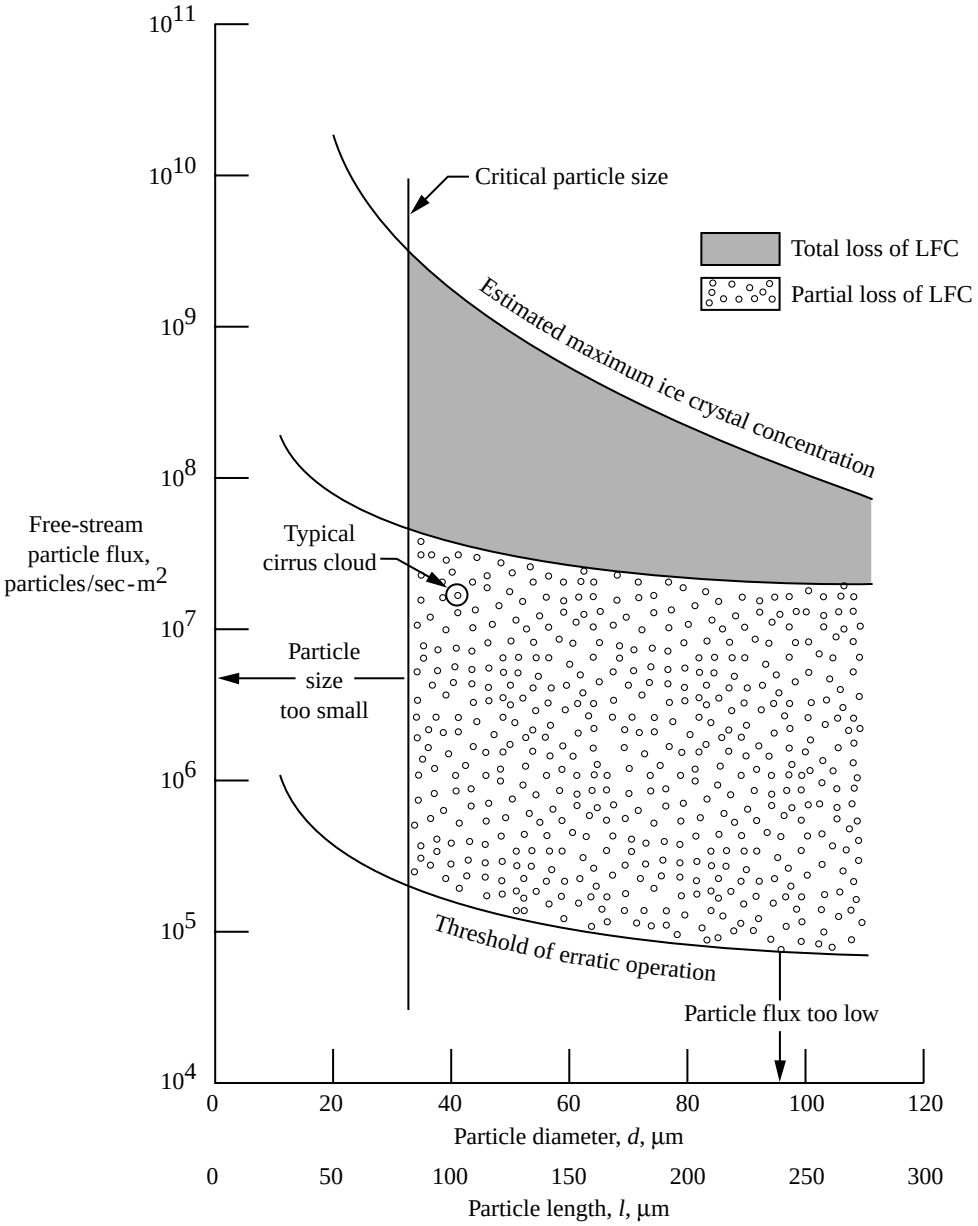

Figure 26. Estimated LFC performance with ice particles in air. h = 40 000 ft; M = 0.75; l/d = 2.5 (ice crystal aspect ratios). (From Fowell and Antonatos 1965.)

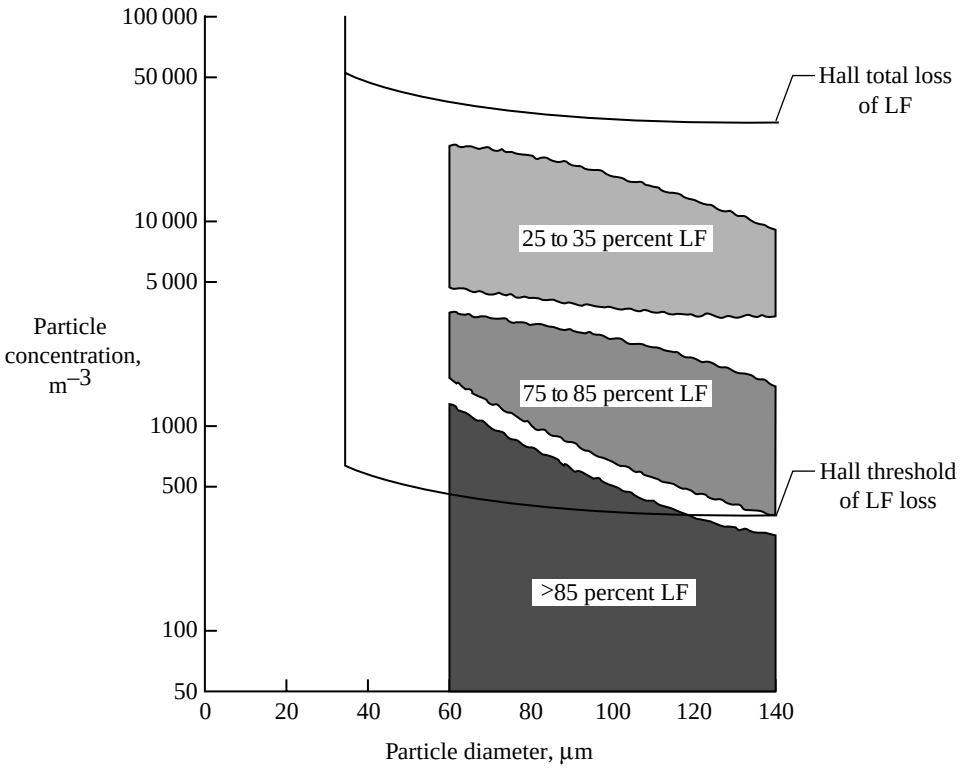

Figure 27. Validation of Hall criteria for impact of cloud particulate on laminar flow using Jetstar aircraft. Flight 1061. (From Davis, Maddalon, and Wagner 1987.)

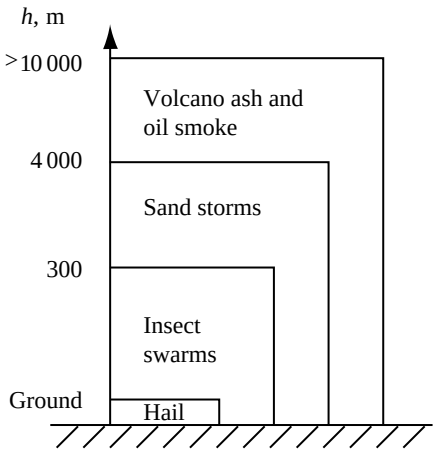

Figure 28. Pollution of atmosphere. (From Meifarth and Heinrich 1992.)

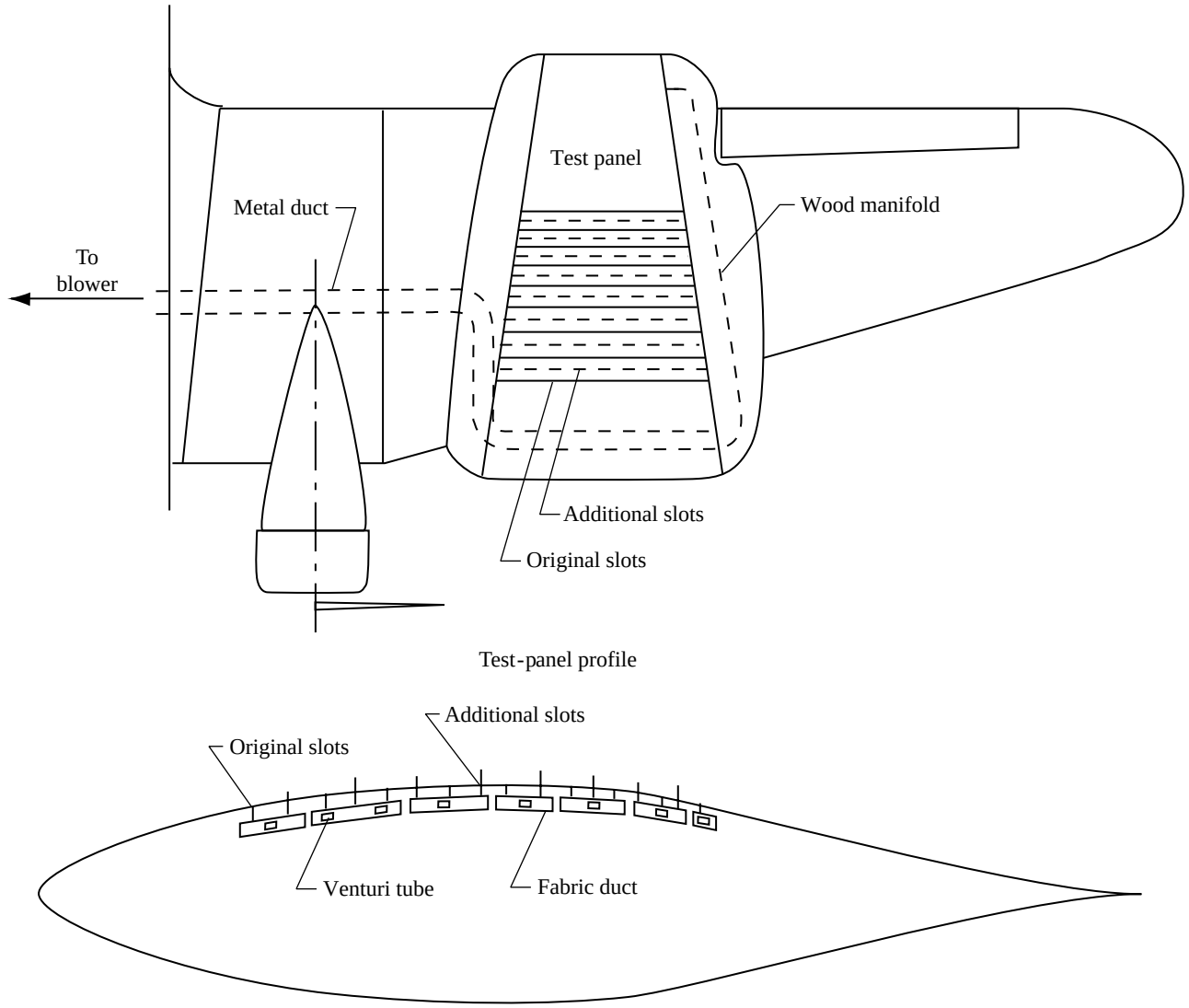

Figure 29. Induction system for slot-suction BLC on NACA 35-215 test panel on B18 wing. (From Zalovcik, Wetmore, and Von Doenhoff 1944.)

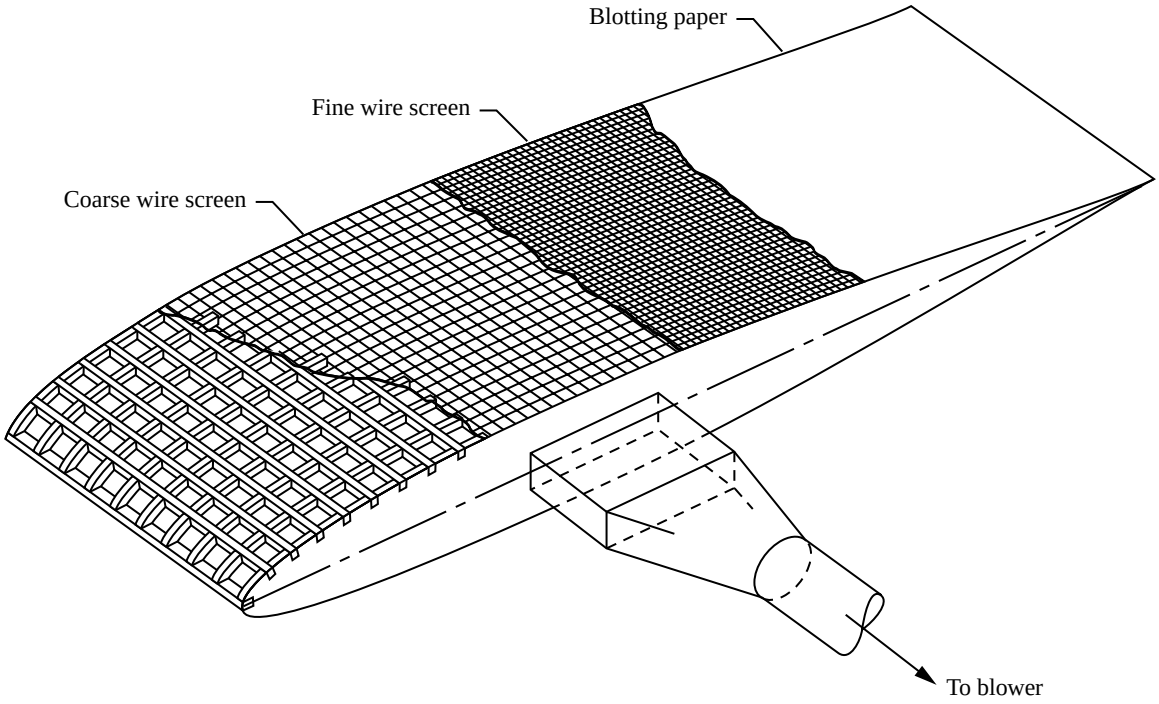

Figure 30. Sketch of method used to construct permeable surfaces for NACA 64A010 LFC airfoil. (From Braslow, Visconti, and Burrows 1948.)

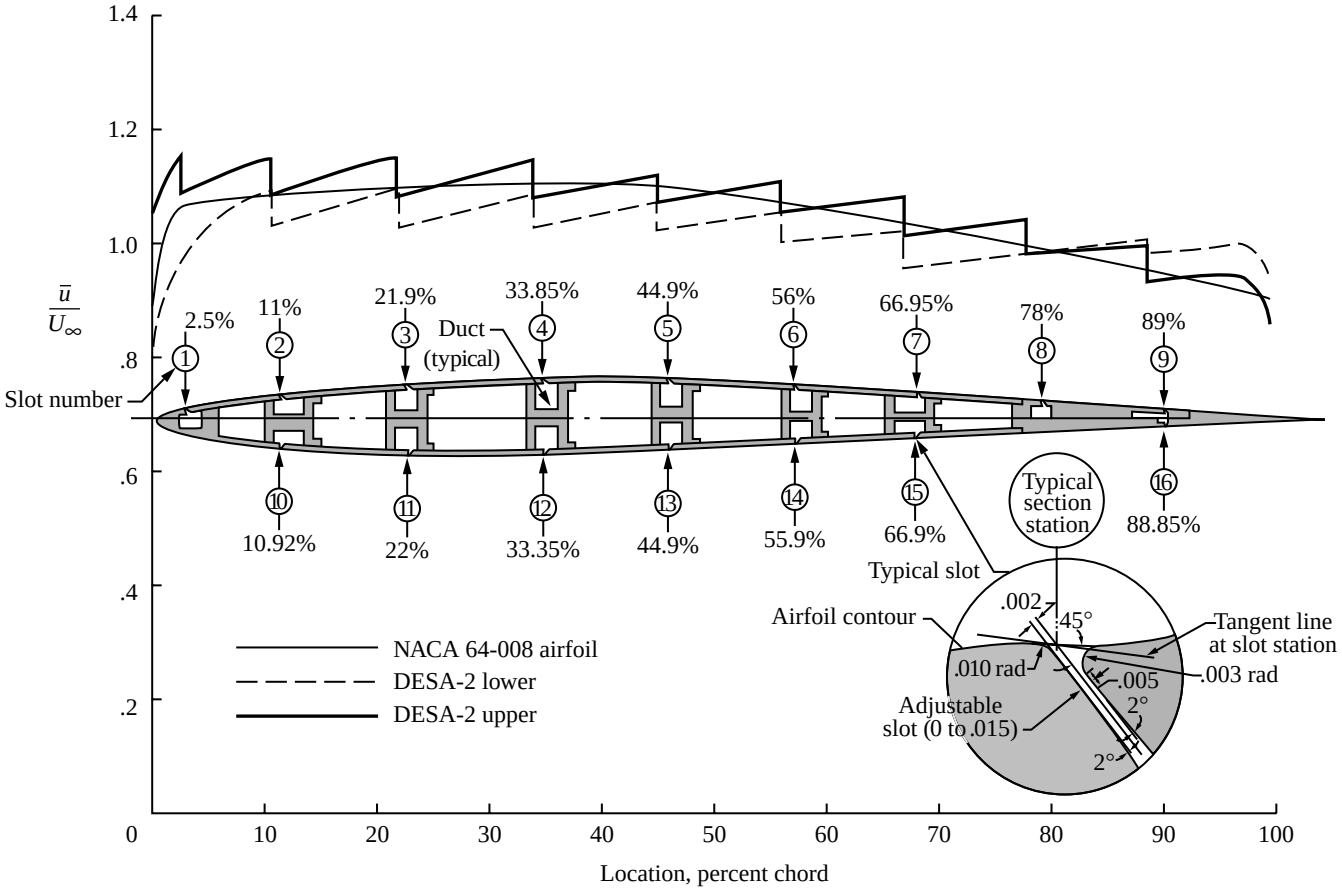

Figure 31. DESA-2 airfoil model and slot-suction induced velocity discontinuities. (From Smith 1953.)

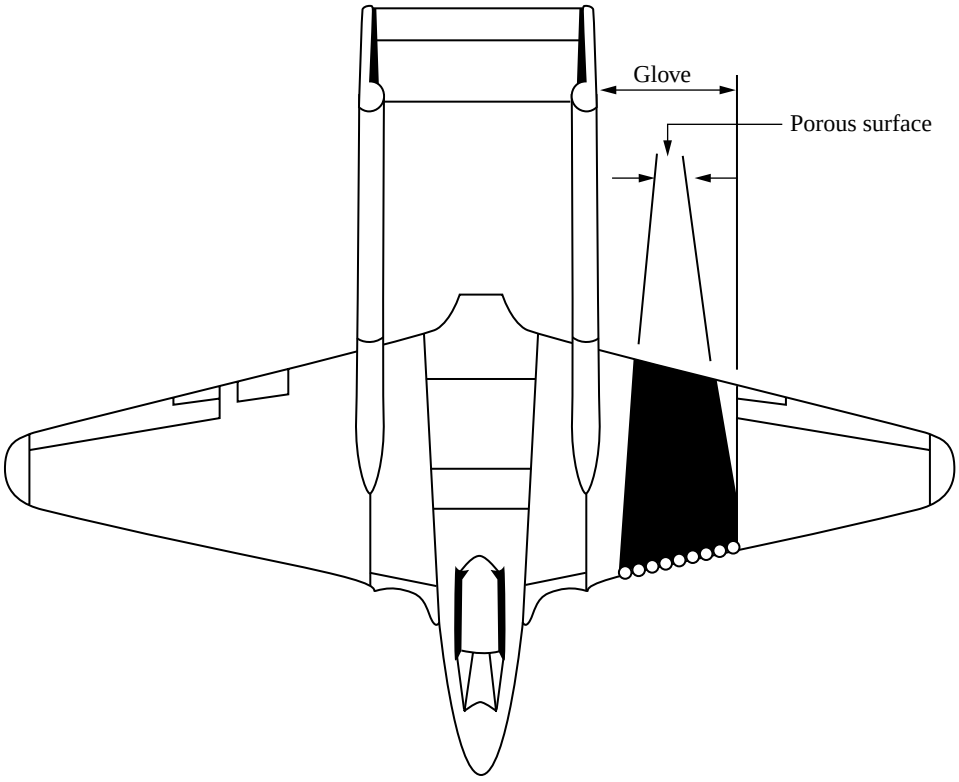

Figure 32. Sketch of Vampire porous-suction LFC flight test aircraft. (From Head, Johnson, and Coxon 1955.)

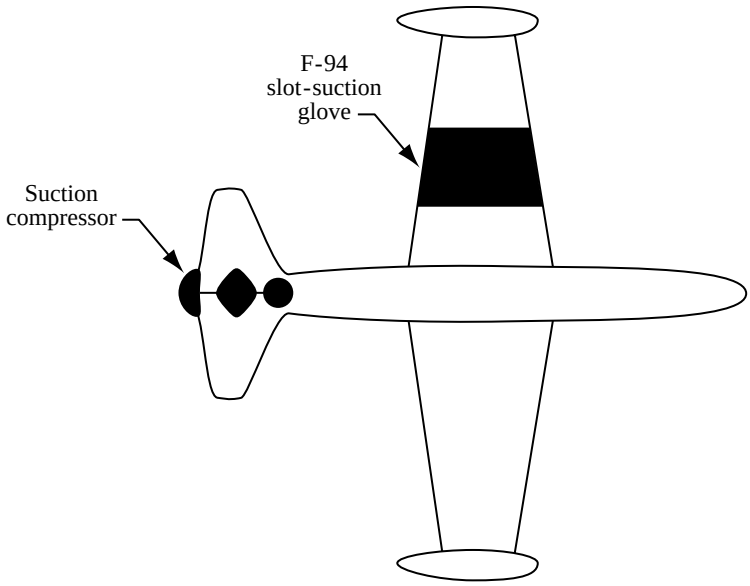

Figure 33. F-94 slot-suction LFC flight test aircraft. (From Carmichael, Whites, and Pfenninger 1957.)

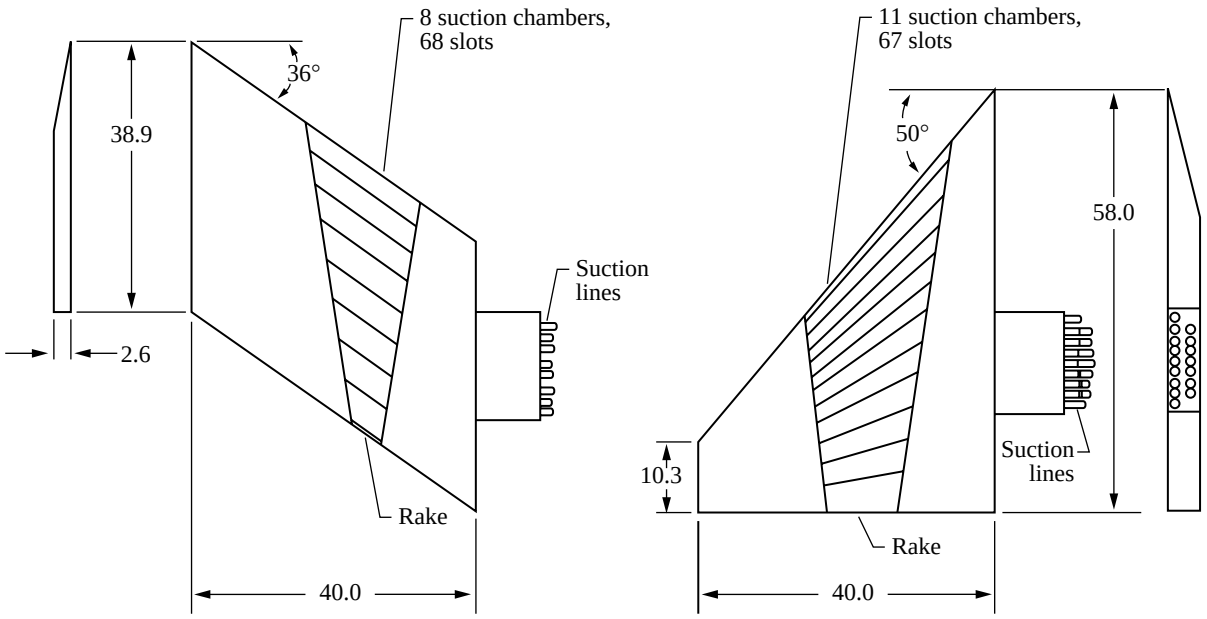

Figure 34. Sketch of supersonic slot-suction swept-wing models tested at AEDC. (From Groth, Pate, and Nenni 1965.)

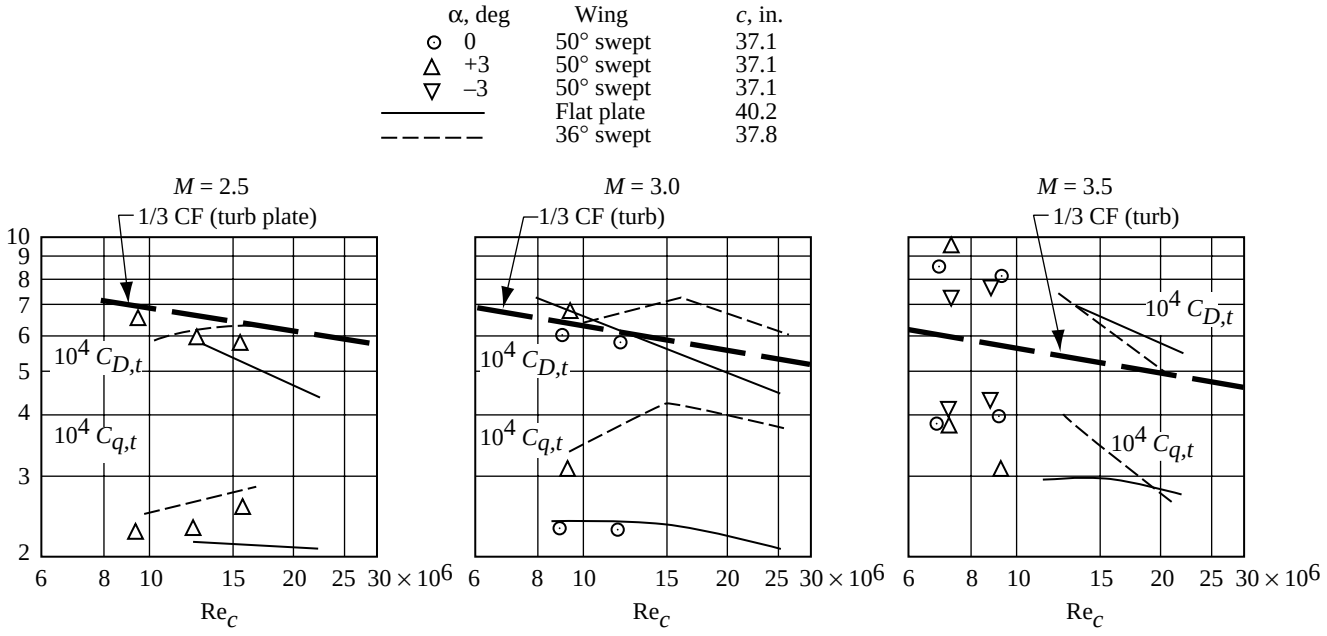

Figure 35. Minimum drag and optimum suction for supersonic slot-suction LFC swept-wing models, one-third turbulent flat-plate drag, and slot-suction flat-plate model drag. (From Groth, Pate, and Nenni 1965.)

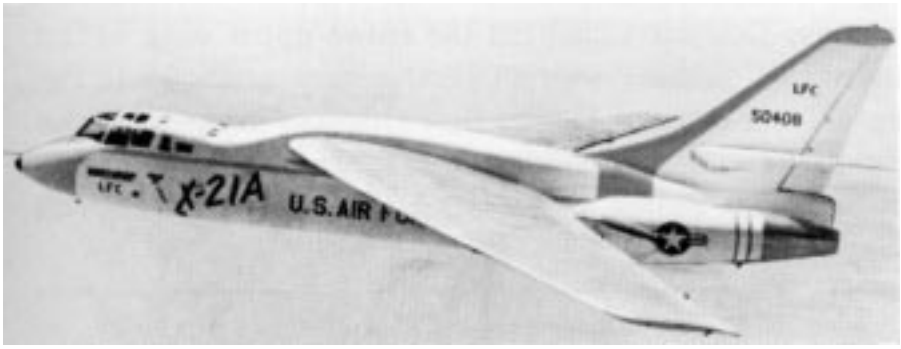

Figure 36. X-21A flight test aircraft. (From Fowell and Antonatos 1995.)

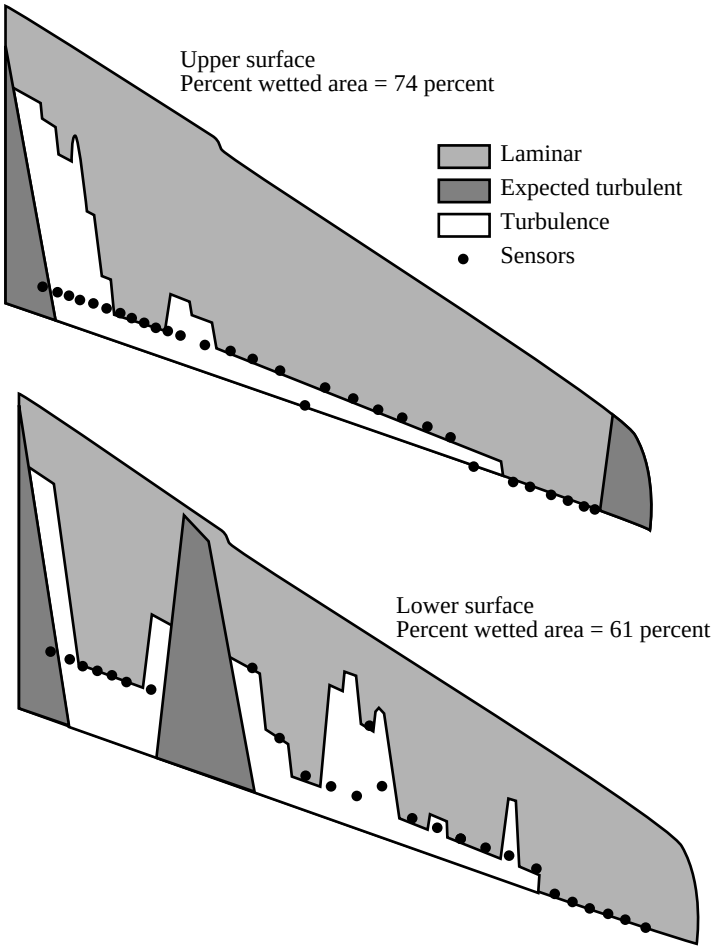

Figure 37. Laminar flow achieved during X-21A flight test for Mach number of 0.7, altitude of 40 000 ft, and chord Reynolds number of 20×10^6, with extended leading edge. (From Fowell and Antonatos 1965.)

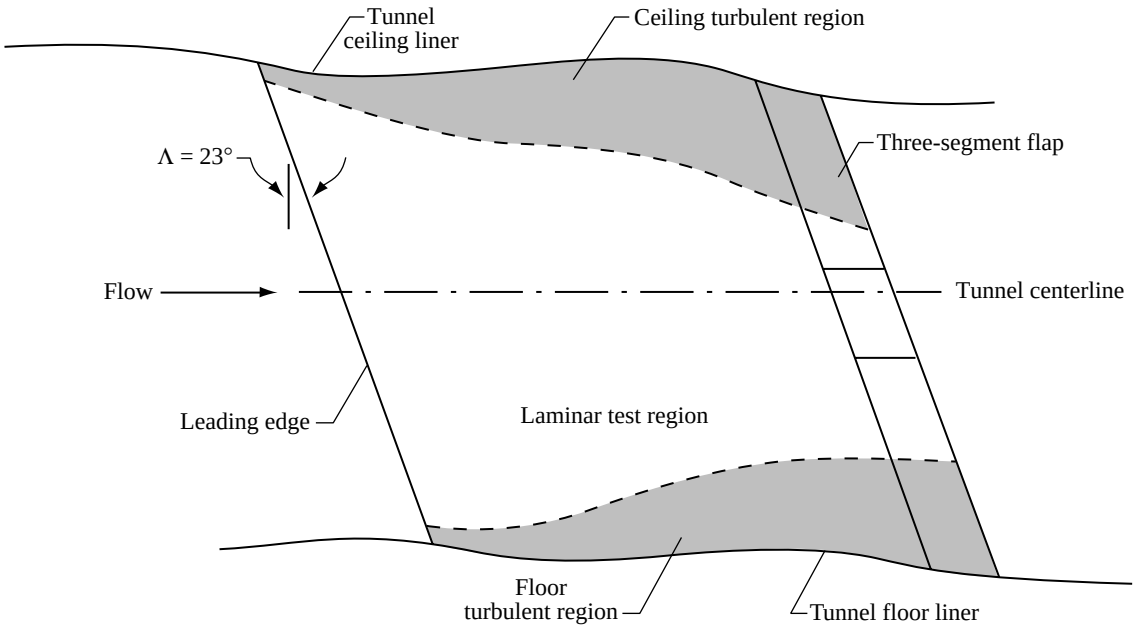

Figure 38. Swept-wing model, liner, and turbulent regions for TPT LFC experiment. (From Bobbitt et al. 1996.)

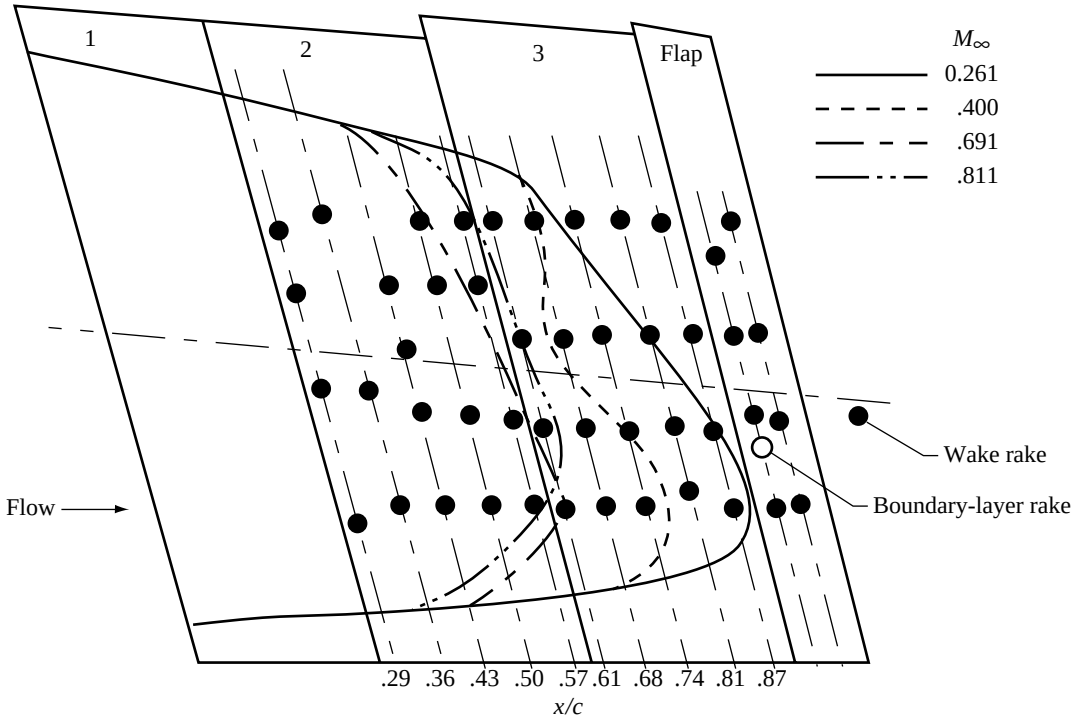

Figure 39. Upper surface transition boundaries for Mach numbers of 0.261 to 0.826, chord Reynolds number of 10×10^6, and full suction. (From Bobbitt et al. 1996.)

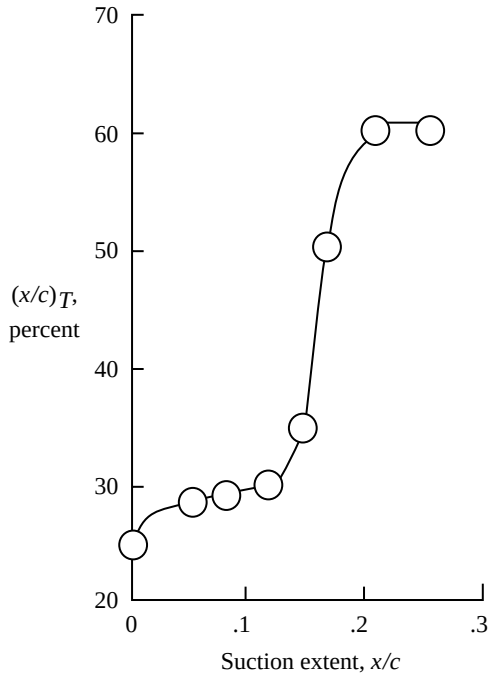

Figure 40. Transition location as function of chordwise extent of suction for Mach number of 0.82 and chord Reynolds number of 15×10^6. (From Bobbitt et al. 1996.)

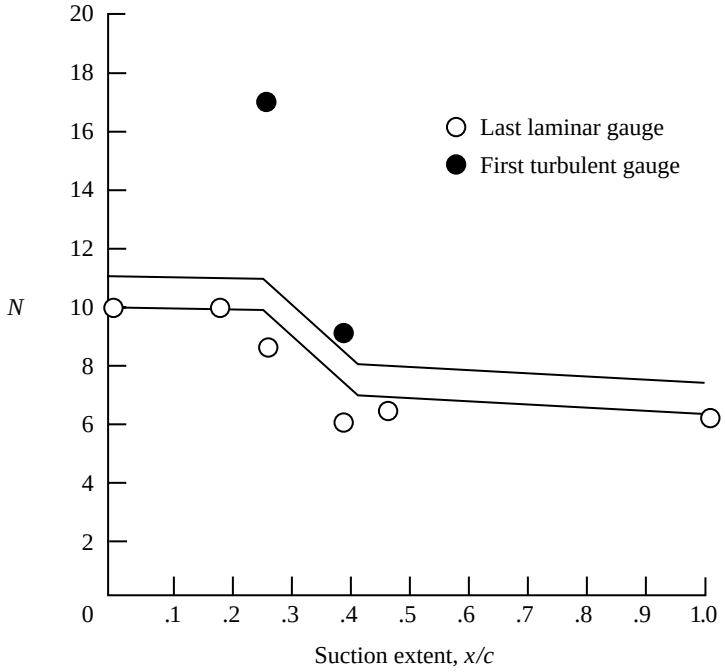

Figure 41. Calculated N-factor values correlated with transition location and amount of chordwise suction extent for TPT LFC experiment for Mach number of 0.82 and chord Reynolds number of 10×10^6. (From Berry et al. 1987.)

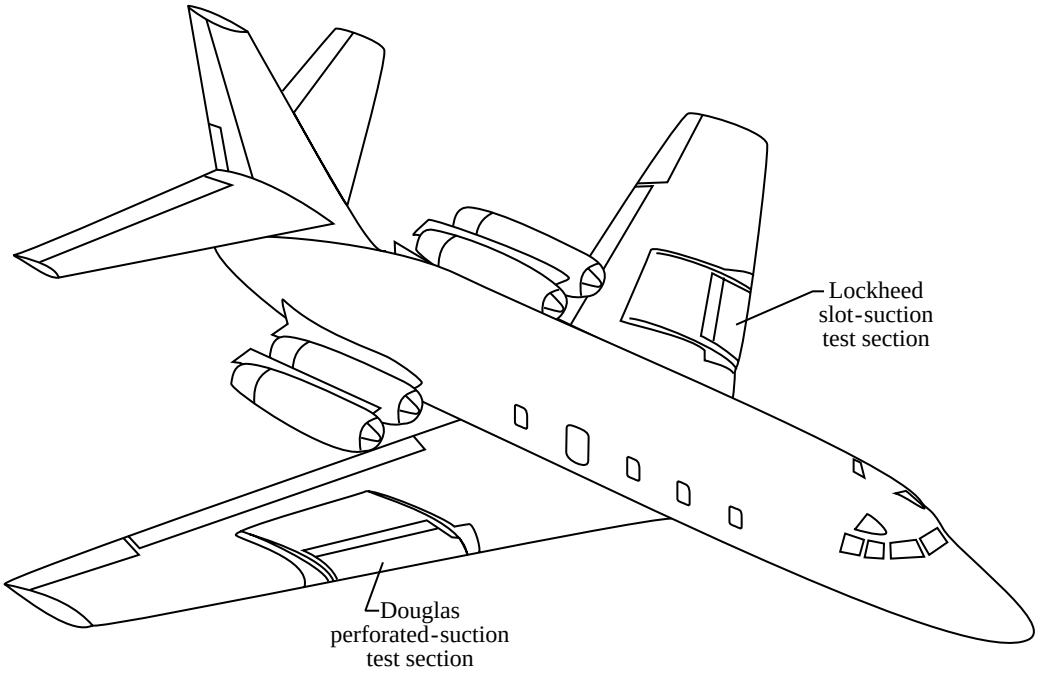

Figure 42. Jetstar leading-edge flight test aircraft. (From Fischer, Wright, and Wagner 1983.)

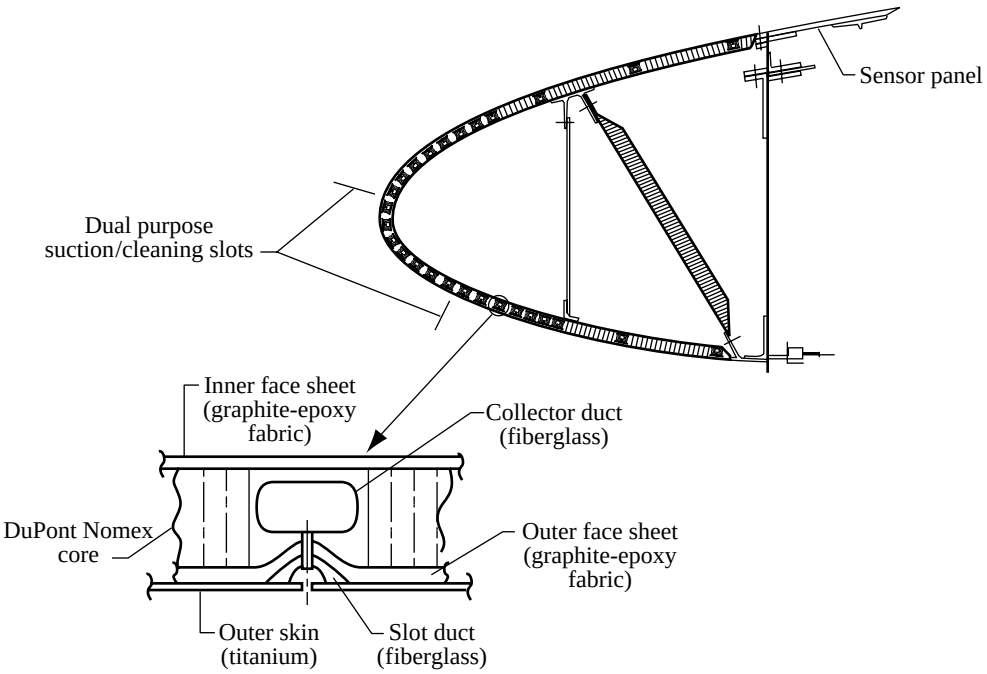

Figure 43. Lockheed test article on Jetstar aircraft. (From Fischer, Wright, and Wagner 1983.)

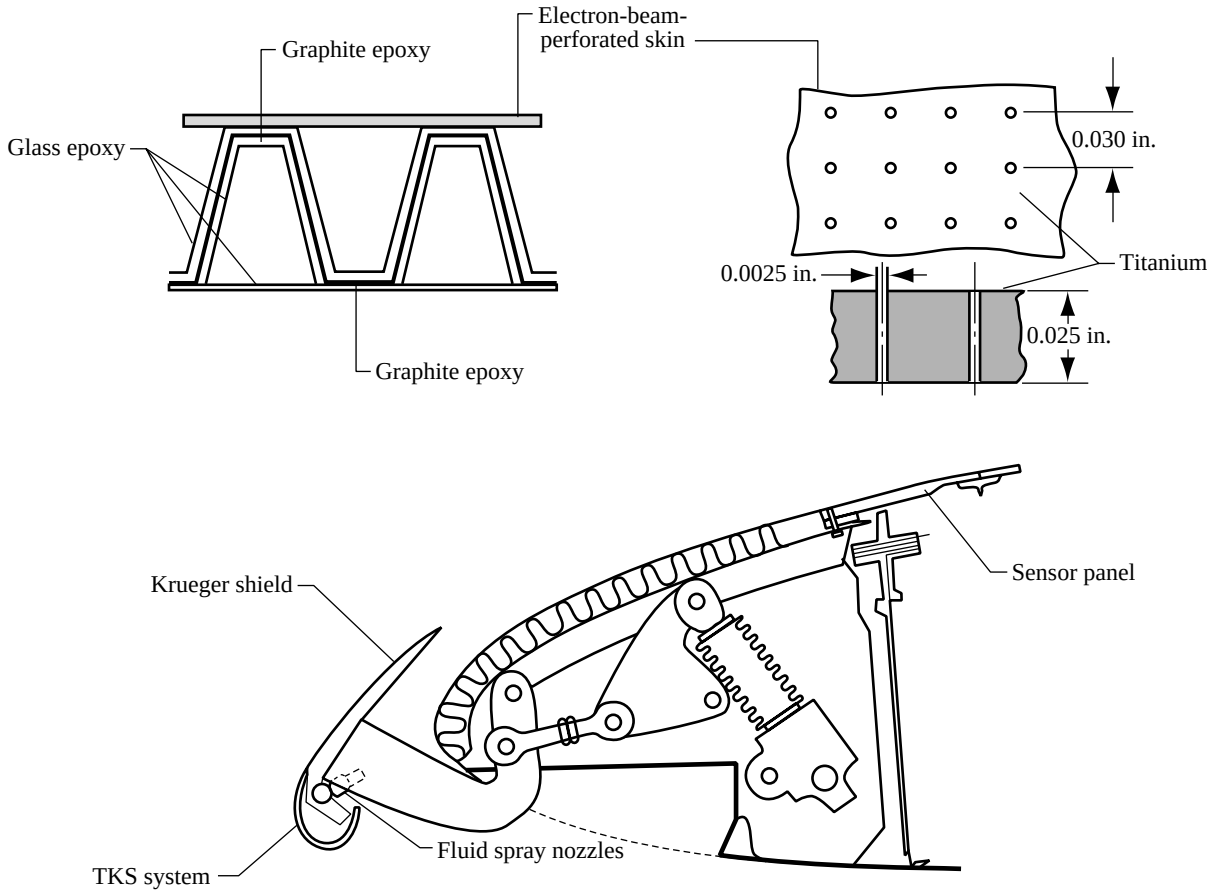

Figure 44. Douglas test article on Jetstar aircraft. (From Fischer, Wright, and Wagner 1983.)

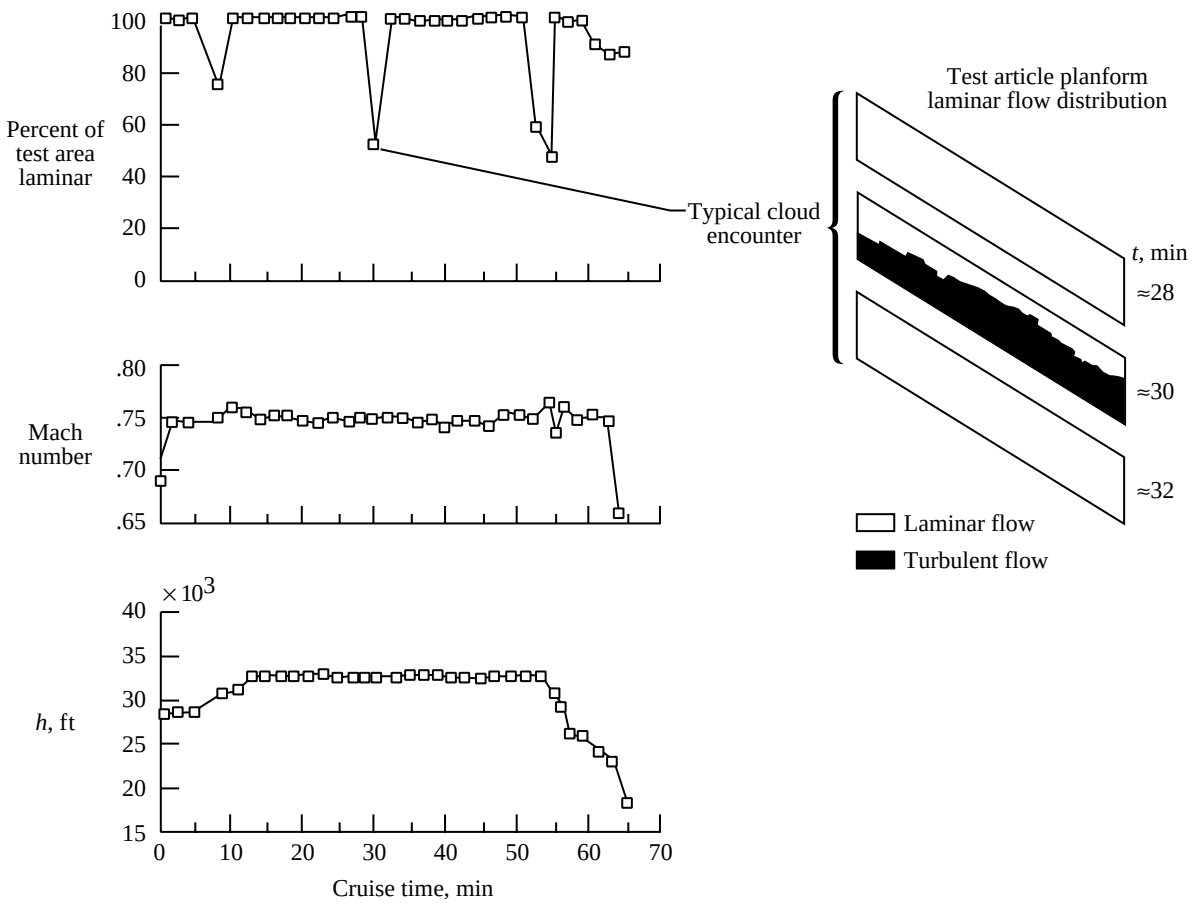

Figure 45. Laminar flow extent on Douglas perforated-suction test article. Mach number and altitude are shown for typical flight with Jetstar. (From Wagner et al. 1992.)

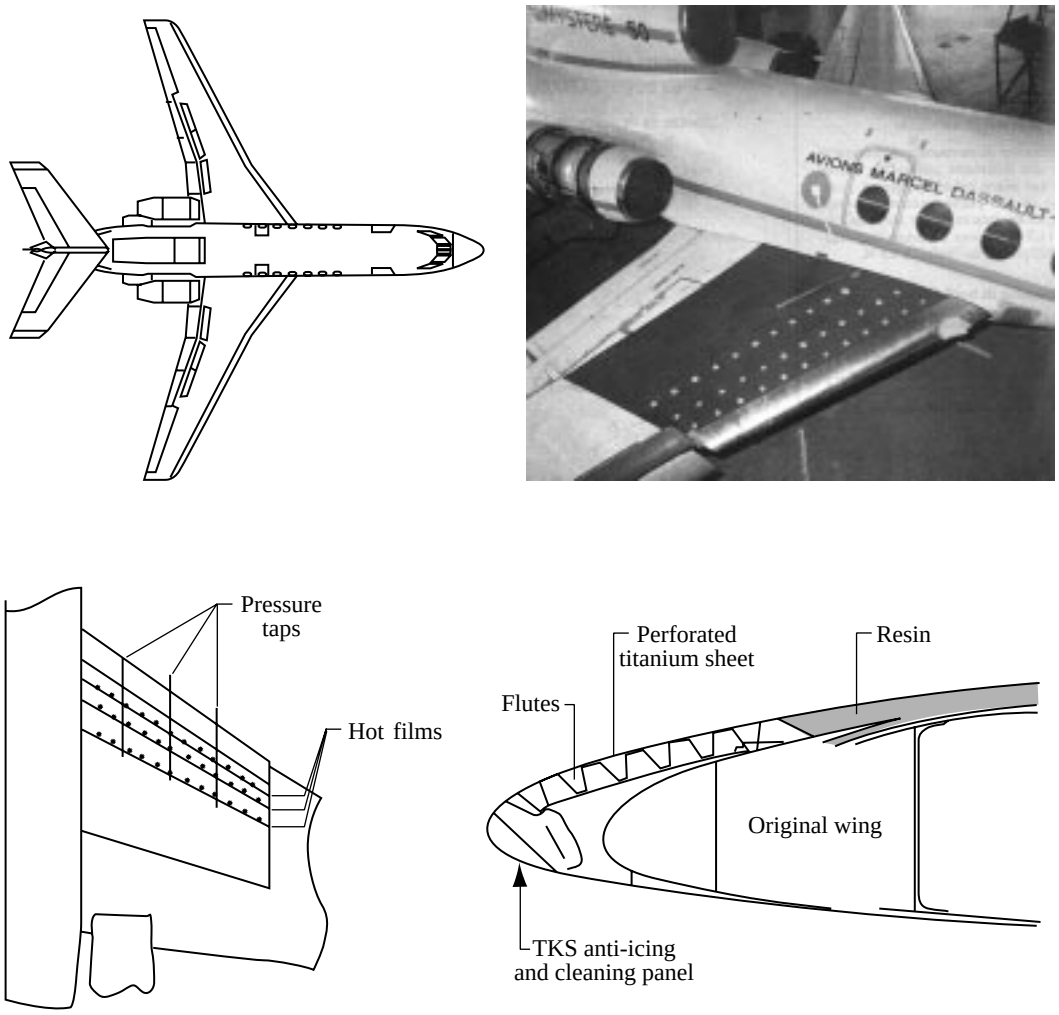

Figure 46. Dassult Falcon 50 HLFC flight demonstrator, instrumentation package, glove, and leading-edge design. (From Bulgubure and Arnal 1992; Courty, Bulgubure, and Arnal 1993.)

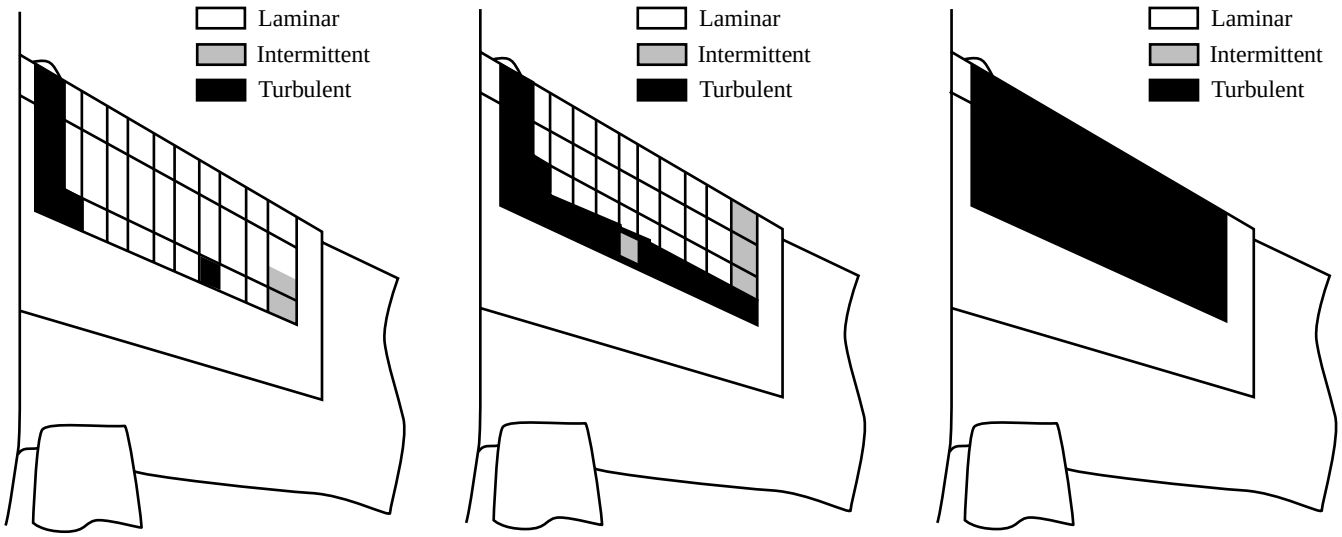

(a) With suction; $\Lambda = 30°$. (b) With suction; $\Lambda = 35°$. (c) Without suction; $\Lambda = 35°$.

Figure 47. Results from Falcon 50 HLFC flight test. Bump 300 mm from wing root. (From Bulgubure and Arnal 1992; Courty, Bulgubure, and Arnal 1993.)

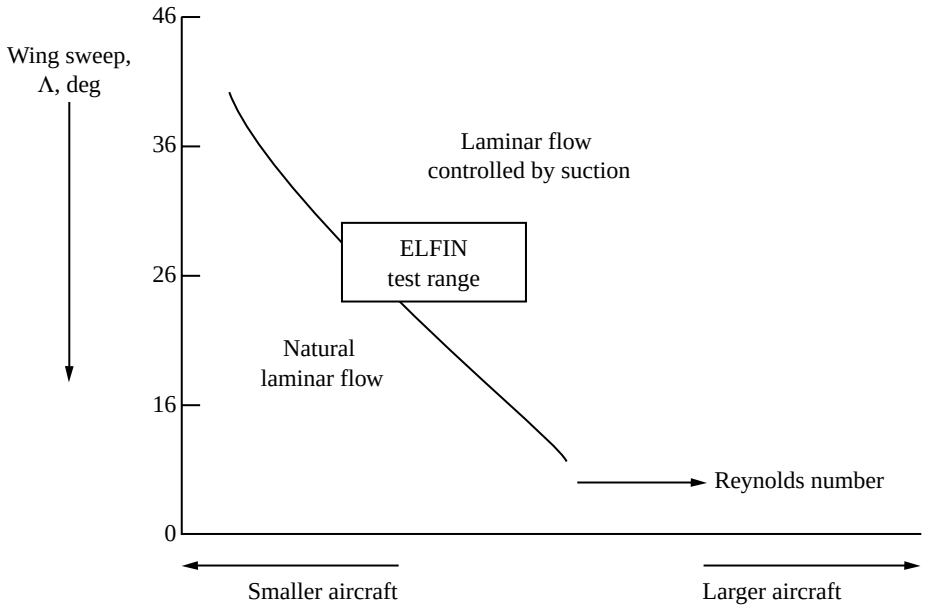

Figure 48. ELFIN test range.

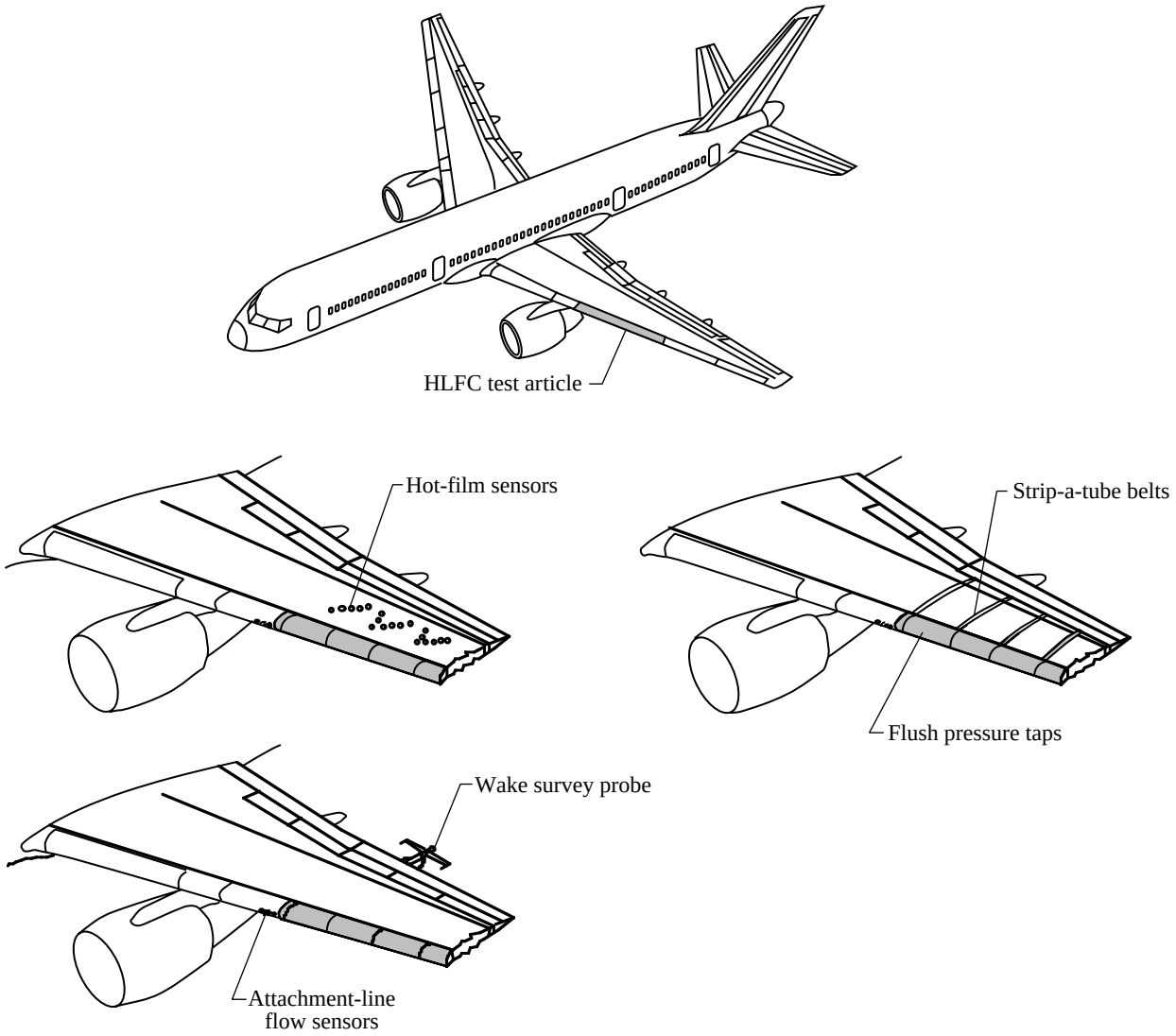

Figure 49. Boeing 757 flight test aircraft with HLFC test section; static pressure, hot-film, and wake-survey instrumentation; and attachment-line flow sensor instrumentation. (From Maddalon 1990, 1991; Collier 1993.)

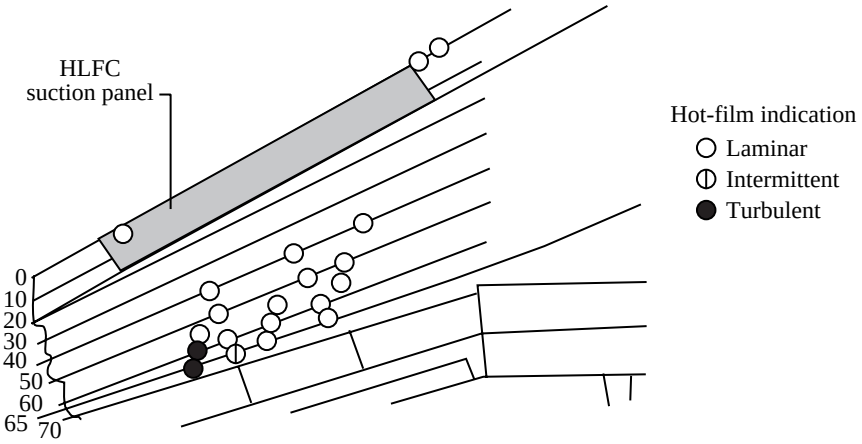

(a) Laminar flow extent; M = 0.82; h = 38 600 ft; C_L = 0.48.

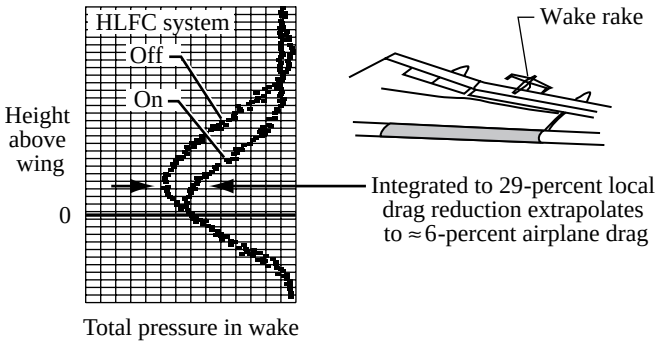

(b) Drag reduction; M = 0.82; C_L = 0.475.

Figure 50. Sample laminar flow extent and drag reduction obtained on Boeing 757 HLFC flight tests. (From Maddalon 1990, 1991; Collier 1993.)

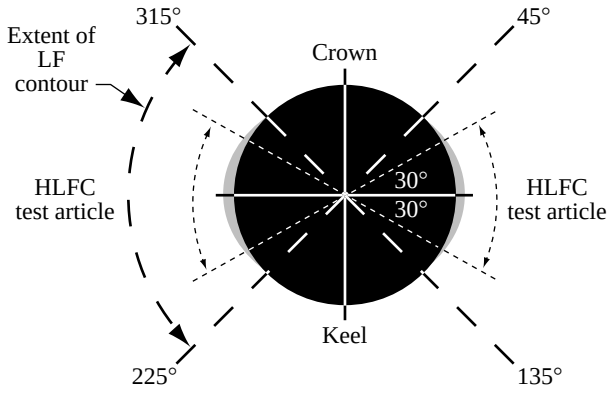

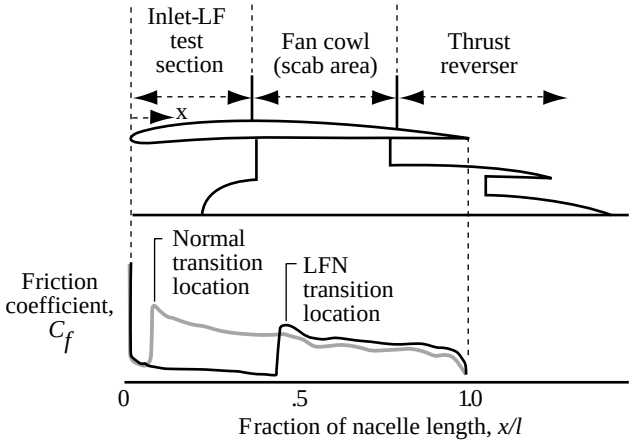

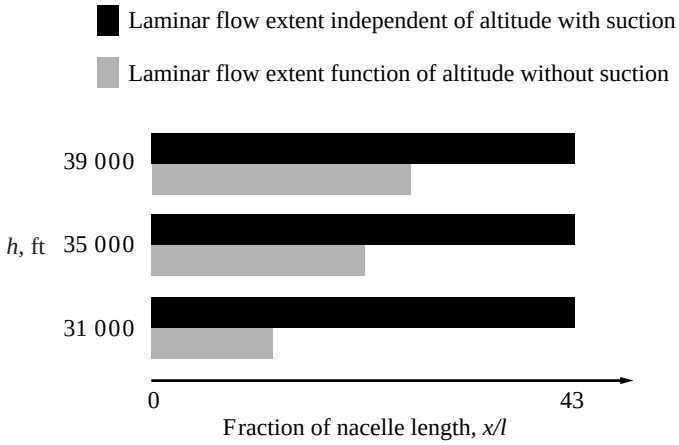

Figure 51. GEAE HLFC nacelle test article flown on Airbus A300/B2 and laminar flow obtained on test article. (From Bhutiani et al. 1993.)

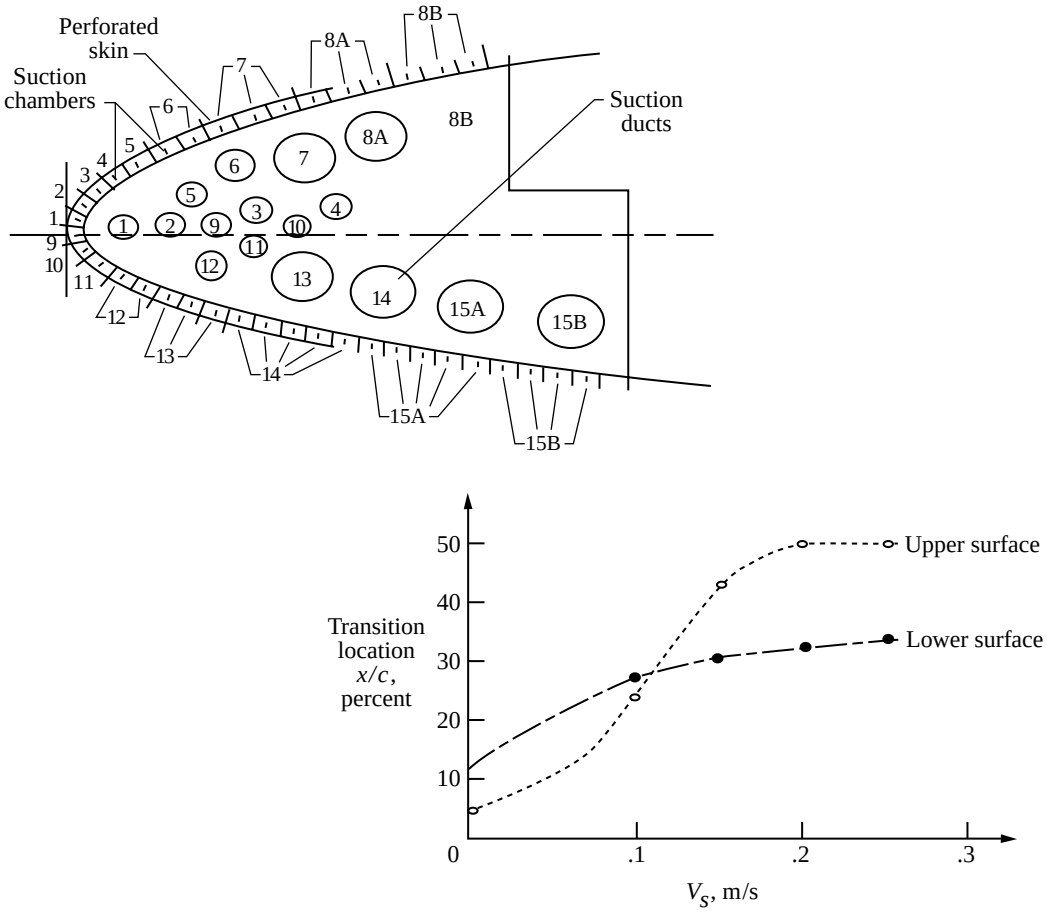

Figure 52. ELFIN large-scale HLFC wind tunnel investigation results from ONERA S1MA. $\Lambda = 28°$; $M = 0.7$; $\alpha = 0°$; $Re = 16.4 \times 10^6$. (From Schmitt, Reneaux, and Priest 1993; Leddy, Charpin, and Garcon 1993; Collier 1993.)

Figure 53. NFL and HLFC flight test article on VFW 614 aircraft. (From Barry et al. 1994; Collier 1993.)

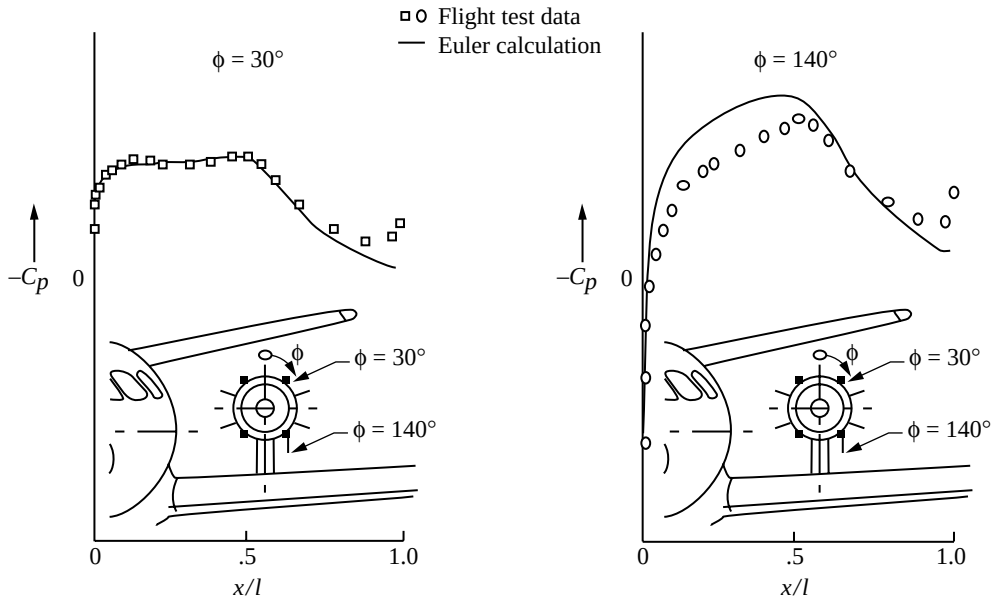

Figure 54. Measured pressure on nacelle test article. (From Barry et al. 1994.)

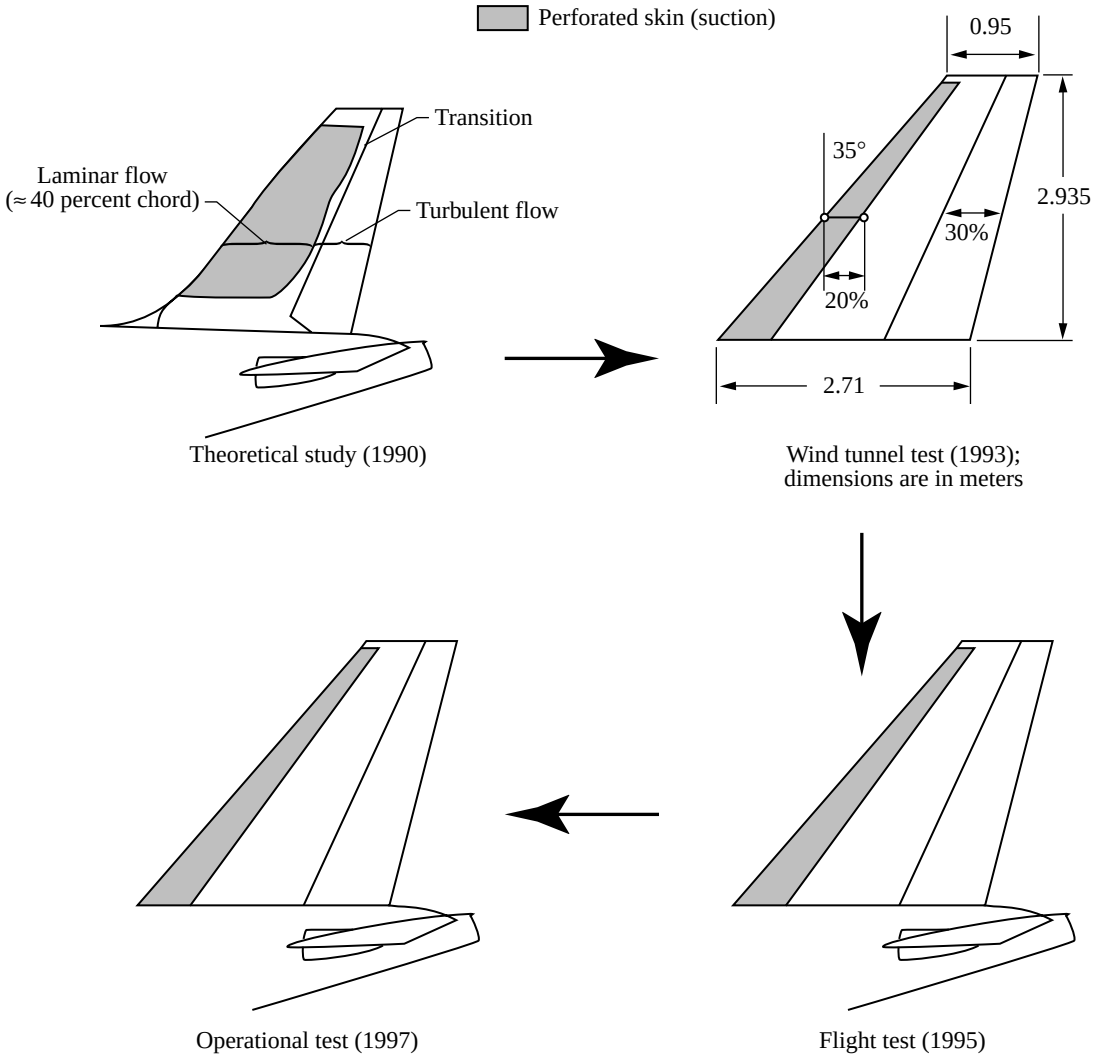

Figure 55. A320 HLFC vertical fin program. (From Robert 1992b.)

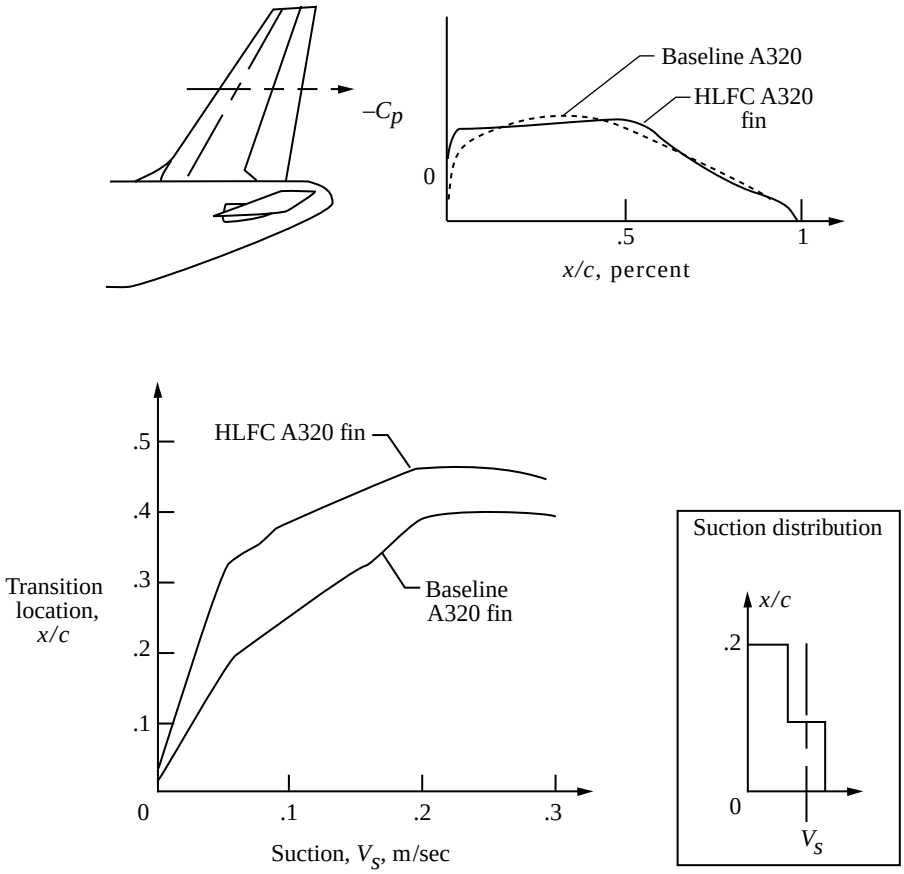

Figure 56. A320 HLFC vertical fin analysis. M = 0.78; Re = 24×10^6. (From Thibert, Reneaux, and Schmitt 1990; Redeker, Quast, and Thibert 1992.)

Figure 57. A320 HLFC vertical fin wind tunnel test in ONERA S1MA. (From Thibert, Reneaux, and Schmitt 1990; Redeker, Quast, and Thibert 1992.)

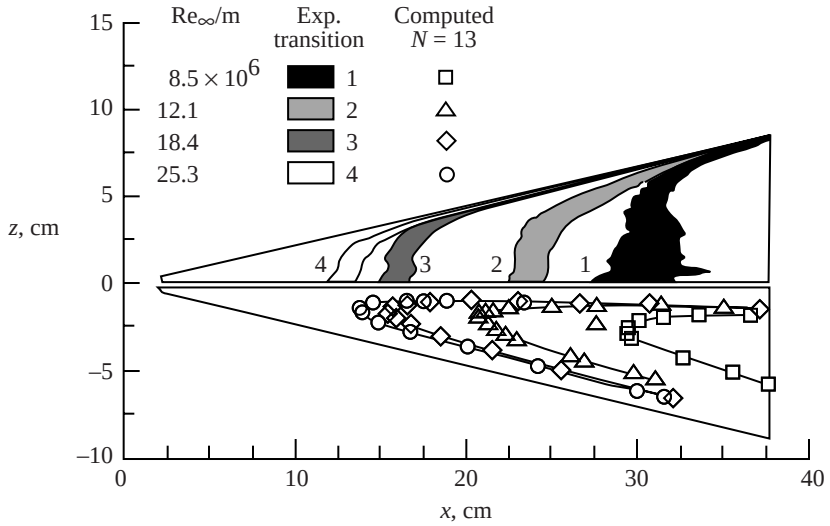

Figure 58. Theoretical correlation of transition location with Reynolds number. (From Cattafesta et al. 1994.)

EC92-09032-2

(a) Single-seat aircraft used for laminar airflow studies.

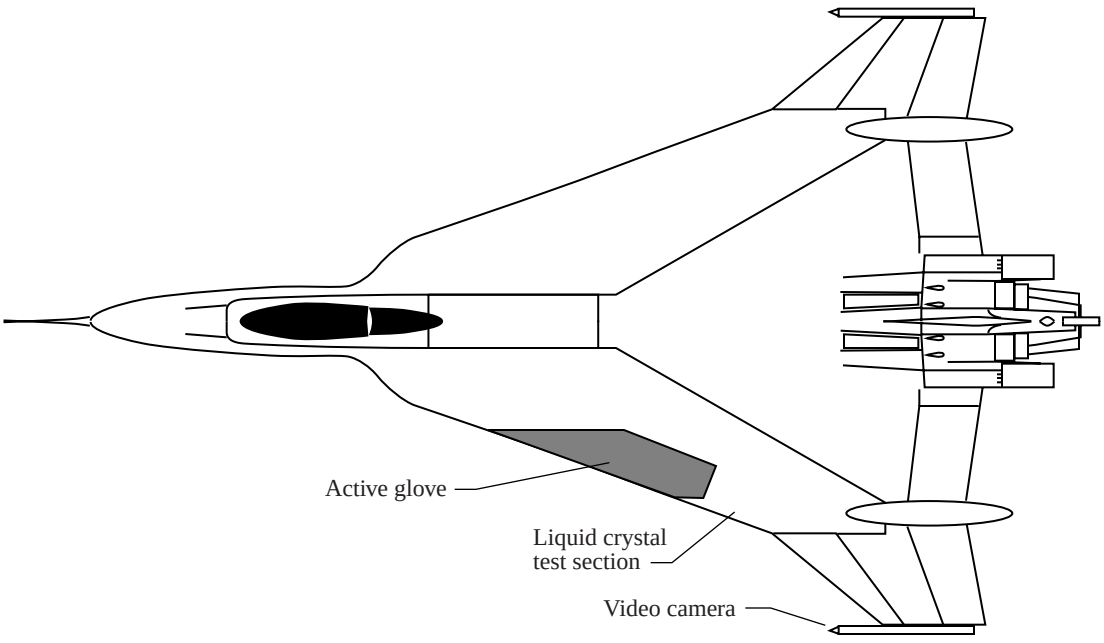

(b) Aircraft with perforated-suction glove. (From Anderson and Bohn-Meyer 1992.)

Figure 59. F-16XL Ship 1.

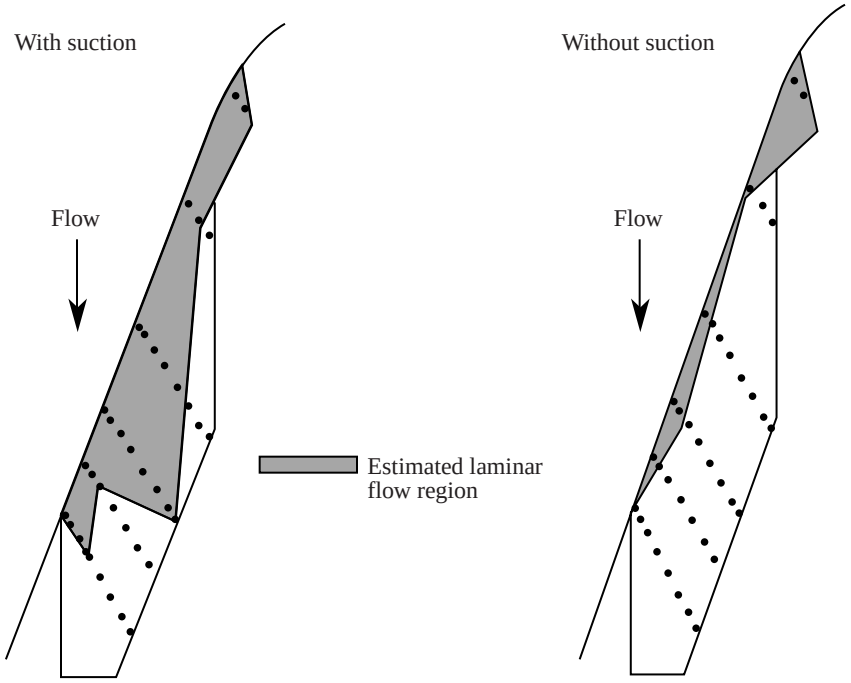

Figure 60. Laminar flow region on perforated-suction glove of F-16XL Ship 1 with and without suction. $M > 1$; $h = 16.7$ km; $\Lambda = 70°$. (From Anderson and Bohn-Meyer 1992.)

EC96-43831-5

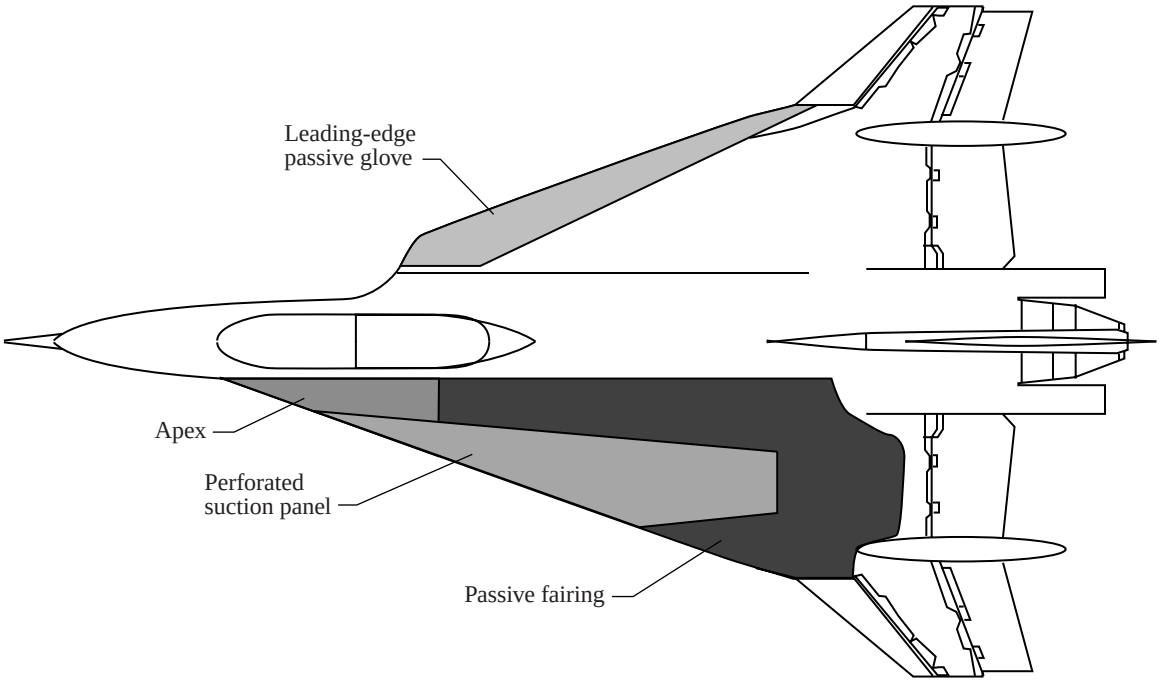

Figure 61. F-16XL Ship 2 supersonic LFC test aircraft. (From Smith 1995.)

REPORT DOCUMENTATION PAGE

Form Approved
OMB No. 07704-0188

1. AGENCY USE ONLY *(Leave blank)*	2. REPORT DATE	3. REPORT TYPE AND DATES COVERED
	October 1998	Technical Publication

4. TITLE AND SUBTITLE
Overview of Laminar Flow Control

5. FUNDING NUMBERS
WU 538-05-15-01

6. AUTHOR(S)
Ronald D. Joslin

7. PERFORMING ORGANIZATION NAME(S) AND ADDRESS(ES)
NASA Langley Research Center
Hampton, VA 23681-2199

8. PERFORMING ORGANIZATION REPORT NUMBER
L-17631

9. SPONSORING/MONITORING AGENCY NAME(S) AND ADDRESS(ES)
National Aeronautics and Space Administration
Washington, DC 20546-0001

10. SPONSORING/MONITORING AGENCY REPORT NUMBER
NASA/TP-1998-208705

11. SUPPLEMENTARY NOTES

12a. DISTRIBUTION/AVAILABILITY STATEMENT
Unclassified–Unlimited
Subject Category 02 Distribution: Standard
Availability: NASA CASI (301) 621-0390

12b. DISTRIBUTION CODE

13. ABSTRACT ***(Maximum 200 words)***

The history of Laminar Flow Control (LFC) from the 1930s through the 1990s is reviewed and the current status of the technology is assessed. Early studies related to the natural laminar boundary-layer flow physics, manufacturing tolerances for laminar flow, and insect-contamination avoidance are discussed. Although most of this publication is about slot-, porous-, and perforated-suction LFC concept studies in wind tunnel and flight experiments, some mention is made of thermal LFC. Theoretical and computational tools to describe the LFC aerodynamics are included for completeness.

14. SUBJECT TERMS	15. NUMBER OF PAGES
Laminar flow control; Transition prediction; Flow control; Review; Natural laminar flow	142
	16. PRICE CODE: A07

17. SECURITY CLASSIFICATION OF REPORT	18. SECURITY CLASSIFICATION OF THIS PAGE	19. SECURITY CLASSIFICATION OF ABSTRACT	20. LIMITATION OF ABSTRACT
Unclassified	Unclassified	Unclassified	